

**The Effect of Inflammation on Stem Cell Mutagenesis and
Carcinogenesis Induced by Azoxymethane in Wild type and
Immune Compromised Mice**

by

Ryan Daniel Whetstone

Chemistry B.A., West Virginia University, 1998

Biotechnology M.S., Johns Hopkins, 2003

Submitted to the Graduate Faculty of
School of Pharmacy in partial fulfillment
of the requirements for the degree of
Doctor of Philosophy

University of Pittsburgh

2014

UNIVERSITY OF PITTSBURGH
SCHOOL OF PHARMACY

This dissertation was presented

by

Ryan Daniel Whetstone

It was defended on

Nov 20, 2014

and approved by

Dr. Kerry Empey, PharmD., Ph.D., Pharmaceutical Sciences

Dr. Pawel Kalinski, M.D., Ph.D., Surgery, Immunology, Bioengineering, and

Inf. Dis. Microbiology

Dr. Song Li, M.D., Ph.D., Pharmaceutical Sciences

Dr. Heth Turnquist, Ph.D., Surgery and Immunology

Dr. Regis Vollmer, Ph.D., Pharmaceutical Sciences

Dissertation Advisor: Dr. Barry Gold, Ph.D., Pharmaceutical Sciences, Chair

Copyright © by Ryan Daniel Whetstone

2014

**The Effect of Inflammation on Stem Cell Mutagenesis and Carcinogenesis Induced by
Azoxymethane in Wild type and Immune Compromised Mice**

Ryan Daniel Whetstone, M.S.

University of Pittsburgh, 2014

Colorectal cancer (CRC) is the third most prevalent cancer in men and women with almost 150,000 new cases diagnosed per year, and almost 50,000 deaths. Inflammation is recognized as a strong risk factor for CRC. The relationship between inflammation potentiating cancer remains unsettled although a common explanation for the role of inflammation involves the formation of reactive oxygen and nitrogen species (RONS). RONS can directly, through oxidation of DNA bases, or indirectly, through the formation of lipid peroxidation products, generate DNA lesions that in turn can lead to increased mutations that activate oncogenes and/or block the function of tumor suppressor genes. To address this fundamental question, C57Bl/6 (B6) WT and TCR β null mice were treated with a DNA damaging agent (azoxymethane, AOM) and/or an inflammatory agent (dextran sulfate sodium, DSS) to mimic an inflammation model of CRC. The carcinogenic and mutagenic effect of the treatments was examined by pathological evaluation of the mouse colons and by measuring the somatic stem cell mutation frequency (MF) in the colon. The results of the carcinogenicity studies show that WT mice are more prone to development of CRC than the TCR β ^{-/-} mice when a low concentration of DSS is used. The mutagenesis results find that DSS, which causes a strong inflammatory response, does NOT result in stem cell mutations in the colon of WT or TCR β ^{-/-} mice. Therefore, inflammation does not potentiate cancer development by increasing the mutation rate. In contrast, AOM causes a significant increase in the colon stem cell MF in both strains but the MF is 50% lower in the

TCR $\beta^{-/-}$ vs. WT mice. Accordingly, we propose that the oncogenic mutations observed in CRC produced by the combination of a genotoxin with an inflammatory agent arise due to the transient creation of a mutator phenotype where stem cells with DNA damage are “forced” to bypass cell cycle arrest and apoptosis because of T-cell supported wound repair and tissue regeneration. We also propose that the effect of DSS treatments after AOM mutagenesis potentiates cancer development by dysregulation of intracellular levels of β -catenin, thereby enhancing the oncogenic effects of AOM mutated β -catenin.

TABLE OF CONTENTS

1.0	INTRODUCTION.....	1
1.1	SCOPE AND SYNOPSIS.....	1
1.2	COLON CANCER FACTS AND STATISTICS.....	2
1.3	FUNCTION AND ARCHITECTURE OF THE LOWER INTESTINE.....	3
1.3.1	Tissue Layers of the Colon and Colorectal Cancer	5
1.3.2	Cell Types, Functions, and Structure of the Colonic Epithelium	9
1.3.2.1	Absorptive Cells	11
1.3.2.2	Goblet Cells.....	12
1.3.2.3	Enteroendocrine Cells.....	12
1.3.2.4	Paneth Cells	14
1.3.2.5	Stem Cells.....	15
1.3.2.6	The Stem Cell Niche.....	20
1.3.2.7	Stem Cell Niche Signaling Governs Stem Cell Behavior.....	23
1.3.2.8	The Niche in Question?.....	25
1.3.2.9	Which Colonic Epithelial Cell is the Potential Cancer Cell?	26
1.4	INFLAMMATION RELATED COLON CANCER INDUCTION MODEL.....	28
1.4.1	Comparative Anatomy of the Human and Mouse Colon	28

1.4.2	A Colon Cancer Inflammation Model	31
1.5	AZOXYMETHANE	32
1.5.1	Azoxymethane (AOM) is a DNA Alkylating Reagent	32
1.5.2	Azoxymethane is a Procarcinogen that is Metabolized into its Active form....	34
1.5.3	AOM displays strong Organotropism	35
1.5.4	Colonic stem cells could be more susceptible to AOM derived DNA Alkylation damage than the differentiated epithelial cells.....	36
1.5.5	DNA Repair, Mutagenesis, and Cytotoxicity	37
1.5.6	Colonic stem cells could be susceptible to O ⁶ mG induced cytotoxicity and mutagenicity than differentiated epithelial cells	39
1.6	DEXTRAN SULFATE SODIUM.....	40
1.6.1	Dextran Sulfate Sodium	40
1.6.2	Treatment with DSS Damages the Colonic Epithelial	41
1.6.3	DSS initiates Colonic Epithelial Injury and Inflammation	44
1.6.4	Inflammation, Bacteria, and RONS.....	46
1.6.5	Bacterial Inflammation Induced by DSS Treatment Modulates Carcinogenesis	50
1.7	AOM+DSS	53
1.7.1	The Genetic Background of a Mouse Strain Modulates the Strains Response to AOM Treatment alone or combine with DSS Treatment	53
1.7.2	AOM Treatment must be closely followed by Treatment with DSS to Induce Colon Cancer	55

1.7.3	Basic research questions	55
2.0	MUTAGENESIS STUDY	57
2.1	SCOPE AND SYNOPSIS.....	57
2.2	INTRODUCTION	57
2.3	DATA	68
2.3.1	Mice Strains and Treatment Groups Studied.....	68
2.3.2	Significance of the Method for Studying G6PD Mutations	68
2.3.3	G6PD Deficient Mutant Crypts.....	69
2.3.3.1	Analysis of G6PD Deficient Mutant Crypts	70
2.3.4	Animal Treatments, Colon Tissue Harvesting and Preparation for G6PD analysis	71
2.3.5	Mutation Frequency and Statistical Analysis	72
2.3.6	G6DP mutation assay results summary table	72
2.4	G6PD MUTATION ASSAY RESULTS SUMMARY	75
2.4.1.1	Analysis of WT AOM treated mice vs. TCR β ^{-/-} AOM treated mice.....	75
2.4.1.2	Analysis of WT AOM treated mice vs. WT AOM+DSS treated mice.....	75
2.4.1.3	Analysis of TCR β ^{-/-} AOM treated mice vs. TCR β ^{-/-} AOM+DSS treated mice	76
2.4.1.4	Analysis of WT AOM+DSS treated mice vs. TCR β ^{-/-} AOM+DSS treated mice	76
2.4.1.5	Analysis of WT DSS treated mice vs. TCR β ^{-/-} DSS treated mice ...	77

2.5	DATA TABLES AND RESULTS FOR THE INDIVIDUAL TREATED GROUPS..	78
2.5.1.1	Results Summary and Analysis of Table 3, previous page.....	79
2.5.1.2	Results Summary and Analysis of Table 4, previous page.....	81
2.5.1.3	Results Summary and Analysis of Table 5, previous page.....	83
2.5.1.4	Results Summary and Analysis of Table 6, previous page.....	85
2.5.1.5	Results Summary and Analysis of Table 7, previous page.....	87
2.5.1.6	Results Summary and Analysis of Table 8, previous page.....	89
2.5.1.7	Results Summary and Analysis of Table 9, previous page.....	91
2.5.1.8	Results Summary and Analysis of Table 10, previous page.....	93
2.6	CALCULATING THE EFFICIENCY OF THE CONVERSION OF AN O⁶-METHYLGUANINE DNA ADDUCT INTO A G6PD MUTATION BY UTILIZING THE STEM CELL MUTATION FREQUENCY.....	94
2.7	SUMMARY AND DISCUSSION.....	98
2.7.1	More G6PD mutant crypts occurred in the WT mice than occur in the immune deficient TCR $\beta^{-/-}$ mice after treatment with AOM?	99
2.7.1.1	α/β T-cell signaling may modulate how a newly divided cell positions itself within the stem cell niche.....	101
2.7.1.2	α/β T-cell signaling may alter a stem cell's epigenetic gene expression to enhance stem cell survival	101
2.7.2	Why were no G6PD mutant crypts detected in the immune competent WT mice and in the immune deficient TCR $\beta^{-/-}$ mice treated with 2% DSS?.....	104

2.7.2.1	The loss of crypt morphology may explain why no G6PD mutant crypts arose in the DSS treated mice	105
2.7.3	Treating the WT mice and the TCR $\beta^{-/-}$ mice with AOM+DSS resulted in a lower G6PD mutation frequency in both strains of mice when compared to the mutation frequency observed after the strains were treated with AOM alone..	106
3.0	CARCINOGENESIS STUDY.....	108
3.1	SCOPE AND SYNOPSIS.....	108
3.2	INTRODUCTION	108
3.2.1	The same mechanisms that immune cells use to provide a benefit for wound repair and tissue regeneration support the growth of cancer cells and their progression toward malignancy.....	111
3.2.2	The earliest cancer cells lack a fully developed tumor microenvironment to support their development and progression, yet are still able to survive and proliferate.....	112
3.2.3	AOM+DSS treatment studies with WT and immune compromised mice.....	113
3.2.4	The potential effects of the loss of α/β T-cell functions on a colon cancer induction model that requires inflammation to promote cancer development..	116
3.3	DATA	121
3.3.1	Mice Strains and Treatment Groups Studied.....	121
3.3.2	The Significance of Studying a Sporadic Colon Cancer Induction model.....	121
3.3.3	Colon cancer induction animal treatments	122

3.3.3.1	Colon Tissue Harvesting and Preparation for H+E Staining	123
3.3.4	H+E Staining and Statistical Analysis	124
3.4	CARCINOGENICITY EXPERIMENTS RESULTS SUMMARY	127
3.4.1.1	Results Summary and Analysis of Table 12, previous page.....	130
3.4.1.2	Results Summary and Analysis of Table 13, previous page.....	132
3.4.1.3	Results Summary and Analysis of Table 14, previous page.....	134
3.4.1.4	Results Summary and Analysis of Table 15, previous page.....	136
3.4.1.5	Results Summary and Analysis of Table 16, previous page.....	139
3.4.2	Differences between the Carcinogenicity Experimental Groups	140
3.4.2.1	Fox n1/J mice developed significantly more carcinomas than the WT mice (Table 11)	140
3.4.2.2	Cancer incidence, multiplicity, and progression was significantly higher in the TCR β ^{-/-} mice after Carcinogenicity Experiment 5 than was observed for the TCR β ^{-/-} mice after Carcinogenicity Experiment 4 (Table 11).....	140
3.5	SUMMARY AND DISCUSSION.....	142
3.5.1	Discussion of the potential reasons why the athymic mice so adversely affected by the DSS treatment	144
3.5.2	Discussion of the potential reasons why the treatment failed to promote tumor development in the athymic mice and in the Fox n1/J mice.....	145
3.5.3	Why did more adenocarcinomas develop in the Fox n1/J mice compared to the athymic mice after the third AOM+DSS treatment?.....	145

3.5.4	Why were the WT mice sensitive to AOM+DSS treatment and the immune compromised TCR β ^{-/-} mice and TCR β ^{-/-} δ ^{-/-} mice resistant to AOM+DSS induced colon cancer by comparison?	146
3.5.5	Why was the significant difference in cancer development observed between the WT mice and the TCR β ^{-/-} mice after the fourth carcinogenicity experiment no longer observed in the WT mice and TCR β ^{-/-} mice after the fifth carcinogenicity experiment? (Table 11)	149
4.0	ARE MUTATIONS THE RATE LIMITNG COMPONENT OF CARCINOGENESIS?	152
4.1	SCOPE AND SYNOPSIS.....	152
4.2	REUSLTS SUMMARY AND ANALYSIS OF THE MUTAGENESIS DATA (TABLE 1) AND CARCINOGENESIS DATA (TABLE 16) FOR THE WT MICE AND TCR β ^{-/-} TREATED WITH 10 MG/KG AOM, 2% DSS AND 10 MG/KG AOM + 2% DSS.....	152
4.3	IF MUTATIONS ARE NOT THE ONLY DETERMINATE FACTOR IN CARCINOGENESIS, THEN WHAT OTHER MECHANISMS WOULD POTENTIATE CANCER CELL DEVELOPMENT?.....	154
4.3.1	Beta-catenin activity is dysregulated by anti-inflammatory immune cell signaling during epithelial restitution	155
5.0	CONCLUSIONS AND SIGNIFICANCE	159
6.0	EXPERIMENTAL DESIGN.....	162
6.1	ANIMAL HUSBANDRY	162
6.2	AZOXYMETHANE DOSING	163

6.3	DEXTRAN SULFATE SODIUM DOSING	164
6.4	TISSUE HISTOLOGY	165
6.4.1	Tissue Collection	165
6.4.2	Paraffin Embedding	166
6.4.2.1	Hematoxylin and Eosin.....	169
6.4.3	Freezing Tissues for Sectioning	169
6.4.3.1	Cutting frozen sections	169
6.4.3.2	Hematoxylin and Eosin.....	170
6.5	ENZYME HISTOCHEMISTRY	171
6.5.1	Tissue Staining Reaction Mixture	171
6.5.1.1	OCT Medium as the Alternative Enzyme Stabilizer	171
6.5.1.2	G6PD enzymatic reaction.....	173
6.5.1.3	pH Adjustment of the OCT Medium	174
6.5.1.4	Assembling the Reaction Mix.....	174
6.5.1.5	Staining Slides for G6PD Activity	177
6.5.2	G6PD Activity Analysis.....	178
6.5.2.1	Assessing G6PD Mutant Crypts and Total Counts	178
6.5.3	Total Counts and Mutation Frequency	179
6.6	STATISTICAL ANALYSIS	180
6.6.1	Student's T-test	180
6.6.2	Fisher's Exact Test	180
APPENDIX A		181
BIBLIOGRAPHY.....		182

LIST OF TABLES

Table 1: G6PD Mutation Assay results summary table.....	73
Table 2. G6PD M.F. results comparison table.....	74
Table 3. WT Untreated Control Mice	78
Table 4. TCR $\beta^{-/-}$ Untreated Control mice	80
Table 5. WT AOM treated mice	82
Table 6. TCR $\beta^{-/-}$ AOM treated mice	84
Table 7. WT DSS treated mice	86
Table 8. TCR $\beta^{-/-}$ DSS treated mice	88
Table 9. WT AOM+DSS treated mice.....	90
Table 10. TCR $\beta^{-/-}$ AOM+DSS treated mice	92
Table 11. Carcinogenicity Experiments Results Summary table.....	128
Table 12. Carcinogenicity Experiment 1	129
Table 13. Carcinogenicity Experiment 2	131
Table 14. Carcinogenicity Experiment 3	133
Table 15. Carcinogenicity Experiment 4	135
Table 16. Carcinogenicity Experiment 5	138

LIST OF FIGURES

Figure 1. The Human Lower Intestine	4
Figure 2. Colonic Epithelial Layers and Cancer Progression	6
Figure 3. Colonic Epithelial Cells and Lineage Differentiation	9
Figure 4. Colonic Epithelial Cell Migration and Differentiation.....	10
Figure 5. Columnar Colonic Epithelial Crypts and the Stem Cell Niche	16
Figure 6. Colonic Epithelial Crypt Domination by a Mutated Stem Cell.....	18
Figure 7. Colonic Epithelial Stem Cells are Separated in the Niche	21
Figure 8. Colonic Epithelial Crypts are Sheathed by Pericryptal Cells.....	22
Figure 9. Colonic Epithelial Stem Cell Division	23
Figure 10. The Mouse Lower Intestine and Comprising Regions	30
Figure 11. Sites of DNA Methylation by Monofunctional Agents.....	33
Figure 12. AOM Metabolism into its DNA Alkylating Form	34
Figure 13. Colonic Epithelial Changes after DSS Treatment.....	43
Figure 14. G6PD Mutant Crypts.....	69
Figure 15. Mouse Colon Swiss-Roll.....	167
Figure 16. G6PD Enzymatic Reaction	173

1.0 INTRODUCTION

1.1 SCOPE AND SYNOPSIS

The purpose of this chapter is to introduce and familiarize the reader with the general knowledge and background material related to our studies. The material covered in this chapter provides significant and extensive details of the colon morphology and the animal model of colon cancer induction used for this work. More specific introductions to each experiment and the results are provided at the beginning of each experimental study chapters 2 and 3. Chapter 1 begins with relevant statistics for colon cancer incidence and mortality, and then reviews colon function and the layers that comprise the colon, with an explanation that the epithelium is the origin of colon adenomas and adenocarcinomas. The chapter then details the types and functions of the cells that comprise the colon and small intestine. Also, the argument is presented that colonic stem cells can fix a mutation and propagate a population of cells that could become the first cancer cells. Chapter 1 then introduces the two-stage colon cancer induction model of a mutagen, azoxymethane (AOM), and an inflammatory agent, dextran sulfate sodium (DSS), and how their action reflects colon cancer development in humans. Chapter 1 details the morphological disruption of the colon architecture and the immune response generated by DSS treatment, with an emphasis on the effects of reactive oxygen and nitrogen species (RONS). Chapter 1 concludes with a review of the strain differences of mice to the induction of colon cancer.

1.2 COLON CANCER FACTS AND STATISTICS

The American Cancer Society estimates that 136,830 cases of colorectal cancer (CRC) will occur in the United States during 2014.⁽¹⁾ 96,380 cases will be colon cancers and 40,000 rectal cancers.⁽¹⁾ Colon cancer is the third most common cancer diagnosed in both men and women.⁽¹⁾ The previous statement, which excludes skin cancers, ranks colon cancer incidence behind lung cancer and cancers of sex-related organs, i.e., prostate, breast.⁽¹⁾⁽²⁾ The World Cancer Research Fund International (WCRF International) reported that 1.4 million cases of CRC were diagnosed worldwide in 2012,⁽³⁾ and it is predicted that there will be 2.4 million cases diagnosed per year by 2035.⁽³⁾

The American Cancer Society also estimates that 50,310 deaths will occur as a result of colon cancer morbidity in the USA during 2014.⁽¹⁾ CRC has the third highest incidence of mortality among both men and women. CRC results in the second highest yearly mortality among cancer related deaths for both men and women combined.⁽¹⁾

The American Cancer Society (ACS) predicts that the lifetime risk of a person developing colorectal cancer is one in twenty.⁽¹⁾ Risk factors for developing CRCs can greatly enhance the probability of an individual developing CRC. ACS categorizes risk factors as; “Risk factors you cannot change”, “Lifestyle related factors”, and “Factors with uncertain, controversial, or unproven effects on CRC”.⁽¹⁾ “Personal history of inflammatory bowel disease” is cited as a risk factor that is not controlled by the individual.⁽¹⁾ Individuals with inflammatory bowel disease (IBD) have a six times greater risk of developing CRC.⁽³⁸⁶⁾ The onset of an inflammatory bowel disease (IBD) may lead to earlier detection and treatment of CRC, as patients diagnosed with an IBD will begin screening for CRC at an earlier time than patients without an IBD.⁽¹⁾ Obesity also increases the risk of an individual developing colon cancer and is

a lifestyle related factor.⁽¹⁾⁽³⁸⁸⁾ Obesity is likely related to diet which is another lifestyle related factor.⁽¹⁾⁽³⁸⁸⁾

1.3 FUNCTION AND ARCHITECTURE OF THE LOWER INTESTINE

The large or lower intestine is comprised of several regions; the cecum, colon, rectum, and anal canal (Figure 1). The cecum is located at the lower right side of the abdominal cavity and forms a dilated pouch-like structure that links the ileum of the small intestine to the large intestine through the ileocecal sphincter.⁽⁴⁾ The ascending colon starts at the cecum and extends upwards toward the thoracic cavity along the right side of the abdominal cavity.⁽⁴⁾ The colon then turns to the left and runs the length of the abdominal cavity just below the liver and stomach,⁽⁴⁾ and this region is called the transverse colon. The colon then moves down the left side of the abdominal cavity and this region is termed the descending colon.⁽⁴⁾ The descending colon then takes on a slight S-shape and is called the sigmoidal colon.⁽⁴⁾ The final portion of the colon is the rectum that lies above the sacrum and ends at the anal canal.⁽⁴⁾ The entire organ is approximately 1.5 meters long.⁽⁴⁾ It is anchored in the abdominal cavity by the peritoneum and rests on the skeletal muscle.⁽⁴⁾

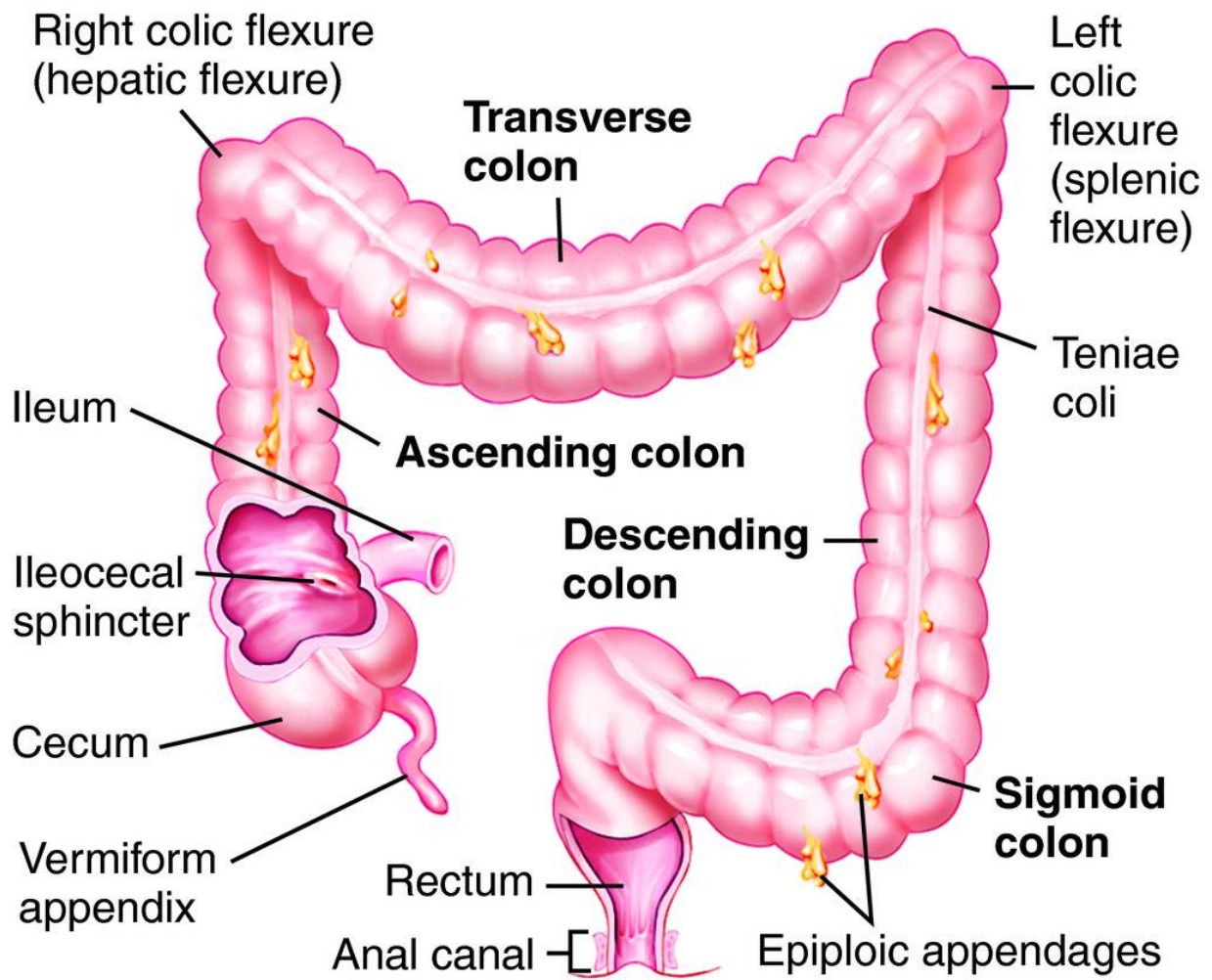


Figure 1. The Human Lower Intestine

(adopted from reference 4)

1.3.1 Tissue Layers of the Colon and Colorectal Cancer

The wall of the colon is comprised of several different layers (Figure 2). The innermost layer bordering the lumen is called the mucosal layer. The mucosal epithelial layer is the source of colonic adenomas and adenocarcinomas⁽⁵⁾(Figure 2). This layer is comprised of three regions; a single sheet of columnar epithelial cells, the lamina propria, and muscularis mucosae.⁽⁴⁾⁽⁵⁾ The epithelium forms long finger-like invaginations which are termed crypts. Colonic crypts extend into the lumen and are defined as columnar due to the fact that they are straight and unbranched⁽¹³⁾(Figure 4).

The crypt architecture is a critical component of the colon's ability to mediate its functions. The shape of the crypts creates a greater surface area than would otherwise be possible if the epithelium was a smooth flat cell layer.⁽⁴⁾⁽¹³⁾ This creates a more extensive contact with the feces as the waste is slowly moved by the reflexive action of the smooth muscle, essentially creating a churning effect.⁽⁴⁾ The crypt shape also ensures that dead epithelial cells are removed and normal turnover of the epithelial cells can be maintained⁽¹⁰⁾(section 1.2.2), as removing dead cells requires frictional interactions with the semi-solid waste to shed the dead cell layer. The different cell types that comprise the epithelial layer are thoroughly discussed in section 1.2.2.

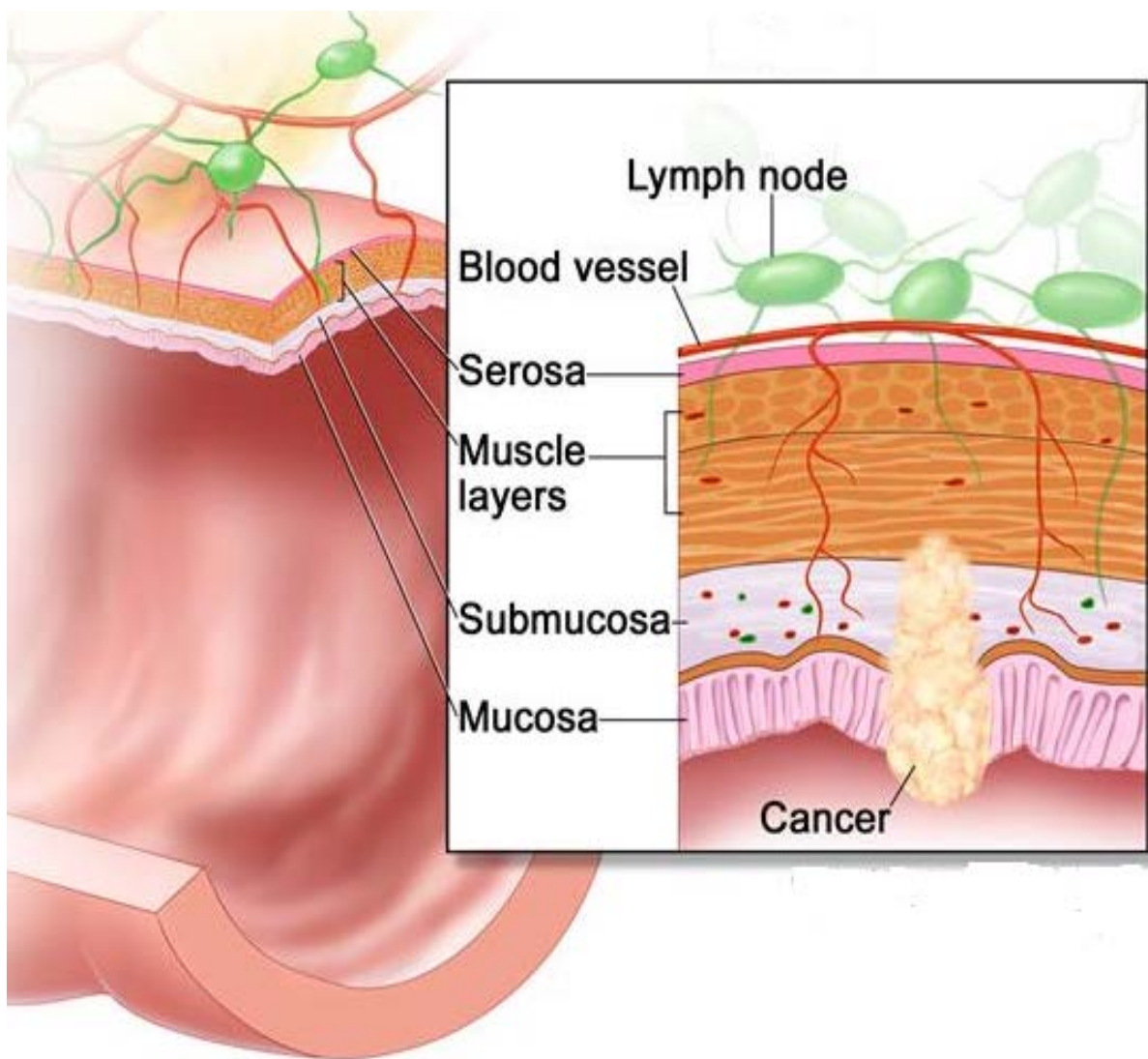


Figure 2. Colonic Epithelial Layers and Cancer Progression

(adopted from reference 5)

Underlying the colonic epithelial layer is the lamina propria. This is a layer of connective tissue that is highly vascularized and heavily populated with immune cells.⁽⁴⁾⁽¹³⁾ The vascularization is necessary for the survival of the epithelial cells, and the immune cells help maintain surveillance and natural tolerance. The lamina propria is a very distinct region under histological examination.⁽¹³⁾ The muscularis mucosae is an innervated smooth muscle that functions in the local movement of the mucosa and aids in the recovery of nutrients.⁽⁴⁾⁽¹³⁾ The enteric nervous system is comprised of at least three different types of neurons.⁽³⁷⁹⁾⁽³⁸⁰⁾ Efferent neurons (motor neurons) carry signals from the central nervous system (CNS) to muscles and glands (effectors).⁽³⁷⁹⁾⁽³⁸⁰⁾⁽³⁸¹⁾⁽³⁸²⁾ Afferent neurons (sensory neurons) relay signals from the mucosa and muscle to nerve centers.⁽³⁷⁹⁾⁽³⁸⁰⁾⁽³⁸¹⁾⁽³⁸²⁾ Interneurons connect and integrate information from sensory neurons to motor neurons.⁽³⁷⁹⁾⁽³⁸⁰⁾⁽³⁸¹⁾⁽³⁸²⁾ The muscularis mucosae also acts as a scaffolding for the mucosal layer.⁽⁴⁾⁽¹³⁾

An adenocarcinoma is a cancer that originates from a glandular cell (Figure 2). In the colon these are the mucus secreting epithelial cells. The progression of a colonic adenocarcinoma is defined by stages.⁽⁵⁾ Each stage describes the degree of invasion of the adenocarcinoma into the layers of colon. For example; Stage I describes a cancer invading through the submucosa and reaching the muscular externa. In Stage IV colon cancer, cancer cells have metastasized via the lymphatic system to other organs.⁽⁵⁾

The submucosa is a layer of connective tissue between the mucosa and muscularis externa⁽⁴⁾⁽¹³⁾(Figure 2). The submucosa is comprised of coarse collagen fibers, large blood and lymphatic vessels, lymph nodes, and autonomic nerve plexi and ganglia.⁽⁴⁾⁽¹³⁾ The submucosa also contains various tissue resident immune cells.⁽⁴⁾⁽¹³⁾ The muscularis externa in the colon is a

smooth muscle.⁽⁴⁾⁽¹³⁾ Smooth muscle is controlled by the autonomic visceral nervous system⁴⁾⁽¹³⁾ The primary function of the colonic muscularis externa is to move solid waste through the abdominal cavity.⁽⁴⁾⁽¹³⁾ The final layer is the serosa, which is comprised of a thin connective layer called the adventitia and the mesothelium layer which secretes serous fluid. Serous fluid is enriched with proteins and moistens internal organs in the body cavity.⁽⁴⁾⁽¹³⁾

Adenocarcinomas are able to invade the mucosal and submucosal layers of the colon. However, in the muscularis externa, adenocarcinomas can continue to advance through the muscle and serosa (Stage II) before spreading to other organs (Stage IV).⁽⁵⁾ Adenocarcinomas do not always penetrate through the muscularis externa (Stage III), but can spread by recruiting the vasculature and metastasize to adjacent lymph nodes (Stage IV).⁽⁵⁾

1.3.2 Cell Types, Functions, and Structure of the Colonic Epithelium

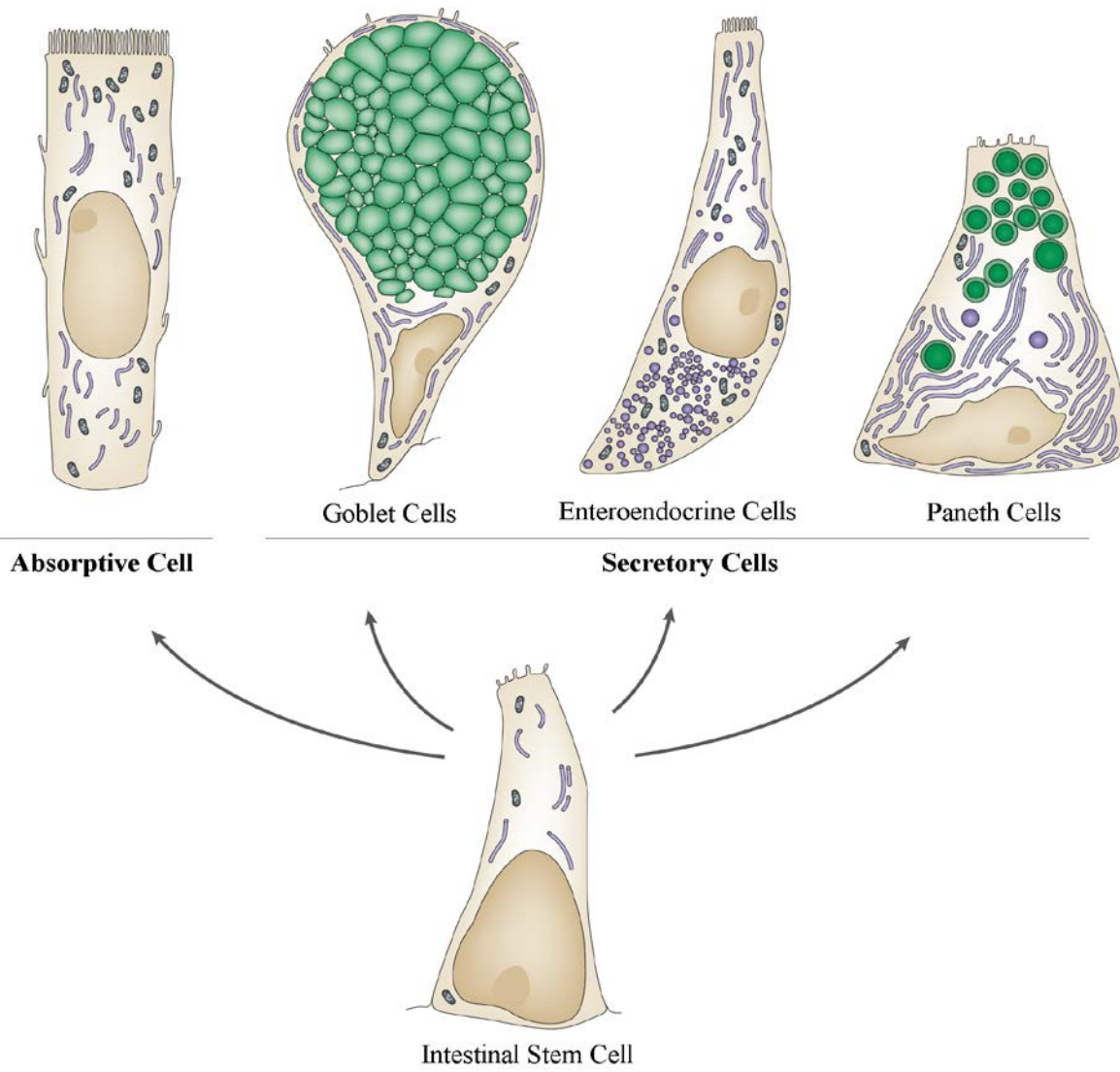


Figure 3. Colonic Epithelial Cells and Lineage Differentiation

(adopted from reference 6)

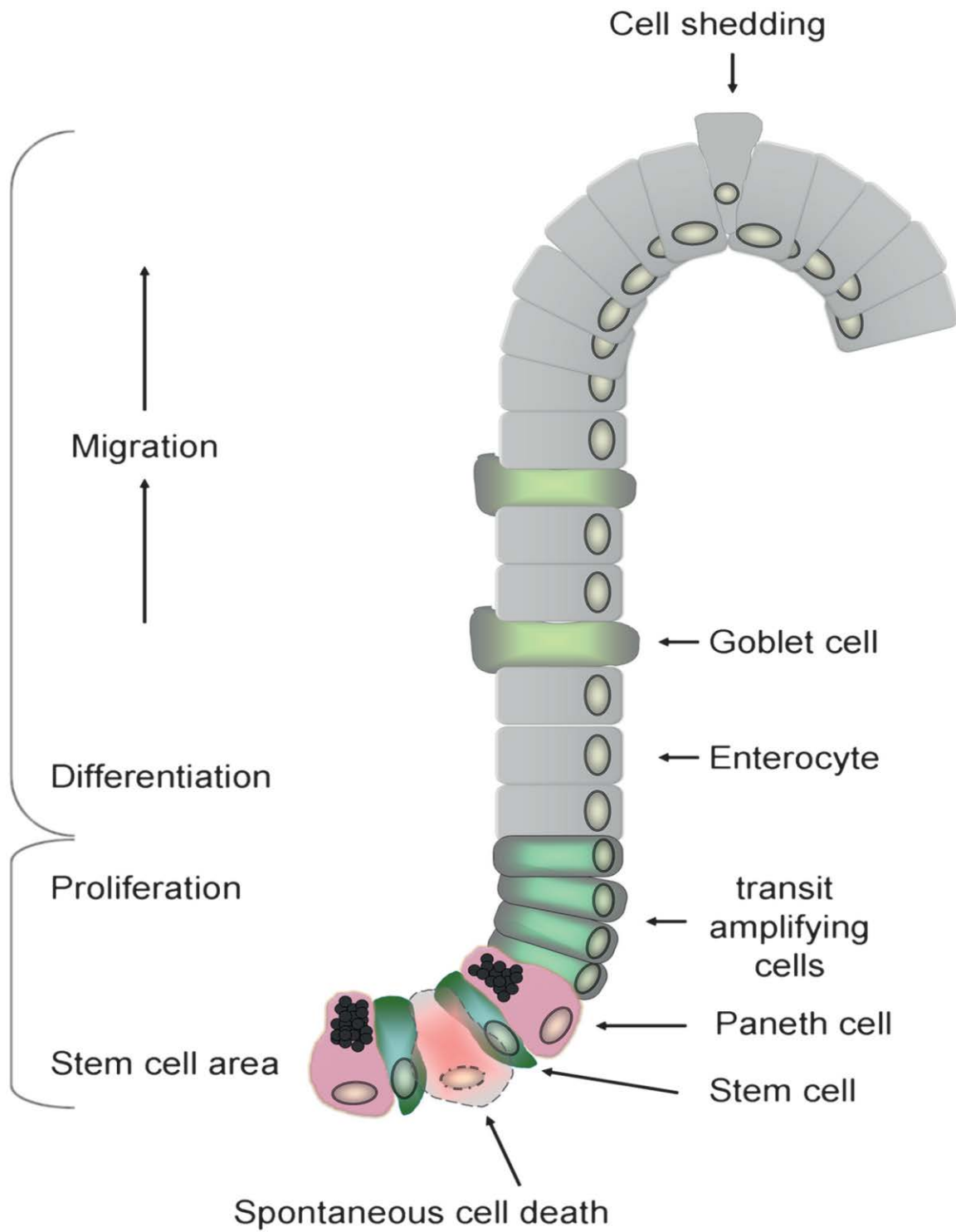


Figure 4. Colonic Epithelial Cell Migration and Differentiation

(adopted from reference 10)

The colonic epithelium is comprised of five distinct cell types (Figure 3). Four of which arise from the lineage differentiation of colonic stem cell progeny (Figure 3). The location of the cells in the columnar shape of the colonic epithelial crypt define the degree of lineage differentiation that the epithelial cells have undergone⁽⁶⁾⁽¹⁰⁾(Figure 4). Stem cells remain fixed in the base of the crypts but the stem cell progeny will migrate out of the stem cell niche and begin lineage differentiation in the transit-amplifying compartment⁽⁶⁾⁽¹⁰⁾(Figure 4). Colonic epithelial cells move in an assembly line fashion from the base of the crypt, progressing thorough lineage differentiation, to the luminal border of the crypt where they are shed⁽⁷⁾⁽⁸⁾(Figure 4). The cells at the luminal border undergo apoptosis to avoid accumulating and disrupting the steady-state turnover of the colonic epithelial cells.⁽⁷⁾⁽⁹⁾⁽¹⁰⁾ Under normal conditions, the introduction of new cells and the loss of existing cells establish an equilibrium.⁽⁷⁾⁽⁹⁾⁽¹⁰⁾ Tissue damage and inflammatory responses disrupt the normal rate of stem cell division and fully differentiated cell loss,⁽¹¹⁾⁽¹²⁾ requiring stem cells to divide at a faster rate to compensate for the sudden depletion of the differentiated cells.

1.3.2.1 Absorptive Cells

Absorptive cells (enterocytes) are abundant in the colonic epithelium lining the lumen. Enterocytes have an apical border on the lumen side of their plasma membrane called the brush border⁽¹³⁾(Figure 3). The apical border extrudes microvilli that increase the surface area of the cells.⁽¹³⁾ This facilitates the recovery of nutrients which enterocytes export through their basal membrane into the lamina propria.⁽¹³⁾ Enterocytes are likely exposed to many agents that generate promutagenic DNA lesions due to the influx of molecules reabsorbed from the undigested wastes. Enterocytes are also susceptible to acquiring mutagenic DNA damage generated by reactive oxygen and nitrogen species (RONS) during immune responses. However,

fully differentiated enterocytes do not undergo cell division under homeostatic conditions. Cell division is a requirement for mutagenesis since DNA must undergo replication for a DNA lesion to cause incorrect nucleobases to be fixed into a cell's genome. Enterocytes are normally retained for a week or less and are then induced to undergo apoptosis.⁽⁸⁾⁽¹⁰⁾ The lack of cell division and their short life span make enterocytes unlikely candidates to become cancer cells.

1.3.2.2 Goblet Cells

Goblet cells are also abundant in the colonic epithelium. They appear to exceed the absorptive cells in some areas of the colon. Goblet cells have an apical border on the luminal side of their plasma membrane⁽¹³⁾(Figure 3). They secrete mucus that assists in moving solid waste, protects the mucosal epithelial cells, and balances the pH of the colonic lumen.⁽⁴⁾⁽¹³⁾ While goblet cells are not at risk from absorbing DNA damaging molecules, they would be susceptible to acquiring mutagenic DNA damage generated by RONS during immune responses. Goblet cells are not dividing under homeostatic conditions, and therefore highly unlikely to fix a lesion into a mutation. Goblet cells are normally retained for less than a week and are then induced to undergo apoptosis.⁽⁸⁾⁽¹⁰⁾ As with the enterocytes, the lack of cell division and a short life span make goblet cells unlikely candidates to become cancer cells.

1.3.2.3 Enteroendocrine Cells

Enteroendocrine cells comprise the largest endocrine system of body.⁽¹⁴⁾ The enteroendocrine cells comprise only one percent of the entire gut epithelium,⁽⁸⁾ yet express a high degree of diversity as fifteen different cell types have been identified. The colonic epithelial enteroendocrine cells lack the diversity of the enteroendocrine cells of the small intestine,

primarily having only three different cell types: enterochromaffin (EC) cells, D cells, and L cells,⁽¹⁵⁾ although other subsets may exist as well.⁽⁸⁾

Enteroendocrine cells display a longer retention time in the colon than enterocytes and goblet cells. Enteroendocrine cells can be retained for up to three weeks vs. a week or less for enterocytes and goblet cells.⁽⁸⁾ Enteroendocrine cells increase their retention time by dissolving their tight cell-cell junctional connections to adjacent cells.⁽⁸⁾ This essentially releases enteroendocrine cells from the assembly line, and allows them to retain a predetermined position within the crypt.

Enteroendocrine cells are secretory and not at risk from absorbing DNA damaging molecules, but are at risk from immune response derived RONS. It is likely enteroendocrine cells have an atypical apoptotic induction signaling pathway vs. enterocytes and goblet cells, due to their long retention time and their dissociation from the typical crypt architecture. Enteroendocrine cells are not dividing under homeostatic conditions, and therefore highly unlikely to fix a lesion into a mutation. However, during severe wound distress fully differentiated cells may undergo cell division to compensate for the loss of tissue integrity.⁽¹⁴⁾ To fix a mutation in its genome, an enteroendocrine cell would need to divide with an unrepaired DNA lesion. Even if enteroendocrine cells could be induced to divide with DNA damage, and the cells were able to resist apoptotic induction, the limited numbers of enteroendocrine cells make them unlikely targets to manifest the first cancer cells.

There is scientific interest in deducing the role of enteroendocrine cells in colonic inflammatory disease and in colon cancer.⁽¹⁵⁾⁽¹⁶⁾ Differentiated enteroendocrine cells have been detected in colorectal carcinomas.⁽¹⁷⁾ Enteroendocrine cells secrete; serotonin, PYY, glicentin and GLP-2 that potentially enhance cellular proliferation within the colonic epithelium. This has

brought forth the hypothesis that CRCs with enteroendocrine support possess a proliferative advantage.⁽¹⁷⁾ In some colonic tumors positive for enteroendocrine cells, the enteroendocrine cells also expressed vascular endothelial growth factor (VEGF).⁽¹⁷⁾ However, it is unclear if the presence of enteroendocrine cells in a CRC actually results in a worse prognosis for patients.⁽¹⁸⁾

1.3.2.4 Paneth Cells

Paneth cells comprise the most unique of the four lineage differentiated cells in terms of their functional capacities. Paneth cells occupy the base of the intestinal crypts, which is also the stem cell niche. Paneth cells, which are named for their discoverer, are secretory cells that secrete antimicrobial peptides; α and β defensins, Lysozyme C, Phospholipases A2, and C-type Lectins.⁽¹⁹⁾ Interestingly, Phospholipases A2 are not expressed by C57Bl/6 mice.⁽¹⁹⁾ Paneth cells are considered to be stem cell niche regulators by expressing Wnt3, Wnt11, Egf, Tgfa and Notch Dll4, and all of these signaling molecules support stem cells.⁽²⁰⁾ Paneth cells are retained significantly longer than other lineage derived cells, possibly 60 days or longer.⁽²¹⁾ Paneth cells are capable of dedifferentiation under ex vivo conditions and reacquire stem cell like proliferative abilities.⁽²¹⁾

If Paneth cells are capable of dedifferentiation in vivo, as suggested by Roth, et al., then they may represent a potential source of new stem cells when crypts are damaged and the current stem cell population is depleted.⁽²¹⁾ If Paneth cells are capable of clonal expansion, then they would also be vulnerable to fixing an inflammation derived RONS DNA lesion into a mutation during DNA replication. As they are also retained for a significant length of time, Paneth cells with a mutation fixed in their genome may be able to progress further toward becoming a cancer cell.

However, Paneth cells are not a normal part of the colonic epithelium,⁽²⁰⁾ and are only found in the small intestine under normal conditions. While a cell that is likely the colonic equivalent has been identified,⁽²⁰⁾ Paneth cells in the colon only arise in colonic disease states such as colitis or CRC.⁽¹⁹⁾⁽²²⁾ Paneth cell development in the distal colon as a result of the onset of colitis is termed metaplasia.⁽¹⁹⁾ Since they are not a component of colonic crypts under homeostatic conditions and, therefore, not a part of the cancer initiation and promotion events, it is difficult to consider Paneth cells as the originating colonic adenocarcinoma cells without further findings. Paneth cell ablation studies only enhance the complexity of defining the role of Paneth cells as these cells can be depleted in the small intestine with no observed phenotype.⁽²³⁾⁽²⁴⁾ Also, it is unknown if Paneth cells can undergo dedifferentiation and clonal expansion in vivo, in the same capacity they are capable of being induced to dedifferentiate ex vivo.

1.3.2.5 Stem Cells

Colonic epithelial stem cells are responsible for generating new cells that allow for the continuous turnover and renewal of the colonic epithelium. The stem cells reside in niches designed to maintain the stem cells unique characteristics of longevity and unlimited proliferative ability.⁽²⁵⁾ Evidence for the existence of a stem cell population occupying the base of a colonic epithelial crypt was deduced to a large extent by the research of the Clevers lab,⁽²⁶⁾ as demonstrated in Figure 5.



Figure 5. Columnar Colonic Epithelial Crypts and the Stem Cell Niche

(adopted from reference 26)

Figure 5. Colonic epithelial stem cells occupy the base of a crypt. Expression of Lrg5-EGFP-IRES-creERT2 coupled to a Cre activated Rosa26-lacZ. LGR5 gene is restricted to stem cells and tamoxifen induced Cre expression led to the activation of the Rosa26-lacZ reporter gene leads to the coloration of the entire crypt as all the stem cell derived progeny cells express lacZ.

To characterize colonic stem cells as Lgr5 expressing cells, mice were generated with a complex knock-in allele. Lgr5 (leucine-rich-repeat-containing G coupled-protein-receptor 5) is an orphan G-coupled protein receptor⁽²⁶⁾ that is rarely expressed in adult tissues, and in the intestines Lgr5 expression is restricted to stem cells.⁽²⁵⁾ The Lgr5 gene was able to be reconstructed to introduce a GFP coding region, an Internal Ribosome Entry Site (IRES) region, and an inducible Cre expressing region.⁽²⁶⁾ The IRES allowed for the translation of the Cre cassette, which was coupled to another reporter gene Rosa26-lacZ.⁽²⁷⁾ In spite of the gene alterations the heterozygote mice generated with the knock-in allele were reported to be healthy and fertile.⁽²⁶⁾

By treating the knock-in mice with tamoxifen the expression of Cre in the stem cells was induced, which then excised the inhibitor of the Rosa26-lacZ gene. If the lacZ reporter is expressed in a cycling stem cell then all of the progeny of that stem cell will express the gene. The lacZ gene hydrolyses the reagent X-Gal into a blue precipitate that will accumulate at the site of the enzyme activity⁽²⁸⁾(Figure 5).

The inducible lacZ reporter expression is critical to understanding why a colonic stem cell produces the originating cells of a colonic adenocarcinoma.⁽²⁹⁾ It is reported that there are approximately 5 stem cells per crypt.⁽³⁰⁾ For an entire crypt to be comprised of lacZ expressing cells, that can metabolize X-Gal, then a lacZ expressing stem cell must be that crypt's active proliferating stem cell, i.e., the dominate stem cell. A stem cell with induced lacZ expression dominating a crypt is equivalent to a stem cell with a fixed mutation surviving and dominating a crypt, so that the progeny cells harboring the mutation eventually occupy the entire crypt (Figure 6).

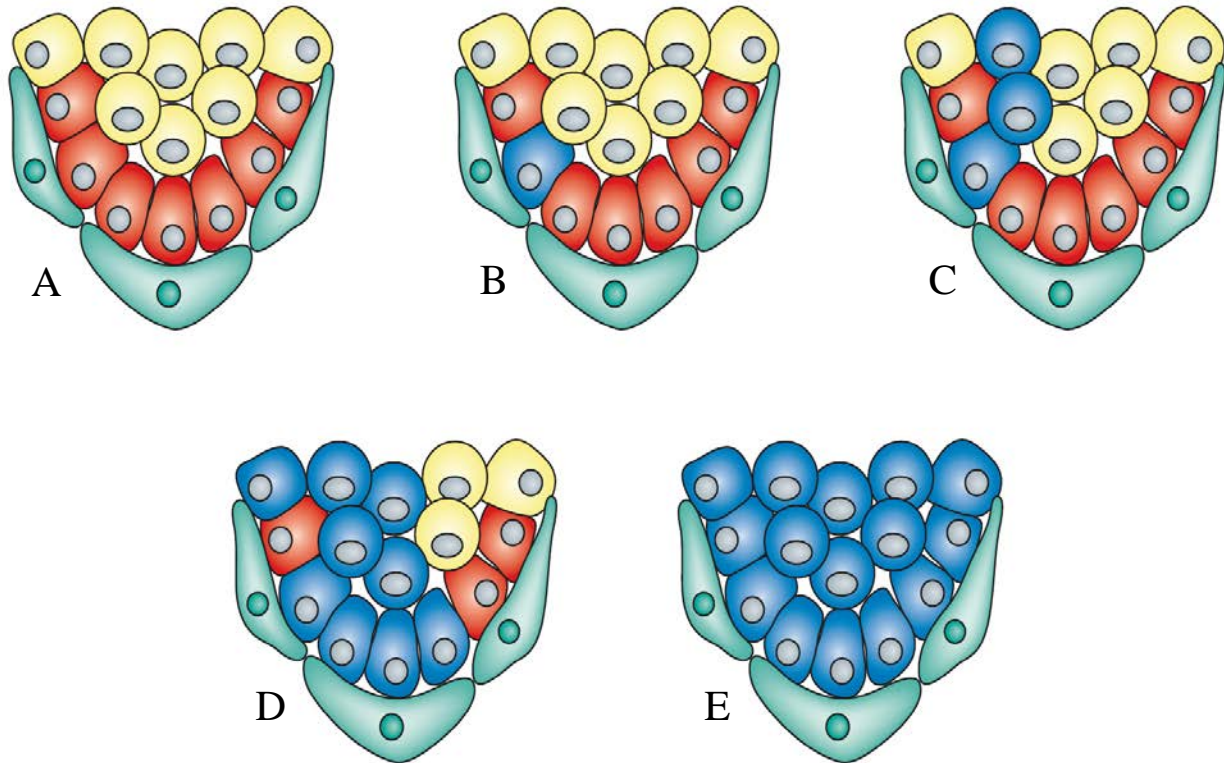


Figure 6. Colonic Epithelial Crypt Domination by a Mutated Stem Cell

(adopted from reference 35)

Figure 6. (A) Colonic epithelial crypt. (B) A stem cell with a fixed mutation (blue) that confers a competitive advantage. (C) The stem cell begins to proliferate. (D) The mutation allows the stem cell to dominate the crypt. (E) All of the clonal cell progeny harbor the mutation.

One of the difficulties in studying colonic epithelial cells is that the majority of the data in the literature focuses on the small intestine. In the small intestine, a stem cell with a mutation that endows a competitive advantage will be more likely to generate self-copies, usurp the dominate stem cell position, and phase out the non-mutated stem cell population⁽³⁰⁾(Figure 6). One example of a mutation that confers a competitive advantage is seen with beta-catenin overexpression or in the regulation of beta-catenin phosphodegradation.⁽³⁰⁾ Even if the chance of the mutated stem cell overtaking the crypt niche increases by only a slight percentage, it still has greater likelihood of usurping the crypt than a normal stem cell.⁽³⁰⁾ The progeny of this mutated stem cell will also harbor the same activated oncogene mutation, or loss of tumor suppressor gene function. While this data is based on research of the small intestine,⁽³⁰⁾ mutated stem cells having an increased probability of dominating crypts in the colon is supported by colonic niche succession studies.⁽³¹⁾

Stem cells are long lived and one crypt will exist in the human colon for an average of 8 years (2.7 to 19 years).⁽³¹⁾ Over time a crypt will deplete its stem cell population until no stem cells remain to propagate new cells needed to replace the differentiated cell turnover in equilibrium. To maintain the colon architecture a crypt must still exist in that location, so a new stem cell niche is created from an adjacent crypt in a process termed niche succession.⁽³¹⁾ A crypt sustained by a stem cell population with an adenomatous polyposis coli (APC) mutation may be retained for an average of 30 years.⁽³¹⁾ The APC mutated stem cells have a competitive advantage that allows them to eventually dominate a stem cell niche, but they also exhibit a prolonged retention time.⁽³⁰⁾⁽³¹⁾ Furthermore, APC mutant crypts are retained longer than normal crypts so an APC mutant stem cell population is likely to be expanded by niche succession.⁽³¹⁾

This will invariably lead to an accumulation of crypts with their entire cell population propagated by APC mutant stem cells.

As colonic epithelial stem cells are readily dividing, an unrepaired DNA adduct could be fixed into a mutation during DNA replication. Stem cells harboring mutations that provide a selective advantage are more likely to dominate a niche and produce progeny. Since colonic stem cells are retained for much longer durations than their lineage differentiated progeny, stem cells represent the most likely cell type of the colonic epithelium to give rise to cells that could manifest as the first cancer cells.⁽²⁹⁾ However, stem cells do not behave independently but are in fact tightly regulated by stem cell niche signaling, and are clearly governed by a different set of parameters than any other epithelial cell type. These include being retained in a set position within the crypt and different parameters for their own turnover and replacement.

1.3.2.6 The Stem Cell Niche

The stem cell niche in any type of tissue is designed to maintain a stem cell population. A stem cell outside of this specialized region will begin lineage differentiation and lose the stem cell defining characteristics. Even a stem cell's gene expression profile diverges greatly from its differentiated progeny.⁽⁶⁾

A stem cell niche is comprised of more cell types than just stem cells, and these cells may or may not contribute to stem cell regulation. In the colonic stem cell niche there are cell types derived from the stem cells as well as; macrophages, dendritic cells, intraepithelial lymphocytes (IELs)⁽³²⁾ and pericryptal cells⁽³³⁾ that all arise from other cell lineages. In the small intestine and colonic crypts, the stem cells are separated by other cells so that the stem cells are not in physical contact with one another⁽²⁵⁾(Figure 7). The colonic stem cells are connected to pericryptal cells on their basolateral border⁽³⁴⁾⁽³⁵⁾(Figure 8). The pericryptal cells connect to the underlining

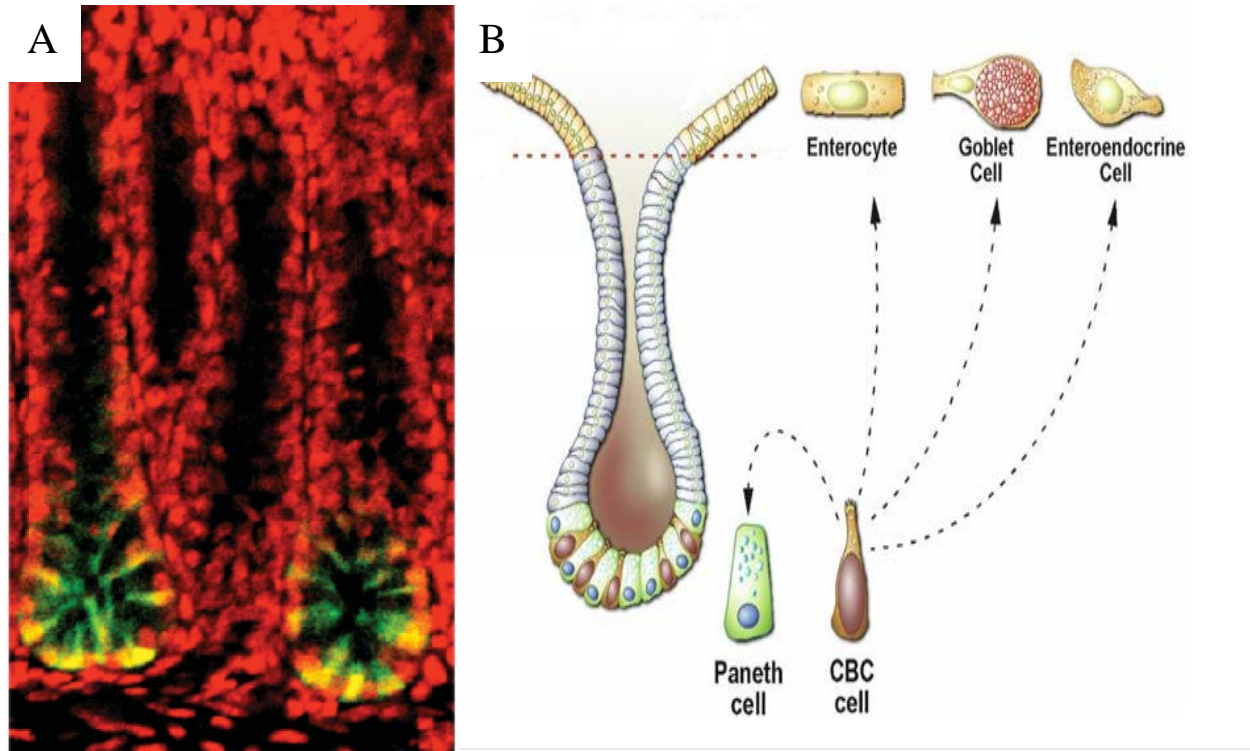


Figure 7. Colonic Epithelial Stem Cells are Separated in the Niche

(adopted from reference 25)

Figure 7. (A) Colonic epithelial stem cells do not border one another in the stem cell niche. This is illustrated by confocal imaging of EGFP in the Lrg5-EGFP-IRES-creERT2 expressing cells. (B) The CBC cells (columnar base cells) represent the Lgr5⁺ expressing stem cells in the small intestine and colon crypts.

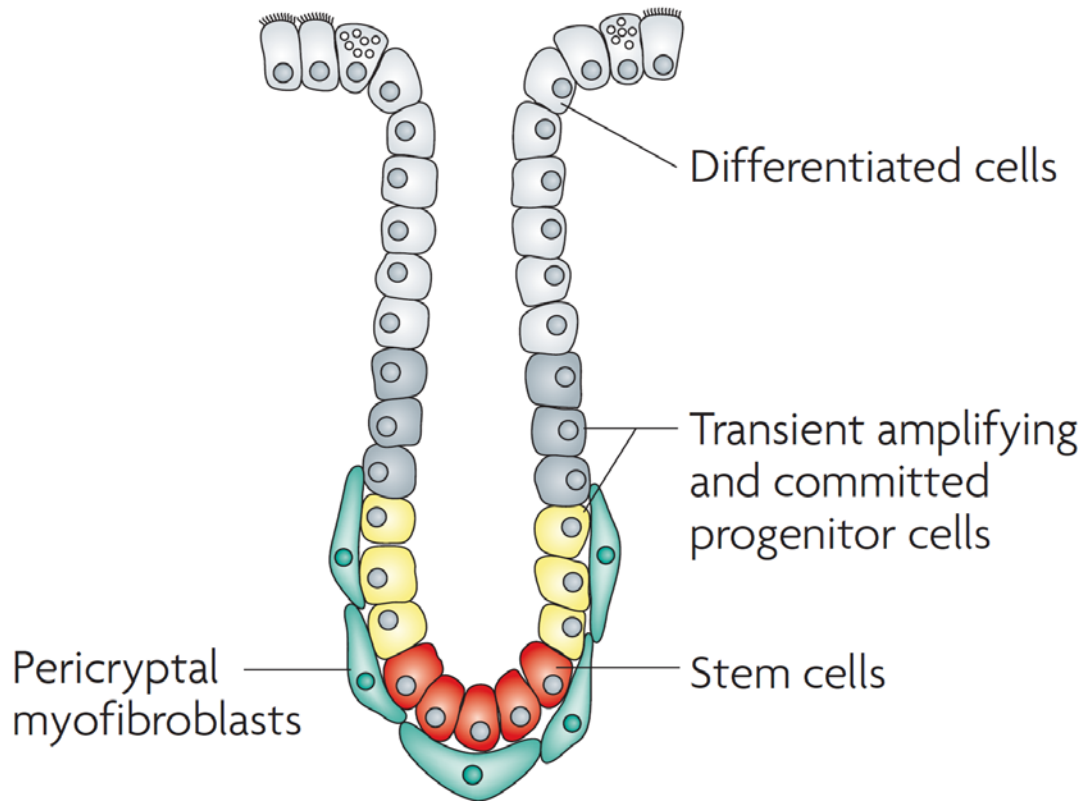


Figure 8. Colonic Epithelial Crypts are Sheathed by Pericryptal Cells

(adopted from reference 35)

Figure 8. Pericryptal cells sheath the colonic crypts starting from the stem cell niche and ascend the crypt. These cells form a bridge for the colonic epithelial cells to the underlying tissue layer. Pericryptal cells actively signal to the stem cell niche and participate in stem cell regulation.

1.3.2.7 Stem Cell Niche Signaling Governs Stem Cell Behavior

Niche signaling governs stem cells and maintains the homeostatic steady-state turnover of colonic crypt cells. Proliferating stem cells are considered to be capable of two types of division, symmetrical and asymmetrical⁽³¹⁾⁽³⁵⁾⁽³⁷⁾⁽³⁸⁾(Figure 9).

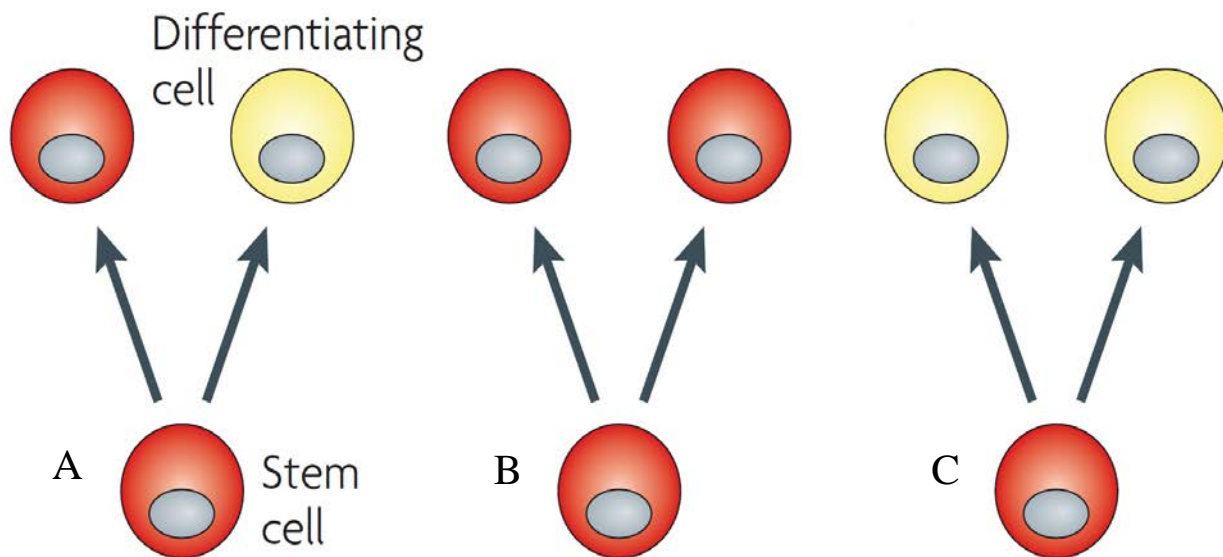


Figure 9. Colonic Epithelial Stem Cell Division

(adopted from reference 35)

Figure 9. Stem cells (RED) are considered to be capable of both (A) asymmetric divisions and (B)(C) symmetric divisions. Asymmetric divisions create one stem cell and one progeny cell (Yellow) to undergo lineage differentiation to maintain the homeostatic epithelial cell turnover. Symmetric division generates 2 stem cells or 2 lineage differentiation cells. Symmetric divisions create more clones of the dominate stem cell or, deletes the dominate stem cell population so a new dominate stem cell can usurp the niche.

Asymmetric stem cell division was first proposed by Dr. John Cairns.⁽³⁷⁾ In an asymmetric division the dominant stem cell divides with one of the new cell copies being retained in the crypt niche (parent cell) and one copy repositioning to undergo lineage differentiation (daughter cell)⁽³⁰⁾⁽³¹⁾⁽³⁵⁾⁽³⁸⁾(Figure 9). Niche signaling determines the lineage differentiation fate of the newly divided cell.⁽⁶⁾ The newly polymerized strands of DNA, that would potentially have fixed a mutation in their genome, may go on to lineage differentiation. Alternatively, the newly polymerized strands of DNA could be retained in the stem cell niche. While it is unknown how asymmetrical division determines the recombination of the DNA strands, the parent stem cell's plasma membrane likely remains anchored in the niche during division, while the daughter cell's plasma membrane moves to the edge of the transit-amplifying compartment. Whether or not this impacts how the DNA recombines remains to be determined, but it is possible that the parent DNA strands are selected for and remain in the parent stem cell.

Symmetrical divisions allow the dominant stem cell to expand its population within the niche by producing replicated copies of itself, copies that are subsequently retained in the niche⁽³¹⁾⁽³⁵⁾⁽³⁸⁾(Figure 9). Alternatively, both copies of the stem cells may proceed to lineage differentiation, allowing the crypt to be usurped by a new dominant stem cell⁽³¹⁾⁽³⁵⁾⁽³⁸⁾(Figure 9). When both copies of the stem cell turnover, it is regarded as an evolutionary adaptation to prevent stem cells that may have fixed mutations from populating a crypt with potential pre-cancer cells,⁽³⁵⁾ or other functionally impaired mutant cells.

For a stem cell to propagate progeny with a fixed mutation it must first undergo cell division having failed to repair DNA damage. The new stem cell clone that harbors a mutation must then assume the dominant position in the niche. In an asymmetric division the original stem cell may harbor the DNA adduct but the daughter cell with the mutation would migrate from the

niche. Therefore, the mutated cell would not remain in a position to usurp the niche. With a symmetric division both the DNA damaged stem cell and the mutated stem cell would be equivalent stem cells. Both stem cells could move to undergo lineage differentiation. Or, both stem cells would be retained in the niche, allowing for the mutant cell to assume the dominate position the niche.

1.3.2.8 The Niche in Question?

What sequence of signals could lead to the survival and proliferation of a stem cell arrested in cell cycle division by DNA damage? Could events such as tissue damage and repair force an arrested stem cell to forego apoptotic induction, bypass unrepaired DNA adducts by recruiting translesion DNA polymerases, and continue to replicate its DNA to complete cell division? Tissue damage and cytotoxicity are accompanied by inflammation. However, it remains unclear if immune cell signaling affects the stem cell niche or would impact the dominate stem cell's survival if it does have damaged DNA.

The cells comprising the colonic stem cell niche are not clearly defined. Consequently, the signaling pathways in the niche are also not defined. In the small intestine, the stem cell niche comprises Paneth cells that separate the stem cells from physically sharing a cell-cell border. In the colon, Paneth cells are rarely expressed and do not constitute a regular part of the colonic crypts. However, as seen in Figure 7, the colonic Lgr5⁺ cells are separated from one another so some cell type occupies the area between the stem cells.

In the small intestine, the stem cell niche is regarded as has having at least two stem cell populations, the Lgr5⁺ expressing cells and the Bmi1 expressing cells.⁽²⁶⁾⁽³⁹⁾ The Bmi1 cells seem to make the Lgr5⁺ stem cells dispensable in the small intestine, as the Lgr5⁺ cells can be depleted and no phenotype is observed.⁽⁴⁰⁾ This has led to the questioning of Lgr5⁺ cells as the intestinal

stem cell population. However, colon crypts lack Bmi1 cells so if Lgr5⁺ cells are not the colonic stem cells then which cells are?⁽³⁹⁾

1.3.2.9 Which Colonic Epithelial Cell is the Potential Cancer Cell?

Colonic stem cells seem to be the only logical cell to be the originating source of cancer cells. Dominant stem cells are undergoing continuous cell division which makes them capable of fixing a mutation into their genome. Stem cells also are retained for extensive periods of time and have unlimited proliferative capability. A dominant stem cell with a mutation could produce an unlimited number of progeny cells harboring that mutation for years, cells that are susceptible to further genetic and epigenetic changes leading to the first cancer cells. Furthermore, stem cells have the support of the stem cell niche to induce cell proliferation, which other colonic epithelial cells lack.

A dominant stem cell forced to arrest cell division due to acquiring DNA lesion damage are likely to be induced to undergo apoptosis.⁽⁴¹⁾ During an inflammatory insult however, an arrested stem cell could potentially be induced to divide and bypass DNA damage as cell turnover rates increase.⁽¹¹⁾⁽¹²⁾ This would make the dominant stem cell(s) susceptible to fixing an oncogenic mutation.

This scenario seems reasonable as it is not known how long a crypt could wait for an arrested stem cell to repair DNA damage and begin renewing the crypt cells under normal conditions. It is also not known how long a crypt could wait for an arrested stem cell under inflammatory conditions. It may be possible that signaling can arise under non-homeostatic conditions which changes a stem cell's rate of division and/or leads to resistance to apoptosis in an effort to keep the stem cell cycling.

Other fully differentiated colonic lineage cells have finite retention times when compared to the stem cells, which can cycle for years. Differentiated cells are readily induced into apoptosis, while stem cells do not turnover by apoptosis but by symmetric cell division under homeostatic conditions. This is a clear indication of the different regulatory parameters of stem cells. Some differentiated epithelial cell types may dedifferentiate *ex vivo*, allowing them to divide and expand their population, but it is not known if this would occur *in vivo*.

Could a dedifferentiated mutant cell divide indefinitely under homeostatic conditions, or would dedifferentiation and clonal expansion be restricted to non-homeostatic conditions? Enterocytes at the edge of a wound dedifferentiate into a motile form and undergo rapid cell cycle division during intestinal wound repair.⁽⁴²⁾ However, all of the dedifferentiated cells mature and turnover rapidly as homeostasis is reestablished,⁽⁴²⁾ making it unlikely their retention time would be sufficient to allow for a cancer cell to manifest.

1.4 INFLAMMATION RELATED COLON CANCER INDUCTION MODEL

1.4.1 Comparative Anatomy of the Human and Mouse Colon

The human and mouse large intestines function in the same capacities that were discussed in section 1.2. The large intestine in both the human and the mouse are comprised of a cecum, colon, and rectum.⁽⁴³⁾ In the mouse the cecum comprises approximately one-third of the large intestine.⁽⁴³⁾ The mouse cecum has a high density of commensal bacteria, and actively ferments solid wastes.⁽⁴³⁾ This contrasts with the human cecum which functions to bridge the small intestine to the colon but lacks an enhanced bacterial presence or functional capacity. The mouse cecum empties into the proximal colon which transitions into the distal colon and then rectum and anus.⁽⁴³⁾ In contrast to the human large intestine, the mouse colon remains a long tube (Figure 10) that parallels the abdominal body cavity beginning behind the liver and running to the anus. The mouse rectum is very short and as a result will easily prolapse when various colonic pathologies occur, including colitis.⁽⁴³⁾

The human and mouse epithelium are comprised of the same layers: mucosa, submucosa, muscularis externa, and serosa,⁽⁴³⁾ discussed in section 1.2.1. Both the human and mouse large intestines are comprised of the same cell types; enterocytes, goblet cells, enteroendocrine cells, and stem cells,⁽⁴³⁾ discussed in section 1.2.2. Both the human and mouse large intestines are colonized by various types of microflora. Immune compromised mice may have protozoal flagellates and ciliates.⁽⁴³⁾ The composition of the microflora can play a role in both ulcerative colitis and carcinogenesis, as discussed in section 1.5.

It is appropriate to question how the data from an experimental model of a pathology will translate to the pathological disease in a human. Can the data generated be of scientific value?

When comparing the large intestines of the mouse and human there are significant similarities in the tissue regions, tissue layers, and epithelial cells. There are also significant differences in the cecum, the shape of the colon, and microflora composition. However, it is feasible that the onset of colitis and colon cancer in the mouse is similar to enough to onset of the diseases in humans to generate data of scientific value.

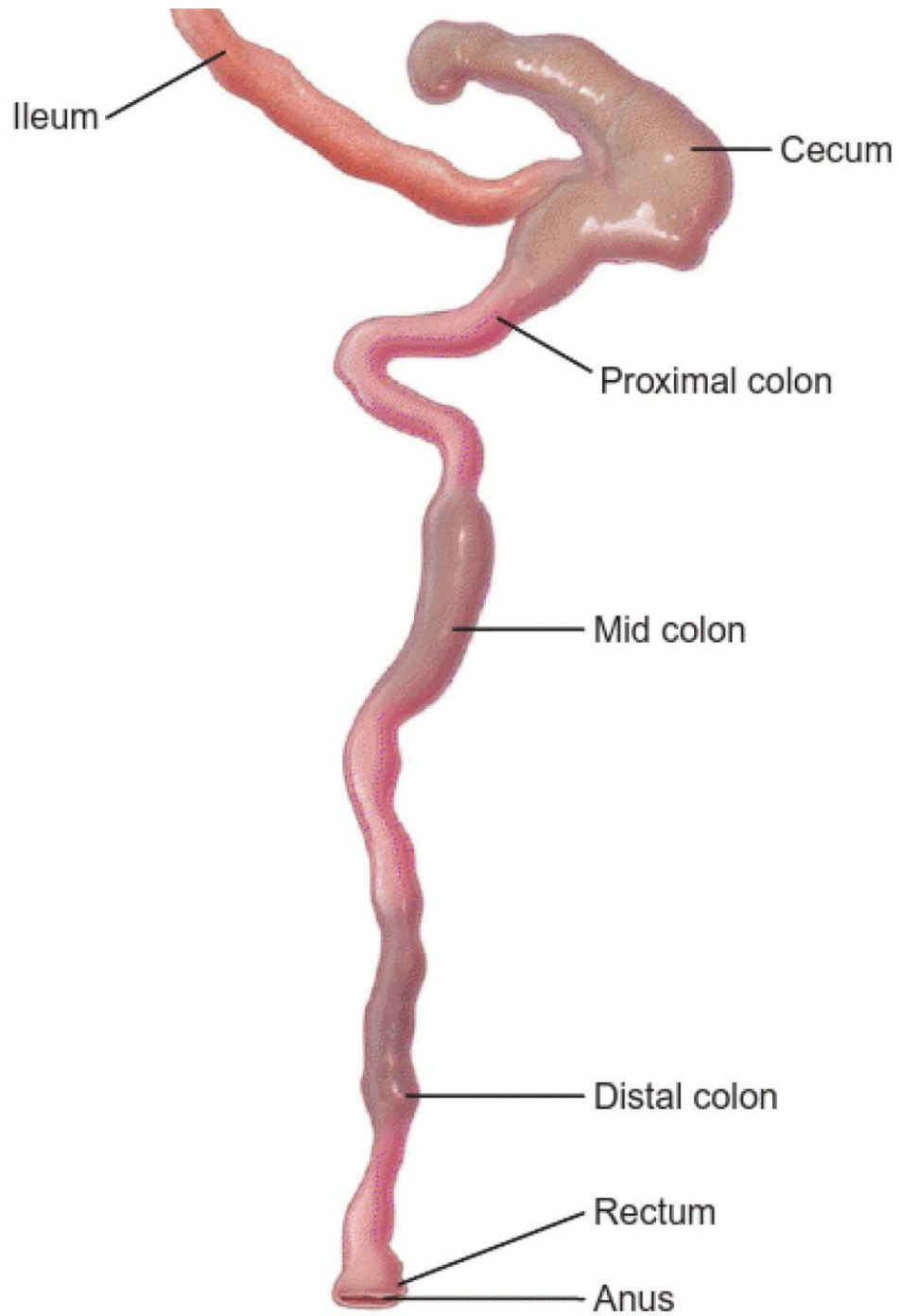


Figure 10. The Mouse Lower Intestine and Comprising Regions

(adopted from reference 43)

1.4.2 A Colon Cancer Inflammation Model

A carcinogenesis animal model that requires two steps via the administration of a mutagen⁽⁴⁴⁾ and an inflammatory agent is referred to as a two-stage carcinogenesis model.⁽⁴⁴⁾ The mutagen may be chemically reactive or metabolized into a chemically reactive form.⁽⁴⁴⁾ The active initiator will react with and damage DNA that results in mutations upon DNA replication.⁽⁴⁴⁾ In contrast, tumor promoters are not directly mutagenic and do not need to react with DNA.⁽⁴⁴⁾ Yet, tumor promoters are strongly associated with the generation of free radicals.⁽⁴⁴⁾ Interestingly, inflammation that results in the generation of reactive oxygen and nitrogen species (RONS) is considered a tumor promoter.

The novel colon cancer induction model developed by Tanaka et. al., utilizes the initiator and promoter concept effectively in the B6 mouse strain that is resistant to carcinogenesis by treatment with an initiating reagent alone.⁽⁴⁵⁾ In the model, azoxymethane (AOM) is the mutagen. One advantage of utilizing AOM is the reagent's organotropism for the colon.⁽⁴⁶⁾ Another advantage of utilizing AOM is that, as a DNA alkylating agent, it causes sporadic mutations, allowing for the study of sporadic colon cancers.⁽⁴⁶⁾⁽⁴⁷⁾⁽⁴⁸⁾ The tumor promoter utilized is dextran sulfate sodium (DSS). DSS recapitulates the onset of human inflammatory bowel disease (IBD).⁽⁴⁶⁾ As previously stated in section 1.1, humans with IBD have a greater risk of developing a CRC than the 1:20 incidence among the general population.

The induction of CRC in mice treated with AOM and DSS is a scientifically accepted model to study the pathogenesis of inflammation related to the development of sporadic colon cancers.⁽⁴⁶⁾ It is reasonable to assume that experimental data derived from this model will impart a greater understanding of the etiology of the disease in humans.

1.5 AZOXYMETHANE

1.5.1 Azoxymethane (AOM) is a DNA Alkylating Reagent

Azoxymethane (AOM) generates DNA lesions that are both cytotoxic and mutagenic. Although cytotoxicity does induce inflammation, the DNA lesions generated by AOM primarily induce apoptosis and not necrotic cell death as will be discussed in this section. Also, the induced inflammation is likely to be rapidly resolved as the cytotoxicity is rapidly reduced within 24h.⁽⁴¹⁾ Through its active metabolic intermediates, AOM methylates DNA. Therefore, AOM is considered a tumor initiator. The chemical structure of AOM is presented in Figure 12. AOM alkylates DNA through an S_N1 substitution reaction.⁽⁴⁹⁾⁽⁵⁰⁾ AOM is a monofunctional alkylating agent in its active form, meaning it contains one active moiety (methyl) that modifies a single site on a nucleobase of a nucleic acid.⁽⁵⁰⁾⁽⁵¹⁾ S_N1-alkylating agents target both ring nitrogens and extracyclic oxygens on the nucleobases.⁽⁵¹⁾

Monofunctional S_N1-alkylating agents primarily generate three DNA adducts, 7-methylguanine (7mG), 3-methyladenine (3mA), and O⁶-methylguanine (O⁶mG)⁽⁵¹⁾(Figure 11). 7mG represents the majority (~60-80%) of the DNA adducts formed by monofunctional S_N1-alkylating agents.⁽⁵²⁾ While 7mG is not cytotoxic or mutagenic,⁽⁵²⁾ spontaneous or enzymatic excision of the methylated guanine results in an abasic site that, if not repaired, is cytotoxic and mutagenic.⁽⁵¹⁾⁽⁵²⁾ 3mA, which accounts for ~10% of DNA adducts formed,⁽⁵¹⁾⁽⁵²⁾ is cytotoxic by disrupting DNA polymerization leading to the induction of apoptosis, or spontaneous depurination can lead to abasic sites.⁽⁵³⁾

O⁶mG, which is formed in ~ 10% yield from AOM, is generated by methylation of the extracyclic oxygen O⁶ of guanine. O⁶mG is potent as both a mutagenic DNA adduct and as a

cytotoxic lesion. The mutagenic effect of O⁶mG arises from the fact that O⁶mG does not arrest DNA replication.⁽⁵⁴⁾⁽⁵⁵⁾ The O⁶mG lesion mismatches with thymine instead of cytosine leading to GC>AT transitional mutations.⁽⁵⁵⁾⁽⁵⁶⁾ O⁶mG is also cytotoxic, as O⁶mG generated mismatched base pairs O⁶mG:T are recognized by enzymatic DNA repair proteins that can induce apoptosis.⁽⁵⁵⁾⁽⁵⁷⁾

It is noteworthy that O⁶mG is only generated in small quantities by monofunctional S_N1-alkylating agents yet O⁶mG is the primary mutagenic lesion in WT DNA repair mice. An example of another monofunctional S_N1-methylating agent being employed as anti-cancer drug is temozolomide.⁽⁵¹⁾ Cancer cell resistance to temozolomide comes from the overexpression of the enzyme that repairs O⁶mG, and from the inactivation of mismatch repair proteins.⁽⁵¹⁾

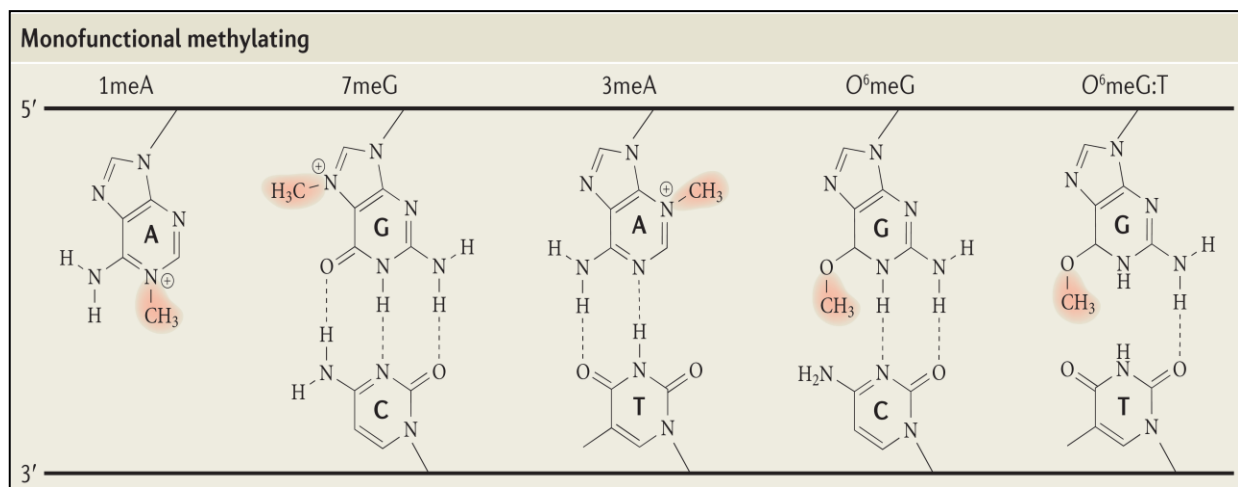


Figure 11. Sites of DNA Methylation by Monofunctional Agents

(adopted from reference 51)

Figure 11. DNA Methylation target sites and the lesions caused by monofunctional S_N1-alkylating agents.

1.5.2 Azoxymethane is a Procarcinogen that is Metabolized into its Active form

AOM, which is itself the metabolite of 1,2-dimethylhydrazine (DMH),⁽⁴⁶⁾ requires metabolic activation to be able to alkylate DNA at nitrogen and extracyclic oxygen atoms.⁽⁴⁶⁾

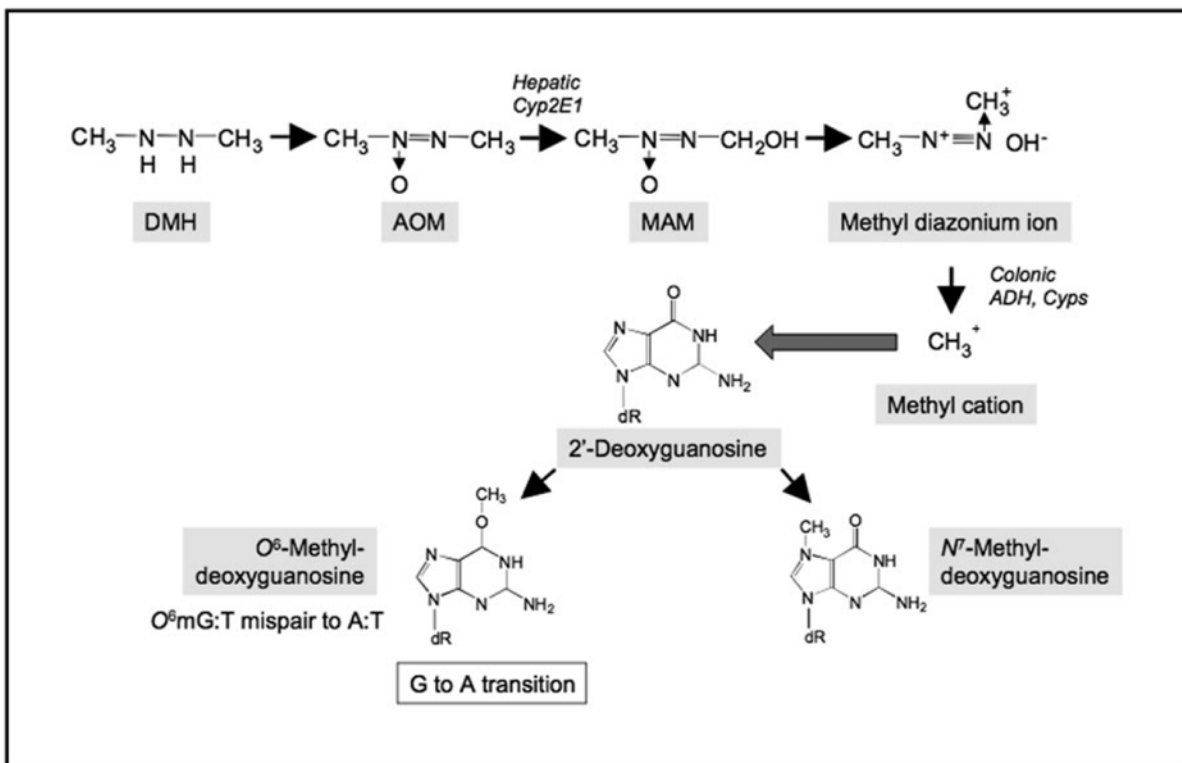


Figure 12. AOM Metabolism into its DNA Alkylating Form

(adopted from reference 46)

Figure 12. AOM, and its precursor DMH, undergo N-oxidation and hydroxylation by CYP2E1 and colonic Aldehyde Dehydrogenase into the DNA reactive methanediazonium ion. This reaction generates the mutagenic O⁶mG DNA adduct.

AOM is metabolized in vivo by the cytochrome P450 CYP2E1 to methylazoxymethanol(MAM)⁽⁵⁸⁾⁽⁵⁹⁾⁽⁶⁰⁾(Figure 12). AOM is prepared in PBS and administered to the mouse via intraperitoneal injection, as discussed in section 5.2. AOM is then absorbed into the bloodstream and perfuses the liver. The AOM permeates into the hepatocytes and once in the hepatocellular cytosol is oxidized and hydrolyzed by CYP2E1 into MAM,⁽⁵⁹⁾ and MAM is exported back into the circulation.

It has been determined in different studies that CYP2E1 is the enzyme most active in metabolizing AOM. Rats treated with disulfiram, a reagent that inhibits CYP2E1 activity, had reduced concentrations of MAM measured in their urine and increased concentrations of unmetabolized AOM measured in their urine and exhaled air when compared to control rats that did not receive disulfiram.⁽⁵⁸⁾ CYP2E1 null 129/SV mice, both male and female, had significantly reduced levels of O⁶mG lesions in their colons and other tissues after treatment with AOM when compared to the WT 129/SV control mice.⁽⁶⁰⁾

1.5.3 AOM displays strong Organotropism

AOM shows significant organotropism for the liver, kidney and colon.⁽⁶⁰⁾⁽⁶¹⁾ The volume of distribution of the AOM metabolite MAM is not known, but significant distribution of MAM to target organs is supported by the level of DNA adducts measured in each tissue.⁽⁶⁰⁾ Since one molecule of MAM potentially generates one adduct via an S_N1 reaction, measuring adduct levels reflects the level of MAM distribution to the various organs of the body. The half-life of MAM is approximately 12 hours, providing time for the MAM to permeate its different target tissues.⁽⁵⁵⁾⁽⁶⁰⁾

Why is the organotropism observed in AOM treatments occurring? One reason that has strong support is that MAM is further metabolized in target organs, such as the colon, due to the expression of aldehyde dehydrogenase (ADH) in those tissues⁽⁴⁶⁾⁽⁶²⁾(Figure 12). MAM is capable of spontaneous degradation to its active methanediazonium ion form, but would need to selectively accumulate in the target organ to alkylate the DNA.⁽⁶³⁾ Schoental suggested that MAM could undergo further metabolism,⁽⁶⁴⁾ and the metabolism of MAM in the target tissue via the expression of a metabolizing enzyme would explain some of the organ specificity.⁽⁶¹⁾

Inhibition of ADH with pyrazole in rats prior to treatment with [¹⁴C]-labeled AOM, decreased exhaled ¹⁴CO₂ and increased urinary excretion of [¹⁴C]MAM when compared to untreated control rats.⁽⁶²⁾ The addition of pyrazole to colonic cytosol homogenate also inhibited ADH activity, which failed to reduce the ADH cofactor NAD⁺ after treatment with pyrazole.⁽⁶²⁾ It is noteworthy that in an ADH^{-/-} null mouse strain showing no activity for ADH in the liver; kidney, lung, and colon, the levels of O⁶mG measured in liver homogenate were not significantly different between the WT and ADH null mice after treatment with methylazoxymethyl acetate (MAMOAc).⁽⁶⁵⁾ This suggests that in the liver there is either spontaneous breakdown of MAM, or other metabolic routes, which lead to O⁶mG adducts.

1.5.4 Colonic stem cells could be more susceptible to AOM derived DNA Alkylation damage than the differentiated epithelial cells

ADH expression could be restricted to the stem cell population in some organs, and ADH has been suggested to be a marker of adult stem cells.⁽⁶⁶⁾⁽⁶⁷⁾ In the colon, the expression of ADH is localized to the very base of the colonic crypts, the location of the stem cell niche.⁽⁶⁷⁾ ADH

expressing cells increased in number and location in colonic adenomas and have been shown to be cancer stem cells.⁽⁶⁷⁾

Colonic stem cells express AHD at detectable levels but differentiated epithelial cells do not. This would suggest colonic stem cells are susceptible to accumulating significantly higher levels of DNA alkylation damage, as a result of the metabolic activation of MAM, than the differentiated cells would be susceptible to. At least some stem cells are undergoing division to support epithelial cell turnover, and rapidly accumulating high levels of DNA adducts could force stem cells to undergo division without arresting the cell cycle in order to repair the adducts.

1.5.5 DNA Repair, Mutagenesis, and Cytotoxicity

Treatment with AOM leads to the generation of three predominant DNA adducts that are biologically significant, as discussed in section 1.4.1 (Figure 11). The quantitatively major lesion, 7mG, is not biologically significant unless it results in a buildup of apurinic sites. Whereas, 3mA and O⁶mG are biologically significant because they are cytotoxic and/or mutagenic.

The 3mA adduct creates a replication block to DNA synthesis.⁽⁵³⁾ The replication blocking effect of 3mA adducts can lead to mutagenesis due to error prone translesion bypass polymerases.⁽⁶⁸⁾ 3mA adducts are repaired by Base Excision Repair (BER) repair, initiated by the enzyme alkyladenine-DNA glycosylase (Aag).⁽⁵³⁾ The adverse effects of 3mA and the resulting BER include; sister chromatid exchange, chromosome aberrations, S-phase arrest, and p53 induction,⁽⁵³⁾ which are all potentially mutagenic or cytotoxic forms of DNA damage.

O⁶mG is biologically significant as a mutagenic DNA lesion. Arguably the most pro-mutagenic lesion formed from AOM. O⁶mG repair can be carried out via at least two enzymatic

DNA repair pathways. The most efficient and desirable way to repair O⁶mG is direct reversal of the lesion. This is accomplished by the demethylation of the methylated extracyclic oxygen of the guanine base by the enzyme O⁶-methylguanine-DNA methyltransferase (MGMT).⁽⁵⁵⁾⁽⁶⁹⁾ MGMT repair is enzymatic, however transferring the methyl group to the cysteine residue in MGMT's active site is irreversible and inactivates the protein.⁽⁶⁹⁾ Hence, it requires one MGMT per O⁶mG lesion to reverse the damage. Thus, the rapid formation of O⁶mG lesions would need to be accompanied by the upregulation of MGMT expression to circumvent the DNA damage. Transgenic mice that have increased expression of MGMT display organ protective effects against AOM induced carcinogenesis, including the colon.⁽⁷⁰⁾⁽⁷¹⁾ While MGMT null B6 mice had significantly higher colon cancer incidence and higher mortality when treated with AOM than WT B6 control mice.⁽⁷²⁾

The O⁶mG lesion does not arrest DNA synthesis, and bypass translesion polymerases frequently generate a mismatched DNA base pairing O⁶mG:T.⁽⁷³⁾⁽⁷⁴⁾ A mismatched DNA base pairing is a substrate for the mismatched DNA repair pathway (MMR). MMR operates through a complex series of interactions and proteins that excise a segment of the newly synthesized DNA strand that contains the T opposite the O⁶mG in the parental strand.⁽⁷⁵⁾

MMR ideally recognizes and reverses O⁶mG:T lesion mispairing,⁽⁷⁶⁾ however MMR proteins do not remove the O⁶mG lesion on the parental DNA strand.⁽⁷⁵⁾ This results in tolerance of the O⁶mG adduct as it is still in the DNA, but is not inducing a mutation or causing cytotoxicity.⁽⁷⁵⁾ However, repeated attempts at repairing the base opposite the O⁶mG lesion results in a futile cycle of repair as the O⁶mG:T pairing is continuously produced by DNA polymerases. This inevitably leads to the accumulation of single-strand DNA gaps, replication

fork collapse, double strand breaks, and chromosomal aberrations,⁽⁵¹⁾ which are all potentially mutagenic or cytotoxic forms of DNA damage.

B6 mice deficient in both MGMT and MMR repair were able to tolerate O⁶mG lesions without experiencing the cytotoxicity and tissue damage observed in MGMT null mice.⁽⁷⁷⁾ However, in the dual repair deficient B6 mice the DNA alkylated cells do not die but instead survive with a high mutation rate. Normal cells can tolerate O⁶mG lesions as long as adequate levels of MGMT are expressed in the cells. However, if MGMT is rapidly exhausted cells become vulnerable to both mutagenesis and cytotoxicity induced by the O⁶mG lesions. Both the upregulation of MGMT and the loss of MMR activity are observed in tumor cells that are resistant to treatment with DNA alkylating agents that generate O⁶mG lesions,⁽⁵¹⁾ as was previously mentioned in section 1.4.1.

1.5.6 Colonic stem cells could be susceptible to O⁶mG induced cytotoxicity and mutagenicity than differentiated epithelial cells

Data reported by Hong et. al. show that MGMT is not constitutively expressed in cells occupying the base of a colonic crypt, including the stem cell niche, in mouse colons stained for MGMT expression after treatment with AOM.⁽⁴¹⁾ In contrast, the fully differentiated cells comprising the luminal edge of the crypt expressed MGMT constitutively before AOM was administered.⁽⁴¹⁾ Over a 12 hour time course, after treatment with AOM, MGMT expression increased in the lower colon crypt region until it reached expression levels equivalent to those in the differentiated cell region.⁽⁴¹⁾ This implies that MGMT expression could be induced by outside signaling, such as immune mediated signaling.

As O⁶mG adduct levels increased in the cells at the base of the crypts, so did the apoptotic index in that region.⁽⁴¹⁾ As MGMT expression levels rose in the cells of the crypt base, the number of apoptotic cells began to decrease.⁽⁴¹⁾ This would indicate that initially O⁶mG lesions are highly cytotoxic to the colonic stem cells due to their low levels of MGMT expression. As discussed in the previous section, direct reversal of O⁶mG lesions by MGMT will enhance cell survival by impeding DNA repair enzymes that initiate apoptosis.

Colonic crypt stem cells and early lineage progenitor cells may already be predisposed to accumulating higher levels of O⁶mG lesions due to the expression of ADH. Without MGMT expression to repair the O⁶mG lesions, the stem cells may be forced to initiate other enzymatic DNA repair pathways, specifically MMR and BER, that readily induce apoptosis. The initial cytotoxicity seen in the stem cells after treatment with AOM could induce signaling that causes an epigenetic expression change in the stem cells. This expression change would be geared toward the survival and continued proliferation of an indispensable cell population.

1.6 DEXTRAN SULFATE SODIUM

1.6.1 Dextran Sulfate Sodium

Dextran Sulfate Sodium (DSS) is a negatively charged sulfated polysaccharide homoglycan of glucose,⁽⁷⁸⁾⁽⁷⁹⁾⁽⁸⁰⁾ produced by the esterification of dextran with chlorosulphonic acid and having approximately two sulphate groups per glucose residue.⁽⁸¹⁾ Dextran is synthesized from sucrose by various bacteria into a complex polysaccharide.⁽⁸²⁾ DSS is comprised of straight and branched polysaccharide chains and is therefore water soluble.⁽⁸⁰⁾⁽⁸³⁾

1.6.2 Treatment with DSS Damages the Colonic Epithelial

Colonic exposure to DSS results in ulcerations, hemorrhage and edema resulting from increased serous fluid swelling, which ultimately decreases or shortens the colon length due to the continuous cycles of tissue repair.⁽⁸³⁾⁽⁸⁴⁾ DSS damage appears primarily superficial to the epithelium, but is capable of damaging the subepithelium and muscularis mucosa as well.⁽⁸³⁾ DSS treatment leads to the rapid onset of acute symptoms that include bloody stools, diarrhea, rectal bleeding and rectal prolapse.⁽⁸³⁾⁽⁸⁴⁾ Chronic symptoms, which are dose-dependent, are weight loss due to a lack of appetite, anemia, rectal prolapse, bacterial infection, colitis, and mortality.⁽⁸³⁾ The duration of the DSS treatment also impacts the severity of the damage. Increasing the concentration and/or the duration of DSS exposure can rapidly change the severity of the symptoms and the mortality observed in the treated mice.

Colonic epithelium changes due to DSS exposure are severe when examined histologically, yet reversible once the DSS exposure ceases. There is a total loss of colonic crypt architecture after 7 days of DSS treatment at both 3% and 5% percent doses⁽⁸⁵⁾⁽⁸⁶⁾(Figure 13). Even at a 1% DSS dose colonic crypts exhibited edema and separate from the muscularis mucosa, and total crypt loss was observed after 7 days of DSS treatment⁽⁸⁶⁾(Figure 13). The duration required to return to homeostasis is significantly shorter at lower DSS concentrations and short treatments, while higher DSS concentrations and longer treatments require much longer intervals to reconstitute the colon tissue.⁽⁸⁹⁾ Histological results also show a massive influx of immune cell populations that included neutrophils, macrophages, and lymphocytes (NK cells, B cells, and T cells).⁽⁸⁵⁾⁽⁸⁶⁾ As will be discussed in the following section, DSS can directly kill immune cells by non-apoptotic pathways. Since this will cause a strong pro-inflammatory

response, many different types of immune cells may influx into the DSS damaged areas of the colon.

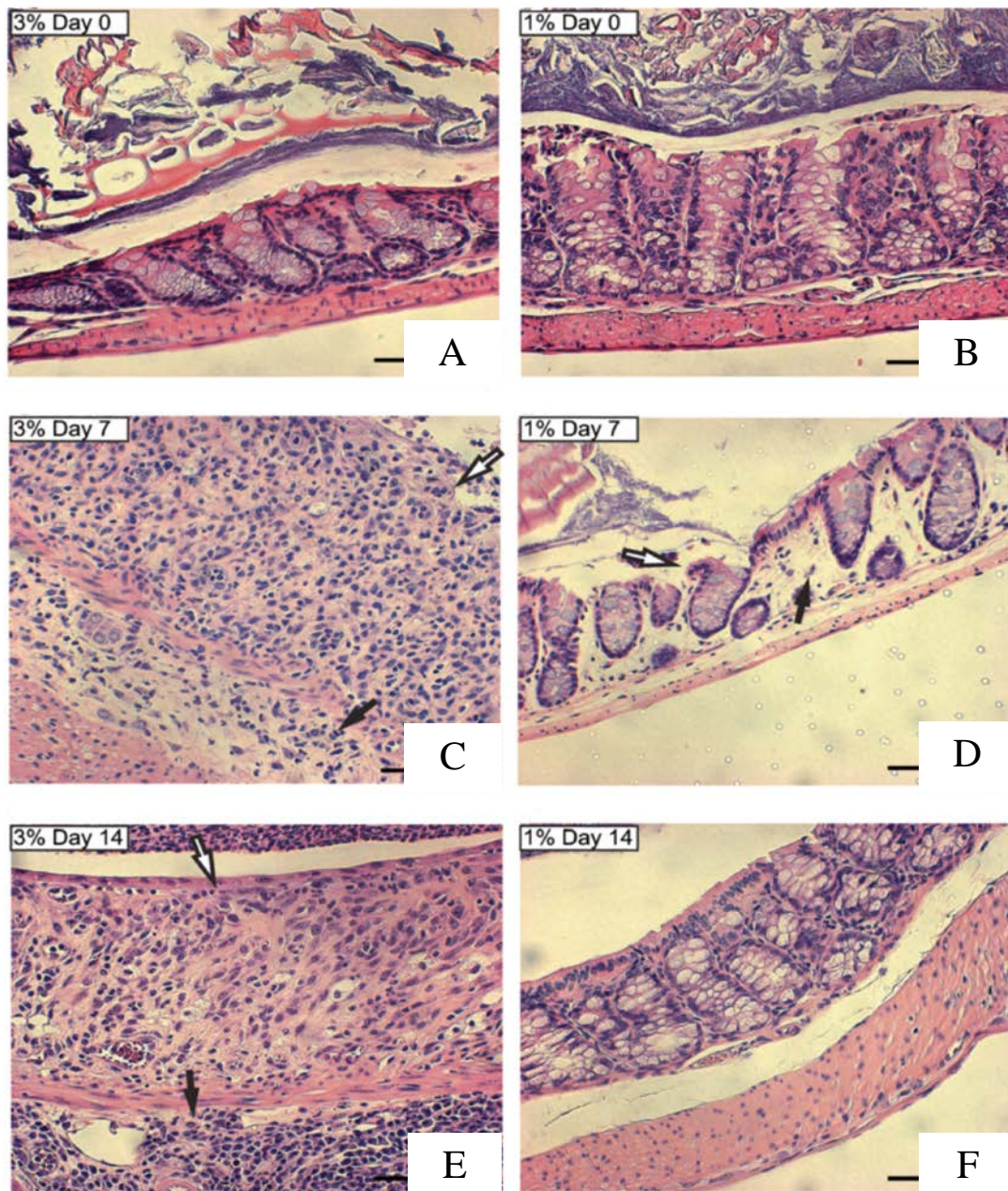


Figure 13. Colonic Epithelial Changes after DSS Treatment

(adopted from reference 142)

Figure 13. (A)(B) Colonic epithelial morphology of WT (B6) mice before DSS treatment. (C) B6 epithelial morphology after 7 days of 3% DSS treatment. (D) B6 epithelial morphology after 7 days of 1% DSS treatment. (E) 7 days after end of the 3% DSS treatment. (F) 7 days after end of the 3% DSS treatment.

1.6.3 DSS initiates Colonic Epithelial Injury and Inflammation

The exact mechanism through which DSS induces injury and initiates inflammation is still undetermined. Preliminary studies with DSS treatment on the colonic mucosa indicated that macrophages are phagocytizing a metachromatic substance detected by toluidine blue staining.⁽⁸⁴⁾⁽⁸⁵⁾ Okayasu et al. showed that colonic macrophages exhibit an altered swollen morphology due to enlarged lysosomes as seen by electron microscopy. Kitajima et al. reported that metachromatic substances were observed after 3 days of DSS treatment in colonic basal pericryptal macrophages, concomitant to the onset of epithelial crypt morphological alterations. If macrophages are undergoing morphological changes, then it is likely they are also undergoing phenotypical changes. Macrophages that have phagocytized DSS molecules are highly likely to be undergoing ischemic cell death, or oncosis,⁽⁸⁷⁾⁽⁸⁸⁾ a form of non-apoptotic cell death. Furthermore DSS exposure depletes colonic tissue resident macrophages and disrupts the maturation and function of infiltrating naïve monocyte populations, the macrophage precursor cells.⁽⁸⁹⁾

If DSS induces macrophage cell death by oncosis, and not apoptosis, then inflammation is being initiated by the detection of non-apoptotic cell death. Oncosis may be partially mediated through intracellular mechanisms, such as PARP activation that depletes intracellular NAD and concomitantly depletes ATP.⁽⁹⁰⁾ While oncosis is a form of programmed cell death, the process differs from apoptosis and autophagy in that oncosis is pro-inflammatory.⁽⁸⁸⁾⁽⁹⁰⁾

The effect of DSS depleting macrophages, and likely other phagocytic cells, leads to immediate deleterious effects. One damaging effect is the disruption of the colonic epithelial cell barrier through the disruption of cell-cell adhesion junctions. Macrophages, dendritic cells, and intraepithelial lymphocytes (IELs) are interspersed throughout the different layers of the

colon.⁽³³⁾⁽⁹¹⁾⁽⁹²⁾ As mentioned previously in section 1.2.2.6, tissue resident myeloid cells and lymphocytes are not derived from colonic stem cells but are of the hematopoietic cell lineage.⁽⁸⁹⁾⁽⁹¹⁾ IELs integrate into the epithelium and form cell-cell adhesions, linking them to the epithelial cells and allowing for direct cell-cell communication.⁽⁹³⁾ Macrophages and dendritic cells localize just below the epithelium in the pericryptal sheath and lamina propria.⁽⁹⁴⁾ Through cell-cell adhesion colonic tissue resident immune cells work with epithelial cells to maintain homeostasis and mediate inflammation.⁽³³⁾⁽⁹¹⁾⁽⁹²⁾⁽⁹⁵⁾ However, tissue resident immune cells do not turnover at the same rate as the epithelial cells.⁽⁹⁶⁾ While data from Penney et al. is based on small intestinal studies, these studies demonstrate the clear differences in cell turnover rates between the two cell lineages.⁽⁹⁶⁾ If a significant depletion in one of the tissue resident immune cell populations occurs, the immune cells will not be renewed at the same rate as the mucosal cells. This will affect the rate at which an inflammatory event can be resolved, tissue repair can be carried out, and colonic homeostasis reestablished.

Treatment with DSS also disrupts epithelial cell tight junction protein expression through the loss of ZO-1 expression.⁽⁹⁷⁾ IELs localize in the epithelium based on their adhesion molecule expression.⁽⁹⁸⁾ It has been demonstrated that DSS treatments disrupted IEL adhesion to epithelial cells, however this finding was based on in vitro studies.⁽⁹⁹⁾ Evidence of the loss of adhesion molecules can also be observed in the histology of DSS induced damage. One of the first changes in the colonic epithelial morphology is the detachment of the base of the colonic crypts from the underlying muscularis mucosa.⁽⁸⁵⁾

A second damaging effect of DSS treatment is the loss of the mucus layer that separates and inhibits bacterial interactions with the colonic epithelium and resident immune cells. Goblet cell numbers were decreased in rat colons in areas of DSS induced colonic ulcers as determined

by histological assessment.⁽¹⁰⁰⁾⁽¹⁰¹⁾ The synthesis of mucus proteins were diminished and numbers of goblet cells devoid of mucus increased with increased duration of epithelium exposure to DSS.⁽¹⁰⁰⁾⁽¹⁰¹⁾ The disruption of mucosal secretions allows the bacteria unimpeded access to physically contact the epithelial cells.⁽¹⁰²⁾ It is noteworthy that a substantial bacterial load is in contact with the colonic epithelium within 12 hours of the onset of DSS treatment.⁽¹⁰²⁾ However, it requires 3 to 5 days before gross symptoms occur and the disruption of epithelial morphology is discernable, and 5 to 7 days for the morbidity to peak.

1.6.4 Inflammation, Bacteria, and RONS

Certain strains of bacteria are tolerated when localized to the exterior surfaces of the body, as their potentially cytotoxic metabolic processes are ameliorated. Mucosal secretion into the lumen is a necessary component of colonic bacterial regulation, as are the tight cell-cell junctions created when colonic epithelial cells link with one another. DSS treatment disrupts this barrier and as a result the colonic microflora are capable of migrating into areas that were previously inaccessible. This leads to the breaking of immune tolerance to the commensal microflora, mediated by the localization of bacteria into the subepithelial region of the epithelium.

The presence of microbiota in both the small intestine and colon does not induce inflammation due to the complex development of natural tolerance. Enterocytes, in particular, play a role in bacterial tolerance. The polarization of enterocyte cells results in two different borders, the luminal brush border and the basolateral border, as discussed in section 1.2.2.2. Both borders express Pattern Recognition Receptors (PPRs) and specifically the PPRs class Toll-like receptors (TLRs).⁽³³⁾⁽⁹⁵⁾⁽¹⁰³⁾ PPRs are the primary initiators of anti-pathogenic responses.⁽¹⁰⁴⁾

Apical brush border PRR signaling is essential to maintaining colonic immune tolerance.⁽³³⁾⁽¹⁰⁵⁾⁽¹⁰⁶⁾ While basolateral PRR signaling initiates inflammatory responses.⁽³³⁾⁽⁹⁵⁾

Once immune tolerance has broken down the tissue resident phagocytic immune cells, the macrophages and dendritic cells, are the first cells to detect and initiate an immune response. PRR activation induces a signaling cascade leading to the activation of various transcription factors,⁽¹⁰⁴⁾ which transcribe the expression of immune mediators that then signal to the infiltrating immune cells.⁽¹⁰⁴⁾

The anti-pathogenic response toward a bacterial infection can be mediated by both innate and adaptive host immune responses. Humoral immune response results in the generation of antibodies by mature B-cells, that specifically bind to epitopes expressed on bacterial cell surface molecules.⁽¹⁰⁷⁾ Antibody binding will impede the bacterial pathogenesis and prime the bacteria to be phagocytized by one of several phagocytic cell types.⁽¹⁰⁷⁾ Humoral immunity is a coordinated response carried out by myeloid and lymphoid immune cells, and is an adaptive immune response due to the targeting of specific bacterial epitopes.⁽¹⁰⁷⁾

Innate antibacterial defense is mediated through immune responses that attack pathogens with non-specific mechanisms. The liver synthesizes proteins capable of directly binding to bacterial cells, such as complement, making them vulnerable to phagocytosis or cytolysis.⁽¹⁰⁸⁾⁽¹⁰⁹⁾⁽¹¹⁰⁾⁽¹¹¹⁾ Phagocytic neutrophils and macrophages express cell surface receptors that capture bacterial cell components, or antibodies and complement covering the bacteria, and ingest them.⁽¹¹⁰⁾⁽¹¹¹⁾⁽¹¹²⁾ Macrophages and neutrophils also secrete antimicrobial peptides and proteases at the site of the infection.⁽¹¹⁰⁾⁽¹¹²⁾ All of these mechanisms attack a broad spectrum of bacterial targets and are not targeting an epitope specific to one strain of bacteria.

Neutrophils and macrophages also generate reactive oxygen and nitrogen species (RONS) to attack bacterial DNA and bacterial cell wall electron transport targets.⁽¹¹⁰⁾⁽¹¹²⁾ Neutrophils and macrophages express enzymes that produce RONS⁽¹¹²⁾⁽¹¹³⁾. These include: (i) NADPH oxidase that oxidizes NADPH to NADP and produces the superoxide radical ($O_2^{\cdot -}$);⁽¹¹⁴⁾ (ii) superoxide dismutase that catalyzes the superoxide radical ($O_2^{\cdot -}$) to molecular oxygen (O_2) and hydrogen peroxide (H_2O_2);⁽¹¹⁵⁾ and (iii) myeloperoxidase that catalyses a reaction between hydrogen peroxide and chloride (Cl^-) to produce the microbicidal hypochlorous acid (HOCl).⁽¹¹⁶⁾

H_2O_2 can freely cross membranes and, therefore, is able to reach phagocytized bacterial targets in lysosomes and extracellular bacterial targets.⁽¹¹⁷⁾ H_2O_2 mediates DNA damage by interacting with intracellular iron to generate neutral hydroxyl radicals ($OH\cdot$) that damage DNA.⁽¹¹⁸⁾⁽¹¹⁹⁾⁽¹²⁰⁾ Myeloperoxidase is transported either intraphagosomally or extracellularly where it catalyses the production of HOCl.⁽¹¹²⁾⁽¹²¹⁾ HOCl chlorinates amines, cytochromes, iron-sulfur proteins, and other vulnerable components of the bacterial cell wall,⁽¹²²⁾⁽¹²³⁾ such as aerobic and anaerobic electron transport systems.⁽¹²³⁾

Nitric Oxide ($NO\cdot$) is a reactive bactericidal molecule produced by inducible Nitric Oxide Synthase (iNOS2).⁽¹²⁴⁾ iNOS2 is a cytokine inducible enzyme that produces $NO\cdot$ by the oxidization of L-arginine.⁽¹²⁴⁾ $NO\cdot$ is capable of diffusing across membranes to directly attack bacterial DNA and other intracellular targets.⁽¹²⁵⁾ $NO\cdot$ molecules may interact with other RONS to mediate attacks on bacterial targets.⁽¹²⁴⁾ One example of this occurs when diffused $NO\cdot$ combines with ($O_2^{\cdot -}$) and generates peroxynitrite ($ONOO^-$),⁽¹²⁶⁾ which occurs without enzymatic catalysation. Modifying RONS and combinations of RONS create a much broader range of

microbicidal activity against many different strains of bacteria.⁽¹²⁴⁾ $\text{NO}\cdot$ and peroxynitrite attack DNA by deaminating nucleobases and generating abasic sites.⁽¹²⁷⁾⁽¹²⁸⁾⁽¹²⁹⁾ Peroxynitrite inactivates bacterial proteins with iron and sulfur clusters.⁽¹³⁰⁾⁽¹³¹⁾ Amino acid residues cysteine and tyrosine are also targets of peroxynitrite mediated damage.⁽¹²⁹⁾

Bacteria have sophisticated mechanisms in place to combat RONS and repair the damage they inflict. Bacteria express various classes of peroxiredoxin enzymes that oxidize a cysteine residue in their active site to sulfenic acid and this enzymatic action reduces peroxides, specifically H_2O_2 into 2 H_2O molecules.⁽¹³²⁾⁽¹³³⁾ The active site is then reset by the reduction of other proteins or molecules, depending on the peroxiredoxin's class.⁽¹³²⁾ Class II peroxiredoxins restore their active site by reducing thiols, primarily glutathione.⁽¹³²⁾ Bacteria express various classes of catalases that rapidly degrade H_2O_2 into 2 $\text{H}_2\text{O} + \text{O}_2$.⁽¹³⁴⁾⁽¹³⁵⁾ Bacteria also express superoxide dismutases that scavenge ($\text{O}_2\cdot^-$) and convert it into H_2O_2 .⁽¹³⁶⁾ Superoxide dismutases activity increases the H_2O_2 levels that the bacteria are exposed to, but decrease the level of ($\text{O}_2\cdot^-$). This strategy relies on catalases and peroxiredoxins to metabolize the H_2O_2 into water. Depleting ($\text{O}_2\cdot^-$) also prevents the generation of other RONS, primarily peroxynitrite.⁽¹³⁶⁾ Bacterial expression of glutathione and similar enzymes mitigate $\text{NO}\cdot$ mediated damage.⁽¹²⁴⁾ Bacteria that express high concentrations of glutathione are resistant to $\text{NO}\cdot$ derived damage when compared to bacteria expressing low levels of glutathione.⁽¹²⁴⁾

Bacteria mitigating the effects of RONS also involve enzymatic DNA repair pathways. MGMT is conserved from bacteria to humans, reversing the O^6mG lesion.⁽¹³⁷⁾ The BER pathway is essential for bacteria to reverse $\text{NO}\cdot$ derived deamination damage.⁽¹³⁸⁾ To overcome the many defenses employed by bacteria that counteract RONS, it is necessary for host phagocytic cells to

generate RONS species in massive amounts. The caveat to producing elevated levels of RONS is that this makes normal host cells at the site of the inflammation vulnerable to the same damage that is intended to eliminate the infectious bacteria.

1.6.5 Bacterial Inflammation Induced by DSS Treatment Modulates Carcinogenesis

As discussed in section 1.3.2., tumor promoters do not directly damage DNA or result in mutations, but they induce inflammation and specifically induce RONS.⁽⁴⁴⁾ The effect of DSS treatment seems to generate two inflammatory immune events. The DSS itself causes a severe disruption of the colonic epithelium, leading to the localization of commensal bacteria into the subepithelial breaking natural tolerance. This then forces the initiation of an antibacterial immune response and delays the repair of the epithelium.

Since dextran is a bacterial derived polymer of glucose, it is reasonable that it would be detectable by one of the many phagocytic cell's surface receptors. Also, DSS only promotes colonic carcinogenesis when mice are treated with a selective molecular weight range of the polymer, 36kD-50kD.⁽¹³⁹⁾ Other molecular weights of the DSS polymer only induce mild inflammation or no inflammation in the colon.⁽¹³⁹⁾ DSS may interact with bacterially synthesized fermentation products that configure the dextran polymers into an inflammation initiating structure.⁽¹⁴⁰⁾

Why does DSS induce oncosis in tissue resident phagocytes that disrupts the colonic epithelium? Why does mucus secretion decrease after DSS exposure? The pathogenic effect of DSS on the colonic epithelium develops independently of the commensal microflora, however the effect of DSS treatment on the development of colitis and carcinogenesis is not independent of the microbiota. Innate

Treatment of germ-free mice with DSS drastically enhances the effect of the DSS. Germ-free IQI/Jic mice treated with 5% DSS experienced a severe pathology that lead to mortality, while conventional mice were able to tolerate the 5% DSS treatment.⁽¹⁴¹⁾ Yet, no evidence of colitis was seen in the histology of the colonic epithelium in the mice that died.⁽¹⁴¹⁾ A 1% DSS dose was tolerated by both germ-free and conventional mice, yet the germ-free animals developed severe colitis 14 days after the DSS treatment ended.⁽¹⁴¹⁾ As previously described in section 1.5.2., DSS treatment has a pronounced dose effect. Apparently, the presence of colonic bacteria ameliorate the DSS treatment in a protective manner. Rose et al., in an experiment not considering bacterial composition, reported that 7 days after a 1% DSS treatment had ended in WT B6 mice the colon had completely recovered from the DSS treatment.⁽¹⁴²⁾ This finding contrasts with the results of the Kitajima et. al. study. Maslowski et. al. reported exacerbated DSS induced inflammation in germ-free B6 mice at 4% DSS treatment.⁽¹⁴³⁾ Interestingly, this outcome was ameliorated by reintroducing gut microbiota from conventional mice to the germ-free mice.⁽¹⁴³⁾

One of the common pathologies seen in human patients with IBD is the dysbiosis of the commensal flora.⁽¹⁴⁴⁾ Microbial dysbiosis resulting from DSS treatment may exacerbate the loss of natural tolerance for commensal flora. Microbial dysbiosis is also likely to prevent the reestablishment of natural tolerance, prolonging the antibacterial proinflammatory response. Bacterially fermented short chain fatty acids (SCFAs) are physiological signaling molecules to various cell receptors.⁽¹⁴⁵⁾⁽¹⁴⁶⁾ SCFA signals are capable of modulating anti-inflammatory immune cells and their functions, including inducing Il-10 expression.⁽¹⁴⁷⁾⁽¹⁴⁸⁾ Dysregulating the normal SCFA expression could partially explain the chronic inflammation in colitis morbidity.

While the presence and composition of commensal microflora can ameliorate DSS damage, defining the effect on cancer promotion is obscure. Specific pathogen free B6 mice treated with antibiotics prior to the induction of colon carcinogenesis with an AOM+DSS treatment were resistant to tumor development as compared to the WT control mice.⁽¹⁴⁹⁾ However, germ-free B6 mice had a much higher tumor multiplicity and more extensive tumor growth in comparison to specific pathogen free B6 mice after AOM+DSS treatment.⁽¹⁵⁰⁾

Il-10^{-/-} B6 mice develop colitis spontaneously without DSS treatment.⁽¹⁵¹⁾ If treated with AOM, the Il-10^{-/-} B6 mice develop colon tumors.⁽¹⁵²⁾ However, germ-free Il-10^{-/-} B6 mice do not develop colitis or any other immune response.⁽¹⁵¹⁾ Therefore, germ-free Il-10^{-/-} B6 mice can be reconstituted with a specific bacterial flora and then treated with AOM, to determine the tumor initiating effect of a bacterial strain.⁽¹⁵²⁾

The tumor promoting activity of reagents such as DSS is strongly associated with the generation of RONS. It is assumed the RONS resulting from DSS treatment is generated purely as a bactericidal innate immune response. The inadvertent RONS mediated damage to the epithelial cells, that causes mutagenic DNA damage and cytotoxicity, is what is thought to potentiate cancer development. However, the cancer potentiation associated with RONS could actually be the result of the physiological signaling that these small molecules mediate.

A study by Ahmad et. al., showed that the expression of multiple cytokines/chemokines were upregulated in WT B6 mice treated with DSS.⁽³⁸³⁾ The investigators reported that the expression of iNOS in macrophages supported that these cells were polarized into their pro-inflammatory M1 phenotype (discussed in section 3.1).⁽²⁸⁸⁾⁽³⁸³⁾ The results support the involvement of the innate immune cells in generating significantly high levels of RONS. Interestingly, the caludin-2 overexpressing transgenic mice in the study by Ahmed, et. al. were

resistant to DSS induced inflammation and showed increased anti-inflammatory adaptive immune Treg cell activity (discussed in section 3.1).⁽³²⁰⁾⁽³²¹⁾⁽³²²⁾⁽³²³⁾⁽³⁸³⁾ While these investigators identify iNOS as pro-inflammatory, NO[•] is capable of regulating the expression of immune mediators that produce both pro and anti-inflammatory effects.⁽¹⁵³⁾⁽¹⁵⁴⁾⁽¹⁵⁵⁾⁽¹⁵⁶⁾⁽¹⁵⁷⁾⁽¹⁵⁸⁾

Beyond the inducible isoforms of NOS, there are several constitutively expressed isoforms found in various tissues, which generate NO[•] involved in signaling pathways that maintain tissue homeostasis.⁽¹⁵⁶⁾ The concentration of RONS in an inflammatory environment impacts how signals are transduced, with high RONS concentrations shifting immune cells toward anti-inflammatory functions.⁽¹⁵⁷⁾⁽¹⁵⁸⁾ NO[•] signaling plays a role in regulating the expression of anti-inflammatory cytokines IL-4, IL-13, TGF-beta, and IL-10.⁽¹⁵⁸⁾ Surgical lacerations in the abdomen of female Balb/c mice treated with a NOS inhibitor exhibit aberrant and delayed wound contraction and repair when compared to the lacerations made in the untreated control mice.⁽¹⁵⁹⁾ The role of RONS in tumor promotion cannot be simply be attributed to cytotoxicity and the potential mutagenic DNA damage resulting from high concentrations of RONS generated to eliminate bacteria.

1.7 AOM+DSS

1.7.1 The Genetic Background of a Mouse Strain Modulates the Strains Response to AOM Treatment alone or combine with DSS Treatment

Different strains of mice exhibit different susceptibilities to colon cancer initiation with AOM treatment. Treating some mouse strains with several doses of AOM will induce colon cancer

development.⁽¹⁶⁰⁾⁽¹⁶¹⁾⁽¹⁶²⁾ In these mouse strains AOM acts as complete carcinogen.⁽⁴⁴⁾ In a study treating various strains of mice with the same AOM dosing regimen, the mice were classified as highly susceptible, moderately susceptible, and resistant.⁽¹⁶⁰⁾ With resistant mouse strains not developing tumors after the same AOM treatment.⁽¹⁶⁰⁾ Balb/c mice are moderately susceptible to AOM induced colon cancer, while B6 mice are resistant when treated with the same AOM dosing regimen.

Mouse strain's exhibit different susceptibility to AOM treatment.⁽¹⁶³⁾ Therefore knowing a mouse strain's susceptibility is crucial to utilizing either AOM or AOM+DSS for the colon cancer induction treatment. Most animal studies require a transgenic or a gene knockout animal,⁽¹⁶³⁾ and many gene knockouts are only available in the B6 background. The B6 mouse strain is resistant to colon cancer induction with AOM treatment.⁽¹⁶³⁾ However, while B6 mice are resistant to AOM treatments used to induce colon cancer they are susceptible to a combined treatment of AOM+DSS.⁽¹⁶⁴⁾

It is not understood why some genetic backgrounds of the inbred mouse strains are resistant to AOM treatments to induce colon tumors. Cross breeding a resistant mouse strain with moderately susceptible strain will lead to an increased susceptibility to AOM treatments in the hybrid mouse strain compared to the resistant background strain.⁽¹⁶²⁾⁽¹⁶⁵⁾ This implies a genetic component to the resistance in some mouse strains, and the resistance may not be a dominate genetic factor.

It is also unclear why mouse strains resistant to AOM treatments used to induce colon cancer are susceptible to a combined AOM+DSS treatment. Strain differences have also been observed in response to AOM+DSS treatments.⁽¹⁶⁴⁾ Balb/c mice show an increased incidence and significantly greater tumor multiplicity after a AOM+DSS treatment in comparison to B6

mice.⁽¹⁶⁴⁾ However, it is unlikely the strain differences to AOM or AOM+DSS treatments are due to differences in commensal flora. As different studies with animals purchased from different suppliers and housed in different facilities still report the same resistance and susceptibility in the various mouse strains.

1.7.2 AOM Treatment must be closely followed by Treatment with DSS to Induce Colon Cancer

The order in which the tumor initiator and promoter are administered is critical to the efficacy of model. Mice must be treated with one AOM dose followed within a few days by a DSS treatment to induce colon cancer.⁽⁴⁵⁾ A commonly employed effective timecourse for an AOM+DSS treatment is to dose the mice with AOM and wait for one week, then treat the mice with DSS for 5 to 7 days. Treating mice with AOM in the middle of a DSS treatment yields a very low tumor incidence,⁽⁴⁵⁾ well below the incidence observed when the reagents are administered in the optimal order. Mice treated with DSS and then treated with AOM, either one day or one week after the DSS treatment ends, did not develop colon tumors.⁽⁴⁵⁾ Mice treated with one dose of AOM do not have any incidence of colon tumors.⁽⁴⁵⁾ Mice treated with one week of DSS do not develop colon tumors.⁽⁴⁵⁾

1.7.3 Basic research questions

Why is the order of the AOM+DSS treatment and timecourse so inflexible to effectively induce colon cancer in mice? This could imply two separate effects of the mutagen and the inflammatory promoter, effects that must follow one another. Tumor promoters are not

mutagenic, yet the cancer promoting effect of DSS treatment is commonly associated with inadvertent cytotoxicity and mutagenesis resulting from RONS generated in response to bacterial infection. Is the DSS acting as a mutagen in a similar manner to the AOM and, if it does, then why is the AOM necessary for the models efficacy?

The immune system response to AOM+DSS treatment factors into every aspect of the model. The AOM treatment leads to apoptosis, and likely necrotic cell death, and then tissue repair to counter the sudden and rapid loss of colonic epithelial cells. Tissue damage from DSS treatment is likely initiated by depleting tissue resident macrophages, and involves immune cells from initiation until resolution, while promoting cancer development through an unknown interplay of cellular signaling and responses. Do immune cells impede or enhance carcinogenesis? Which immune cells could be involved in mediating the promotion of cancer?

The AOM+DSS model of colon cancer induction is utilized exclusively as a combine treatment in experimental studies. We will attempt to break the model into its individual components to assess the effect of each agent on the colonic epithelium and colon cancer development. We will also attempt to dissect the role of the immune response as either a source of mutations, or cell mediated pro-survival signaling, that would circumvent apoptotic induction. This would inadvertently lead to the survival of stem cells with mutations, that are capable of producing a population of cells that potentially would develop into cancer.

2.0 MUTAGENESIS STUDY

2.1 SCOPE AND SYNOPSIS

Chapter 2 presents the results and discussion of the mutagenesis study. The chapter is divided into three sections. The first section is an introduction to the study and provides new material that supports the relevance of the basic research questions and concludes by clearly stating the basic research aim and an overview of the experimental method. The second section of Chapter 2 outlines the significance of the study, the experimental design, the important details of the enzyme histochemistry assay and the statistical analyses. The experimental data and results tables are then presented. The third section presents a summary of the experimental results and then a discussion of those results, including possible explanations and interpretations.

2.2 INTRODUCTION

Elucidation of the etiology of human colon cancer remains a difficult challenge facing medical science. Certain colon cancer cases are the result of an inheritable genetic risk factor, and the most well characterized of these is familial adenomatous polyposis (FAP).⁽¹⁶⁶⁾ FAP is the result of an adenomatous polyposis coli (APC) mutation in the Wnt signaling pathway that regulates the phosphodegradation of the transcription factor beta-catenin.⁽¹⁶⁷⁾ However, hereditary colon

cancer cases represent approximately 5% of the total number of colon cancer cases,⁽¹⁶⁶⁾ while the vast majority are sporadic cancer cases. A tissue associated chronic inflammatory disease significantly increases an individual's chances for developing cancer.⁽¹⁾ The onset of the chronic inflammatory disease ulcerative colitis is a high risk factor for developing a sporadic colon cancer.⁽¹⁾

In well characterized two-stage models of cancer induction, both in the skin and intestinal epithelium, treatment with an inflammatory agent is required to potentiate cancer development.⁽⁴⁴⁾ It is unclear exactly how inflammation potentiates cancer development, but tumor promoting reagents induce the expression of radical oxygen and nitrogen species (RONS) from phagocytic immune cells.⁽⁴⁴⁾⁽¹¹²⁾ A commonly employed two-stage colon cancer induction model treats mice with azoxymethane (AOM),⁽⁴⁵⁾ a reagent that acts as the mutagenic tumor initiator,⁽⁴⁴⁾ and dextran sulfate sodium(DSS) which induces acute and chronic colonic inflammation.⁽⁴⁴⁾⁽⁴⁵⁾

Treatment with AOM is mutagenic and cytotoxic as a result of creating substantial DNA alkylation damage,⁽⁴⁹⁾⁽⁵⁰⁾⁽⁵¹⁾ as discussed in section 1.4. AOM is metabolized by enzymes into its DNA alkylating active metabolite⁽⁵⁸⁾⁽⁶⁰⁾⁽⁶¹⁾⁽⁶²⁾(Figure 12). The primary mutagenic DNA alkylation lesion generated by an AOM treatment is O⁶-methylguanine (O⁶mG)⁽⁵¹⁾⁽⁵⁵⁾⁽⁵⁶⁾(Figure 11). DNA lesions generated by AOM are cytotoxic by blocking DNA replication that induces apoptosis.⁽⁵¹⁾⁽⁵²⁾⁽⁵³⁾

AOM can both initiate and promote colon cancer in some inbred mouse strains,⁽¹⁶⁰⁾⁽¹⁶¹⁾⁽¹⁶²⁾ acting as a complete carcinogen,⁽⁴⁴⁾ as discussed in section 1.6.1. While other inbred strains of mice are resistant to AOM treatment as a complete carcinogen.⁽¹⁶³⁾ The susceptibility or resistance seen to AOM treatments acting as a carcinogen highlights how significantly the

different inbred mouse strains vary genetically. AOM is desirable to utilize as a sporadic colon cancer initiator for its ease of administration, for the reproducibility of AOM treatments, and its colon specific organotropism.

To conduct a sporadic colon cancer study utilizing the B6 inbred mouse strain and employing AOM as the mutagenic initiator requires that the mice are treated with DSS,⁽¹⁶⁴⁾⁽¹⁶⁷⁾ as the mice of the B6 genetic background are resistant to treatment with AOM alone.⁽¹⁶³⁾ The adverse effects of DSS treatments on mice are discussed in section 1.5. DSS treatments are easily administered and the outcomes of the treatments are reproducible, once the dosing has been optimized to account for strain related morbidity and possible mortality.⁽¹⁶⁷⁾

AOM+DSS treatment renders B6 mice susceptible to colon cancer induction, circumventing the B6 strain resistance to AOM treatments. So long as the mice are treated with AOM first, followed shortly afterward by the DSS treatment in a very precise timecourse⁽⁴⁵⁾ as discussed in section 1.6.2. Treatment with DSS leads to the onset of inflammation and colitis in mice, with a very similar pathology to colitis morbidity in humans as determined by histological assessment.⁽⁸⁴⁾

What is the role of inflammation as a tumor potentiating mechanism? DSS initiates inflammation and colon mucosal damage by inducing cell mediated oncosis in colon tissue resident macrophages,⁽⁸⁴⁾⁽⁸⁵⁾⁽⁸⁷⁾⁽⁸⁸⁾ as discussed in section 1.5.3. Through this effect DSS treatments disrupt cell-cell tight junction adhesion proteins that link epithelial cells together and to the tissue resident immune cell populations integrated into the epithelium.⁽⁹⁷⁾⁽⁹⁸⁾⁽⁹⁹⁾ By disrupting the mucosal barrier commensal microflora are subsequently freed to migrate into the underlying mucosal regions that were previously inaccessible, breaking the natural tolerance that was established with the microbiota.⁽³³⁾⁽⁹³⁾⁽⁹⁵⁾ The proinflammatory signaling caused by the

apoptosis of tissue resident macrophages following their uptake of DSS molecules,⁽⁸⁴⁾⁽⁸⁵⁾⁽⁸⁸⁾⁽⁹⁰⁾ and the basolateral detection of bacteria by enterocytes through toll-like receptors in the subepithelial regions of the colon,⁽⁸⁸⁾⁽⁹⁰⁾ engages the immune system response.

The initiation of the innate anti-bacterial immune response will cause an influx of myeloid lineage phagocytic cells,⁽¹¹⁰⁾ as discussed in section 1.5.4. Monocytes, which are the myeloid lineage precursors of macrophages and dendritic cells, and neutrophils express enzymes specifically to generate RONS intended to attack bacterial DNA and bacterial cell wall electron transport targets.⁽¹¹⁰⁾ Among the most important bactericidal RONS are; the superoxide radical ($O_2^{\cdot-}$), hydrogen peroxide (H_2O_2), nitric oxide ($NO\cdot$), and peroxynitrite ($ONOO^-$), which is a spontaneous non-enzymatic combination of ($O_2^{\cdot-}$) and $NO\cdot$.⁽¹¹⁴⁾⁽¹¹⁵⁾⁽¹²⁴⁾⁽¹²⁶⁾ These small molecules diffuse across non-polar plasma membranes and attack intracellular bacterial DNA and proteins and also target cell wall aerobic and anaerobic respiratory proteins.⁽¹¹⁷⁾⁽¹²⁵⁾⁽¹²⁹⁾⁽¹³⁰⁾ Innate antimicrobial responses to bacterial infections produce high concentrations of RONS to eliminate the pathogens, placing normal healthy cells near the inflammatory environment at risk of exposure to significantly elevated levels of RONS.⁽¹⁶⁸⁾ Colonic epithelial cells are placed in exactly that scenario after DSS treatment is initiated.

All aerobic organisms are exposed to endogenously generated intracellular RONS.⁽¹⁶⁸⁾⁽¹⁶⁹⁾ In mammalian cells, reactive oxygen species (ROS) are produced mainly in the mitochondria as a result of the normal metabolism of cellular oxygen.⁽¹⁷⁰⁾⁽¹⁷¹⁾ $NO\cdot$ is also produced in mitochondria and, therefore, so is endogenous peroxynitrite.⁽¹⁷²⁾⁽¹⁷³⁾ Mammalian cells eliminate intracellular RONS by multiple antioxidant mechanisms, and these mechanisms maintain a homeostatic balance with the endogenously generated RONS levels to prevent cellular damage.⁽¹⁷⁴⁾⁽¹⁷⁵⁾ Mammalian cells express catalases, peroxiredoxins, and super oxide dismutases,

as well as other antioxidant enzymes to eliminate RONS.⁽¹⁷⁶⁾⁽¹⁷⁷⁾ The enzyme functions have been conserved from the bacterial isoforms of the enzymes, the antioxidant enzyme mechanisms of action are discussed in section 1.5.4.

Oxidative stress is a term used to describe a state in which the intracellular RONS levels exceed a mammalian cell's ability to detoxify the RONS. Excessive H₂O₂ damages DNA by reacting with intracellular iron to generate neutral hydroxyl radicals (OH·), which then reacts with purine and pyrimidine bases.⁽¹⁷⁸⁾ In vitro, at least 20 oxidized DNA bases have been identified,⁽¹⁶⁸⁾⁽¹⁶⁹⁾ although some may not occur in vivo. Of these oxidation lesions, 8-oxoguanine (8-hydroxyguanine) is considered highly significant, and measuring 8-oxoguanine levels is used as a marker of the overall ROS damage occurring in a tissue.⁽¹⁶⁸⁾⁽¹⁷⁸⁾ Unrepaired 8-oxoguanine lesions are mutagenic by creating G>T and A>C nucleobase transversions.⁽¹⁷⁹⁾ 8-oxoguanine is also mutagenic at the site of the lesion as polymerases insert adenine and not cytosine in the newly polymerized DNA strand opposite the lesion.⁽¹⁸⁰⁾ Reactive nitrogen species (RNS) arising from NO· modifications deaminate DNA bases causing abasic sites and DNA strand breaks.⁽¹⁸¹⁾⁽¹⁸²⁾ The subsequent polymerase detection of this DNA damage activates enzymatic DNA repair that can induce apoptosis.

Proteins are also targets of RONS mediated damage and can act as indirect mutagenic agents. Amino acids, both free and incorporated into proteins, are targets of oxidative damage.⁽¹⁸³⁾ RONS oxidized DNA polymerases can have diminished fidelity for incorporating the correct DNA bases into a newly polymerized DNA strand and create mutations.⁽¹⁶⁸⁾ Oxidized amino acids in DNA repair proteins can cause the failure to repair DNA damage and force a cell into apoptosis.⁽¹⁶⁸⁾

The peroxidation of lipids is another indirect mutagenic initiator. Lipid peroxidation resulting from RONS degrade lipids into carbonyl products, such as malondialdehyde (MDA).⁽¹⁸⁴⁾ MDA, which is both electrophilic and nucleophilic, can react with DNA to form adducts.⁽¹⁸⁵⁾⁽¹⁸⁶⁾ MDA-guanine lesions lead polymerases to insert G>A transitions and G>T transversions with equal frequency to the correct G>C pairing.⁽¹⁸⁷⁾ MDA lesions are repaired by the nucleotide excision repair pathway.⁽¹⁸⁷⁾

Alkyladenine-DNA glycosylase (Aag) is a mammalian DNA base excision repair (BER) enzyme that is required for the identification and removal of some RONS generated DNA adducts.⁽¹⁸⁸⁾ Aag recognizes and initiates BER repair of lipid peroxidation adducts 1,N2-ethenoguanine and 1,N6-ethenoadenine, but Aag also has a broad specificity of adduct targets generated by deamination.⁽¹⁸⁸⁾⁽¹⁸⁹⁾⁽¹⁹⁰⁾ Aag also repairs the 3-methyladenine adduct generated by AOM treatment,⁽⁵³⁾ as discussed in section 1.4.5. B6 mice deficient for Aag^{-/-} showed increased tumor multiplicity and more severe inflammation when compare to WT B6 mice after AOM+DSS treatment.⁽¹⁸⁸⁾ The inflammation score was used to assess the severity of the tissue inflammation.⁽¹⁸⁸⁾ Alkbh2 is a mammalian DNA repair enzyme that repairs lipid peroxidation generated DNA and RNA adducts 1,N6-ethenoadenine and 3,N4-ethenocytosine.⁽¹⁹¹⁾⁽¹⁹²⁾ B6 mice deficient for Alkbh2^{-/-} showed increased tumor multiplicity and more severe inflammation when compare to WT B6 mice after AOM+DSS treatment.⁽¹⁹²⁾ In the same study B6 mice deficient in both Aag^{-/-} and Alkbh2^{-/-} also showed increased tumor multiplicity and more severe inflammation when compare to WT B6 mice after AOM+DSS treatment.⁽¹⁹²⁾ These studies demonstrated that mice deficient in DNA repair enzymes necessary to eliminate oxidative DNA adducts have an enhanced susceptibility to cancer development. These studies also suggest that unrepaired DNA

adducts lead to the accumulation of mutations, and further implying that DSS treatments are mutagenic through RONS mediated damage.

Three different studies examining colon cancer induction by AOM+DSS treatment in mice deficient for MGMT^{-/-} and Msh6^{-/-} (mutS homolog 6), Aag^{-/-}, and Alkbh2^{-/-} DNA repair enzymes demonstrated that DNA repair reduces colon cancer,⁽⁵⁵⁾⁽¹⁹²⁾ as all of the DNA repair enzyme deficient strains of mice had a significantly higher tumor incidence and multiplicity than the WT control mice.⁽⁵⁵⁾⁽¹⁹²⁾ Understanding how successful DNA repair relates to cancer susceptibility is essential scientific knowledge, but it remains unclear how this knowledge relates to carcinogenesis in WT mice and in humans? The overwhelming number of cancers occur in humans that have normal DNA repair enzyme activity.

The generation of significantly elevated levels of RONS in mammalian tissues resulting from combating infections and other disease morbidity, epidermal exogenous exposure to ionizing UV radiation, and ingested drugs and other chemical agents, would seem to represent an insurmountable obstacle to preventing tissue destruction and/or carcinogenesis. However, these RONS generating insults, while occurring infrequently, are not unique or even rare events. Even chronic inflammatory diseases, that cause oxidative stress, do not immediately lead to an increased cancer risk. For example, ulcerative colitis does not increase cancer risk for 8-10 years after its onset in patients.⁽¹⁹³⁾

Mitochondrial DNA is at even greater risk than nuclear DNA to oxidative stress, as mitochondria already generate substantial levels of RONS endogenously.⁽¹⁷⁸⁾⁽¹⁹⁴⁾ However, mitochondrial DNA repair mechanisms are the same as the nuclear DNA repair mechanisms, since mitochondrial DNA repair enzymes are encoded in the nuclear DNA.⁽¹⁹⁴⁾⁽¹⁹⁵⁾ Mammalian cells express a BER glycosylase family specifically to remove 8-oxoguanine oxidation lesions

from DNA.⁽¹⁹⁶⁾⁽¹⁹⁷⁾ Also, mammalian cells protect their intracellular components with several classes of antioxidant enzymes that utilize multiple mechanisms to eliminate RONS species, as was previously discussed. The innate immune system would not utilize an anti-pathogenic mechanism based on the generation of excessively high RONS levels without cellular mechanisms in place to prevent tissue damage and carcinogenesis. However, inflammation and the subsequent generation of RONS is strongly associated with carcinogenesis as RONS is produced by tumor potentiating inflammatory reagents.

In the AOM+DSS two-stage colon cancer induction model, treatment with one dose of AOM followed by one treatment with DSS leads to a high incidence of tumors in several different strains of mice.⁽¹⁶⁴⁾ However, treating mice with one dose of the mutagen AOM does not induce colon tumor development.⁽⁴⁵⁾ Even in inbred mouse strains susceptible to AOM treatments, it requires multiple doses to induce colon tumor development,⁽¹⁶⁰⁾⁽¹⁶¹⁾⁽¹⁶²⁾ as discussed in section 1.6.1. One treatment with DSS does not lead to colon cancer development.⁽⁴⁵⁾ Twenty-five CBA/J mice treated with nine treatments of 3% DSS, resulted in tumor incidence in twelve of the mice.⁽¹⁹⁸⁾ While this DSS treatment regimen resulted in a 50% tumor incidence, the DSS concentration was high compared to the DSS concentrations needed to induce colon tumors in AOM+DSS studies, and number of DSS treatment cycles was uncommonly high. Meira et. al. treated ten WT B6 mice with five treatments of 2.5% DSS and induced two colon tumors.⁽¹⁸⁸⁾ In the same paper they treated a separate set of seven WT B6 with seven cycles of 2.5% DSS and did not observe any colon tumors.⁽¹⁸⁸⁾ The DNA repair deficient B6 mice were more susceptible to tumor induction with a DSS treatment, after seven cycles of 2.5% DSS treatment seven out of eighteen Aag^{-/-} deficient B6 mice showed tumor incidence.⁽¹⁸⁸⁾ These studies clearly indicated that oxidative stress is leading to RONS derived DNA damage, and the DNA repair deficient B6

mice are more susceptible to oxidative lesions inducing cancer than the WT B6 mice. However, even at high DSS concentrations and multiple cycles of DSS treatment there is little to no carcinogenic effect on the WT B6 mice. The duration and severity of the DSS treatments required to induce a low tumor incidence in the WT B6 mouse strain suggests that DSS is a poor mutagenic agent, yet still possesses a high efficacy as a tumor potentiating agent.

The AOM+DSS treatment makes it impossible to compare the effect of the two individual reagents separately in a study. Few studies have dissected the model to attempt to understand the individual effect of the AOM and the DSS treatments, only focusing on the combine effect of the treatment. Here, we propose to study the mutagenic and cytotoxic effect of the AOM treatment, the DSS treatment, and the combine AOM+DSS treatment that is necessary to induce colon cancer development.

The critical initiating event in cancer cell development is the fixation of a mutation in a somatic cell's genome. The mutation must occur in or affect the function of an oncogene or tumor suppressor gene. To fix a mutation into the genome of a cell requires several mutually exclusive events to occur. A DNA damaging agent must interact with a cell's DNA to generate a potential mutagenic adduct that must not be repaired. Then the cell must undergo cell division and during DNA replication the polymerase must make an error in the base pairing where the newly polymerized DNA strand would acquire the mutation. All of this must occur without the cell undergoing apoptosis. While there is a very low probability of all of these events occurring, the cancer incidence seen in the human population is quite high and cancer risk increases with age.

The measurement of DNA adduct levels in colon tissue has been associated with cancer incidence, as DNA damaging lesions are mutagenic initiators.⁽¹⁹⁹⁾⁽²⁰⁰⁾ The measurement of DNA

adducts in the colon requires the tissue be excised and homogenized to extract the total DNA for analysis. While measuring potentially mutagenic DNA adducts levels does correlate high adduct levels to an increased risk of colon cancer development, it does not allow for analysis of actual mutations generated. An adduct generating a fixed mutation in a somatic cell's DNA is a low probability event. The rationale for measuring adduct levels is that high adduct levels overwhelm a cell's ability to mitigate the DNA damage, increasing the probability that a mutation will be generated; as mice deficient in the DNA repair of oxidative lesion and mice deficient in the repair of AOM generated methyl adducts are more susceptible to colon cancer incidence. (55)(188)(192)

In contrast to measuring DNA levels, it is possible to study the generation of actual mutations formed in vivo. The glucose-6 phosphate dehydrogenase (G6PD) gene is a constitutively expressed X-linked gene with several hundred known mutations caused by various DNA damaging agents. G6PD is the rate-limiting enzyme in the synthesis of pentose phosphates, and is a critical antioxidant by supplying NADPH that is used against ROS generated lipid peroxidases and in reducing H₂O₂ levels.⁽²⁰¹⁾ G6PD mutations are also non-lethal to a cell. An enzyme histochemistry assay allows for the measurement of colonic epithelial crypts completely populated by G6PD mutant cells.⁽²⁰²⁾⁽²⁰³⁾ This assay measures the number of colonic stem cells that fixed a somatic G6PD mutation, avoided apoptotic induction, and continued to undergo cell division and generate progeny.

We propose to study the generation of somatic stem cell mutations by treating mice with AOM, DSS, and AOM+DSS treatments. By measuring colonic crypts in male mice deficient in G6PD activity, we will ascertain the mutagenic potential of AOM, DSS, and AOM+DSS. We will treat both WT B6 mice and T-cell receptor (TCR) α/β deficient B6 mice in this study. The

purpose of using the α/β T-cell deficient mice is to impair both pro-inflammatory and anti-inflammatory immune cell response. We will ascertain if the immune response supports or impedes the fixation of colonic somatic stem cell mutations. The animals in this study are the same mice in the carcinogenicity experimental group 5 presented in Chapter 3. Therefore, no other strains of mice, either WT or genetically modified, were incorporated into this study. Also, no other analysis of the effect of the microflora composition on carcinogenesis were performed for this work.

As previously discussed, the pro-inflammatory immune response is associated with cancer development. However, anti-pathogenic immune responses lead to cytotoxicity and do not support cell survival. Anti-inflammatory immune cell mediation resolves pro-inflammatory events and is a component of tissue repair and regeneration. As discussed in section 1.5.5., the potential role of RONS and the immune response in potentiating cancer may actually involve enhancing stem cell survival and proliferation.

In applying AOM, DSS, and AOM+DSS treatments to the WT B6 mice and α/β T-cell deficient B6 mice, we predict to see greater numbers of G6PD deficient colonic crypts in the AOM+DSS treated mice. Only the AOM+DSS treated mice will develop colon cancer.⁽⁴⁵⁾ We also predict to see greater numbers of G6PD deficient colonic crypts in the WT mice in comparison to the α/β T-cell deficient mice, if the role of T-cells is potentially mutagenic or enhancing cell survival. If the role of the T-cells is purely related to eliminating potential tumor cells, then we would predict greater numbers of G6PD deficient colonic crypts in the α/β T-cell deficient mice in comparison to the WT mice, due to the loss and/or impairment of α/β T-cell mediated cytotoxicity.

2.3 DATA

2.3.1 Mice Strains and Treatment Groups Studied

Male (B6) WT mice and $\text{TCR}\beta^{-/-}$ mice were divided into four treatment groups. Untreated controls (administered PBS), 10 mg/kg AOM, 2% DSS, and combine 10 mg/kg AOM + 2% DSS. The presentation and analysis of each of these results and a summary of the combine results, which includes comparisons of the treatments effects on each of the strains, are presented in this section.

2.3.2 Significance of the Method for Studying G6PD Mutations

The G6PD mutation assay allows for the in vivo detection of somatic stem cell mutations. Mutations in G6PD are only one of many mutations that can occur after treatment with AOM. In relation to carcinogenesis, mutations occurring in oncogenes or tumor suppressor genes are likely the critical targets. However, measuring G6PD activity allows for an estimation of the incidence of random somatic mutations in colonic stem cells without any selection pressure. Therefore, mutations in G6PD provide a conservative estimation of the random gene mutations that arise from AOM treatment. The G6PD assay also allows for comparisons of the effect of the AOM and AOM+DSS treatment on mutagenesis between WT mice and different strains of gene knockout mice.

2.3.3 G6PD Deficient Mutant Crypts

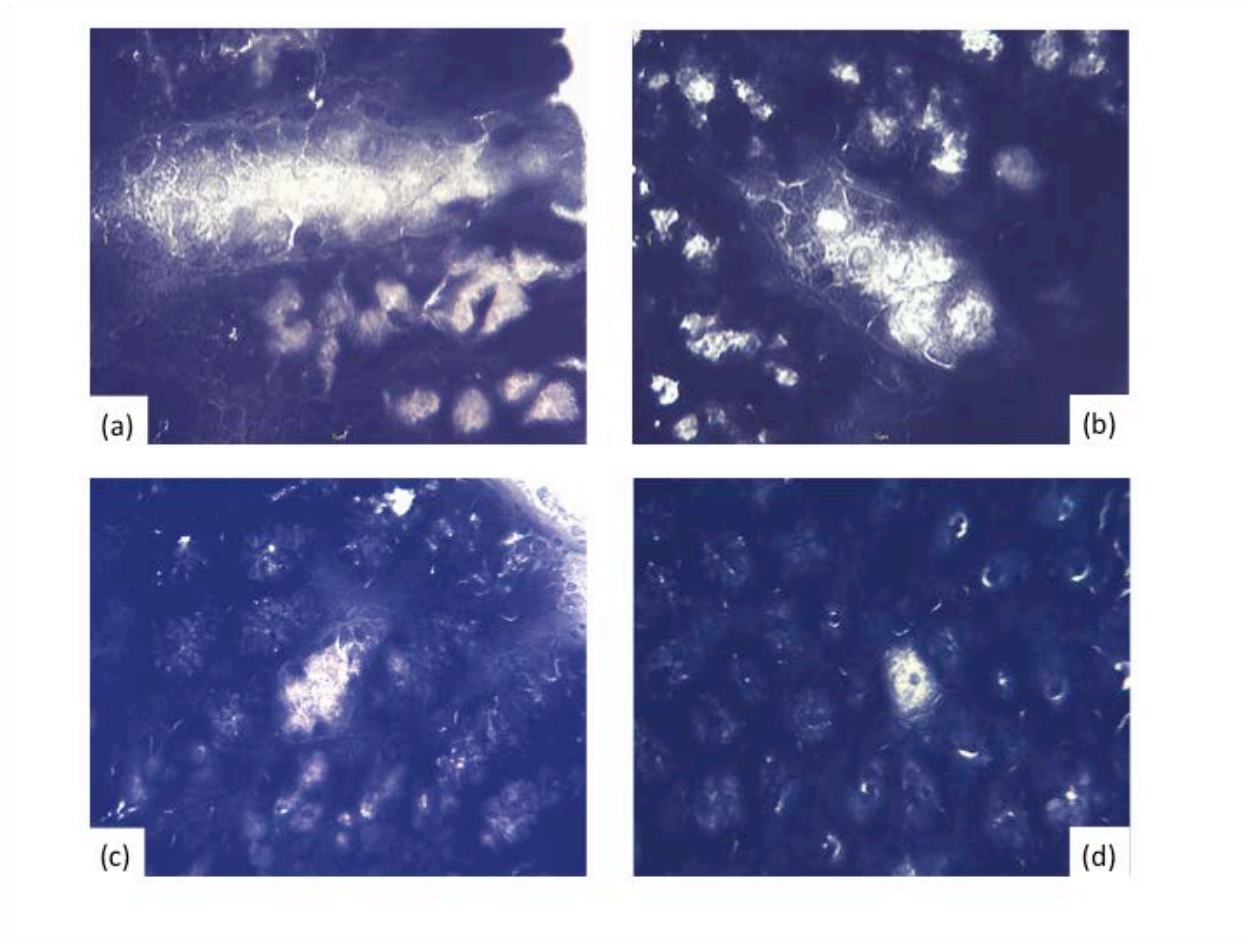


Figure 14. G6PD Mutant Crypts

Figure 14. Representative G6PD mutant crypts in WT mice (**a & b**) and $\text{TCR}\beta^{-/-}$ mice (**c & d**) treated with 10 mg/kg AOM + 2% DSS. G6PD deficient crypts, and the cells that comprise them, appear transparent or white in contrast to the formazan containing “blue” staining crypts. **a & c** are representative of crypts viewed horizontally. **b & d** are vertically viewed crypts.

2.3.3.1 Analysis of G6PD Deficient Mutant Crypts

The generation of a G6PD mutant crypt requires that a mutation is fixed in the G6PD loci in the X chromosome of the male mice. If a newly replicated stem cell, with its G6PD gene inactivated, rises to dominate a crypt, all of the progeny cells will also lack G6PD activity. The G6PD deficient mutant crypts cannot oxidize glucose-6 phosphate, and cannot reduce nitro blue tetrazolium (NBT) into formazan. When the G6PD enzyme is functional, the NBT in the reaction mix will be reduced to insoluble formazan and precipitate out of the reaction mixture, accumulating at the location of the enzyme and “staining” cells with a deep blue color. Without the accumulation of reduced insoluble formazan, the cells will not stain and, therefore, will not acquire the deep blue color. Thus, the fully mutant crypts stand out as “white” in a dark blue background (Figure 14). The cells on the periphery of the mutant crypts acquire some color as a result of the submucosal pericryptal cells and immune cells that comprise the “sheath” surrounding the crypt. These cell populations anchor to the basal axis of the epithelial cells, and are not derived from the G6PD deficient epithelial stem cell, so these cells will express normal G6PD and reduce NBT to formazan. Potential false mutant crypts can occur when the tissue is very slightly torn, or in a region where the color of the stain was very light but the crypts are normal in appearance. However, these conditions are easy to distinguish from the optimal staining regions and were not regarded as G6PD mutant crypts. Another approach used to eliminate false mutants was to cut two sequentially located tissue sections and stain them on the same slide under the exact same conditions, with the same batch of reaction mix. As the sequential sections were only seven microns apart, it is highly probable G6PD mutant crypts will be represented in the exact same location on both slides. Hence a true G6PD mutant crypt will be identifiable in sequential sections. However, not every section is identical as tissue folds and

tears can occur, or the staining may have a poor quality in the region where the mutant crypt is located. Regardless, a conservative and consistent characterization of a mutant G6PD crypt in consecutive sections reduces the probability of missing a true G6PD mutant or identifying a false mutant.

2.3.4 Animal Treatments, Colon Tissue Harvesting and Preparation for G6PD analysis

Six WT mice and six TCR $\beta^{-/-}$ mice were treated with one i.p. injection of sterile PBS (200 μ l) and represented the untreated control groups. The AOM treated groups were comprised of twelve WT mice and twelve TCR $\beta^{-/-}$ mice treated with one i.p. injection of 10 mg/kg AOM. The DSS treated groups were comprised of twelve WT mice and twelve TCR $\beta^{-/-}$ mice treated with 2% DSS for one week. The AOM+DSS treated groups were comprised of twelve WT mice and twelve TCR $\beta^{-/-}$ mice and were treated with 10 mg/kg AOM + 2% DSS, where the 10 mg/kg i.p. injection of AOM was followed one week later by a one week treatment with 2% DSS. The mice were then housed for 90 days in the sterile animal facility. The 90 day timecourse was sufficient for carcinogenesis based on previous carcinogenicity experiments. This data is presented in Chapter 3. However, no mutagenesis studies were conducted on any of the treated animal groups except the above mentioned animal groups. Therefore, the 90 day timecourse for the mutagenesis analysis was based off of the cancer development data. Upon completion of the timecourse, the mice were euthanized and their colons excised, immersed in OCT medium (Tissue-Tek® Optimal Cutting Temperature Compound, Ted Pella, Inc., Redding, CA), and frozen on liquid N₂. Sections were then cut for each animal and stained for G6PD activity. Sections were generated until a minimum of 10,000 colon crypts had been observed per animal. Sections were

also analyzed for G6PD mutant crypts. Full details of the experimental methods are written in Chapter 5.

2.3.5 Mutation Frequency and Statistical Analysis

The mutation frequency (M.F.) is the ratio of G6PD mutant crypts observed in the histological sections from a mouse's colon divided by the total number of colonic crypts assessed for that mouse's colon. As it is unlikely any one study would have the time and resources necessary to examine all of the colonic crypts in all of the mice used in a study, the M.F. estimates the total number of G6PD mutated colonic crypts that would arise in an animal after treatment with a carcinogen. Combining the M.F. results for all of the animals in one treatment group will allow for the calculation of the average M.F. for that group.

Calculating the M.F. allows for a statistical analysis of differences within or between treated groups of animals. In this study, the t-test was sufficient to perform the statistical analysis of the different treated groups of mice. Before statistical comparisons were made, the data sets were administered the normality test to show the values of the data followed a Gaussian distribution. Also, the F-test for Two Data Sets was used to determine the equality of variances between the data sets being compared. All of the data sets satisfied the requirements for the t-test to be used to analyze the data. The software used and details of the statistical methods are discussed in section 5.

2.3.6 G6DP mutation assay results summary table

Table 1: G6PD Mutation Assay results summary table

Mouse Strain (B6)	Treatment	Incidence of Mutant Crypts	G6PD Mutant Crypts	Total # Crypts Analyzed	M.F. ($\times 10^{-4}$)
WT	solvent	0/6 mice	0	$> 10^5$	< 0.02
TCR $\beta^{-/-}$	solvent	0/6 mice	0	$> 10^5$	< 0.02
WT	AOM	10/12 mice	43	96821	4.44 ^{a,b}
TCR $\beta^{-/-}$	AOM	11/12 mice	59	288512	2.04 ^{a,c}
WT	DSS	0/12 mice	0	133770	< 0.02
TCR $\beta^{-/-}$	DSS	1/12 mice	1	163406	0.06
WT	AOM+DSS	7/12 mice	17	161755	1.05 ^{b,d}
TCR $\beta^{-/-}$	AOM+DSS	5/12 mice	7	167374	0.42 ^{c,d}

a) WT AOM vs. TCR $\beta^{-/-}$ AOM ($p=0.03749$) t-test

Result: The M.F. is significantly higher in the WT AOM treated group compared to the TCR $\beta^{-/-}$ AOM treated group.

b) WT AOM vs. WT AOM+DSS ($p=0.0041$) t-test

Result: The M.F. is significantly higher in the WT AOM treated group compared to the WT AOM+DSS treated group.

c) TCR $\beta^{-/-}$ AOM vs. TCR $\beta^{-/-}$ AOM+DSS ($p=0.00039$) t-test

Result: The M.F. is significantly higher in the TCR $\beta^{-/-}$ AOM treated group compared to the TCR $\beta^{-/-}$ AOM+DSS treated group.

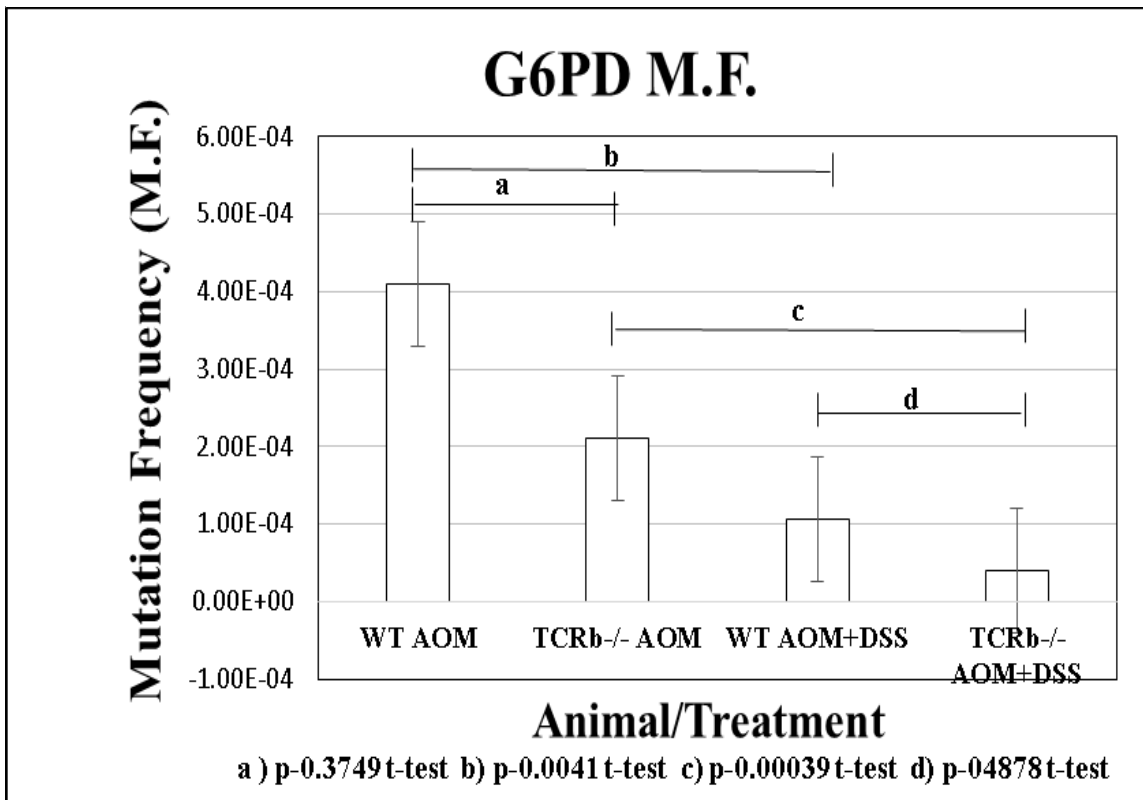
d) WT AOM+DSS vs. TCR $\beta^{-/-}$ AOM+DSS ($p=0.04878$) t-test

Result: The M.F. is significantly higher in the TCR $\beta^{-/-}$ AOM treated group compared to the TCR $\beta^{-/-}$ AOM+DSS treated group.

G6PD: Glucose-6 Phosphate Dehydrogenase AOM: Azoxymethane

DSS: Dextran Sulfate Sodium M.F. = Mutation Frequency

Table 2. G6PD M.F. results comparison table



2.4 G6PD MUTATION ASSAY RESULTS SUMMARY

2.4.1.1 Analysis of WT AOM treated mice vs. TCR $\beta^{-/-}$ AOM treated mice

The G6PD M.F. is significantly higher in the WT AOM treated mice when compared to the TCR $\beta^{-/-}$ AOM treated mice ($p=0.037$) (Table 1). The immune competent WT mice exhibited greater numbers of stem cells that acquired a mutation in the G6PD gene loci during DNA replication, avoided apoptotic induction by DNA repair pathways, rose to dominate the stem cell niche, and proliferated to produce the epithelial cells of the crypt, when compared to the TCR $\beta^{-/-}$ AOM treated mice. The significance of this result indicated that stem cells are more likely to replicate with unrepaired DNA alkylation damage when α/β T-cells are viable.

2.4.1.2 Analysis of WT AOM treated mice vs. WT AOM+DSS treated mice

The G6PD M.F. is significantly higher in the WT AOM treated mice when compared to the WT AOM+DSS treated mice ($p=0.0041$) (Table 1). It is likely the reduction in the occurrence of G6PD mutant crypts is the result of the DSS damage and subsequent tissue repair reducing the overall number of crypts in the colon, including crypts with AOM derived mutated stem cells. As both the AOM and AOM+DSS treatments were administered to WT mice, which are immune competent, the decrease in G6PD mutant crypts cannot be linked to a deficiency in the immune response. Nor could consideration be given to expression differences between DNA repair enzymes or detoxifying enzymes due to strain differences. As discussed in section 1.5.2, treatment with DSS significantly disrupts the colonic epithelial and results in a shortening of the colon.⁽⁸³⁾⁽⁸⁴⁾ In this study mice receiving a DSS treatment always had a reduced the colon length when compared to the mice that did not receive a DSS treatment. However, the reduction in

colon lengths was not significantly different in the mice that received the DSS treatment in comparison to the mice that did not receive the DSS treatment. A discussion of these results will be presented in section 2.6.

2.4.1.3 Analysis of TCR β ^{-/-} AOM treated mice vs. TCR β ^{-/-} AOM+DSS treated mice

The G6PD M.F. is significantly higher in the TCR β ^{-/-} AOM treated mice compared to the TCR β ^{-/-} AOM+DSS treated mice ($p=0.00039$) (Table 1). As with the WT mice, it is likely that the effect of the DSS treatment is the reason for the decreased numbers of the G6PD mutant crypts observed in the TCR β ^{-/-} AOM+DSS mice treated when compared to the TCR β ^{-/-} AOM treated mice.

2.4.1.4 Analysis of WT AOM+DSS treated mice vs. TCR β ^{-/-} AOM+DSS treated mice

The G6PD M.F. is significantly higher in the WT AOM+DSS compared to the TCR β ^{-/-} AOM+DSS ($p=0.04878$) (Table 1). The p-value is virtually 0.05, indicating that the statistical significance is marginal. As previously discussed, it is unlikely that the expression of DNA repair enzymes or detoxifying enzymes would be altered in the TCR β ^{-/-} mice when compared to the WT mice, and therefore would not explain the significant difference in the G6PD M.F. between the two strains of mice. Treatment with DSS reduced the G6PD M.F. in the WT AOM treated mice by 75% of the value calculated for the G6PD M.F. in the WT AOM treated mice without the DSS treatment. There was an equivalent 75% decrease in G6PD M.F. observed in the TCR β ^{-/-} AOM treated mice after treatment with DSS. The decrease of the M.F. in both mouse strains by a 75% reduction shows that the effect of the DSS treatment was equivalent on both the WT mice and the TCR β ^{-/-} mice.

The significant impact of the DSS treatment on the mutagenesis is that it reduced the G6PD M.F. Treatment with the inflammatory reagent DSS did not result in an increase in the G6PD M.F.; therefore, it did not increase the number of G6PD mutant crypts after the AOM treatment. Also, the effect of DSS treatment on the G6PD M.F. did not depend on the immune status of the mice. Both the immune competent WT mice and the immune deficient $\text{TCR}\beta^{-/-}$ mice showed the same reduction in their respective G6PD M.F. after the DSS treatment.

2.4.1.5 Analysis of WT DSS treated mice vs. $\text{TCR}\beta^{-/-}$ DSS treated mice

No G6PD deficient mutant crypts were observed in the WT DSS treated mice. One G6PD mutant was observed in the $\text{TCR}\beta^{-/-}$ DSS treated mice. However, this is likely a spontaneous mutation and not a result of the DSS treatment.⁽²⁰⁴⁾ This result is highly significant as the RONS produced by the DSS treatment did not cause G6PD mutant crypts in either the immune competent or immune deficient mice, although, it is thought that RONS should generate somatic stem cell mutations,⁽¹⁷⁸⁾⁽¹⁷⁹⁾⁽¹⁸¹⁾⁽¹⁸³⁾⁽¹⁸⁸⁾⁽¹⁹²⁾ as discussed in section 2.1. This result strongly suggests that the DNA repair of RONS derived oxidative lesions was equivalent in both strains of mice. Also, this result strongly suggests that the oxidative stress did not significantly overwhelm the cellular repair of RONS derived oxidative DNA damage, and that inflammation's role in carcinogenesis is not due to a mutagenic effect.

2.5 DATA TABLES AND RESULTS FOR THE INDIVIDUAL TREATED GROUPS

Table 3. WT Untreated Control Mice

WT B6 Untreated Control Mice				
Table 3. Incidence: <u>No mice had G6PD mutant crypts</u>				
WT B6 (6)	Treatment	# of G6PD Mutant Crypts	Total # of Crypts Observed	Mutation Frequency (M.F.)
M1	PBS	0	10,000 +	n/a
M2	PBS	0	10,000 +	n/a
M3	PBS	0	10,000 +	n/a
M4	PBS	0	10,000 +	n/a
M5	PBS	0	10,000 +	n/a
M6	PBS	0	10,000 +	n/a
<u>Result:</u> No G6PD mutant crypts were observed in the WT control mice. <u>Treatment:</u> 200 ul PBS i.p. injection. <u>G6PD:</u> Glucose-6 Phosphate Dehydrogenase. <u>n/a:</u> not applicable				

2.5.1.1 Results Summary and Analysis of Table 3, previous page

There were no G6PD mutant colonic crypts observed in the histology sections generated from the WT untreated control mice. Other studies have reported spontaneous G6PD mutants in mouse colons at very low numbers, ($<0.04 \pm 0.02 \times 10^{-4}$), that are well below the values observed after treatment with a mutagenic tumor initiator.⁽²⁰⁴⁾ This observation is consistent with other reported studies.

Table 4. TCRβ^{-/-} Untreated Control mice

TCRβ^{-/-} B6 Untreated Control Mice				
Table 4. Incidence: <u>No mice had G6PD mutant crypts</u>				
TCRβ^{-/-} B6 (6)	Treatment	# of G6PD Mutant Crypts	Total # of Crypts Observed	Mutation Frequency (M.F.)
M1	PBS	0	10,000 +	n/a
M2	PBS	0	10,000 +	n/a
M3	PBS	0	10,000 +	n/a
M4	PBS	0	10,000 +	n/a
M5	PBS	0	10,000 +	n/a
M6	PBS	0	10,000 +	n/a
<p><u>Result:</u> No G6PD mutant crypts were observed in the TCRβ^{-/-} control mice. <u>Treatment:</u> 200 ul PBS i.p. injection. <u>G6PD:</u> Glucose-6 Phosphate Dehydrogenase <u>n/a:</u> not applicable</p>				

2.5.1.2 Results Summary and Analysis of Table 4, previous page

No G6PD mutant colonic crypts observed in the histology sections generated from the TCR $\beta^{-/-}$ untreated control mice.

Table 5. WT AOM treated mice

WT B6 treated with AOM				
Table 5. Incidence: 11 out of 12 mice had G6PD mutant crypts				
WT B6 (12)	Treatment	# of G6PD Mutant Crypts	Total # of Crypts Observed	Mutant Frequency (M.F.)
M1	AOM	5	10564	4.73e ⁻⁰⁴
M2	AOM	5	6422	7.79e ⁻⁰⁴
M3	AOM	13	10805	1.20e ⁻⁰³
M4	AOM	1	5265	1.90e ⁻⁰⁴
M5	AOM	2	6368	3.14e ⁻⁰⁴
M6	AOM	2	6524	3.07e ⁻⁰⁴
M7	AOM	0	6282	0
M8	AOM	0	8889	0
M9	AOM	5	9195	5.44e ⁻⁰⁴
M10	AOM	5	10640	4.70e ⁻⁰⁴
M11	AOM	1	8064	1.24e ⁻⁰⁴
M12	AOM	4	7803	5.13e ⁻⁰⁴
Totals		43	96821	4.44e⁻⁰⁴
<p>Results: 43 G6PD mutant crypts were observed in the WT AOM treated mice. Treatment: 10 mg/kg b.w. AOM i.p. injection G6PD: Glucose-6 Phosphate Dehydrogenase AOM: Azoxymethane</p>				

2.5.1.3 Results Summary and Analysis of Table 5, previous page

Forty-three G6PD mutant crypts were observed in the twelve WT mice treated with AOM. There is variability in the distribution of G6PD mutant crypts observed in each WT AOM treated mouse. One limitation of the experimental method used to determine the M.F. is that not every crypt can be observed due to practical reasons. G6PD mutant crypts can be present in the tissue that did not appear in the tissue sections assessed. Each mouse is likely to have variable expression of the enzymes that metabolize AOM, variability in the volume of distribution of the AOM active metabolite, and variable expression of DNA repair enzymes. Therefore, it is not surprising to observe variability in the numbers of G6PD mutant crypts between the mice.

Table 6. TCRβ^{-/-} AOM treated mice

TCRβ^{-/-} B6 treated with AOM				
Table 6. Incidence: 9 out of 12 mice had G6PD mutant crypts				
TCRβ^{-/-} B6 (12)	Treatment	# of G6PD Mutant Crypts	Total # of Crypts Observed	Mutant Frequency (M.F.)
M1	AOM	2	20795	9.62e ⁻⁰⁵
M2	AOM	11	21574	5.10e ⁻⁰⁴
M3	AOM	9	27933	3.22e ⁻⁰⁴
M4	AOM	6	22618	2.65e ⁻⁰⁴
M5	AOM	0	31952	0
M6	AOM	2	24786	8.07e ⁻⁰⁵
M7	AOM	8	27206	2.94e ⁻⁰⁴
M8	AOM	4	28164	1.42e ⁻⁰⁴
M9	AOM	5	16795	2.98e ⁻⁰⁴
M10	AOM	2	19916	1.00e ⁻⁰⁴
M11	AOM	3	20436	1.47e ⁻⁰⁴
M12	AOM	7	26337	2.66e ⁻⁰⁴
Totals		59	288512	2.04e⁻⁰⁴

Results: 59 G6PD mutant crypts were observed in the TCRβ^{-/-} AOM treated mice.
Treatment: 10 mg/kg bw AOM i.p. injection
G6PD: Glucose-6 Phosphate Dehydrogenase
AOM: Azoxymethane

2.5.1.4 Results Summary and Analysis of Table 6, previous page

Fifty-nine G6PD mutant crypts were observed in the twelve TCR $\beta^{-/-}$ mice treated with AOM.

Table 7. WT DSS treated mice

WT B6 treated with DSS				
Table 7. Incidence: <u>No mice had G6PD mutant crypts</u>				
WT B6 (12)	Treatment	# of G6PD Mutant Crypts	Total # of Crypts Observed	Mutation Frequency (M.F.)
M1	DSS	0	11914	1.00e ⁻⁰⁶
M2	DSS	0	10193	1.00e ⁻⁰⁶
M3	DSS	0	11285	1.00e ⁻⁰⁶
M4	DSS	0	11395	1.00e ⁻⁰⁶
M5	DSS	0	12780	1.00e ⁻⁰⁶
M6	DSS	0	11280	1.00e ⁻⁰⁶
M7	DSS	0	13881	1.00e ⁻⁰⁶
M8	DSS	0	8183	1.00e ⁻⁰⁶
M9	DSS	0	14094	1.00e ⁻⁰⁶
M10	DSS	0	17224	1.00e ⁻⁰⁶
M11	DSS	0	11541	1.00e ⁻⁰⁶
Total		0	133770	1.00e⁻⁰⁶
<p><u>Results:</u> No G6PD mutant crypts were observed in the WT DSS treated mice. <u>Treatment:</u> 2% DSS in drinking water for seven days. <u>G6PD:</u> Glucose-6 Phosphate Dehydrogenase <u>DSS:</u> Dextran Sulfate Sodium</p>				

2.5.1.5 Results Summary and Analysis of Table 7, previous page

There were no G6PD mutant crypts observed in the histology sections generated from the WT mice treated with DSS.

Table 8. TCRβ^{-/-} DSS treated mice

TCRβ^{-/-} B6 treated with DSS				
Table 8. Incidence: <u>One mouse had one G6PD mutant crypt</u>				
TCRβ^{-/-} B6 (12)	Treatment	# of G6PD Mutant Crypts	Total # of Crypts Observed	Mutation Frequency (M.F.)
M1	DSS	0	13464	1.00e ⁻⁰⁶
M2	DSS	0	13640	1.00e ⁻⁰⁶
M3	DSS	0	15121	1.00e ⁻⁰⁶
M4	DSS	0	14737	1.00e ⁻⁰⁶
M5	DSS	0	13716	1.00e ⁻⁰⁶
M6	DSS	0	11280	1.00e ⁻⁰⁶
M7	DSS	0	17208	1.00e ⁻⁰⁶
M8	DSS	1	14339	6.97e ⁻⁰⁵
M9	DSS	0	14118	1.00e ⁻⁰⁶
M10	DSS	0	11767	1.00e ⁻⁰⁶
M11	DSS	0	12608	1.00e ⁻⁰⁶
M12	DSS	0	11408	1.00e ⁻⁰⁶
Total		1	163406	6.1197e⁻⁰⁶
Results: One G6PD mutant crypts were observed in the TCRβ ^{-/-} DSS treated mice.				
Treatment: 2% DSS in drinking water for seven days				
G6PD: Glucose-6 Phosphate Dehydrogenase				
DSS: Dextran Sulfate Sodium				

2.5.1.6 Results Summary and Analysis of Table 8, previous page

There was one G6PD mutant crypt observed in the histology sections generated from the TCR $\beta^{-/-}$ DSS treated mice. The one mutant crypt is likely a spontaneous mutant and is unlikely to have been generated as a result of the DSS treatment.⁽²⁰⁴⁾

Table 9. WT AOM+DSS treated mice

WT B6 treated with AOM+DSS				
Table 9. Incidence: 7 out of 12 mice had G6PD mutant crypts				
WT B6 (12)	Treatment	# of G6PD Mutant Crypts	Total # of Crypts Observed	Mutant Frequency (M.F.)
M1	AOM+DSS	2	12879	1.55e ⁻⁰⁴
M2	AOM+DSS	0	13862	0
M3	AOM+DSS	2	10605	1.89e ⁻⁰⁴
M4	AOM+DSS	1	12490	8.01e ⁻⁰⁵
M5	AOM+DSS	0	16672	0
M6	AOM+DSS	3	16134	1.86e ⁻⁰⁴
M7	AOM+DSS	1	11513	8.69e ⁻⁰⁵
M8	AOM+DSS	3	15846	1.89e ⁻⁰⁴
M9	AOM+DSS	0	18767	0
M10	AOM+DSS	0	15456	0
M11	AOM+DSS	5	13015	3.84e ⁻⁰⁴
M12	AOM+DSS	0	4516	0
Totals		17	161755	1.05e⁻⁰⁴
<p>Results: 17 G6PD mutant crypts were observed in the WT AOM+DSS treated mice.</p> <p>Treatment: 10 mg/kg b.w. AOM i.p. injection + 2% DSS in the drinking water for seven days</p> <p>G6PD: Glucose-6 Phosphate Dehydrogenase</p> <p>DSS: Dextran Sulfate Sodium AOM: Azoxymethane</p>				

2.5.1.7 Results Summary and Analysis of Table 9, previous page

Seventeen G6PD mutant crypts were observed in the twelve WT mice treated with AOM+DSS. The colons of these mice were excised at 90 days after the completion of the DSS treatment, so this was clearly not a transient effect caused by the DSS induced tissue damage and subsequent tissue repair and regeneration (discussed in section 1.5). Also, most of the WT AOM+DSS treated mice had tumors in their colons. This reduced the number of normal crypts per slide when compared to the mice that were not treated with AOM+DSS, as dysplastic crypts from the tumor tissue were not included in the total counts. No G6PD mutant crypts were observed in the tumor tissue. Nor were there any complete G6PD mutant tumors, although these have been reported in other studies.⁽²⁰⁵⁾

Table 10. TCRβ^{-/-} AOM+DSS treated mice

TCRβ^{-/-} B6 treated with AOM+DSS				
Table 10. Incidence: 5 out of 12 mice had G6PD mutants				
TCRβ^{-/-} B6 (12)	Treatment	# of G6PD Mutant Crypts	Total # of Crypts Observed	Mutant Frequency (M.F.)
M1	AOM+DSS	0	11340	0
M2	AOM+DSS	1	12704	7.87e ⁻⁰⁵
M3	AOM+DSS	0	15290	0
M4	AOM+DSS	2	15331	1.30e ⁻⁰⁴
M5	AOM+DSS	1	15696	6.37e ⁻⁰⁵
M6	AOM+DSS	1	16928	5.91e ⁻⁰⁵
M7	AOM+DSS	2	13441	1.49e ⁻⁰⁴
M8	AOM+DSS	0	10898	0
M9	AOM+DSS	0	13650	0
M10	AOM+DSS	0	10409	0
M11	AOM+DSS	0	20540	0
M12	AOM+DSS	0	11147	0
Totals		7	167374	4.182e⁻⁰⁵
Results: 17 G6PD mutant crypts were observed in the TCRβ ^{-/-} AOM+DSS treated mice.				
Treatment: 10 mg/kg b.w. AOM i.p. injection + 2% DSS in the drinking water for seven days				
G6PD: Glucose-6 Phosphate Dehydrogenase				
DSS: Dextran Sulfate Sodium AOM: Azoxymethane				

2.5.1.8 Results Summary and Analysis of Table 10, previous page

Seven G6PD mutant crypts were observed in the twelve $\text{TCR}\beta^{-/-}$ mice treated with AOM+DSS. $\text{TCR}\beta^{-/-}$ AOM+DSS treated mice also had tumors that further decreased the amount of normal crypts. No G6PD mutant tumors, or G6PD mutant crypts within the tumor tissue, were observed during the analysis.

2.6 CALCULATING THE EFFICIENCY OF THE CONVERSION OF AN O⁶-METHYLGUANINE DNA ADDUCT INTO A G6PD MUTATION BY UTILIZING THE STEM CELL MUTATION FREQUENCY

The M.F. is calculated by dividing the number of G6PD mutant crypts by the total number of crypts assessed. G6PD mutant crypts arise from stem cells that have fixed a mutation in the G6PD gene. Generating a mutation is a complex process that involves multiple cellular pathways and events. Studies have used the detection of DNA adducts as a predictor of mutagenesis.⁽¹⁹⁹⁾⁽²⁰⁰⁾ However, the formation of a DNA lesion does not indicate that a mutation will arise as a result of the lesion.

Measuring the actual occurrence of a mutation in a marker gene, G6PD, indicates that a DNA lesion was effectively converted into an actual DNA mutation. Treating mice with AOM produces the pro-mutagenic DNA lesion O⁶mG in colon epithelial cells,⁽⁴⁹⁾⁽⁵⁰⁾⁽⁵¹⁾ as discussed in section 1.4. O⁶mG levels have been determined in the colon after AOM treatment.⁽²⁰⁶⁾ Knowing the level of colonic O⁶mG adducts after an AOM dose and calculating the M.F. of G6PD mutant crypts allows for an estimation of the efficiency of O⁶mG adduct conversion into a G6PD mutation.

For a stem cell to fix a somatic mutation several events must occur. The parent stem cell must undergo division while harboring a DNA lesion without the lesion being repaired and without cell cycle arrest and the subsequent induction of apoptosis.⁽⁴¹⁾⁽⁷¹⁾⁽⁷²⁾⁽⁷⁷⁾ The DNA polymerase must insert an incorrect DNA base, or mismatch, across from the DNA lesion.⁽⁵¹⁾ While some DNA polymerases, such as translesion synthesis polymerases, exhibit poor accuracy in pairing DNA bases during DNA replication,⁽⁷³⁾⁽⁷⁴⁾ a correct base pairing can still be produced despite the presence of the DNA lesion.

Assuming that O⁶mG adducts are the critical lesion in the generation of a G6PD mutation,⁽⁴¹⁾⁽⁵⁵⁾⁽⁷¹⁾⁽⁷²⁾⁽⁷³⁾⁽⁷⁴⁾ estimating the number of O⁶mG adducts generated in the colon by a 10 mg/kg dose of AOM,⁽²⁰⁶⁾ and knowing the number of possible phenotypic guanine targets in G6PD gene loci,⁽²⁰⁷⁾⁽²⁰⁸⁾ an estimation of the efficiency in which O⁶mG adducts are converted into G6PD mutations can be made:

a) A 10 mg/kg dose of AOM will generate 1.2×10^5 O⁶mG adducts per colonic stem cell, based on a reported 14 mg/kg dose of AOM producing 78 pmol O⁶mG/ μ mol guanine bases in the proximal and distal colon of WT B6 mice, and that there are a total of 2×10^9 guanine bases/stem cell.

b) There are ~400 potential guanine base targets in the G6PD gene loci that could lead to a G6PD null phenotype, and this number is based on phenotypic G6PD deficiency studies in humans.⁽²⁰⁷⁾⁽²⁰⁸⁾ This makes the odds generating an O⁶mG adduct at a potential phenotypic mutating base in the G6PD gene loci of a stem cell equal to $(400 \text{ guanine target bases}) / (2 \times 10^9 \text{ total guanine O}^6\text{mG adducts}) = 2.0 \times 10^{-7}$.

c) Multiplying the odds of an O⁶mG adduct occurring at a phenotypic G6PD mutation target base (hit) multiplied by the number of O⁶mG adducts per stem cell ($2.0 \times 10^{-7} \times 1.2 \times 10^5$) = 2.4×10^{-2} O⁶mG adducts at potential phenotypic mutating guanine bases in the G6PD gene loci/stem cell.

d) A million crypts represents a conservative estimate of the number of crypts in the mouse large intestine based on the reported value of 1.1×10^6 crypts in the mouse small intestine,⁽²⁰⁹⁾ and knowing that the mouse colon is ~ one quarter of the small intestine's length.⁽⁴³⁾ The greater the number of crypts the more colonic stem cells will be present,

increasing the number of G6PD phenotypic mutant target bases, and therefore the chance of observing a G6PD mutated crypt in the colon increases proportionately.

e) It is reported there are roughly 5 stem cells per crypt,⁽³⁰⁾ and multiplying the number of O⁶mG adducts at potentially phenotypic G6PD mutant target bases by in the total number of stem cells per colon (2.4×10^{-2} O⁶mG adducts at potential mutating sites) x (5×10^6 stem cells/total crypts) = 1.2×10^5 O⁶mG adducts at G6PD mutating sites per mouse colon.

f) If one hundred percent of O⁶mG adducts at the G6PD mutating sites generated phenotypic mutations, then 1.2×10^5 G6PD mutant crypts would be expected to be observed in the colon.

g) The observed G6PD M.F. in the WT AOM treated mice was 4.4×10^{-4} . Multiplying the G6PD M.F. by the total number of colon crypts (4.4×10^{-4} G6PD mutants/total crypts assessed) x (1×10^6 total colon crypts) = 400 G6PD mutant crypts/colon.

f) Dividing the observed number of G6PD mutant crypts per colon by the expected number of G6PD mutant crypts per colon at a 100% O⁶mG adduct conversion efficiency (4×10^2)/(1.2×10^5) = 0.003, or 0.3% O⁶mG adduct conversion efficiency.

Only 0.3% of all of the O⁶mG adducts formed at potential phenotypic G6PD mutating sites in the G6PD gene loci are successfully converted into phenotypic somatic stem cell mutations in the male WT B6 mouse colon. Interestingly, this value reasonably approximates the value reported in WT *E.coli* studies⁽²¹⁰⁾⁽²¹¹⁾ for the efficiency of O⁶mG adducts converted into mutations.

If only 0.3% of O⁶mG adducts are converted into phenotypic G6PD mutations, how many mutations actually manifest in genes critical to carcinogenesis? A somatic G6PD stem cell mutation is only a conservative marker of mutagenesis in stem cells, and it is assumed many

more different somatic mutations occurred in stem cells throughout the colon. However, the O6mG adduct conversion efficiency demonstrates how rare of an event mutagenesis actually is. How likely is it that one or more phenotypic somatic mutations would occur in a stem cell, if any O6mG adducts are converted into mutations? Can mutagenesis really be the rate limiting step in carcinogenesis?

Beta-catenin is an oncogenic transcription factor and a component of the E-cadherin cell-cell adhesion protein complex that would likely have a significantly lower conversion efficiency than G6PD. Beta-catenin is frequently mutated after AOM treatments.⁽²¹²⁾⁽²¹³⁾⁽²¹⁴⁾⁽²¹⁵⁾⁽²¹⁶⁾ There are five potential phenotypic mutating guanine bases in beta-catenin, and as there are two alleles that can be mutated. Therefore are ten total potential guanine bases that lead to phenotypic mutations.⁽²¹⁴⁾ This compares to the 400 phenotypic mutating guanine bases in G6PD on the x-linked allele in the male mice.⁽²⁰⁷⁾⁽²⁰⁸⁾ There are significantly fewer potential sites for phenotypic beta-catenin mutations than there are with phenotypic G6PD mutations, signifying that phenotypic beta-catenin mutations are an extremely rare event. However, in a study assessing beta-catenin mutations in AOM+DSS induced colon tumors there was a 100% incidence of phenotypic mutations in beta-catenin.⁽²¹⁵⁾

The value of studying actual somatic stem cell mutations is that real differences can be elucidated between test groups. WT mice generated mutations with greater efficiency than the TCR β ^{-/-} mice. This implies that a competent immune response potentiates mutagenesis through stem cell survival and enhances DNA replication with unrepaired DNA lesions present in a stem cell. So what differences will be observed in cancer development between the two strains of mice?

2.7 SUMMARY AND DISCUSSION

The study of the effects of AOM, DSS, and AOM+DSS treatment on G6PD mutagenesis provides several important insights into the relationship between DNA damage and inflammation. The WT mice treated with AOM had a significantly higher G6PD M.F. than the immune deficient $\text{TCR}\beta^{-/-}$ mice, implying a role for the α/β T-cell mediated immune signaling in the fixation of mutations in stem cells. The role of inflammation as a tumor promoter that generates RONS is thought in part to involve oxidative DNA damage and mutagenesis. Yet, WT mice and $\text{TCR}\beta^{-/-}$ mice treated with DSS did not have a statistically different G6PD M.F. than the untreated control mice and actually there was no M.F. to compare between the treated groups. When treated with the combination of AOM+DSS WT mice showed a significantly higher G6PD M.F. compared to the $\text{TCR}\beta^{-/-}$ mice, but the G6PD M.F. in both of the strains decreased by approximately 75% relative to the M.F. calculated for the corresponding mice treated with AOM as a single agent. Therefore, the DSS treatment had a deleterious impact on the generation or survival of stem cells with somatic mutations, not an enhancing effect. Calculating the efficiency of converting a pro-mutagenic O^6mG adduct into a somatic stem cell mutation in the WT mice demonstrated how rare mutations actually are relative to the number of adducts that are formed. Furthermore, mutations must be phenotypic to affect cancer development. Since the conversion efficiency was calculated based on an actual count of somatic stem cell mutations, the efficiency of converting an O^6mG adduct into a mutation is even lower in the immune deficient mice than the 0.3% efficiency calculated for the WT mice. The observation of stem cell mutations in AOM treated mice that subsequently do not develop colon

tumors, strongly implies that mutations are not the rate limiting step in cancer development and other factors related to the immune response play a critical role in carcinogenesis.

2.7.1 More G6PD mutant crypts occurred in the WT mice than occur in the immune deficient TCR β ^{-/-} mice after treatment with AOM?

Studying G6PD M.F. requires that a phenotypic G6PD mutation occurs in newly polymerized DNA strands during stem cell division. After the stem cell divides and the DNA recombines, the DNA strands with the mutation in the G6PD loci must be retained in the stem cell niche and assume the dominate position to propagate the crypt with G6PD mutant cells.

As discussed in section 1.4.6., a study by Hong et. al. reported that the base regions of colonic crypts, including the stem cell niche, showed severe cytotoxicity immediately after treatment with AOM.⁽⁴¹⁾ It is likely the rapid increase in DNA adducts levels induced cytotoxicity that depleted the crypt stem cells. To attempt to reconstitute the stem cell population the remaining dominate stem cell(s) would need to bypass cell cycle arrest and DNA repair, and undergo symmetrical stem cell divisions⁽³⁵⁾(Figure 9), as discussed in section 1.2.2.7. The outcome of a symmetrical division is that two equivalent stem cells are produced.⁽³⁵⁾ Therefore, if the parent stem cell divides with unrepaired O⁶mG lesions a mutation could be fixed in the newly polymerized DNA strands, and the DNA strands with the mutation will be retained in the niche after the DNA recombines, unless both stem cells move to lineage differentiation.⁽³⁵⁾

This would mean a stem cell with a somatic mutation is in a position to usurp the niche and propagate the cells of the crypt. If the mutation confers a selective advantage then the mutated stem cell will be more likely to assume the dominate position.⁽³⁰⁾ A mutation may even enhance the stem cell's survival or elongate its retention time.⁽³¹⁾ One example of this is seen in

the APC gene in human colon cancer,⁽³¹⁾ which is mutated in ~80% of sporadic human colon cancer cases as well as being an inheritable mutation(FAP).⁽²¹⁷⁾ APC mutations provide both a selective advantage and enhance the stem cell's retention time in the dominate position of the niche.⁽³⁰⁾⁽³¹⁾ Interestingly, a G6PD mutation would not confer a selective advantage on a stem cell. A G6PD mutation could impair a cell's ability to combat RONS mediated damage,⁽²⁰⁵⁾ but should not otherwise deleteriously impact a cell.

Could α/β T-cell signaling play a role in inducing more symmetrical stem cell divisions and potentially expanding a stem cell population with a somatic mutation? WT mice had a significantly higher G6PD M.F. vs. the $\text{TCR}\beta^{-/-}$ mice after treatment with AOM. In this way α/β T-cell signaling could have inadvertently led to both the generation of somatic stem cell mutations and also prime stem cells with mutations to propagate a colonic crypt.

The colonic stem cell populations in the $\text{TCR}\beta^{-/-}$ mice would not have received α/β T-cell signaling support. Therefore, the $\text{TCR}\beta^{-/-}$ mice had fewer stem cells successfully fix a mutation, and the newly mutated stem cell usurped the stem cell niche, resulting in a significantly lower G6PD M.F. in comparison to the WT mice. While asymmetrical stem cell division is capable of producing DNA strands with a fixed mutation, there is a least a 50% chance the cell copy with mutated DNA strands is not retained in the stem cell niche but moves to undergo lineage differentiation. If α/β T-cell signaling does help to produce more stem cells with a somatic G6PD stem cell mutation, this would partially explain why there was a significant difference in the G6PD M.F. between the two strains of mice.

2.7.1.1 α/β T-cell signaling may modulate how a newly divided cell positions itself within the stem cell niche

A mechanism through which α/β T-cell signaling could direct stem cell division toward a symmetrical cell division may be through modulating the expression of the cell-cell adhesion protein junctions on the basolateral border of the stem cells. Pericryptal cells, macrophages, dendritic cells, and tissue resident intraepithelial (IELs) T-cells, form cell-cell adhesions junctions on the basal border of the stem cells. This then anchors the stem cells to the subepithelial and fixes them in place, as well as establishing signaling pathways outside of the niche.⁽⁶⁾⁽³²⁾⁽³³⁾⁽³⁴⁾⁽³⁵⁾⁽³⁶⁾

α/β T-cell signaling can modulate all of these cell types and could influence how stem cells reposition themselves within the niche. The colonic Lgr5⁺ expressing stem cells do not share a border in the stem cell niche⁽²⁵⁾(Figure 7), so at least one of the cell copies produced after a stem cell divides must reposition itself within the niche. This is critical to determining the fate of the cell: if it is destined to undergo lineage differentiation or remain in the niche. So α/β T-cell signaling may generate more “slots” for the stem cells, positions within the niche where a stem cell will receive the signaling support necessary to retain its stem cell characteristics and maintain its functions.

2.7.1.2 α/β T-cell signaling may alter a stem cell’s epigenetic gene expression to enhance stem cell survival

The study by Hong et. al. demonstrated that the cells in the base regions of colonic crypts, the stem cell niche, had significantly lower MGMT expression under homeostatic conditions than the fully differentiated epithelial cells on the luminal border of the crypt.⁽⁴¹⁾

Consequently, treatment with AOM showed substantial apoptotic induction in the stem cell niche, and significantly fewer cells died in the luminal regions of the crypts.⁽⁴¹⁾ Twelve hours after the AOM treatment, the MGMT expression levels in the niche were equivalent to the levels of MGMT expression in the fully differentiate cells and the apoptotic cell numbers substantially decreased.⁽⁴¹⁾

α/β T-cell signaling impact the change in MGMT expression observed in the stem cell niche. If the $\text{TCR}\beta^{-/-}$ mice were unable to upregulate MGMT expression after the AOM treatment due to a lack of α/β T-cell signaling, then they may experience more stem cells dying than in the WT mice. This could explain why the G6PD M.F. was significantly lower in the $\text{TCR}\beta^{-/-}$ mice after the AOM treatment when compared to the WT mice.

One caveat to this hypothesis is that increased MGMT expression would repair the O^6mG lesions and drive down the mutation rate. While this is invariably true, the more significant impact could be that increased MGMT expression allows stem cells to avoid apoptosis. This would inadvertently enhance stem cell survival and allow some stem cells to successfully fix mutations during DNA replication before the DNA lesions are repaired.

Another possible mechanism by which α/β T-cell signaling might play a role in stem cell mutagenesis is inducing translesion DNA polymerase expression, or inducing the preferential utilization of translesion polymerases during DNA replication once a lesion has been detected. α/β T-cells induce translesion DNA polymerases to replicate variable regions of the antibody gene loci, as part of their role in the maturation of B-cells into antibody producing plasma cells. This ensures that DNA replication of the variable regions of antibody binding sites have a high degree of variability. So that the target bacterial cell surface antigens are constantly susceptible

to antibody binding.⁽²¹⁸⁾ This proves that α/β T-cells possess the ability to modulate translesion DNA polymerases in select scenarios.

Could α/β T-cell signaling also lead to the preferential use of translesion DNA polymerases in DNA alkylation damaged stem cells, as a means of preventing cell cycle arrest to keep the stem cells dividing? While this would increase the risk of cells acquiring mutations, it could also help to explain how stem cells increase their rate of cell division and compensate for the loss of epithelial cells during an inflammatory event.⁽¹¹⁾⁽¹²⁾ This could explain why the G6PD M.F. was significantly lower in the $\text{TCR}\beta^{-/-}$ mice after the AOM treatment when compared to the WT mice.

2.7.2 Why were no G6PD mutant crypts detected in the immune competent WT mice and in the immune deficient TCR β ^{-/-} mice treated with 2% DSS?

The most direct answer to this question is that the oxidative stress resulting from the actions of the innate immune response did not overwhelm the colonic stem cell's ability to mitigate the RONS derived DNA damage. G6PD mutant crypts are the result of a stem cell that has fixed a mutation in the G6PD gene, and this result demonstrates that no stem cells fixed a G6PD mutation and subsequently came to dominate a crypt. Also, the lack of G6PD mutant crypts in both strains of mice after the DSS treatment shows this result was not related to the immune status of the mice.

It is significant that at least one DSS treatment is not leading to cancer promotion by acting as a mutagen. As somatic G6PD mutations in stem cells act as a marker for mutagenesis, it suggests a very low number of mutations resulted in any genes. In the carcinogenic AOM+DSS treatments, mutations must manifest as a result of the AOM derived DNA alkylation damage. So the DSS treatment is not amplifying the number of mutations in the colonic stem cells.

Could NO \cdot generation actually initiate anti-apoptotic, immune suppressive, and tissue regenerative mechanisms that inadvertently protect burgeoning cell populations with oncogenic/tumor suppressor mutations? Studies have suggested that NO \cdot can mediate several anti-inflammatory effects as well as survival effects on cells,⁽¹⁵⁸⁾⁽¹⁵⁹⁾ as discussed in section 1.5.5. NO \cdot inhibits neutrophil β 2 integrin function, decreases endothelial P-selectin expression and reduces chemotactic responses to various chemokines, such as interleukin (IL)-8 and monocyte chemotactic protein-1 (MCP-1).⁽³⁸⁴⁾ NO \cdot concentration is a factor in the transition from Th1 to

Th2 immune mediation.⁽³⁵⁸⁾⁽³⁸⁴⁾⁽³⁸⁵⁾ The association of RONS generated by treatments with tumor promoters acting as a mutagen may not have been accurate. The multifaceted capabilities of RONS acting as signaling molecules, especially at higher than normal intracellular and extracellular concentrations,⁽¹⁵⁸⁾⁽³⁵⁸⁾⁽³⁸⁴⁾⁽³⁸⁵⁾ could explain part of the mechanism through which DSS treatments potentiate cancer development.

2.7.2.1 The loss of crypt morphology may explain why no G6PD mutant crypts arose in the DSS treated mice

DSS treatment is very disruptive to the colon architecture, even at low doses. So much so that it is impossible to determine where the stem cell niche is located after the DSS treatment (Figure 13). There could have been sufficient spatial separation from the site of the anti-pathogenic innate immune response to decrease the concentration of RONS molecules reaching the stem cells, so that they had no deleterious impact. Therefore, the cancer promoting mechanism of DSS must occur during the tissue restoration which could be partially mediated by NO[•] signaling.

The result of the DSS treatment in this study does not mean other tumor promoting reagents applied to different tissues are not mutagenic. However, tumor promoting reagents are considered to be poor carcinogens when used independently of a tumor initiator.⁽⁴⁴⁾ The fact that no G6PD mutants were observed in the DSS treated mice, at one dose, corroborates this theory.

2.7.3 Treating the WT mice and the TCR β ^{-/-} mice with AOM+DSS resulted in a lower G6PD mutation frequency in both strains of mice when compared to the mutation frequency observed after the strains were treated with AOM alone

After treatment with AOM+DSS the G6PD M.F. calculated for both the WT mice and the TCR β ^{-/-} mice was approximately 75% lower for both strains than the M.F. calculated after the AOM treatment for both strains. This decrease in the observed number of G6PD mutant crypts, and the corresponding decrease in M.F., is likely due to destructive effect of the DSS treatment on the colon. DSS treatments result in several deleterious effects on the treated mice and invariably cause a shortening of the entire colon length when compared to untreated mice, as discussed in section 1.5.2. The loss of colon length due to scarring depleted the total number of colonic crypts, including crypts with mutated stem cells. Alternatively, as G6PD is a critical antioxidant, the DSS treatment may have selectively killed stem cells with a somatic G6PD mutation as these cells would have been more susceptible the cytotoxic effects of RONS.⁽²⁰⁵⁾

It was much more difficult to generate a total count of 10,000 crypts observed per animal with mice that received a DSS treatment than with the mice that did not undergo a DSS treatment. The DSS treatment reduced the number of crypts appearing on each section of colon tissue in both strains of mice when compared to mice that did not receive DSS treatments. The mice treated with AOM+DSS also had fewer crypts per slide than the other treatment groups due to the presence of tumor tissue.

The effect of the DSS treatment following an AOM treatment was a significant reduction in the number of mutated stem cells and therefore a reduction in potential cancer cells. This result is paradoxical to the assumed effect of DSS treatment potentiating cancer

development. G6PD mutant stem cells act as a marker for mutagenesis. A reduction in G6PD mutant crypts means that a substantial number of crypts with stem cells harboring phenotypic somatic mutations in any gene were also eliminated. Therefore, DSS treatments should lower the probability of cancer incidence in a mouse after treatment with AOM. However, colon cancer development in WT mice, regardless of the strain, is substantial after treatment with AOM+DSS. This relationship will be related to the carcinogenicity data for these same treated groups of mice in the Summary Chapter (Chapter 4).

3.0 CARCINOGENESIS STUDY

3.1 SCOPE AND SYNOPSIS

Chapter 3 presents the results of several different carcinogenesis experiments and a discussion of those results. The first section is an introduction to the carcinogenesis experiments and provides new material focusing on the immune system and how different immune cells may affect colon cancer induction by AOM+DSS. The goal is to help the reader understand the relevance and novelty of treating T-cell deficient mice with AOM+DSS to determine how colon cancer may develop in a immune compromised animal. The second section outlines the significance of the study, the experimental design, the important details of the assay and the statistical analyses. The experimental data and results tables will then be presented. The final section is a summary of the experimental results and a discussion, including possible explanations and interpretations of how and why the results occurred.

3.2 INTRODUCTION

A tissue associated chronic inflammatory disease significantly increases an individual's chances for developing cancer. Chronic inflammatory colitis is a high risk factor for CRC.⁽¹⁾ The first person credited with studying the relationship between inflammation and cancer was Rudolph

Virchow, who suggested that lymphatic infiltrate discovered in solid tumor samples supported the cancer pathology.⁽²¹⁹⁾

The function of the immune system is to eliminate infectious agents, such as viruses, bacteria, small parasites, and even large helminthes. Considering the sheer number of different and potentially lethal infectious agents in the environment, the immune response has evolved a substantial number of mechanisms to combat infections. However, immune responses represent considerable risk to the host tissue environment where disease or wounding occurs. The immune response tightly regulates cytolytic cell activity and minimizes the duration of the immune response, to prevent immune cell mediated damage to the host tissue while still eliminating pathogenic threats. Dysregulation of the immune response can lead to severe morbidity and mortality. The pathology of cancer requires multiple levels of immune dysregulation. Primarily, cancer progression requires that cancer cells either remain undetected by cytolytic immune cells and/or impair their cytolytic activity.

Immune cells are unique in the body as cells that exist and function as individual units. Immune cells are able to traffic throughout the body by moving through the circulatory and lymphatic systems, and infiltrate into areas of inflammation. Some immune cells become tissue resident cells that integrate into a tissue's normal structure and remain a part of the normal tissue architecture. The colonic epithelium incorporates macrophages, dendritic cells (DCs), and intraepithelial lymphocytes (IEL) T-cells, among others. Immune cells exhibit a wide range of functional plasticity, while fully differentiated cells in other tissues specialize to fulfill one set of functions.

Immune cells support tissue wound repair and regeneration.⁽²²⁰⁾⁽²²¹⁾⁽²²²⁾⁽²²³⁾ Neutrophils and monocytes debride wound areas of dead cell components and pathogens.⁽²²³⁾ Monocytes

express TGF-beta(transforming growth factor beta) upon infiltrating into inflamed and wounded tissues.⁽²²⁴⁾⁽²²⁵⁾⁽²²⁶⁾⁽²²⁷⁾ TGF-beta induces macrophages and DCs to express angiogenic and lymphangiogenic growth factors, such as VEGF(vascular endothelial growth factors), TGF-alpha(transforming growth factor alpha) and IGF-1(insulin-like growth factor 1).⁽²²⁸⁾⁽²²⁹⁾⁽²³⁰⁾⁽²³¹⁾⁽²³²⁾⁽²³³⁾ IGF-1 is a mitogenic growth factor and causes the partial dedifferentiation of epithelial cells, altering an epithelial cell's morphology from a columnar axial polarized shape into a flattened motile cell capable of migrating into the wound space.⁽²³⁴⁾⁽²³⁵⁾ The physiological process of epithelial cell migration into the wound space in an attempt to reconstitute the epithelial barrier is termed epithelial restitution.⁽²³⁵⁾ α/β T-cells, which are discussed extensively in section 3.1.4, express IL-4/IL-13 expression polarize monocyte maturation into the M2 macrophage phenotype which drives immune suppression and tissue regeneration.⁽³⁰⁵⁾⁽³⁰⁶⁾⁽³⁰⁷⁾⁽³⁰⁸⁾

γ/δ IELs support colonic epithelial wound repair mechanisms by expressing keratinocyte growth factor (KGF) after the γ/δ IELs are activated by a tissue insult.⁽²²¹⁾ KGF (KGF-1 and 2) is a member of the fibroblast growth factor (FGF) family of protein ligands that modulate multiple pathways of growth and regeneration.⁽²³⁶⁾ WT B6 mice, that express KGF-2, showed enhanced repair and regeneration of epidermal lacerations when compared to $Tcr\delta^{-/-}$ B6 mice.⁽²³⁷⁾ WT B6 mice treated with dextran sulfate sodium (DSS) at a 2.5% dose for 5 days showed enhanced colonic epithelial repair and regeneration in comparison to $Tcr\delta^{-/-}$ B6 mice.⁽²³⁸⁾

3.2.1 The same mechanisms that immune cells use to provide a benefit for wound repair and tissue regeneration support the growth of cancer cells and their progression toward malignancy

The colonic tumor microenvironment is hypoxic and hypoglycemic due to the high metabolic demands of cancer cells mitogenic activity.⁽²³⁹⁾⁽²⁴⁰⁾⁽²⁴¹⁾ Anaerobic glycolysis causes hypoglycemia that may induce oncogenic mutations in K-ras and other genes,⁽²³⁹⁾ and produces lactic acid and carbon dioxide causing acidosis in the local tumor environment.⁽²⁴²⁾⁽²⁴³⁾⁽²⁴⁴⁾ An acidic physiological pH can lead to misfolding and dysregulation in many proteins, although a few proteins can enhance their functional capacity in acidic environments.

For these reasons the tumor microenvironment is highly cytotoxic compared to normal tissue, and many tumor cells die through necrosis as a result. Many normal cells bordering the tumor tissue also die through necrosis, leading to a highly inflammatory environment. Modifying immune cells to assume wound healing phenotypes may be a necessary component of tumor malignancy, as hypoxic conditions seem to be the driving force behind tumor cell metastasis,⁽²⁴⁵⁾ and immune cell mediated angiogenesis and lymphangiogenesis provide tumor cells the ability to metastasize.⁽²⁴⁶⁾⁽²⁴⁷⁾

Tumor cells release chemottractant cytokines that induce the migration of immune cells into the tumor environment by expressing chemottractant cytokines.⁽²⁴⁸⁾⁽²⁴⁹⁾ Many different immune cells can function in support of the tumor microenvironment. Tumor-associated macrophages (TAMs) are macrophages in a tumor environment that support tumor progression and impede cytolytic anti-tumor cell mediated immune responses.⁽²⁵⁰⁾⁽²⁵¹⁾⁽²⁵²⁾⁽²⁵³⁾ To counter the hypoxia, hypoglycemia, and acidosis in the tumor microenvironment, TAMs express the same array of angiogenic and lymphangiogenic growth factors expressed by normal macrophages

during tissue wound repair.⁽²⁵³⁾⁽²⁵⁴⁾⁽²⁵⁵⁾⁽²⁵⁶⁾ The function and behavior of TAMs resembles the M2 macrophage phenotype (M2 cells) that mediates wound repair responses and facilitates the anti-inflammatory immune suppression of inflammation.⁽²⁵¹⁾⁽²⁵²⁾⁽²⁵⁷⁾⁽²⁵⁸⁾⁽²⁵⁹⁾⁽²⁶⁰⁾ This implies that TAMs begin as monocytes that are polarized into M2 cells before they manifest as TAM populations, although macrophages and TAMs show extensive heterogeneity both within and between their respective populations.⁽²⁵³⁾⁽²⁶¹⁾⁽²⁶²⁾⁽²⁶³⁾

Tumor microenvironments also affect DCs, as VEGF expression by TAM's will prevent DC maturation and maintains high numbers of immature DCs.⁽²⁶⁴⁾⁽²⁶⁵⁾⁽²⁶⁶⁾ Inhibiting DC maturation would severely impair or completely inhibit the generation of cytolytic T-cells, as DCs would not traffic to nearby lymph nodes to activate and expand cytolytic T-cell populations that specifically target tumor antigens.⁽²⁶⁴⁾⁽²⁶⁵⁾⁽²⁶⁶⁾

3.2.2 The earliest cancer cells lack a fully developed tumor microenvironment to support their development and progression, yet are still able to survive and proliferate

As cancer cells are able to induce immune cells to stimulate angiogenesis they help to satisfy their own energy demands. In addition, cancer cells prevent immune cell mediated cytolytic and/or cytotoxic elimination of the cancer cells. However, tumor microenvironments develop after cancer cells have manifested in tissues, and are required for the more advanced stages of cancer rather than the early stages of cancer. Cancer cells should be more vulnerable to energy depletion and cytolytic cell attacks during the earliest stages of cancer development. Early stage cancer cells must lack the ability to remodel the vasculature and alter their environment to compensate for the energy demands of anaerobic glycolysis. Moreover, the

expression of intracellular stress signaling proteins should mark cancer cells for cytolytic deletion by natural killer (NK) cells.⁽²⁶⁷⁾⁽²⁶⁸⁾⁽²⁶⁹⁾

While it is likely that significant numbers of early stage cancer cells are either killed by cytolytic immune cells or die by necrosis, enough cancer cells persist to alter their microenvironment and conscript immune cell support. This implies that some immune modulation occurs in the earliest stages of cancer, perhaps even potentiating the development of the first cancer cells. What would be the result of a sporadic colon cancer induction model used to treat immune compromised mice? Would cancer development be enhanced in the immune compromised animals, or possibly impaired when compared to immune competent WT mice?

3.2.3 AOM+DSS treatment studies with WT and immune compromised mice

Several studies have examined the relationship of colon cancer induction after treatment with AOM+DSS in immune deficient mice. These studies addressed the role of TLR/NLR PRRs receptors that initiate inflammatory responses in colon cancer development.⁽¹⁰⁴⁾⁽²⁷⁰⁾⁽²⁷¹⁾ The reason for studying these receptors is the unique relationship the colon exhibits with commensal microbiota. Many cells of the body express PRRs including macrophages; DCs, and neutrophils, but also endothelial and epithelial cells.⁽³³⁾⁽⁹³⁾⁽⁹⁴⁾⁽⁹⁵⁾⁽¹¹⁰⁾⁽¹¹²⁾ It is through TLR/NLR signaling that natural tolerance for microbiota is established and broken.⁽³³⁾⁽⁹³⁾⁽⁹⁵⁾⁽¹⁰³⁾⁽¹⁰⁵⁾⁽¹⁰⁶⁾ DSS disrupts the colon architecture allowing bacteria access to the subepithelial regions of the colon, which induces inflammation when bacteria are detected in this region,⁽³³⁾⁽⁹⁵⁾ as discussed in section 1.5.4.

When WT B6 mice and TLR2^{-/-} B6 mice were treated with AOM+DSS it was found that the TLR2^{-/-} B6 mice developed significantly more and larger colon tumors than the WT B6

control mice.⁽²⁷²⁾ It was also reported that colonic epithelium of TLR2^{-/-} B6 mice had altered immune responses and dysregulated cell proliferation during colitis, which resulted in inflammation derived growth signals and that potentiated neoplastic growth.⁽²⁷²⁾ The investigators concluded that TLR2 signaling inhibits colon cancer development in WT B6 mice.⁽²⁷²⁾

In another study in which that treated WT B6 mice and TLR4^{-/-} B6 mice were treated with AOM+DSS it was shown that the TLR4^{-/-} B6 mice were resistant to colon cancer development in comparison to the WT B6 mice.⁽²⁷³⁾ WT B6 mice treated with AOM+DSS developed significantly more tumors in comparison to the TLR4^{-/-} B6 mice treated with AOM+DSS.⁽²⁷³⁾ The TLR4^{-/-} B6 mice also exhibited a significantly decreased number of tumors per animal and a significantly decreased tumor size.⁽²⁷³⁾ The investigators concluded that TLR4 signaling potentiates colon cancer development in WT B6 mice.⁽²⁷³⁾

In a third study in which WT B6 mice and NLR3^{-/-} B6 mice treated with AOM+DSS, the NLR3^{-/-} B6 mice developed significantly more colon tumors with significantly larger size and weight than the WT B6 mice.⁽²⁷⁴⁾ Interestingly, in this study the cancer development was assessed by endoscopy as well as H+E histological evaluation in both mouse strains.⁽²⁷⁴⁾ The investigators concluded NLR3 and inflammasome signaling inhibits colon cancer development in WT B6 mice.⁽²⁷⁴⁾

Studies examining the effect of AOM+DSS treatment inducing colon cancer in TLR/NLR deficient mice showed conflicting results in that TLR/NLR receptors may either potentiate or inhibit colon cancer development. Explaining these discrepant results will likely require a deeper understanding of the inflammatory response initiated by each of these receptors. These results also imply that each TLR/NLR will have its own individual effect on AOM+DSS induced colon

cancer development, and the effect will not be synonymous for all of the receptors in a specific class.

TLR/NRL receptors are initiators of inflammation, but what colon cancer development result would occur in an immune deficient mouse lacking the cells that mediate the immune response? α/β T-cells (thymus derived cells) are the dominate effectors of the adaptive immune response, comprising both cytolytic cells and immune response mediators. α/β T-cells are a complex heterogeneous population of cells, often capable of overlapping and compensatory functions. An α/β T-cell deficient animal would be severely immune compromised, and therefore, would represent a compelling test group to determine how a cancer induction treatment would affect an immune compromised animal model.

A study was done on T-cell deficient B6 mice treated with AOM (10 mg/kg b.w.), but the mice did not receive a DSS treatment. In this study five AOM treatments were administered to $\text{TCR}\alpha^{-/-}$ B6 mice, $\text{TCR}\delta^{-/-}$ B6 mice, and WT B6 mice.⁽²⁷⁵⁾ Interestingly, the investigators choose to study the WT B6 mice although they are resistant to colon cancer induction by AOM treatments.⁽¹⁶⁰⁾ In this study only the $\text{TCR}\delta^{-/-}$ B6 mice developed colon cancer, with only one tumor reported in six $\text{TCR}\delta^{-/-}$ B6 mice after five months.⁽²⁷⁵⁾ However, after seven months five out of ten $\text{TCR}\delta^{-/-}$ B6 mice treated with AOM developed tumors.⁽²⁷⁵⁾ The results of this study confirmed that the WT B6 mice are resistant to AOM treatments inducing colon cancer, but interestingly so were the $\text{TCR}\alpha^{-/-}$ B6 mice. This study also indicated a role for γ/δ T-cells in resisting colon cancer development in WT B6 mice.

We predict that the lack of α/β T-cells in the immune compromised mice will reduce the incidence, multiplicity, and progression of colon cancer in a model that involves inflammation, when compared to the WT immune competent mice. This prediction is based on the rational that

inflammation, and the multitude of immune responses that result from inflammation, are required to promote cancer development. The dysregulation of the immune response by the lack of α/β T-cells will inhibit, not enhance, cancer development. This prediction contrasts with the idea that the immune response is required to impede cancer development.

3.2.4 The potential effects of the loss of α/β T-cell functions on a colon cancer induction model that requires inflammation to promote cancer development

The thymus is a small organ of the thoracic cavity, sitting superior to the heart. The primary function of the thymus is to induce the expression of the thymus cell receptor (TCR) on T-cell precursors, that must interact with the intraepithelial of the thymus.⁽²⁷⁶⁾⁽²⁷⁷⁾ The T-cell precursors will express the beta and alpha chains of the T-cell receptor and the CD4 and CD8 co-stimulatory molecules that will determine the T-cells phenotype.⁽²⁷⁶⁾⁽²⁷⁷⁾⁽²⁷⁸⁾⁽²⁷⁹⁾⁽²⁸⁰⁾

Athymic mice do not properly develop the intraepithelial of the thymus to facilitate the expression of the α/β TCR, as the athymic mice are null for the expression of the Fox p1 transcription factor.⁽²⁸¹⁾ This means that athymic mice are α/β T-cell deficient. A beta chain null mouse would lack the beta chain gene loci and not express the beta chain of the α/β TCR, also resulting in an α/β T-cell deficient phenotype.

CD8⁺ α/β T-cells (CTLs) are the cytolytic T-cells that identify and lyse virally infected cells.⁽²⁸²⁾ CTLs are predominate to other cytolytic cell populations, which utilize less specific recognition signals to identify cells for cytolysis, as employing the less specific mechanisms of selecting cells for cytolysis would result in more extensive and severe tissue destruction.

α/β T-cell deficient mice will lack CTLs and consequently would be vulnerable to viral infections, and unable to impede cancer cell development by selectively eliminating cancer cells through CTL cytolysis. Cancer cells may express detectable non-self antigens from degraded proteins that are altered due to mutations or novel proteins expressed due to genomic instability, such as carcinoembryonic-antigen (CEA) in colon cancer.⁽²⁸³⁾⁽²⁸⁴⁾ CTLs could be a critical component of cancer cell elimination, if CTLs were not immune suppressed by the tumor microenvironment.⁽²⁸⁵⁾⁽²⁸⁶⁾

CD4⁺ α/β T-cells Th1 (T-helper 1) cells are immune pro-inflammatory mediators. They express, Interferon-gamma (IFN γ), Lymphotoxin α (LT α), IL-2, and TNF-beta, among other cytokines to mediate the elimination of pathogens.⁽²⁸⁶⁾⁽²⁸⁷⁾ IFN γ expression modulates several immune responses to enhance CTL activity. IFN γ also polarizes macrophages into their anti-microbial M1 phenotype, which generates RONS.⁽²⁸⁸⁾

Th1 cell mediation potentiates CTLs and other anti-microbial mechanisms, and as α/β T-cell deficient mice also lack CTLs, burgeoning cancer cells would have less potent anti-tumor cell cytolytic immune responses to attenuate in α/β T-cell deficient mice. Interestingly, the lack of Th1 cell mediation may also attenuate RONS generation as deficient IFN γ expression would repress the polarization of monocytes into M1 macrophages. A reduction in RONS may impede cancer development in the α/β T-cell deficient mice.

CD4⁺ α/β T-cells Th17 (T-helper 17) cells are also pro-inflammatory mediators. Interestingly, Th-17 cell mechanisms are directed toward non-immune cells to induce immune responses. Th-17 cells mediate anti-pathogenic responses to extracellular pathogens, including bacteria and fungi, through the expression of IL-17a, IL-17f,⁽²⁸⁹⁾ and array of other cytokines to potentiate the activity of neutrophils and monocytes.⁽²⁹⁰⁾⁽²⁹¹⁾⁽²⁹²⁾⁽²⁹³⁾⁽²⁹⁴⁾ IL-22 is an IL-10 family

cytokine expressed by Th17 cells that enhances colonic epithelial barrier protection, maintains homeostasis, and enhances tissue repair.⁽²⁹⁵⁾⁽²⁹⁶⁾⁽²⁹⁷⁾⁽²⁹⁸⁾ However, IL-22 expression may also exacerbate chronic inflammatory conditions, such as psoriasis, rheumatoid arthritis, and ulcerative colitis.⁽²⁹⁹⁾⁽³⁰⁰⁾⁽³⁰¹⁾

The lack of Th17 mediated signaling in α/β T-cell deficient mice could strongly diminish neutrophil and monocyte activity. Diminishing phagocyte function could significantly reduce ROS generation that is associated with potentiating cancer development. The loss of Th17 mediated IL-22 expression in α/β T-cell deficient mice may impair wound repair and tissue regeneration, or conversely could result in a less severe immune response.

CD4⁺ α/β T-cells Th2 (T-helper 2) cells mediate anti-inflammatory signals that suppress Th1 polarized immune responses. Th2 cells express IL-4, IL-13, and other cytokines.⁽³⁰²⁾⁽³⁰³⁾⁽³⁰⁴⁾ IL-4 and IL-13 expression polarize monocyte maturation into the M2 macrophage phenotype which drives immune suppression and tissue regeneration.⁽³⁰⁵⁾⁽³⁰⁶⁾⁽³⁰⁷⁾⁽³⁰⁸⁾ Interestingly, many of the Th2 derived cytokines exacerbate allergic reactions by enhancing eosinophil and mast cell functions, and causing IgE antibody class-switch.⁽³⁰⁹⁾⁽³¹⁰⁾⁽³¹¹⁾⁽³¹²⁾⁽³¹³⁾⁽³¹⁴⁾⁽³¹⁵⁾⁽³¹⁶⁾⁽³¹⁷⁾⁽³¹⁸⁾⁽³¹⁹⁾

α/β T-cell deficient mice lacking Th2 cell mediated signaling would not be able to drive monocyte polarization into M2 macrophages through the expression of IL-4/IL-13. This would impact the development of the tumor microenvironment, as Th2 cells are recruited by cancer cells to facilitate the development of TAMs, as discussed in section 3.1.1. Without the normal TAM development would tumors be more or less capable of progressing to the advanced metastatic stages of colon cancer?

CD4⁺ α/β T-cells T-regulatory cells (Treg) suppress immune responses to restore tissue homeostasis, as well as maintaining self-tolerance in auto-immune diseases. Tregs express IL-10,

IL-35, and TGF-beta, to suppress immune responses.⁽³²⁰⁾⁽³²¹⁾⁽³²²⁾⁽³²³⁾ IL-10 inhibits monocytes from expressing multiple cytokines and chemokines to prevent INF γ from polarizing monocytes into M1 macrophages,⁽³²⁴⁾⁽³²⁵⁾⁽³²⁶⁾⁽³²⁷⁾⁽³²⁸⁾ inhibits M1 macrophage functions,⁽³²⁹⁾ and inhibits the development of DCs, both classical and plasmacytoid, from monocytes.⁽³³⁰⁾⁽³³¹⁾

IL-10 expression inhibits neutrophil phagocytosis and the killing of phagocytosed bacteria.⁽³³²⁾⁽³³³⁾⁽³³⁴⁾⁽³³⁵⁾ Interestingly, IL-10 expression does not directly inhibit CTLs and may actually enhance CTLs cytolytic activity.⁽³³⁶⁾⁽³³⁷⁾ IL-10 also enhances activated cytolytic NK cells, and does not directly suppress them⁽³³⁸⁾ but does drive down INF γ expression. TGF-beta also mediates immunosuppression to facilitate the initiation of tissue repair. TGF-beta inhibits NK (natural killer) cell activation, cytokine production, and cytolytic activity.⁽³³⁹⁾⁽³⁴⁰⁾ TGF-beta mediated T-cell immunosuppression seems to be directed against CD4⁺ α/β T-cells.⁽³⁴¹⁾

Tregs are recruited to tumor microenvironments where they mediate immune suppression through the previously discussed mechanisms.⁽³⁴²⁾⁽³⁴³⁾⁽³⁴⁴⁾⁽³⁴⁵⁾⁽³⁴⁶⁾⁽³⁴⁷⁾ Cancer cells in α/β T-cell deficient mice would lack the multiple immune suppressive benefits that Tregs would provide in a tumor microenvironment. However, a reduction in IL-10 expression could result in enhanced RONS production for a longer duration in α/β T-cell deficient mice that may potentiate cancer development.

Could innate cytolytic NK cell and γ/δ T-cell populations have enhanced anti-tumor cell cytolytic activity in Treg deficient mice? Would this drive down cancer incidence in the α/β T-cell deficient mice?

Both NK cells and γ/δ T-cell populations (peripheral circulating γ/δ T-cells and γ/δ IEL cells) will have normal development and a normal range of functions in α/β T-cell deficient mice. Both populations are potent anti-tumor cell cytolytic cells.⁽³⁴⁸⁾⁽³⁴⁹⁾⁽³⁵⁰⁾⁽³⁵¹⁾ Interestingly,

both populations may mediate cytolytic activity against tumor cells through NKG2D expression.⁽³⁴⁸⁾⁽³⁴⁹⁾⁽³⁵²⁾ The cytolytic potential of these cell populations, and the pro-inflammatory responses they can mount, will not be suppressed by Tregs in the α/β T-cell deficient mice.

3.3 DATA

3.3.1 Mice Strains and Treatment Groups Studied

Male (B6) Fox n1/J, Fox n1^{nu}/J athymic, WT, TCR $\beta^{-/-}$, TCR $\delta^{-/-}$, TCR $\beta^{-/-}\delta^{-/-}$ strains of mice were treated with AOM, DSS, or AOM+DSS to induce colon cancer. A summary table of these experimental results, that compares the colon cancer induction outcomes for each of the treatments on each of the strains, will be presented in this section. For a more comprehensive analysis of the results of each experiment, a table detailing the outcome of each experiment will be presented that will include a results summary.

3.3.2 The Significance of Studying a Sporadic Colon Cancer Induction model

The AOM+DSS treatment is a two-stage colon cancer induction model.⁽⁴⁴⁾ Treatment with AOM+DSS approximates sporadic colon cancer development in humans.⁽⁴⁶⁾ As the majority of colon cancer cases lack a known hereditary mutation as the primary driving force behind colon cancer incidence, sporadic colon cancer models are more reflective of the cancer development seen in most patients.⁽²¹⁷⁾ As the causative mutations of cancer are not predetermined, the effect of inducing colon cancer on a genetic knockout mouse strain can produce a novel result when compared to the WT mouse strain. Studying colon cancer induction in an immune compromised mouse model is not the same experiment as inoculating an immune compromised athymic or SCID mouse with cancer cells from another animal. The former study relates to the development of new cancer cells, while latter study reflects the effects of the immune response on established cancer cells. Treating α/β T-cell deficient mice with a sporadic colon cancer induction model

will provide novel insight into the development of colon cancer in an immune compromised system when compared to an immune competent WT mouse.

3.3.3 Colon cancer induction animal treatments

During the course of this work five different colon cancer induction animal experiments were performed using WT mice and immune compromised mice treated of the B6 mouse strain (Table 10):

Carcinogenicity Experiment 1: 20 Fox n1/J mice and 20 Fox n1^{nu}/J athymic mice were treated with one 10 mg/kg dose of AOM followed after one week by a 2% DSS treatment lasting one week.

Carcinogenicity Experiment 2: 20 Fox n1/J mice and 20 Fox n1^{nu}/J athymic mice were treated with one 10 mg/kg dose of AOM followed after one week by a 1% DSS treatment lasting one week.

Carcinogenicity Experiment 3: 15 Fox n1/J mice and 15 Fox n1^{nu}/J athymic mice were treated with one 15 mg/kg dose of AOM followed after one week by a 1.5% DSS treatment lasting one week.

Carcinogenicity Experiment 4: 12 WT mice, 10 TCR β ^{-/-} mice, 10 TCR δ ^{-/-} mice, and 10 TCR β ^{-/-} δ ^{-/-} mice were treated with one 15 mg/kg dose of AOM followed after one week by a 1.5% DSS treatment lasting one week.

Carcinogenicity Experiment 5: 6 WT mice and 6 TCR β ^{-/-} mice were treated with 200 ul of PBS. 12 WT mice and 12 TCR β ^{-/-} mice were treated with one 10 mg/kg dose of AOM. 12 WT mice and 12 TCR β ^{-/-} mice with treated with one 2% DSS treatment lasting one week. 12 WT

mice and 12 TCR $\beta^{-/-}$ mice were treated with one 10 mg/kg dose of AOM followed after one week by one 2% DSS treatment lasting one week.

3.3.3.1 Colon Tissue Harvesting and Preparation for H+E Staining

After the completion of their respective DSS treatments, the Fox n1/J mice and Fox n1^{nu}/J athymic mice used in Carcinogenicity Experiments 1, 2, and 3 were housed in the sterile animal facility for 120 days. At the end of the timecourse the mice were euthanized and their colons excised, placed in 4% formalin, and embedded in paraffin. Sections were cut and mounted on slides for H+E staining histological analysis.

After the completion of the DSS treatment the WT, TCR $\beta^{-/-}$, TCR $\delta^{-/-}$ mice, and TCR $\beta^{-/-}\delta^{-/-}$ mice used in Carcinogenicity Experiment 4 were housed in the sterile animal facility for 90 days. Upon completion of the timecourse the mice were euthanized and their colons excised, placed in 4% formalin, and embedded in paraffin. Sections were cut and mounted on slides for H+E staining histological analysis.

After the completion of the DSS treatment the WT mice and TCR $\beta^{-/-}$ mice used in Carcinogenicity Experiment 5 were housed in the sterile animal facility for 90 days. Upon completion of the timecourse the mice were euthanized and their colons excised, immersed in OCT medium (Tissue-Tek® Optimal Cutting Temperature Compound, Ted Pella, Inc., Redding, CA), and frozen on liquid N₂. Sections were then cut for each animal, the slides were placed in 4% formalin for 3 hours, and H+E stained histological analysis. Full details of all of the experimental methods are written in Chapter 5.

3.3.4 H+E Staining and Statistical Analysis

All of the histological analysis was performed by a medical pathologist. Briefly, in the normal colonic crypt architecture crypts appear as long test tube like glands with a regular diameter top to bottom, and display regular spacing between the crypts. The cells are in a single layer and have small nuclei, and goblet cells are abundant in the normal colon architecture.

Adenomas have small flat or polypoidal crypts that are similar in size, and have an approximate glandular size. There is more stromal space between the crypts, and there is more lymphatic infiltrate than is observed in the normal colon crypt architecture. The cells of the adenoma crypts have elongated nuclei that resemble a cigar like shape. The adenoma cells may or may not layer. Crypts at the edge of the adenoma do not exhibit any signs of invasion into the normal tissue layers. Also, adenomas do not show desmoplasia, the development of dense fibrous connective tissue from proliferating fibroblasts.⁽³⁵³⁾

Adenocarcinomas have large polypoidal crypts of varying glandular sizes. There is very scant stroma between the crypts and heavy lymphatic infiltrate. The cells of the adenocarcinoma crypts have large round nuclei and prominent nucleoli. Nucleoli are granular structures forming within the nucleus of a cell, composed of protein and RNA, for ribosomal RNA synthesis and the formation of ribosomes.⁽³⁵⁴⁾ The adenocarcinoma cells form layers and the crypts appear to thicken in comparison to normal epithelial crypts. Crypts at the edge of the adenocarcinoma bordering the normal tissue do exhibit signs of invasion into the normal tissue layers. Adenocarcinoma crypts are also positive for desmoplasia.

Although the carcinogenesis results of the AOM+DSS treatments were generated with only standard histological evaluation performed by a clinical pathologist, more advanced immunohistochemistry techniques could potentially distinguish between adenomas and

carcinomas. The expression of various marker proteins in human samples have shown significant changes in their expression between normal, adenomas, and adenocarcinomas. It has not been reported if the quantification of the expression of these marker proteins would correlate to mouse samples in the B6 background.

p53 expression was reported to have a significantly higher expression rate in colonic carcinomas in comparison to adenomas.⁽³⁷³⁾ Adenomas with high-grade dysplasia also showed more p53 expression.⁽³⁷³⁾ p53 is a tumor suppressor⁽³⁷⁴⁾ and it seems counterintuitive that p53 expression would increase in more progressed colonic epithelial cancer cell populations. No mutations in p53 that would inactivate the protein were reported in the article by Saleh, et. al.⁽³⁷³⁾ Nor were any mutations in mdm2 reported. Mdm2 serves as a negative regulator of p53 activity.⁽³⁷⁵⁾ p53 expression levels may indicate differences in the colonic tumors resulting from the AOM+DSS treated mice in this study. However, further studies in mice may be required to determine if p53 expression levels vary significantly between adenomas and adenocarcinomas as they appear to in human cancers.

Studies have also attempted to associate PCNA and CD34 expression levels to the progression of human colonic tumors.⁽³⁷⁶⁾⁽³⁷⁷⁾ The expression of PCNA (proliferating cell nuclear antigen) was found to be significantly higher in carcinoma cells than in adenomas and normal epithelial cells.⁽³⁷⁷⁾ CD34 expression levels were also significantly higher in colonic carcinoma cells than in adenoma cells or normal epithelial cells. CD34 (hematopoietic progenitor cell antigen) is a multifunctional protein that mediating the attachment of stem cells to the bone marrow extracellular matrix or directly to stromal cells.⁽³⁷⁸⁾ Both CD34 and PCNA expression levels may indicate differences in the colonic tumors resulting from the AOM+DSS treated mice in this study. However, further studies in mice may be required to determine if the expression

levels of either protein vary significantly between adenomas and adenocarcinomas as they appear to in human cancers.

Statistically significant differences in colon cancer incidence among the mice in the different experiments were determined using the Fisher's Exact Test. Cancer incidence (yes or no) is a categorical variable having no intrinsic value,⁽³⁵⁵⁾ and differences in categorical variables between two test groups undergoing the same treatment can be determined using a contingency table.⁽³⁵⁶⁾ The Fisher's Exact Test is a contingency table test best utilized when the treatment groups have small sample sizes.⁽³⁵⁷⁾ The t-test was used to determine the statistical differences in the multiplicity (total number of tumors), numbers of adenomas, and the number of adenocarcinomas, between treated groups of mice in the different experiments. Before statistical comparisons were made, the data sets were administered the normality test to show the values of the data followed a Gaussian distribution. Also, the F-test for Two Data Sets was used to determine the equality of variances between the data sets being compared. All of the data sets satisfied the requirements for the t-test to be used to analyze the data. The software used and details of the statistical methods are discussed in section 5.

3.4 CARCINOGENICITY EXPERIMENTS RESULTS SUMMARY

Table 11. Carcinogenicity Experiments Results Summary table

Experiment (#) Treatment	Mouse Strain (B6)	Incidence	Adenoma	Carcinoma	Multiplicity (Total)
Experiment I 10 mg/kg AOM 2% DSS	Fox n1/J	14/20	6	16	22
	Fox n1 ^{nu} /J athymic	n/a	n/a	n/a	n/a
Experiment II 10 mg/kg AOM 1% DSS	Fox n1/J	6/20	6	n/a	6
	Fox n1 ^{nu} /J athymic	3/20	3	n/a	3
Experiment III 15 mg/kg AOM 1.5% DSS	Fox n1/J	12/14	11 ^a	22 ^{b,g}	32
	Fox n1 ^{nu} /J athymic	11/12	19 ^a	7 ^b	26
Experiment IV 15 mg/kg AOM 1.5% DSS	WT	7/12 ^{c,d}	7	6 ^g	13 ^{e,f}
	TCRβ ^{-/-}	1/10 ^{c,h}	1 ⁱ	0	1 ^{e,j}
	TCRδ ^{-/-}	3/9	3	0	3
	TCRβ ^{-/-} δ ^{-/-}	1/9 ^d	1	0	1 ^f
Experiment V* 10 mg/kg AOM 2% DSS	WT	10/12	11	10	21
	TCRβ ^{-/-}	11/12 ^h	10 ⁱ	12	22 ^j

Results: $p=0.01180$ t-test

a) $p=0.02016$ t-test

e) $p=0.02369$ t-test

i) $p=0.01180$ t-test

b) $p=0.04593$ t-test

f) $p=0.02513$ t-test

j) $p=9.250e^{-05}$ t-test

c) $p=0.02630$ Fisher's exact test

g) $p=0.02660$ t-test

n/a = not applicable

d) $p=0.03750$ Fisher's exact test

h) $p=0.0151$ Fisher's exact test

Note:* no tumors developed in mice treated with AOM, treated with DSS, or were untreated.

Table 12. Carcinogenicity Experiment 1

Experiment I: Fox n1/J mice vs. Fox n1^{nu}/J athymic mice (B6) treated with AOM+DSS					
Table 12.					
Treatment	Mouse Strain (B6)	Incidence	Adenoma	Carcinoma	Multiplicity (Total)
10 mg/kg AOM 2% DSS	Fox n1/J	14/20	6	16	22
	Fox n1 ^{nu} /J athymic	n/a*	n/a*	n/a*	n/a*

Results:
Incidence: 14 out of 20 Fox n1/J mice developed tumors.
Adenomas: 6 adenomas occurred in the Fox n1/J mice.
Carcinomas: 16 carcinomas occurred in the Fox n1/J mice.
Multiplicity: 22 total tumors occurred in the Fox n1/J mice.
n/a: not applicable.

Note: *19 out of the 20 Fox n1^{nu}/J athymic mice died as a result of the 2% DSS treatment.

3.4.1.1 Results Summary and Analysis of Table 12, previous page

The Fox n1/J mice showed a high tumor incidence (70%), multiplicity (22 developed in 14 mice), and progression (16 out of 22 tumors were classified as carcinomas), after treatment with AOM+DSS. Fox n1/J mice are not immune compromised as these mice are heterozygotes for the Foxn1 transcription factor. The Foxn1 gene plays a part in the development of the intraepithelial of the thymus.⁽²⁸¹⁾ Since Fox n1/J mice have normal expression of one allele of the Foxn1 gene, their immune development should be normal.

73% of the total tumors in the Fox n1/J mice had progressed to carcinomas. The Fox n1/J mice exhibited a potent response to the 2% DSS treatment. The animals displayed the adverse symptoms common to severe DSS induced inflammation that included; blood in the stools, soft wet enlarged stools, rectal bleeding, and prolapsed rectums occurred in the mice after the DSS treatment.

The athymic mice could not tolerate the 2% DSS dose, and all of the mice died or were euthanized by seven days after the initiation of the DSS treatment. As they are immune compromised this result could indicate delayed and/or impaired colonic epithelial repair due to the loss of α/β T-cell mediated signaling. For example; if the expression of IL-22 was significantly reduced in the athymic mice compared to the WT mice, then the athymic mice might have experienced an impaired tissue wound repair response in the colon epithelium. However, the lack of the Foxn1 gene expression causes other developmental defects in the athymic mice, so more research would be needed to determine if the lack of α/β T-cell mediated signaling impacted this result.

Table 13. Carcinogenicity Experiment 2

Experiment II: Fox n1/J mice vs. Fox n1^{nu}/J athymic mice (B6) treated with AOM+DSS					
Table 13.					
Treatment	Mouse Strain (B6)	Incidence	Adenoma	Carcinoma	Multiplicity (Total)
10 mg/kg AOM 1% DSS	Fox n1/J	6/20	6	n/a	6
	Fox n1 ^{nu} /J athymic	3/20	3	n/a	3

Results:

Incidence: 6 out of 20 Fox n1/J mice developed tumors.
3 out of 20 Fox n1^{nu}/J athymic mice developed tumors.

Adenomas: 6 adenomas occurred in the Fox n1/J mice.
3 adenomas occurred in the Fox n1^{nu}/J athymic mice.

Carcinomas: No carcinomas occurred in the Fox n1/J mice.
No carcinomas occurred in the Fox n1^{nu}/J athymic mice.

Multiplicity: 6 total tumors occurred in the Fox n1/J mice.
3 total tumors occurred in the Fox n1^{nu}/J athymic mice.

n/a: not applicable.

Statistical Analysis: There were no statistical differences in the tumor incidence or multiplicity between the two strains of mice.

3.4.1.2 Results Summary and Analysis of Table 13, previous page

There were no significant differences in the tumor incidence or tumor multiplicity between the Fox n1/J mice and the athymic mice with this AOM+DSS treatment. Also, no adenocarcinomas developed in either strain. Only mild adverse effects of the DSS treatment were observed; soft stools with very little or no blood, no rectal bleeding, and no prolapsed rectums occurred. The effect of the 1% DSS dose as a tumor promoter on the immune compromised athymic mice could not be effectively assessed or compared to the immune competent control Fox n1/J mice since neither mouse strain exhibited a significant inflammatory response to the DSS treatment to potentiate tumor development, and produce a statically distinguishable difference between the strains.

Table 14. Carcinogenicity Experiment 3

Experiment III: Fox n1/J mice vs. Fox n1^{nu}/J athymic mice (B6) treated with AOM+DSS					
Table 14.					
Treatment	Mouse Strain (B6)	Incidence	Adenoma	Carcinoma	Multiplicity (Total)
15 mg/kg AOM 1.5% DSS	Fox n1/J	12/14	11 ^a	22 ^b	32
	Fox n1 ^{nu} /J athymic	11/12	19 ^a	7 ^b	26

Results:

Incidence: 12 out of 14 Fox n1/J mice developed tumors.
11 out of 12 Fox n1^{nu}/J athymic mice developed tumors.

Adenomas: 11 adenomas occurred in the Fox n1/J mice.
19 adenomas occurred in the Fox n1^{nu}/J athymic mice.

Carcinomas: 22 carcinomas occurred in the Fox n1/J mice.
7 carcinomas occurred in the Fox n1^{nu}/J athymic mice.

Multiplicity: 32 total tumors occurred in the Fox n1/J mice.
26 total tumors occurred in the Fox n1^{nu}/J athymic mice.

Statistical Analysis: a) *p*-0.02016 t-test;
Significantly higher numbers of adenomas occurred in the Fox n1^{nu}/J athymic mice when compared to the Fox n1/J mice.

b) *p*-0.04593 t-test;
Significantly higher numbers of adenocarcinomas occurred in the Fox n1/J mice when compared to the Fox n1^{nu}/J athymic mice.

3.4.1.3 Results Summary and Analysis of Table 14, previous page

Note that the AOM dose was increased from 10 mg/kg to 15 mg/kg to attempt to enhance the carcinogenic effect of the AOM+DSS treatment. Both strains of mice were able to tolerate the 15 mg/kg AOM treatment and the 1.5% DSS treatment. Typical adverse symptoms resulting from the DSS treatment were observed, but no mice died or had to be euthanized due to the adverse effects of the DSS treatment.

There was no significant difference in the tumor incidence or multiplicity between the Fox n1/J mice and the athymic mice. A significantly higher number of adenomas occurred in the athymic mice (19 adenomas) when compared to the Fox n1/J mice (11 adenomas) ($p=0.02016$ t-test). Also, a significantly higher number of adenocarcinomas occurred in the Fox n1/J mice (22 carcinomas) when compared to the athymic mice (7 carcinomas) ($p=0.04593$ t-test).

The lack of α/β T-cell populations in the immune deficient athymic mice did not lead to a significant change in the tumor incidence or multiplicity vs. the immune competent Fox n1/J mice. However, there is a significant difference in tumor progression between the two strains of mice.

Table 15. Carcinogenicity Experiment 4

Experiment IV: WT, TCRβ^{-/-}, TCRδ^{-/-}, and TCRβ^{-/-}δ^{-/-} mice (B6) treated with AOM+DSS					
Table 15.					
Treatment	Mouse Strain (B6)	Incidence	Adenoma	Carcinoma	Multiplicity (Total)
15 mg/kg AOM 1.5% DSS	WT	7/12 ^{c,d}	7	6	13 ^{e,f}
	TCR β ^{-/-}	1/10 ^c	1	0	1 ^e
	TCR δ ^{-/-}	3/9	3	0	3
	TCR β ^{-/-} δ ^{-/-}	1/9 ^d	1	0	1 ^f

Results:

Incidence: 7 out of 12 WT mice developed tumors.
 1 out of 10 TCR β ^{-/-} mice developed tumors.
 3 out of 9 TCR δ ^{-/-} mice developed tumors.
 1 out of 9 TCR β ^{-/-} δ ^{-/-} mice developed tumors.

Adenomas: 7 adenomas occurred in the WT mice.
 1 adenomas occurred in the TCR β ^{-/-} mice.
 3 adenomas occurred in the TCR δ ^{-/-} mice.
 1 adenomas occurred in the TCR β ^{-/-} δ ^{-/-} mice.

Carcinomas: 6 carcinomas occurred in the WT mice.

Multiplicity: 13 total tumors occurred in the WT mice.
 1 tumor occurred in the TCR β ^{-/-} mice.
 3 total tumors occurred in the TCR δ ^{-/-} mice.
 1 tumor occurred in the TCR β ^{-/-} δ ^{-/-} mice.

Statistical Analysis: **c)** *p*-0.0263 Fisher's Exact Test **d)** *p*-0.0375 Fisher's Exact Test;
 A significantly higher incidence of tumors occurred in the WT mice when compared to the (c) TCR β ^{-/-} mice and the (d) TCR β ^{-/-} δ ^{-/-} mice.
e) *p*-0.02369 t-test **f)** *p*-0.02513 t-test;
 A significantly higher number of tumors occurred in the WT mice when compared to the (e) TCR β ^{-/-} mice and the (f) TCR β ^{-/-} δ ^{-/-} mice.

3.4.1.4 Results Summary and Analysis of Table 15, previous page

The Fox n1^{nu}/J mice were poor breeders with high mortality among the pups, and orders could not be efficiently filled. Due to the difficulty of obtaining the athymic mice, and the problem of determining a tolerable DSS dose, the immune compromised athymic mice were replaced with TCR β ^{-/-} mice, TCR δ ^{-/-} mice, TCR β ^{-/-} δ ^{-/-} mice. The control mice for these knockout B6 mice strains is the WT mouse. The immune compromised T-cell deficient phenotype of the athymic and T-cell knockout mice should be the same.

The WT mice had a significantly higher incidence of mice with tumors (7 mice) than the TCR β ^{-/-} mice in which one mouse had one tumor ($p=0.0263$ Fisher's Exact Test). The tumor multiplicity was also significantly greater in the WT mice (13 tumors) than in the TCR β ^{-/-} mice (one tumor) ($p=0.02369$ t-test). Seven adenomas and six carcinomas developed in the WT mice while the TCR β ^{-/-} mice developed only one adenoma. With nearly half of the tumors classified as adenocarcinomas, there is also a more rapid cancer cell progression in the WT mice.

The TCR β ^{-/-} δ ^{-/-} mice responded to the AOM+DSS treatment in nearly identical fashion to the TCR β ^{-/-} mice. The WT mice had significantly higher incidence of mice with tumors (7 mice) compared to one mouse with one tumor in the TCR β ^{-/-} δ ^{-/-} mice ($p=0.0375$ Fisher's Exact Test). The total number of tumors was also significantly greater in the WT mice (13 tumors) than in the TCR β ^{-/-} δ ^{-/-} mice where only one tumor developed ($p=0.02513$ t-test). As with the TCR β ^{-/-} mice, there was only one adenoma and no carcinomas in the TCR β ^{-/-} δ ^{-/-} mice. However, these values are not significantly different from the numbers of adenomas and adenocarcinomas in the WT mice.

The TCR δ ^{-/-} mice were not significantly different from the WT mice in tumor incidence or tumor multiplicity after the AOM+DSS treatment. Three TCR δ ^{-/-} mice did have adenomas,

with one adenoma developing per mouse, which was approximately half of number of adenomas observed in the WT mice. There were no adenocarcinomas reported in the $\text{TCR}\delta^{-/-}$ mice.

While all of the immune compromised strains of mice showed inhibited colon tumor development, the α/β T-cell deficient mice and the T-cell double knockout mice showed the most significant restriction in cancer development. Emphasizing α/β T-cells as the most significant T-cell type related to DSS mediated tumor promotion. The mechanisms through which α/β T-cells mediate anti-pathogenic and tissue repair responses are thoroughly discussed in section 3.1.

Table 16. Carcinogenicity Experiment 5

Experiment V: WT mice and TCRβ^{-/-} mice (B6) treated with AOM, DSS, AOM+DSS, or untreated (Carcinogenicity Results for Mutagenesis Data)					
Table 16.					
Treatment	Mouse Strain (B6)	Incidence	Adenoma	Carcinoma	Multiplicity (Total)
PBS	WT	0/6	n/a	n/a	n/a
	TCR β ^{-/-}	0/6	n/a	n/a	n/a
10 mg/kg AOM	WT	0/12	n/a	n/a	n/a
	TCR β ^{-/-}	0/12	n/a	n/a	n/a
2% DSS	WT	0/12	n/a	n/a	n/a
	TCR β ^{-/-}	0/12	n/a	n/a	n/a
10 mg/kg AOM 2% DSS	WT	10/12	11	10	21
	TCR β ^{-/-}	11/12	10	12	22

Results:

Incidence: 10 out of 12 WT mice developed tumors.
11 out of 12 TCR β ^{-/-} mice developed tumors.

Adenomas: 11 adenomas occurred in the WT mice.
10 adenomas occurred in the TCR β ^{-/-} mice.

Carcinomas: 10 carcinomas occurred in the WT mice.
12 carcinomas occurred in the TCR β ^{-/-} mice.

Multiplicity: 21 total tumors occurred in the WT mice.
22 total tumors occurred in the TCR β ^{-/-} mice.

n/a: not applicable

Statistical Analysis: There were no statically significant differences in the tumor incidence, multiplicity, or progression between the WT mice and the TCR β ^{-/-} mice.

3.4.1.5 Results Summary and Analysis of Table 16, previous page

The AOM used in this experiment was a higher purity (98%) compound than the AOM used in the previous experiment (90%). The (98%) AOM led to toxicity and mortality (one-third of the mice treated died) at the 15 mg/kg dose. Therefore, the AOM dose had to be lowered so the mice could tolerate the AOM treatment. The DSS dose was increased to enhance the carcinogenic effect of the AOM+DSS treatment. As the WT mice and the $\text{TCR}\beta^{-/-}$ mice were more tolerant of the DSS treatment than the Fox n1 deficient mice, it was reasonable to assume a 0.5% increase in the DSS dose would be tolerated by both strains of mice. The WT mice and the $\text{TCR}\beta^{-/-}$ mice exhibited only mild adverse effects of the 2% DSS treatment, although several mice developed prolapsed rectums near the end of the timecourse.

There were no tumors reported in the WT mice and the $\text{TCR}\beta^{-/-}$ mice treated with PBS (untreated), 10 mg/kg AOM, or 2% DSS. There were no statically significant differences in the tumor incidence, multiplicity, or progression between the WT mice and the $\text{TCR}\beta^{-/-}$ mice treated with 10 mg/kg AOM + 2% DSS treatment. This is a striking contrast to the previous experiment which showed a strong inhibition of cancer development in the immune compromised mice. The WT mice and $\text{TCR}\beta^{-/-}$ mice show nearly identical numbers of tumor incidence, multiplicity, adenomas, and carcinomas.

3.4.2 Differences between the Carcinogenicity Experimental Groups

3.4.2.1 Fox n1/J mice developed significantly more carcinomas than the WT mice (Table 11)

Fox n1/J mice developed significantly more carcinomas (22 carcinomas) than the WT mice (6 carcinomas) using the same AOM+DSS treatment doses ($p=0.02660$ t-test). The Fox n1/J mice are heterozygotes for the Fox n1 transcription factor gene so these mice should be expressing the gene normally, as they carry one copy of the allele. However, the Fox n1/J mice are clearly more susceptible to DSS induced inflammation, as they exhibited more severe adverse effects of the DSS treatment when compare the WT mice treated at the same DSS dose. This result may indicate that the Fox n1/J mice heterozygotes have a significantly different differential gene expression than the WT mice.

3.4.2.2 Cancer incidence, multiplicity, and progression was significantly higher in the TCR $\beta^{-/-}$ mice after Carcinogenicity Experiment 5 than was observed for the TCR $\beta^{-/-}$ mice after Carcinogenicity Experiment 4 (Table 11)

There was a striking increase in the tumor incidence, multiplicity, and progression in the TCR $\beta^{-/-}$ mice after the 10 mg/kg AOM + 2% DSS treatment used in Carcinogenicity Experiment 5 (Table 11) vs. what resulted in the TCR $\beta^{-/-}$ mice after the 15 mg/kg AOM + 1.5% DSS treatment used in Carcinogenicity Experiment 4 (Table 11). The tumor incidence increased from one mouse in ten TCR $\beta^{-/-}$ mice after Carcinogenicity Experiment 4 to eleven mice in twelve TCR $\beta^{-/-}$ mice after Carcinogenicity Experiment 5. The tumor multiplicity increased from one tumor in the TCR $\beta^{-/-}$ mice after Carcinogenicity Experiment 4 to twenty-two total tumors in the

TCR $\beta^{-/-}$ mice after Carcinogenicity Experiment 5. The number of adenomas increased from one in the TCR $\beta^{-/-}$ mice after Carcinogenicity Experiment 4 to ten adenomas in the TCR $\beta^{-/-}$ mice after Carcinogenicity Experiment 5. Finally, no adenocarcinomas developed in the TCR $\beta^{-/-}$ mice after Carcinogenicity Experiment 4, but twelve developed in the TCR $\beta^{-/-}$ mice with the AOM+DSS treatment used in Carcinogenicity Experiment 5.

A DSS dose effect has been observed in AOM+DSS studies,⁽¹⁶⁷⁾ DSS treatments range from a 1-5% concentration for one week, so a 0.5% DSS dose increase can produce a substantially more severe colonic inflammation. Also, the composition of the colonic microbiota, both the bacterial strains and density, can alter the tolerance to the DSS dose of the mice being treated.⁽¹⁴¹⁾⁽¹⁴³⁾

3.5 SUMMARY AND DISCUSSION

Studying the effect of colon carcinogenesis induced by AOM+DSS treatment on immune competent mice and immune compromised mice produced results that were both insightful and confounding. The 2% DSS treatment in the first experiment was toxic to the Fox n1^{nu}/J athymic mice, while the 1% DSS treatment in the second experiment failed to elicit a severe enough inflammatory response to potentiate cancer development in either mouse strain. In the third experiment, the Fox n1^{nu}/J athymic mice had significantly more adenomas and significantly fewer adenocarcinomas than Fox n1/J mice, while the mice had a similar total number of tumors. This result suggests a role for α/β T-cell mediated tumor promotion, where the immune competent mice have more rapid progression of cancer cell development. In the fourth experiment the AOM+DSS treated WT mice had a significantly higher cancer incidence, multiplicity, and faster progression of cancers than the TCR $\beta^{-/-}$ mice and TCR $\beta^{-/-}\delta^{-/-}$ mice. These results would indicate that cancer cell development is actually being impeded in the absence of α/β T-cell mediated signaling.

The fifth experiment was performed to study the mutagenic and carcinogenic effect of the AOM, DSS, and AOM+DSS treatments. In the fifth experiment there was no statistical difference between the WT mice and TCR $\beta^{-/-}$ mice in cancer incidence, multiplicity, or the progression of cancer after treatment with AOM+DSS. The result seen in the TCR $\beta^{-/-}$ mice occurred in response to a 0.5% DSS dose increase between the fourth and fifth carcinogenicity experiments. This could suggest that the severity of the inflammation may determine how immune cells respond after treatment with DSS, and it is possible the α/β T-cell mediated signaling that is absent in the TCR $\beta^{-/-}$ mice was compensated for by other cells in a more severe

inflammation. Interestingly, there was a very significant increase in the cancer incidence, multiplicity, and progression of cancer observed in the $\text{TCR}\beta^{-/-}$ mice treated in the fifth carcinogenicity experiment in comparison to the $\text{TCR}\beta^{-/-}$ mice treated in the fourth carcinogenicity experiment. However, there was no significant difference in cancer incidence and tumor multiplicity in the WT mice treated in the fifth carcinogenicity experiment in comparison to the WT mice treated in the fourth carcinogenicity experiment.

If the severity of the inflammation potentiates cancer development, then factors that determine the severity of an inflammatory event must be a significant factor impacting carcinogenesis. A deficiency in α/β T-cell mediated signaling impeded cancer development in a mild or moderate inflammatory environment, but a more severe inflammation in the colon negated the inhibition seen in the α/β T-cell deficient mice. The results of these studies would suggest that immune competent WT mice are in fact more susceptible to cancer development than α/β T-cell deficient mice.

3.5.1 Discussion of the potential reasons why the athymic mice so adversely affected by the DSS treatment

Treating the athymic mice with 2% DSS for one week resulted in 19 out of 20 mice dying or being euthanized (Table 12). It is likely the athymic mice were affected more severely than the Fox n1/J mice due to the composition of their commensal microflora. Germ-free and some specific-pathogen free mice are more severely affected by high doses of DSS, and it is likely the microbiota in the athymic mice were not able to protect the colon epithelium. This result is reminiscent of the effect of DSS treatments above 1% in germ-free mice reported in the literature.⁽¹⁴¹⁾⁽¹⁴³⁾ While the athymic mice were littermates of the Fox n1/J mice, the animals are eventually housed separately. Since the athymic mice are not all siblings it is likely their floral composition diverged from the Fox n1/J mice.

The athymic mice may also have been unable to tolerate higher DSS doses due to deficient immune cell signaling. IEL T-cells are strongly associated with homeostatic functions and tissue repair in the colonic epithelium,⁽³²⁾⁽²³⁷⁾ and the lack of resident IELs in the athymic mice could have delayed or impaired the initiation of the epithelial wound repair. Also, the loss of the Fox n1 gene expression impairs the intraepithelial development of the thymus, so it is possible wound repair and regeneration responses in other epithelial tissues may experience impaired effects as well. These different explanations are also not necessarily mutually exclusive.

3.5.2 Discussion of the potential reasons why the treatment failed to promote tumor development in the athymic mice and in the Fox n1/J mice

As discussed in section 1.5.5 and 2.1, the composition of the colonic microbiota can mitigate the adverse effects of the DSS treatment by increasing the animal's tolerance for the DSS dose. This would mean that mice with certain colonic microbiota would require DSS treatments at higher doses to potentiate cancer development than other mice would require with different flora. This effect may even be strain independent. While the 2% DSS dose was clearly toxic to the athymic mice, the 1% DSS treatment did not induce a severe enough immune response to potentiate cancer development in either mouse strain. The small numbers of adenomas developing in the immune competent Fox n1/J mice supports this conclusion (Table 13). Based on their response to the 2% DSS treatment from the first trial, the Fox n1/J mice did not have a severe enough immune response to potentiate cancer development.

3.5.3 Why did more adenocarcinomas develop in the Fox n1/J mice compared to the athymic mice after the third AOM+DSS treatment?

While the tumor incidence and multiplicity were not significantly different between the Fox n1/J mice and athymic mice, significantly more adenocarcinomas developed in the Fox n1/J mice after treatment with AOM+DSS (Table 14). The role of the immune response in cancer development is expected to impede and inhibit cancer cell progression and pathology. However, the immune competent mice had more tumors progress to cancers than the immune compromised mice during the same timecourse.

If the anti-bacterial innate immune response is resolved quickly, as the pro-inflammatory response is suppressed by Treg cells and Th2 cells, then tissue repair and regeneration can be initiated within a short duration from the onset of the DSS treatment. In the athymic mice, lacking immune suppressive α/β T-cells, the innate immune response against the bacteria may be prolonged in comparison to the Fox p1/J mice. This hypothesis would suggest that the cancer potentiating effect of inflammation is a part of the repair and regeneration of the colon epithelium. Therefore, the quicker the tissue repair can be initiated the more potent the cancer development will be. This would also suggest that a significant component the cancer potentiating effect of inflammation lies in the duration of the inflammatory response, specifically related to how rapidly the pro-inflammatory response can be ended and repair initiated. As discussed in section 3.5.1., the reasons the athymic mice experienced a greater toxicity to the DSS treatment, such as a potential delay in epithelial repair initiation, may have led to a latency in cancer development as well.

3.5.4 Why were the WT mice sensitive to AOM+DSS treatment and the immune compromised $\text{TCR}\beta^{-/-}$ mice and $\text{TCR}\beta^{-/-}\delta^{-/-}$ mice resistant to AOM+DSS induced colon cancer by comparison?

In the fourth carcinogenicity experiment the WT mice had a 60% tumor incidence, with the mice developing an equivalent number of adenomas and carcinomas (Table 15). Interestingly, in both the $\text{TCR}\beta^{-/-}$ mice and the $\text{TCR}\beta^{-/-}\delta^{-/-}$ mice only one animal developed one adenoma per group (Table 15). In the previous section 3.5.3., the suggestion was made that the cancer potentiating effect of the DSS treatment is enhanced by a rapid resolution of the anti-pathogenic immune response. This result also suggests that the more rapidly α/β T-cell signaling moves toward anti-

inflammatory signaling, the stronger the tumor potentiating effect of DSS derived inflammation becomes. The duration of the anti-bacterial inflammatory response occurring in the WT mice would be considered normal, as the WT mice have immune suppressive Treg cells and Th2 cells to resolve the pro-inflammatory response. The $\text{TCR}\beta^{-/-}$ mice and $\text{TCR}\beta^{-/-}\delta^{-/-}$ mice are likely to have a dysregulated duration of an innate pro-inflammatory response, favoring an inappropriately long duration of an innate pro-inflammatory response and delaying the onset of tissue repair.

Resolution of the pro-inflammatory response does not mean the end of immune cell signaling. As discussed in section 3.1, one of the outcomes of Treg and Th2 cell signaling is the modulation of monocyte differentiation. Through IL-10 signaling Tregs inhibit Th1 cells to drive down the expression of $\text{INF}\gamma$ that polarizes monocytes into the M1 macrophage phenotype.⁽³²⁴⁾⁽³²⁵⁾⁽³²⁶⁾⁽³²⁷⁾⁽³²⁸⁾ Th2 derived IL-4/IL-13 modulate infiltrating monocytes to adopt the tissue regenerative M2 macrophage phenotype (M2 cells).⁽³⁰⁵⁾⁽³⁰⁶⁾⁽³⁰⁷⁾⁽³⁰⁸⁾ M2 cells express an array of cytokines, such as VEGF and IGF-1, that support angiogenesis, lymphangiogenesis, and epithelial restitution.⁽²²⁹⁾⁽²³⁰⁾⁽²³¹⁾⁽²³¹⁾⁽²³³⁾⁽²³⁴⁾⁽²³⁵⁾ M2 cells may even express $\text{NO}\cdot$ as an anti-inflammatory extracellular signaling molecule.⁽¹⁵⁷⁾⁽¹⁵⁸⁾

DSS exposure is particularly devastating to colonic epithelial macrophages and DCs. The onset of the DSS pathology initiates with the oncosis of macrophages as they phagocytize the dextran based molecule.⁽⁸⁴⁾⁽⁸⁵⁾ The only functional macrophages would be newly derived from the influx of monocytes into the site of inflammation, although DSS also disrupts monocyte maturation.⁽⁸⁹⁾ Still, the WT mice would be more capable of polarizing monocytes into M2 cells than the α/β T-cell deficient mice as WT mice have Th2 cells. The presence of the M2 cells in the WT mice could lead to more rapid immune suppression and onset of epithelial repair than the

α/β T-cell deficient mice would experience. The fact that the WT mice are more susceptible to colon cancer induction with an AOM+DSS treatment suggests that α/β T-cell mediated modulation of the monocytes into M2 cells could be an important component of DSS mediated tumor promotion.

The $\text{TCR}\delta^{-/-}$ mice, which are γ/δ T-cell deficient, did not show a significant decrease in tumor incidence or multiplicity from the WT mice due to the small sample sizes of the animal treatment groups. However, no adenocarcinomas developed in these mice after the AOM+DSS treatment. As these mice are α/β T-cell competent the conclusions addressing the results of the AOM+DSS treatment on the $\text{TCR}\beta^{-/-}$ B6 mice would not apply to this result.

γ/δ T-cells comprise only a small percentage of the peripheral T-cell population, but are strong presence in the tissue resident IELs. $\text{TCR}\delta^{-/-}$ mice have been shown to have delayed colonic epithelial repair after treatment with DSS in comparison to WT mice.⁽²³⁸⁾ γ/δ IELs supply critical growth factors to the colonic epithelium.⁽²³⁶⁾ Also, γ/δ IELs would be one of the very first immune cells activated by DSS induced damage, helping to shape the initial immune response before the influx of circulating immune cells.⁽²²¹⁾ The less potent effect of the AOM+DSS treatment on tumor induction in the $\text{TCR}\delta^{-/-}$ mice in comparison to the WT mice could suggest a role for the γ/δ IEL subset in potentiating inflammation induce carcinogenesis, although this role is likely to be concomitant with the α/β T-cells.

Interestingly, the restricted cancer development in the α/β T-cell deficient mice does not eliminate the possibility that innate cytolytic cells, NK cells and γ/δ T-cells, may have an increased efficacy of anti-tumor cell cytotoxicity in the absence of Tregs. It could be possible that the α/β T-cell deficient mice express less TGF-beta to inhibit innate cytolytic cells, as the pro-

inflammatory response is also likely diminished without α/β T-cells.⁽²⁴¹⁾⁽²⁴²⁾ An absence of Tregs and reduced levels of TGF-beta expression would allow innate cytolytic cells to avoid the strong immunosuppressive restrictions they normally operate under.

3.5.5 Why was the significant difference in cancer development observed between the WT mice and the TCR β ^{-/-} mice after the fourth carcinogenicity experiment no longer observed in the WT mice and TCR β ^{-/-} mice after the fifth carcinogenicity experiment? (Table 11)

There was a very significant difference in carcinogenesis between the TCR β ^{-/-} mice treated in the fourth carcinogenicity experiment and the TCR β ^{-/-} mice treated in the fifth carcinogenicity experiments (Table 11). The increase in tumor incidence, multiplicity, adenomas, and carcinomas in the TCR β ^{-/-} mice after the 10 mg/kg AOM + 2% DSS treatment used in Carcinogenicity Experiment 5 resulted in there being no significant difference in cancer development between the WT mice and TCR β ^{-/-} mice in the fifth carcinogenicity experiment (Table 16). However, the WT mice did not have a significant change in cancer development between the fourth and the fifth carcinogenicity experiments (Table 11). It is interesting that the values of the cancer incidence, multiplicity, adenomas and carcinomas between the WT mice and the TCR β ^{-/-} mice are very similar. Is it possible that the increased inflammation resulting from the higher DSS dose led to compensation for the deficient α/β T-cell mediated signaling?

It can be concluded that α/β T-cell mediated signaling is not indispensable to inflammation potentiating cancer development. If compensatory signaling occurred that caused the α/β T-cell deficient mice to adopt a similar phenotype to the WT mice in a more severe inflammatory event, then which cells and signaling molecules could have been responsible for

this? It has already been suggested that RONS, such as $\text{NO}\cdot$, can lead to anti-inflammatory signaling when RONS is generated in high concentrations.⁽¹⁵⁷⁾⁽¹⁵⁸⁾ It has been reported that high concentrations of RONS signaling may also polarize monocyte differentiation into M2 cells.⁽³⁵⁸⁾ If high RONS concentrations do polarize monocytes into M2 cells, then this could generate M2 cells in the $\text{TCR}\beta^{-/-}$ mice during a severe inflammatory insult. The M2 cells would then be able supply the normal levels of cytokines that potentiate epithelial wound repair. This would effectively be compensating for the loss of Th2 cell signaling in the $\text{TCR}\beta^{-/-}$ mice that would normally polarize influxing monocytes into M2 cells, through the expression of IL-4/13. This compensation may help to resolve the pro-inflammatory response in a shorter duration, one that matches the WT mice thereby potentiating cancer development. In WT mice with normal Th2 cell development and signaling, the impact of the RONS concentrations would be less significant to M2 cell polarization. This would partially explain why the WT mice did not have a significant change in cancer development between the fourth and fifth carcinogenicity experiments.

IL-10 represents an intriguing possibility as a compensatory signaling molecule. While Tregs are an important source of IL-10 expression, IL-10 is expressed by other cell types including M2 macrophages. IL-10 may also be expressed by enterocytes in response to insults, as was shown by a study using a human enterocyte cell culture line.⁽³⁵⁹⁾ IL-10 must be expressed by cells other than α/β T-cells in the $\text{TCR}\beta^{-/-}$ mice as these animals do not spontaneously develop colitis. IL-10^{-/-} mice will spontaneously develop colitis, unless they are germ-free, and this spontaneous inflammation acts as a tumor promoter if the IL-10^{-/-} mice are treated with AOM.⁽¹⁵¹⁾⁽¹⁵²⁾

Since there was so little difference in the carcinogenicity data between the WT mice and the $\text{TCR}\beta^{-/-}$ mice with more severe inflammation, uninhibited innate cytolytic cell activity must

not have an impact on this result. In spite of the absence of Tregs, innate cytolytic cell activity did not lead to a reduction in the tumors in the $\text{TCR}\beta^{-/-}$ mice. Understanding why innate anti-tumor cells (NK cells and γ/δ T-cells) did not eliminate cancer cells, in an environment that should have left their cytolytic anti-tumor cell activity enhanced, could represent an important research question.

4.0 ARE MUTATIONS THE RATE LIMITING COMPONENT OF CARCINOGENESIS?

4.1 SCOPE AND SYNOPSIS

The first section of Chapter 4 presents a summary of the mutagenesis data from Chapter 2 and its relationship to the carcinogenesis experimental data in Chapter 3. The following section discusses a possible explanation for the results.

4.2 RESULTS SUMMARY AND ANALYSIS OF THE MUTAGENESIS DATA (TABLE 1) AND CARCINOGENESIS DATA (TABLE 16) FOR THE WT MICE AND TCR β ^{-/-} TREATED WITH 10 MG/KG AOM, 2% DSS AND 10 MG/KG AOM + 2% DSS

One of the significant results of this study indicates that although mutagenesis is indispensable to carcinogenesis, mutations are not the sole determinate factor in cancer development. Also, mutagenesis is not the mechanism through which DSS induced inflammation potentiates cancer. What effects could inflammation have on a cell with an oncogenic mutation to drive it toward becoming a cancer cell?

A significantly higher G6PD M.F. occurred in the WT mice than occurred in the TCR β ^{-/-} mice after one treatment with AOM (Table 1). As G6PD mutations are a conservative marker for

somatic stem cell mutations, it is likely many different types of mutations were fixed in colonic stem cells that subsequently produced progeny cell populations harboring those mutations. However, in spite of the likely oncogenic mutations in certain stem cells, no tumors developed in the WT mice or the $\text{TCR}\beta^{-/-}$ mice after one treatment with AOM (Table 16). This result would indicate that the mutations generated by the AOM treatment were not the primary driving force behind cancer development.

It is generally assumed that RONS resulting from the DSS induced inflammation leads to a substantial increase in mutations. However, DSS did not cause somatic stem cell mutations in G6PD in either mouse strain (Table 1). No tumors developed in the WT mice or the $\text{TCR}\beta^{-/-}$ mice after one treatment with DSS (Table 16). While it is possible that somatic stem cell mutations did occur as a result of RONS damage generated by the DSS treatment, these mutations did not lead to tumor development. The immune status of the mice did not impact the occurrence of G6PD mutant crypts after treatment with DSS, however, this result contrasts the AOM treatment where the immune status of the mice did impact the occurrence of G6PD crypts (Table 1).

A significant cancer development resulted in both the WT mice and in the $\text{TCR}\beta^{-/-}$ mice after one treatment with 10 mg/kg AOM + 2% DSS treatment (Table 16). Interestingly, the immune status of the mice did not impact the colon cancer development after the 10 mg/kg AOM + 2% DSS treatment (Table 16). This is despite the fact that the G6PD M.F. was significantly higher in the WT mice in comparison to the $\text{TCR}\beta^{-/-}$ mice (Table 1). This difference in the G6PD M.F was observed after both the AOM treatment and the AOM+DSS treatment. Conventional understanding says that mutations are the driving cause of carcinogenesis. However, in this work the G6PD M.F. did not correlate to tumor burden in either strain of mice.

4.3 IF MUTATIONS ARE NOT THE ONLY DETERMINATE FACTOR IN CARCINOGENESIS, THEN WHAT OTHER MECHANISMS WOULD POTENTIATE CANCER CELL DEVELOPMENT?

It has been proposed that the pre-cancer cell population arises from a colonic epithelial stem cell with an oncogenic somatic mutation.⁽²⁹⁾ This process begins with a stem cell suffering DNA alkylation damage from treatment with AOM. This cell must successfully complete cell division with the unrepaired lesion leading to a mutation, and the cell harboring the mutation must remain a stem cell in the stem cell niche. Furthermore, the mutated stem cell must usurp the dominate position in the niche and begin to propagate cells. A mutated stem cell is more likely to dominate a niche if the mutation confers a selective advantage.⁽³⁰⁾⁽³¹⁾ So which gene, if mutated, is oncogenic and provides a selective advantage to stem cells?

Beta-catenin is a transcription factor that is strongly associated with colon cancer development.⁽²¹²⁾ Beta-catenin is regulated by a multiprotein phosphodestruction complex that phosphorylates specific amino-acids on beta-catenin targeting it for ubiquitin-proteasome degradation. The phosphodestruction complex itself can be regulated through extracellular Wnt signaling,⁽²¹³⁾ where the complex is transiently inactivated by Wnt binding to allow for beta-catenin DNA binding and transcription. The phosphodestruction complex is mutated, primarily in the APC protein,⁽³¹⁾ in the vast majority of colon cancers in both mice and humans.⁽²¹⁷⁾ However, AOM treatments frequently induce beta-catenin mutations in mice that prevent the phosphorylation of beta-catenin by GSK-3, a protein of the phosphodestruction complex.⁽²¹⁴⁾⁽²¹⁵⁾⁽²¹⁶⁾ A somatic mutation in beta-catenin would confer a selective advantage to a stem cell, enhancing the likelihood it could usurp a stem cell niche and propagate a population of epithelial cells expressing a mutated beta-catenin resistant to phosphodegradation.⁽³⁰⁾⁽³¹⁾

Yet, AOM treatments are not enough to cause colon cancer development in B6 mice.⁽¹⁶⁰⁾⁽¹⁶¹⁾ Could B6 mice be resistant to AOM induced mutations? If that were the case then treatment with AOM followed by treatment with DSS would not create colon cancer susceptibility in the B6 mice.⁽¹⁶⁴⁾ Does treatment with DSS affect beta-catenin in a way that is unique in comparison to other oncogenes, one that leads to an enhancement of a mutated beta-catenin protein's activity?

4.3.1 Beta-catenin activity is dysregulated by anti-inflammatory immune cell signaling during epithelial restitution

Beta-catenin is a transcription factor that also combines with E-cadherin to form tight cell-cell adhesion junctions linking epithelial cells together and forming a barrier to the lumen of the colon.⁽²¹⁷⁾ Binding beta-catenin into the catenin binding domain of E-cadherin is essential for maintaining epithelial cell-cell adhesion junctions,⁽²¹⁷⁾ while also allowing beta-catenin to act as an intracellular signaling molecule in response to extracellular modulation of a cell's plasma membrane. In fact, beta-catenin activity is regulated by forming cell-cell adhesion protein complexes as well as through beta-catenin phosphodegradation.⁽³⁶⁰⁾⁽³⁶¹⁾⁽³⁶²⁾

Treatment with DSS disrupts the epithelial layer through dysregulating tight cell-cell junction complexes.⁽⁹⁷⁾⁽⁹⁸⁾ In turn this would dysregulate beta-catenin by increasing the free intracellular concentration of the transcription factor. Cells with a normal form of beta-catenin may be able to compensate for an increase in free intracellular beta-catenin levels through phosphodegradation, but cells with a mutated beta-catenin that prevents phosphorylation may be forced to function with the higher than normal intracellular concentration of beta-catenin. These cells would then be vulnerable to enhanced beta-catenin activity driving the cells toward

carcinogenesis. It is important emphasize that increased intracellular beta-catenin levels are not the result of increased beta-catenin transcription and translation, but are resulting from a decrease in E-cadherin complex cell-cell junctions.

Beta-catenin activity is dysregulated by anti-inflammatory immune cell signaling during epithelial restitution. Treatment with DSS causes epithelial cell death but so does treatment with AOM, bacterial and viral infections, wounds, etc... However, DSS treatment causes a loss of colonic crypt morphology and, depending on the severity of the DSS induced damage and inflammation, the disrupted colon architecture can persist for weeks after the DSS treatment ended.⁽⁸⁵⁾⁽⁸⁶⁾ Epithelial restitution is a physiological process where undamaged epithelial cells at the edge of a wound will migrate into the wound space to reconstitute the epithelial barrier.⁽²³⁵⁾ To accomplish this epithelial cells, primarily enterocytes, can assume a motile non-columnar non-axial morphology by eliminating many E-cadherin cell-cell junctions among other significant changes.⁽²³⁴⁾⁽²³⁵⁾ Epithelial cells in this form are considered to be partially dedifferentiated and are capable of undergoing mitotic cell division.⁽²³⁴⁾⁽²³⁵⁾

Insulin-like growth factor 1 (IGF-1) is a mitogenic growth factor that induces the partial dedifferentiation of epithelial cells.⁽²³³⁾⁽²³⁴⁾ IGF-1 is expressed by M2 cells, that are polarized from monocytes by Th2 cells through the expression of IL-4/13.⁽³⁰⁵⁾⁽³⁰⁶⁾⁽³⁰⁷⁾⁽³⁰⁸⁾ If DSS treatment leads to polarizing M2 cells that express IGF-1, then epithelial cells are being induced into a partially dedifferentiated state that will contribute to the disrupted crypt architecture. If a stem cell with a somatic mutation in beta-catenin, which either prevents beta-catenin phosphorylation or inactivates the phosphodegradation complex, is generating progeny then those cells would be vulnerable to enhanced beta-catenin activity while they are in the dedifferentiated state. Therefore, the DSS treatment is effectively creating a window of opportunity for enhanced beta-

catenin activity, which then potentiates carcinogenesis in epithelial cells with mutated beta-catenin regulation.

This window of beta-catenin dysregulation can be opened by rapidly resolving the pro-inflammatory response, leading to M2 cells polarized from monocytes through anti-inflammatory signaling. Anti-inflammatory and wound repair induced dysregulation of epithelial cell turnover will also prolong the window of beta-catenin dysregulation. An increased rate of stem cell division will provide more cells with mutated beta-catenin, while epithelial cells will be able to resist normal apoptotic induction in attempting to reconstitute the wounded epithelium and maintain a partially dedifferentiated state for a significant length of time.⁽¹¹⁾⁽¹²⁾ As DSS treatments can lead to a disrupted crypt morphology that persists for several weeks, the cells with the mutated beta-catenin could experience a significant length of time with beta-catenin having enhanced activity. This duration in a dedifferentiated state must be long enough to cause further changes in a few of these cells to progress into cancer cells.

Treatment with AOM had to generate somatic beta-catenin mutations, as a single treatment with DSS did not lead to any detected G6PD mutations, but the mice that only received an AOM treatment did not develop cancer. So despite the likelihood of crypts with dominant stem cells harboring a somatic mutation in beta-catenin, these cell populations did not experience an additional level of beta-catenin dysregulation that potentiated cancer development without the DSS treatment. Whether a stem cell divides symmetrically or asymmetrically, both cell copies would rapidly assume their designated position in the normal crypt niche architecture. The newly divided cell would only transiently have a motile morphology, and once it relocates within the niche, would assume a normal columnar axial morphology with an identifiable apical-basal axis. The cells would then express the appropriate level of E-cadherin cell-cell junctions and

normalize the free intracellular beta-catenin levels. Regulating beta-catenin levels through E-cadherin cell-cell junction complexes must be sufficient to prevent enhanced beta-catenin transcriptional activity in cells with a beta-catenin mutation that inhibits phosphodegradation. Also, nearly all stem cell divisions are asymmetrical so cells will progress to lineage differentiation and turnover before the mutated beta-catenin will have time to produce a deleterious carcinogenic effect.

5.0 CONCLUSIONS AND SIGNIFICANCE

The work presented here generated several important basic scientific findings. While it will require more studies and time to gauge the overall impact of our results, they still provide several important observations. These observations challenge some long standing ideas and could force a reexamination of established dogma related to chemical carcinogenesis and the role of inflammation.

- 1) The work herein indicates that a fully competent immune system enhances the survival and continued cell division of DNA alkylation damaged colonic stem cells. While α/β T-cell deficient mice exhibited a reduction in the survival DNA alkylation damaged colonic stem cells. This result is significant in several ways. For the first time this result suggests that immune cells and the immune response, at least partially mediated by α/β T-cells, protects or enhances the survival of colonic stem cells with DNA alkylation damage. The increase in stem cell mutations in wild type vs. TCR null mice represents an entirely new functional capacity for immune cells that had previously not been elucidated. As α/β T-cells already are components of a myriad of immune cell mediated functions it may not be surprising to see these cells implicated in a new capacity. The enhanced damaged stem cell survival may be an effect of the activity of multiple immune cells, and not solely a α/β T-cell mediated response. The significance to carcinogenesis may be even more profound, as it seems that involvement of the immune system in responding to

cytotoxicity resulting from DNA alkylation damage leads to the development of an expanded pre-cancer cell population. It would be interesting to know if the enhance survival of DNA alkylated stem cells is restricted to colonic stem cells or if any DNA alkylated cell would be protected from cell death.

- 2) Our work demonstrated that DSS does not yield somatic stem cell mutations in either wild type or TCR null mice. This is a critical observation as inflammatory agents, such as DSS, have been associated with the generation of RONS and it is widely assumed that RONS leads to oxidative DNA lesions that cause an increase in the mutation rate. This is clearly incorrect in mice with a normal DNA repair capacity. This result forces the question of the actual function of the inflammatory agent, which is required for tumorigenesis.
- 3) The DSS treatment following the AOM treatment actually reduced the number of somatic stem cell mutations in both the WT and α/β T-cell deficient mice. However, the cancer incidence, multiplicity and progression, was not significantly different between two strains of mice at the higher 2% DSS but lower dose of AOM, although the M.F. was significantly higher in the WT mice. The significance of this result confirms that the generation of somatic stem cell mutations does not correlate with colon cancer development. The generation of mutations in critical target cells appears to not be the rate-limiting step in cancer development.
- 4) We calculated for the first time the in vivo conversion efficiency of an O⁶mG lesion into a somatic stem cell mutation based on the observed G6PD M.F. and the level of O⁶mG lesions in the colon. The value of 0.3% from the analysis demonstrates that measuring adduct levels does not necessarily correlate with mutations. Only a fraction of adducts are

converted in mutations, due to DNA repair, cell death, correct coding during polymerization.

- 5) In this work, we demonstrated that α/β T-cell deficient mice had reduced colon cancer in comparison to WT mice after treatment with AOM+DSS at lower DSS concentrations. However, this insensitivity was lost when the concentration in DSS was increased. An increased concentration of DSS would cause the development of a more severe inflammation. The significance of this result is that the deficient α/β T-cell signaling in the TCR $\beta^{-/-}$ mice could have been compensated for when the mice were exposed to a more severe inflammatory event. This finding could mean that α/β T-cell mediated signaling can potentiate colon cancer development.

This work generated several significant questions. In Chapter 3, a potential role for α/β T-cells supporting colon cancer development by polarizing M2 macrophages is discussed and this could be an important future research aim. In Chapter 4, a possible mechanism by which DSS, in a dose dependent manner may dysregulate cytoplasmic and nuclear beta-catenin levels by disrupting E-cadherin cell-cell junctions was introduced. This would release AOM mutated beta-catenin from the cell junction into the cytoplasm. This could be a very significant basic research question to pursue as it would explain why the concentration of DSS correlates better with carcinogenicity than the dose of AOM.

6.0 EXPERIMENTAL DESIGN

6.1 ANIMAL HUSBANDRY

The animals used in the work are both wild type (WT) and immunocompromised mice. All B6 strains (WT, athymic, TCR $\beta^{-/-}$, TCR $\delta^{-/-}$, TCR $\beta^{-/-}\delta^{-/-}$) were housed in the University of Pittsburgh vivarium. The mice were housed ≤ 4 mice per cage, in plastic cages with filter covers that were specially designed to hold immunocompromised animals. A HEPA-Filtered Laminar Air Flow system provided air to the cages. This system prevents the introduction of potential pathogens to the cages by filtering 99.97% of air-borne pathogens 0.3 μm and larger.⁽³⁶⁶⁾ All of the mice received irradiated chow and autoclaved water in autoclaveable water bottles designed to fit the cages.

All animal injections were carried out in a clean room under a Class II Type A biological safety cabinet that was thoroughly sterilized before use. All water bottles containing DSS solution were prepared in the aforementioned animal facility's clean room. Food and water consumption were not monitored during these studies.

6.2 AZOXYMETHANE DOSING

AOM was administered to the mice via intraperitoneal injection (i.p.).⁽⁴⁵⁾ AOM was acquired from Sigma-Aldrich (Sigma-Aldrich, St. Louis MO). AOM is a neat liquid with a density of 0.991 g/ml in its native form. The AOM used in the initial experiments was a practical grade, ($\geq 90\%$ by GC). The AOM used for the mutagenesis/carcinogenesis study was $\geq 98\%$ pure. As previously reported, the practical grade AOM was discontinued, which is why the experiments were conducted with the higher purity material.

A single stock solution of AOM (10 mg/kg or 15 mg/kg b.w.) was prepared in phosphate buffered saline (PBS) (Thermo Fisher Scientific Inc., Waltham MA) to ensure that all of the mice received the same AOM. The PBS was purchased sterilized by filtration through a 0.2 Micron Filter. The PBS (pH 7.4) is comprised of 11.9 mM phosphate, 137 mM sodium chloride and 2.7 mM potassium chloride. As the PBS was at an initial 10X concentration, it was diluted using ultrapure water to a 1X concentration for the final AOM stock solution. The final amount of AOM and volume of PBS for each stock solution was determined by the number of mice receiving an AOM treatment in the experiment. One tuberculin syringe (26 gauge) (Thermo Fisher Scientific Inc., Waltham MA) was prepared for each mouse receiving an AOM dose.

An example calculation for an experimental trial where 40 mice were dosed with AOM at 10 mg/kg b.w. is as follows:

$$\left(\frac{10 \text{ mg AOM}}{\text{kg b.w.}} \right) = \left(\frac{0.010 \text{ mg AOM}}{\text{g b.w.}} \right)$$

Since the mice weight between 20-30 g at 6-8 weeks of age, with a few outliers above and below this range, the calculation is converted to mg/g b.w.

$$\left(\frac{0.010 \text{ mg AOM}}{\text{g b.w.}} \right) \times \left(\frac{30 \text{ g b.w.}}{30 \text{ g b.w.}} \right) = \left(\frac{0.30 \text{ mg AOM}}{30 \text{ g b.w.}} \right)$$

A 200 µl volume of PBS was used per injection, which was adjusted for mice weighting less than 30 g. So a 30 g mouse would receive 0.30 mg AOM dose in 200 µl of PBS via i.p injection. The AOM stock solution is stable overnight at 4 °C in the dark. For trials with large numbers of mice, all of the syringes were prepare in advance and the mice were dosed the following day.

6.3 DEXTRAN SULFATE SODIUM DOSING

IUCAC requirements stated that mice needed to be provided with excess drinking water during an animal treatment involving a reagent administered ab libitum. It was determined that a 300 ml volume of DSS solution per cage would last for more than 7 days. As each mouse was expected to drink 6 to 7 ml of water per day and there were a maximum of 4 mice per cage. The daily consumption of DSS solution was not monitored since the individual consumption per mouse could not be determine.

DSS (36-50 kDa) (MP grade colitis grade, white powder, MPBiomedicals LLC, Santa Ana CA) is a water soluble powder that goes into solution with moderate shaking and no heating at the concentrations used in these studies. The DSS solution was prepared in a biosafety hood where DSS powder was added to autoclaved water bottles. The bottles were resealed before being removed from the hood. Once in the animal facility, the DSS solutions were transferred into sterilized water bottles for the cages from the original containers.

6.4 TISSUE HISTOLOGY

6.4.1 Tissue Collection

All mice were euthanized by CO₂ asphyxiation followed by cervical dislocation. The final weight of the animal was then recorded. Dissections were performed in the immunocompromised procedure rooms of the University of Pittsburgh animal facility. Dissections were carried out in the aforementioned sterilized biosafety hoods. The abdominal cavity was washed gently with sterile PBS to remove bedding dust, urine, and to prevent hairs from entering into the body cavity. The animal's body was pinned with 18 G needles to a styrofoam cutting board and the abdominal cavity opened from just above the anus to the base of the sternum. The skin, body fat, and peritoneum were carefully removed from the open cavity. The seminal vesicle, urinary bladder, prostate, and perputial gland were excised. The small intestine that comprises most of the organ mass in lower body cavity, along with the liver, was moved out of the body cavity but not excised. The lower intestine was excised beginning just below the cecum. The point of excision is arbitrary as each animal's lower intestine varied based on both the size and weight of the animal, and also on the treatment that the animal received (untreated, AOM, DSS and AOM+DSS). The lower intestine was excised down to the rectum. If the animal's rectum had prolapsed, this tissue was recovered separately. The colons were then placed full length on a cutting board and carefully sliced along one side using the blade of a micro-dissection scissor. Feces were then removed and the colons quickly washed in clean sterile PBS. Tears in the tissue were infrequent and if they did occur were only in one location. The presence of the rectum allowed for proper tissue orientation to be retained if a tear did occur. The colon lengths were measured at this time. Other organs harvested were the liver and spleen. All

of the livers and spleens collected were weighted and immediately placed into 4% formalin and stored at 4 °C.

6.4.2 Paraffin Embedding

The excised lower intestines were placed in 4% formalin and stored at 4 °C overnight. The paraffin embedding of the colons was performed following a standard protocol with modifications.⁽³⁶⁷⁾ The colon sections were Swiss-rolled after the 70% ethanol step of the protocol. The Swiss-roll was created by fully extending the flat colon and placing the end of the colon that was excised from the cecum on a matchstick or the thick edge of a pipet tip. The colon is then rolled over itself until all of the tissue is coiled around the stick ending at the rectum. It is common practice that the luminal side of the colon face outward in the rolled shape. An example of an H+E stained section of mouse colon in the Swiss-roll shape is shown in Figure 15.



Figure 15. Mouse Colon Swiss-Roll

(adopted from reference 43)

Formalin Fixation and Paraffin Embedding Protocol:

1. 4% Formalin at stored at 4 °C overnight.
2. 50% Ethanol for 3-4 hours at RT.
3. 50% Ethanol for 3-4 hours at RT.
4. 70% Ethanol at 4 °C overnight.
5. Tissues are Swiss-rolled.
6. 85% Ethanol ½ hour at RT.
7. 90% Ethanol ½ hour at RT.
8. 100% Ethanol for 1 hour at RT.
9. 100% Ethanol for 1 hour at RT.
10. Xylene for 1-2 hours at RT.
11. Xylene for 1-2 hours at RT.
12. Paraffin for 1-2 hours at 60 °C.
13. Paraffin for 1-2 hours at 60 °C.
14. Paraffin for overnight at 60 °C.
15. Paraffin for 2-4 hours at 60 °C.

The paraffin incubations are necessary to remove the xylene from the tissue. The paraffin blocks are then prepared by filling a tissue mold with melted paraffin (65 °C), immersing the Swiss-rolled colon in the melted paraffin, and then waiting until the block solidifies completely as it cools at room temperature.

6.4.2.1 Hematoxylin and Eosin

Sections from each tissue were cut at 5 μm using a standard microtome. Sections for each colon were H+E stained using a standard protocol.⁽³⁶⁸⁾ H+E staining was performed by the UPMC Pathology Department. Pathology findings were reported by Dr. Shi-Fan Kuan (Department of Pathology).

6.4.3 Freezing Tissues for Sectioning

After measuring their length, the excised colons were opened longitudinally to remove feces then immediately washed in clean sterile PBS, Swiss-rolled, and placed in a tissue mold. The colons were then completely immersed in OCT medium (Tissue-Tek® Optimal Cutting Temperature Compound, Ted Pella, Inc., Redding, CA). The mold was then placed in a bench-Dewar containing a small volume of liquid N₂. The mold is held so that its plastic base was just in contact with the liquid N₂ until the OCT medium had frozen completely solid. The frozen tissue block was then stored at -80 °C until tissue sections were generated. No fixative was used during this process, as that would inactivate the G6PD enzyme.

6.4.3.1 Cutting frozen sections

H+E analysis requires only one section of tissue from the Swiss-rolled colons, normally taken from the center of the tissue block. To determine the number of G6PD mutant crypts in a colon, multiple regions of the tissue need to be assessed. Frozen tissue sections were cut at a thickness of 7 μm using a fixed-blade cryostat at -25 °C. Two consecutive sections were placed on each slide. Two slides, or four consecutive sections, were cut to represent one level. The next region (level) was sectioned at a minimum distance of 50 μm from the last section of the

previous level. This distance ensured that the crypts assessed for each level did not duplicate one another.

Generating optimal frozen sections using the cryostat requires controlling the room temperature and humidity using a dehumidifier. The cryostat chamber, where the tissue and blade sit, is extremely humid and the blade was frequently wiped with 100% ethanol to remove the OCT medium residue that accumulates during cutting. Before sectioning was resumed, the dry blade was also wiped with a normal dryer sheet to dissipate any accumulated static charge. This was performed to prevent sections from curling or floating off of the blade before they could be adhered to a slide. All of the slides with the frozen sections were stored at -80 °C.

6.4.3.2 Hematoxylin and Eosin

Each slide with a frozen section was fixed in 4% formalin for 3 hours before being H+E stained. Sections from each colon were H+E stained using a standard protocol⁽³⁶⁸⁾ in the UPMC Pathology Department. Pathology findings were reported by Dr. Shi-Fan Kuan.

6.5 ENZYME HISTOCHEMISTRY

6.5.1 Tissue Staining Reaction Mixture

6.5.1.1 OCT Medium as the Alternative Enzyme Stabilizer

The reaction mixture is a formulation modified from protocols described by Williams et al.,⁽²⁰⁵⁾ and Van Noorden et. al.⁽³⁶⁹⁾ The polyvinyl alcohol (PVA) used for in the original protocols was replaced by OCT medium. Some enzymes, such as G6PD, can diffuse out of the cells on an unfixed tissue section if the sections are placed in an aqueous solution. The PVA acts a stabilizer for these enzymes in the tissue sections to be analyzed.⁽³⁷⁰⁾ The stabilizer in the reaction media does allow for the diffusion of small molecules, such as the reagents necessary for the G6PD enzymatic reaction.

There were several reasons that the OCT medium was used to replace the PVA as the stabilizer in the reaction mixture. The PVA is acidic and quite viscous at the solution percentages (18% and greater) necessary to facilitate the enzyme histochemistry reaction while preventing the diffusion of the G6PD enzyme. Attempting to adjust the solution pH caused a decrease in the viscosity of the PVA solution and resulted in the diffusion of the G6PD enzyme into the reaction mix. Solubilizing PVA is difficult as it requires heating at very high temperatures for a long period of time. Even solubilizing the PVA in a pH adjusted phosphate buffer did not result to a consistently reproducible reaction mixture at the correct pH and viscosity. Also, ascertaining the pH of the PVA solution was impossible due to the viscosity of the reaction mixture. The high viscosity of the PVA solution prevented the reagents from distributing evenly, as the mixture could not be effectively shaken to homogeneity. These problems lead to poor and inconsistent

overall tissue staining in which different areas of the tissue sections stained with variable efficacy.

The OCT medium, which is comprised of approximately 10% PVA, offered a solution to all of the aforementioned problems. The OCT medium could be pH adjusted with a minimal volume of aqueous phosphate buffer while retaining the necessary solution viscosity. The pH could be accurately determined with a least one type of pH paper (Hydrion Microfine Paper, Brooklyn NY). With only vigorous hand shaking, the mixture would become homogeneous. At pH 7.2-7.4 the OCT reaction mixture has a characteristic crystal clear deep red color after all of the reagents are in solution.

6.5.1.2 G6PD enzymatic reaction

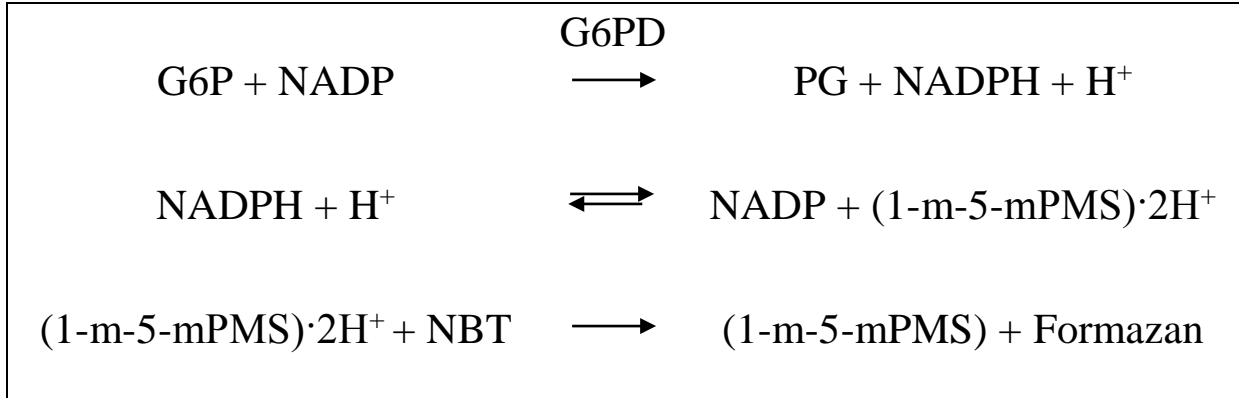


Figure 16. G6PD Enzymatic Reaction

(adopted from reference 371)

Figure 16. G6PD oxidizes G6P and reduces NBT to insoluble Formazan
The G6PD enzyme substrate is Glucose-6 phosphate (G6P). G6P is oxidized into phosphogluconate (PG). β -Nicotinamide adenine dinucleotide phosphate (NADP) is the cofactor. Magnesium chloride (MgCl) is utilized in the enzyme binding pocket when occupied by G6P. 1-methoxy-5-methylphenazinium methyl sulfate (1-m-5mPMS) acts as a transient electron carrier. Nitro Blue Tetrazolium (NBT) is reduced into Formazan.

Detecting the presence or absence of G6PD activity is actually the result of cells acquiring, or staining, insoluble Formazan which has a dark blue color. G6P is oxidized into PG by G6PD releasing $2e^-$ (electrons) which is an irreversible modification of the enzyme substrate. One hydrogen (H) will transfer to NADP forming NADPH. As enzyme cofactors are only reversibly modified, the NADPH can be oxidized to NADP and facilitate the oxidation of

another G6P molecule. 1-m-5mPMS transiently acquires 2 H⁺ molecules and transfers them to NBT, reducing the NBT into the insoluble Formazan. As 1-m-5mPMS is also transiently modified, one molecule of 1-m-5mPMS can reduce many NBT molecules. Formazan is insoluble and diffuses out of solution, localizing where it is reduced, so the presence of the blue color in a cell indicates the G6PD enzyme is active.

6.5.1.3 pH Adjustment of the OCT Medium

The largest alteration from other previously reported G6PD staining protocols was replacing the PVA solution with the OCT medium. The OCT medium is approximately pH 6. However, the G6PD enzymatic reaction occurs optimally at pH 7.2-7.4 or the physiological pH. The pH of the OCT medium can be adjusted by adding an aqueous buffered solution, e.g., phosphate buffer (PB). A 200 mM concentration of PB (pH 7.4) allowed for the adjustment of the OCT medium pH while only minimally increasing the volume of solution. 2 ml of 200 mM PB was used to adjust 35 ml of OCT to pH 7.2-7.4. This additional volume did not reduce the viscosity of the OCT medium significantly and adversely impact the G6PD enzymatic reaction.

6.5.1.4 Assembling the Reaction Mix

The final volume of the reaction mixture was set at 40 ml. The mixture was prepared fresh for use on each day.⁽³⁶⁹⁾ 35 ml of OCT medium was placed into a standard 50 ml centrifuge tube and 2 ml of 200 mM PB (pH 7.4) was added to the tube and shaken vigorously. This affords a characteristic effervescent mixture. To avoid diluting the viscosity of the OCT medium, the reaction reagents were solubilized in the minimum necessary volume of PB before they were added.

The final concentration of each reagent, following the method by Williams et al.,⁽²⁰⁵⁾ was 5 mM G6P (Sigma-Aldridge, St Louis MO); 2 mM NADP (AppliChem Inc., St. Louis MO), 5 mM MgCl₂ (Sigma-Aldridge, St Louis MO), 0.35 mM 1-m-5mPMS (Sigma-Aldridge, St Louis MO) and 0.8 mM NBT (Life Technologies, Grand Island NY), respectively. 1-m-5mPMS replaced the 5-methylphenazinium methyl sulfate used in the original method as the electron transfer mediator due to its superior stability and activity.⁽³⁷²⁾

For each reagent the initial concentration was derived for a 40 ml final volume. Using the dilution equation $(C)_c(V)_c=(C)_d(V)_d$ to determined the initial concentration for each reagent:

$$\text{G6P: } (200 \text{ mM G6P})(1 \text{ ml})=(5 \text{ mM})(40 \text{ ml})$$

Dissolve 60.8 mg G6P into (0.94 ml 200 mM PB) in a 2 ml microcentrifuge tube.

$$\text{NADP: } (80 \text{ mM NADP})(1 \text{ ml})=(2 \text{ mM})(40 \text{ ml})$$

Dissolve 61.2 mg NADP into (0.94 ml 200 mM PB) in a 2 ml microcentrifuge tube.

$$\text{MgCl}_2: (200 \text{ mM MgCl}_2)(1 \text{ ml})=(5 \text{ mM})(40 \text{ ml})$$

Dissolve 40.66 mg MgCl₂ into (0.96 ml 100 mM PB) in a 2ml microcentrifuge tube.

$$\text{1-m-5mPMS: } (56 \text{ mM 1-m-5mPMS})(0.25 \text{ ml})=(0.35 \text{ mM})(40 \text{ ml})$$

Dissolve 4.71 mg 1-methoxy-5-methylphenazinium into (0.25 ml 200 mM PB) in a 1 ml microcentrifuge tube.

Once each reagent was fully dissolved into solution, the solution was then added to the pH adjusted OCT medium. The resulting reaction mixture was then shaken vigorously to form a deep crystal red homogenate. The pH was then checked at this step (pH 7.4) as a final confirmation the reaction mix was assembled correctly.

The solution should be highly effervescent and not appear cloudy. If the solution is cloudy, the pH is off and the mixture had to be discarded. The OCT medium is normally the source of this problem and that lot of OCT must be discarded and new OCT used. Since each reagent was solubilized in PB (pH 7.4), it further insulated the OCT medium from pH changes. This buffering is critical since both G6P and NADP are acidic in solution and, therefore, would lower the pH below 7.4. The tube containing the reaction mixture was wrapped in foil to minimize exposure to light. One of the purposes of using 1-m-5mPMS is to eliminate the light sensitivity of the reaction mixture.⁽³⁷²⁾

The reaction mixture was then stored at room temperature while the final component, NBT, was solubilized. NBT is highly insoluble and requires boiling in a solution mixture of N,N-dimethylformamide (DMF) (N,N-Dimethylformamide Molecular Biology Reagent, Sigma-Aldridge, St Louis MO) and 100% ethanol to solubilize the NBT.⁽³⁶⁹⁾

NBT: $(250 \text{ mM NBT})(0.8 \text{ ml}) = (5 \text{ mM})(40 \text{ ml})$

0.4 ml DMF and 0.4 ml 100% EtOH were added to 163.53 mg NBT in a 2 ml microcentrifuge tube with an O-ring lid. The lid was loosely closed (not tightly sealed) and the solution brought to a vigorous boil in an oil bath until the NBT was in solution. This must be done in a room with low humidity. The DMF and 100% EtOH (1:1) volume was determined by Van Noorden et al.⁽³⁶⁹⁾ to be 2% of the final reaction mixture's volume.

Once the NBT is solubilized and removed from the oil bath, it was allowed to cool to room temperature and then added to the OCT reaction mixture and shaken vigorously. This changes the reaction mixture to an orange-red colored solution. Unlike the other reagents, the NBT would

transiently fall out of solution when added to the reaction mixture but with continued shaking would quickly go back into solution. At this point, the reaction mixture was placed in a 37 °C warm room for 1 h.

6.5.1.5 Staining Slides for G6PD Activity

The enzyme histochemistry reaction was carried out in a 37 °C warm room to ensure that the temperature of all of the components was the same. The warm room also had high humidity that facilitated the reaction. Attempting the enzymatic reaction in an incubation oven or on a slide warmer led to poor and inconsistent staining efficacy.

Tissue staining for G6PD activity was performed by building wells using two 1.5 cm x 0.15 cm steel washers (interior diameter x height) that were sealed together using silicone grease. Parafilm was then cut to fit the base of the well with the center cut out and the well placed over the tissue section on the slide. The parafilm on the bottom of the washer created a seal between the slide and the washer that maintained the media on the tissue section by preventing diffusion. This construct gave a well with a 0.4-0.5 ml volume so that each tissue section in the study would receive approximately the same volume of the G6PD reaction mixture.

The frozen slides were incubated at 37 °C in a warm room for 10 min to equilibrate the slide temperature. The OCT reaction mixture, at 37 °C, was then added to each tissue section (2 sections per slide) for 45-50 min. After the incubation period the slides were removed from the warm room, the wells were carefully lifted off of the slides, and the slides were set on their long edge to allow the reaction medium to drain. The slides were then placed in 100 mM PB (pH 7.4) for 30-60 min to remove the OCT mixture from the tissue without disturbing the tissue staining. The slides were placed in distilled water for 5-10 min to remove PB salts and then sealed with

fluoro-gel (Fluoro-gel with TRIS buffer Cat. # 17985-11, Electron Microscopy Sciences, Hatfield PA).

6.5.2 G6PD Activity Analysis

6.5.2.1 Assessing G6PD Mutant Crypts and Total Counts

Slides were analyzed for mutant crypts under a Leitz Orthoplan-Pol light microscope. To assess the number of G6PD mutant crypts in the colons of the animals it was necessary to observe different regions of the colon. Generating tissue sections and levels was previously described in section 5.4.3.1. The reason that consecutive sections were generated was two-fold. First, it was to prevent losing data due to inadequate tissue sectioning or staining. It is impossible to evaluate the quality of each section at the time the sections are being cut. Tissue areas are vulnerable to folds, tears, or simply adhere poorly to the slide. Sections of the tissue that are cut closely together will duplicate the same crypts. Therefore, assessing consecutive sections improves the chances of properly evaluating a colon region.

Second, G6PD mutant crypts will appear on consecutively cut sections. This presents an internal control for the proper identification of a G6PD mutant crypt. Certain crypts or clusters of crypts may also stain poorly and can produce false G6PD mutant crypts. A true G6PD mutant crypt can be correctly identified by appearing on two consecutive sections in the same location. The verification of a G6PD mutated crypt required two independent observers to identify the same crypt. Each G6PD mutant crypt was then imaged at 40x magnification and catalogued using a Mitocam 2500 5.0M Pixel camera (Motic, Hong Kong) and Motic Images Plus 2.0 software.

To calculate the total number of observed crypts, one level was selected as representative of all of the levels assessed in that animal. As the tissue surface area varied between levels, a section from the level with the least amount of surface area was selected for total crypt quantification. The total surface area of this section was then imaged at 10x magnification and catalogued. The image files were then individually opened in ImageJ (NIH Free Software) and using the Cell Counter feature each crypt was flagged. The software recorded the total number of flags (crypts) per image. The final number of crypts for each image was then recorded.

6.5.3 Total Counts and Mutation Frequency

After all of the image files (>15 images per section) were analyzed, the total number of crypts in the level was determined by adding the final numbers from each image. This number was then multiplied by the number of levels assessed for each mouse. For example, a total count of 1,250 crypts per level multiplied by 8 levels assessed would give a total count of 10,000 crypts assessed. A minimum of 10,000 crypts were assessed from each colon.

To determine the M.F. for each animal, the number of G6PD mutant crypts was divided by the total number of crypts counted. For example; 5 G6PD mutant crypts divided by 12,386 total crypts would give a M.F. of 4.04×10^{-4} . Once the M.F. was calculated for each animal, an average M.F. could be determined for each treatment group.

6.6 STATISTICAL ANALYSIS

6.6.1 Student's T-test

The unpaired t-test compares the means of two unmatched groups, comparing the effect of a treatment and a strain, assuming that the values follow a Gaussian distribution. The normality test was utilized to show that the values of the data sets followed a Gaussian distribution. The F-test determined the equality of variances between the data sets being compared. The unpaired t-test and normality test were conducted with Prism 4 (GraphPad Software, Inc., La Jolla, CA) and the F-test for Two Data Sets was conducted with XLSTAT (Addinsoft, New York NY).

6.6.2 Fisher's Exact Test

The Fisher's Exact Test is a contingency table test used to derive an exact p-value for assessing the difference between two categorical data sets.⁽³⁵⁶⁾ Categorical data sets represent data sets that have no intrinsic values assigned to them.⁽³⁵⁵⁾ The Fisher's Exact Test is best utilized for small sample sizes.⁽³⁵⁷⁾ The Fisher's Exact Test was conducted using GraphPad QuickCals Analyze a 2x2 contingency table online: <http://graphpad.com/quickcalcs/contingency1/>

APPENDIX A

LIST OF ABBREVIATIONS

ACS = American Cancer Society	MMR = Mismatched DNA repair
ADH = Aldehyde Dehydrogenase	M.F. = Mutation Frequency
AOM = Azoxymethane	NO· = Nitric Oxide
APC = Adenomatous Polyposis Coli	O ⁶ mG = O ⁶ -methylguanine
B6 = C57Bl/6	OCT medium = Optimal Cutting Temperature
BER = Base Excision Repair	PVA = Polyvinyl Alcohol
CRC = Colorectal cancer	RONS = Reactive Oxygen and Nitrogen Species
DSS = Dextran Sulfate Sodium	
FAP = Familial Adenomatous Polyposis	
G6PD = Glucose-6 Phosphate Dehydrogenase	
H ₂ O ₂ = Hydrogen Peroxide	
IBD = Inflammatory bowel disease	
IEL = Intraepithelial lymphocytes	
MAM = methylazoxymethanol	
MGMT = O ⁶ -methylguanine-DNA methyltransferase	

BIBLIOGRAPHY

- 1) What are the key statistics about colorectal cancer?. (n.d.). What are the key statistics about colorectal cancer?. Retrieved April 28, 2014, from <http://www.cancer.org/cancer/colonandrectumcancer/detailedguide/colorectal-cancer-key-statistics>
- 2) Common Cancer Types. (n.d.). - *National Cancer Institute*. Retrieved April 28, 2014, from <http://www.cancer.gov/cancertopics/types/commoncancers>
- 3) Colorectal cancer. (n.d.). *statistics*. Retrieved April 28, 2014, from http://www.wcrf.org/cancer_statistics/data_specific_cancers/colorectal_cancer_statistics
- 4) Shier, D., Butler, J., & Lewis, R. (2004). *Digestive System*. Hole's Human Anatomy and Physiology. New York: McGraw-Hill.
- 5) Colon Cancer Treatment (PDQ®). (n.d.). - National Cancer Institute. Retrieved May 2, 2014, from <http://www.cancer.gov/cancertopics/pdq/treatment/colon/Patient/page2#Keypoint8>
- 6) Crosnier, C., D. Stamataki and J. Lewis (2006). "Organizing cell renewal in the intestine: stem cells, signals and combinatorial control." *Nat Rev Genet* **7**(5): 349-359.
- 7) Creamer, B., R. G. Shorter and J. Bamforth (1961). "The turnover and shedding of epithelial cells. I. The turnover in the gastro-intestinal tract." *Gut* **2**: 110-118.
- 8) Roth, K. A., S. Kim and J. I. Gordon (1992). "Immunocytochemical studies suggest two pathways for enteroendocrine cell differentiation in the colon." *Am J Physiol* **263**(2 Pt 1): G174-180.
- 9) Eisenhoffer, G. T., P. D. Loftus, M. Yoshigi, H. Otsuna, C.-B. Chien, P. A. Morcos and J. Rosenblatt (2012). "Crowding induces live cell extrusion to maintain homeostatic cell numbers in epithelia." *Nature* **484**(7395): 546-549.
- 10) Gunther, C., H. Neumann, M. F. Neurath and C. Becker (2013). "Apoptosis, necrosis and necroptosis: cell death regulation in the intestinal epithelium." *Gut* **62**(7): 1062-1071.

- 11) Edelblum, K. L., F. Yan, T. Yamaoka and D. B. Polk (2006). "Regulation of apoptosis during homeostasis and disease in the intestinal epithelium." Inflamm Bowel Dis **12**(5): 413-424.
- 12) Peterson, L. W. and D. Artis (2014). "Intestinal epithelial cells: regulators of barrier function and immune homeostasis." Nat Rev Immunol **14**(3): 141-153.
- 13) SIU SOM Histology GI. (n.d.). SIU SOM Histology GI. Retrieved May 3, 2014, from <http://www.siumed.edu/~dking2/erg/gicells.htm#absorp>
- 14) Fan, Y. and A. Bergmann (2008). "Apoptosis-induced compensatory proliferation. The Cell is dead. Long live the Cell!" Trends Cell Biol **18**(10): 467-473.
- 15) Moran, G. W., F. C. Leslie, S. E. Levison, J. Worthington and J. T. McLaughlin (2008). "Enteroendocrine cells: neglected players in gastrointestinal disorders?" Therap Adv Gastroenterol **1**(1): 51-60.
- 16) Gunawardene, A. R., B. M. Corfe and C. A. Staton (2011). "Classification and functions of enteroendocrine cells of the lower gastrointestinal tract." Int J Exp Pathol **92**(4): 219-231.
- 17) Gulubova, M. and T. Vlaykova (2008). "Chromogranin A-, serotonin-, synaptophysin- and vascular endothelial growth factor-positive endocrine cells and the prognosis of colorectal cancer: an immunohistochemical and ultrastructural study." J Gastroenterol Hepatol **23**(10): 1574-1585.
- 18) Lloyd, R. V., G. Schroeder, M. D. Bauman, J. E. Krook, L. Jin, R. M. Goldberg and G. H. Farr, Jr. (1998). "Prevalence and Prognostic Significance of Neuroendocrine Differentiation in Colorectal Carcinomas." Endocr Pathol **9**(1): 35-42.
- 19) Bevins, C. L. and N. H. Salzman (2011). "Paneth cells, antimicrobial peptides and maintenance of intestinal homeostasis." Nat Rev Micro **9**(5): 356-368.
- 20) Sato, T., J. H. van Es, H. J. Snippert, D. E. Stange, R. G. Vries, M. van den Born, N. Barker, N. F. Shroyer, M. van de Wetering and H. Clevers (2011). "Paneth cells constitute the niche for Lgr5 stem cells in intestinal crypts." Nature **469**(7330): 415-418.
- 21) Roth, S., P. Franken, A. Sacchetti, A. Kremer, K. Anderson, O. Sansom and R. Fodde (2012). "Paneth cells in intestinal homeostasis and tissue injury." PLoS One **7**(6): e38965.
- 22) Pai, R. K., L. A. Rybicki, J. R. Goldblum, B. Shen, S. Y. Xiao and X. Liu (2013). "Paneth cells in colonic adenomas: association with male sex and adenoma burden." Am J Surg Pathol **37**(1): 98-103.

- 23) Garabedian, E. M., L. J. Roberts, M. S. McNevin and J. I. Gordon (1997). "Examining the role of Paneth cells in the small intestine by lineage ablation in transgenic mice." J Biol Chem **272**(38): 23729-23740.
- 24) Durand, A., B. Donahue, G. Peignon, F. Letourneur, N. Cagnard, C. Slomianny, C. Perret, N. F. Shroyer and B. Romagnolo (2012). "Functional intestinal stem cells after Paneth cell ablation induced by the loss of transcription factor Math1 (Atoh1)." Proc Natl Acad Sci USA **109**(23): 8965-8970.
- 25) Barker, N., M. van de Wetering and H. Clevers (2008). "The intestinal stem cell." Genes Dev **22**(14): 1856-1864.
- 26) Barker, N., J. H. van Es, J. Kuipers, P. Kujala, M. van den Born, M. Cozijnsen, A. Haegbarth, J. Korving, H. Begthel, P. J. Peters and H. Clevers (2007). "Identification of stem cells in small intestine and colon by marker gene Lgr5." Nature **449**(7165): 1003-1007.
- 27) Komar, A. A. and M. Hatzoglou (2011). "Cellular IRES-mediated translation: the war of ITAFs in pathophysiological states." Cell Cycle **10**(2): 229-240.
- 28) Reporter Detection Kits. (n.d.). LacZ Reporter Gene System : beta-galactosidase reporter gene and kits. Retrieved May 29, 2014, from <http://www.invivogen.com/lac-z-reporter-gene-system>
- 29) Barker, N., R. A. Ridgway, J. H. van Es, M. van de Wetering, H. Begthel, M. van den Born, E. Danenberg, A. R. Clarke, O. J. Sansom and H. Clevers (2009). "Crypt stem cells as the cells-of-origin of intestinal cancer." Nature **457**(7229): 608-611.
- 30) Vermeulen, L., E. Morrissey, M. van der Heijden, A. M. Nicholson, A. Sottoriva, S. Buczacki, R. Kemp, S. Tavaré and D. J. Winton (2013). "Defining stem cell dynamics in models of intestinal tumor initiation." Science **342**(6161): 995-998.
- 31) Kim, K. M., P. Calabrese, S. Tavaré and D. Shibata (2004). "Enhanced stem cell survival in familial adenomatous polyposis." Am J Pathol **164**(4): 1369-1377.
- 32) Peterson, L. W. and D. Artis (2014). "Intestinal epithelial cells: regulators of barrier function and immune homeostasis." Nat Rev Immunol **14**(3): 141-153.
- 33) Richman, P. I., R. Tilly, J. R. Jass and W. F. Bodmer (1987). "Colonic pericrypt sheath cells: characterisation of cell type with new monoclonal antibody." J Clin Pathol **40**(6): 593-600.
- 34) Li, A., K. Hasui, S. Yonezawa, S. Tanaka and E. Sato (1999). "Immunohistochemical analysis of pericryptal fibroblast sheath and proliferating epithelial cells in human colorectal adenomas and carcinomas with adenoma components." Pathol Int **49**(5): 426-434.

- 35) Humphries, A. and N. A. Wright (2008). "Colonic crypt organization and tumorigenesis." Nat Rev Cancer **8**(6): 415-424.
- 36) Haegebarth, A. and H. Clevers (2009). "Wnt signaling, Lgr5, and stem cells in the intestine and skin." Am J Pathol **174**(3): 715-721.
- 37) Cairns, J. (1975). "Mutation selection and the natural history of cancer." Nature **255**(5505): 197-200.
- 38) Morrison, S. J. and J. Kimble (2006). "Asymmetric and symmetric stem-cell divisions in development and cancer." Nature **441**(7097): 1068-1074.
- 39) Yan, K. S., L. A. Chia, X. Li, A. Ootani, J. Su, J. Y. Lee, N. Su, Y. Luo, S. C. Heilshorn, M. R. Amieva, E. Sangiorgi, M. R. Capecchi and C. J. Kuo (2012). "The intestinal stem cell markers Bmi1 and Lgr5 identify two functionally distinct populations." Proc Natl Acad Sci U S A **109**(2): 466-471.
- 40) Tian, H., B. Biehs, S. Warming, K. G. Leong, L. Rangell, O. D. Klein and F. J. de Sauvage (2011). "A reserve stem cell population in small intestine renders Lgr5-positive cells dispensable." Nature **478**(7368): 255-259.
- 41) Hong, M. Y., R. S. Chapkin, C. P. Wild, J. S. Morris, N. Wang, R. J. Carroll, N. D. Turner and J. R. Lupton (1999). "Relationship between DNA adduct levels, repair enzyme, and apoptosis as a function of DNA methylation by azoxymethane." Cell Growth Differ **10**(11): 749-758.
- 42) Iizuka, M. and S. Konno (2011). "Wound healing of intestinal epithelial cells." World J Gastroenterol **17**(17): 2161-2171.
- 43) Treuting, P. M., & Dintzis, S. M. (2012). Lower Gastrointestinal Tract. Comparative Anatomy and Histology a Mouse and Human Atlas. Oxford: Academic.
- 44) Boyland, E. (1985). "Tumour initiators, promoters, and complete carcinogens." Br J Ind Med **42**(10): 716-718.
- 45) Tanaka, T., H. Kohno, R. Suzuki, Y. Yamada, S. Sugie and H. Mori (2003). "A novel inflammation-related mouse colon carcinogenesis model induced by azoxymethane and dextran sodium sulfate." Cancer Sci **94**(11): 965-973.
- 46) Rosenberg, D. W., C. Giardina and T. Tanaka (2009). "Mouse models for the study of colon carcinogenesis." Carcinogenesis **30**(2): 183-196.
- 47) Thurnherr, N. and K. Reinhart (1975). "[Induction of colonic carcinoma in mice using 1,2 dimethylhydrazine hydrochloride]." Schweiz Med Wochenschr **105**(18): 585-586.

- 48) Neufert, C., C. Becker and M. F. Neurath (2007). "An inducible mouse model of colon carcinogenesis for the analysis of sporadic and inflammation-driven tumor progression." Nat Protoc **2**(8): 1998-2004.
- 49) Warwick, G. P. (1963). "THE MECHANISM OF ACTION OF ALKYLATING AGENTS." Cancer Res **23**: 1315-1333.
- 50) Beranek, D. T. (1990). "Distribution of methyl and ethyl adducts following alkylation with monofunctional alkylating agents." Mutat Res **231**(1): 11-30.
- 51) Fu, D., J. A. Calvo and L. D. Samson (2012). "Balancing repair and tolerance of DNA damage caused by alkylating agents." Nat Rev Cancer **12**(2): 104-120.
- 52) Drablos, F., E. Feyzi, P. A. Aas, C. B. Vaagbo, B. Kavli, M. S. Bratlie, J. Pena-Diaz, M. Otterlei, G. Slupphaug and H. E. Krokan (2004). "Alkylation damage in DNA and RNA repair mechanisms and medical significance." DNA Repair (Amst) **3**(11): 1389-1407.
- 53) Engelward, B. P., J. M. Allan, A. J. Dreslin, J. D. Kelly, M. M. Wu, B. Gold and L. D. Samson (1998). "A chemical and genetic approach together define the biological consequences of 3-methyladenine lesions in the mammalian genome." J Biol Chem **273**(9): 5412-5418.
- 54) Larson, K., J. Sahm, R. Shenkar and B. Strauss (1985). "Methylation-induced blocks to in vitro DNA replication." Mutat Res **150**(1-2): 77-84.
- 55) Bugni, J. M., L. B. Meira and L. D. Samson (2009). "Alkylation-induced colon tumorigenesis in mice deficient in the Mgmt and Msh6 proteins." Oncogene **28**(5): 734-741.
- 56) Snow, E. T., R. S. Foote and S. Mitra (1984). "Base-pairing properties of O6-methylguanine in template DNA during in vitro DNA replication." J Biol Chem **259**(13): 8095-8100.
- 57) Karran, P. and M. Bignami (1992). "Self-destruction and tolerance in resistance of mammalian cells to alkylation damage." Nucleic Acids Res **20**(12): 2933-2940.
- 58) Fiala, E. S. (1977). "Investigations into the metabolism and mode of action of the colon carcinogens 1,2-dimethylhydrazine and azoxymethane." Cancer **40**(5 Suppl): 2436-2445.
- 59) Sohn, O. S., H. Ishizaki, C. S. Yang and E. S. Fiala (1991). "Metabolism of azoxymethane, methylazoxymethanol and N-nitrosodimethylamine by cytochrome P450IIE1." Carcinogenesis **12**(1): 127-131.
- 60) Sohn, O. S., E. S. Fiala, S. P. Requeijo, J. H. Weisburger and F. J. Gonzalez (2001). "Differential effects of CYP2E1 status on the metabolic activation of the colon carcinogens azoxymethane and methylazoxymethanol." Cancer Res **61**(23): 8435-8440.

- 61) Feinberg, A. and M. S. Zedeck (1980). "Production of a highly reactive alkylating agent from the organospecific carcinogen methylazoxymethanol by alcohol dehydrogenase." Cancer Res **40**(12): 4446-4450.
- 62) Grab, D. J. and M. S. Zedeck (1977). "Organ-specific effects of the carcinogen methylazoxymethanol related to metabolism by nicotinamide adenine dinucleotide dependent dehydrogenases." Cancer Res **37**(11): 4182-4189.
- 63) Fiala, E. S., C. Kulakis, G. Christiansen and J. H. Weisburger (1978). "Inhibition of the metabolism of the colon carcinogen, azoxymethane, by pyrazole." Cancer Res **38**(12): 4515-4521.
- 64) Schoental, R. (1973). "The mechanisms of action of the carcinogenic nitroso and related compounds." Br J Cancer **28**(5): 436-439.
- 65) Fiala, E. S., N. Caswell, O. S. Sohn, M. R. Felder, G. D. McCoy and J. H. Weisburger (1984). "Non-alcohol dehydrogenase-mediated metabolism of methylazoxymethanol in the deer mouse, *Peromyscus maniculatus*." Cancer Res **44**(7): 2885-2891.
- 66) Ginestier, C., M. H. Hur, E. Charafe-Jauffret, F. Monville, J. Dutcher, M. Brown, J. Jacquemier, P. Viens, C. G. Kleer, S. Liu, A. Schott, D. Hayes, D. Birnbaum, M. S. Wicha and G. Dontu (2007). "ALDH1 is a marker of normal and malignant human mammary stem cells and a predictor of poor clinical outcome." Cell Stem Cell **1**(5): 555-567.
- 67) Huang, E. H., M. J. Hynes, T. Zhang, C. Ginestier, G. Dontu, H. Appelman, J. Z. Fields, M. S. Wicha and B. M. Boman (2009). "Aldehyde dehydrogenase 1 is a marker for normal and malignant human colonic stem cells (SC) and tracks SC overpopulation during colon tumorigenesis." Cancer Res **69**(8): 3382-3389.
- 68) Monti, P., I. Traverso, L. Casolari, P. Menichini, A. Inga, L. Ottaggio, D. Russo, P. Iyer, B. Gold and G. Fronza (2010). "Mutagenicity of N3-methyladenine: a multi-translesion polymerase affair." Mutat Res **683**(1-2): 50-56.
- 69) Oh, H. K., A. K. Teo, R. B. Ali, A. Lim, T. C. Ayi, D. B. Yarosh and B. F. Li (1996). "Conformational change in human DNA repair enzyme O6-methylguanine-DNA methyltransferase upon alkylation of its active site by SN1 (indirect-acting) and SN2 (direct-acting) alkylating agents: breaking a "salt-link"." Biochemistry **35**(38): 12259-12266.
- 70) Dumenco, L. L., E. Allay, K. Norton and S. L. Gerson (1993). "The prevention of thymic lymphomas in transgenic mice by human O6-alkylguanine-DNA alkyltransferase." Science **259**(5092): 219-222.
- 71) Zaidi, N. H., T. P. Pretlow, M. A. O'Riordan, L. L. Dumenco, E. Allay and S. L. Gerson (1995). "Transgenic expression of human MGMT protects against azoxymethane-induced

- aberrant crypt foci and G to A mutations in the K-ras oncogene of mouse colon." Carcinogenesis **16**(3): 451-456.
- 72) Wirtz, S., G. Nagel, L. Eshkind, M. F. Neurath, L. D. Samson and B. Kaina (2010). "Both base excision repair and O6-methylguanine-DNA methyltransferase protect against methylation-induced colon carcinogenesis." Carcinogenesis **31**(12): 2111-2117.
- 73) Haracska, L., S. Prakash and L. Prakash (2000). "Replication past O(6)-methylguanine by yeast and human DNA polymerase eta." Mol Cell Biol **20**(21): 8001-8007.
- 74) Choi, J. Y., G. Chowdhury, H. Zang, K. C. Angel, C. C. Vu, L. A. Peterson and F. P. Guengerich (2006). "Translesion synthesis across O6-alkylguanine DNA adducts by recombinant human DNA polymerases." J Biol Chem **281**(50): 38244-38256.
- 75) Karran, P. and M. Bignami (1994). "DNA damage tolerance, mismatch repair and genome instability." Bioessays **16**(11): 833-839.
- 76) Rasmussen, L. J. and L. Samson (1996). "The Escherichia coli MutS DNA mismatch binding protein specifically binds O(6)-methylguanine DNA lesions." Carcinogenesis **17**(9): 2085-2088.
- 77) Klapacz, J., L. B. Meira, D. G. Luchetti, J. A. Calvo, R. T. Bronson, W. Edelmann and L. D. Samson (2009). "O6-methylguanine-induced cell death involves exonuclease 1 as well as DNA mismatch recognition in vivo." Proc Natl Acad Sci U S A **106**(2): 576-581.
- 78) Editors of Encyclopaedia Britannica. (n.d.). polysaccharide (chemical compound). Encyclopedia Britannica Online. Retrieved June 17, 2014, from <http://www.britannica.com/EBchecked/topic/469090/polysaccharide>
- 79) polysaccharide. (n.d.). Merriam-Webster. Retrieved June 17, 2014, from <http://www.merriam-webster.com/dictionary/polysaccharide>
- 80) Chassaing, B., J. D. Aitken, M. Malleshappa and M. Vijay-Kumar (2014). "Dextran sulfate sodium (DSS)-induced colitis in mice." Curr Protoc Immunol **104**: Unit 15.25.
- 81) DEXTRAN SULFATE SODIUM SALT (36,000-50,000 M.Wt.) MP Grade (02160110) - MP Biomedicals." DEXTRAN SULFATE SODIUM SALT (36,000-50,000 M.Wt.) MP Grade (02160110) - MP Biomedicals. N.p., n.d. Web. 18 June 2014. <http://www.mpbio.com/product.php?pid=02160110>
- 82) Bailey, R. W. and E. J. Bourne (1961). "Intracellular glycosidases of dextran-producing bacteria." Nature **191**: 277-278.
- 83) Solomon, L., S. Mansor, P. Mallon, E. Donnelly, M. Hoper, M. Loughrey, S. Kirk and K. Gardiner (2010). "The dextran sulphate sodium (DSS) model of colitis: an overview." Comparative Clinical Pathology **19**(3): 235-239.

- 84) Okayasu, I., S. Hatakeyama, M. Yamada, T. Ohkusa, Y. Inagaki and R. Nakaya (1990). "A novel method in the induction of reliable experimental acute and chronic ulcerative colitis in mice." Gastroenterology **98**(3): 694-702.
- 85) Kitajima, S., S. Takuma and M. Morimoto (1999). "Changes in colonic mucosal permeability in mouse colitis induced with dextran sulfate sodium." Exp Anim **48**(3): 137-143.
- 86) Rose, W. A., 2nd, K. Sakamoto and C. A. Leifer (2012). "Multifunctional role of dextran sulfate sodium for in vivo modeling of intestinal diseases." BMC Immunol **13**: 41.
- 87) Majno, G. and I. Joris (1995). "Apoptosis, oncosis, and necrosis. An overview of cell death." Am J Pathol **146**(1): 3-15.
- 88) Trump, B. F., I. K. Berezsky, S. H. Chang and P. C. Phelps (1997). "The pathways of cell death: oncosis, apoptosis, and necrosis." Toxicol Pathol **25**(1): 82-88.
- 89) Bain, C. C., C. L. Scott, H. Uronen-Hansson, S. Gudjonsson, O. Jansson, O. Grip, M. Williams, B. Malissen, W. W. Agace and A. M. Mowat (2013). "Resident and pro inflammatory macrophages in the colon represent alternative context-dependent fates of the same Ly6Chi monocyte precursors." Mucosal Immunol **6**(3): 498-510.
- 90) Fink, S. L. and B. T. Cookson (2005). "Apoptosis, pyroptosis, and necrosis: mechanistic description of dead and dying eukaryotic cells." Infect Immun **73**(4): 1907-1916.
- 91) Cheroutre, H., F. Lambomez and D. Mucida (2011). "The light and dark sides of intestinal intraepithelial lymphocytes." Nat Rev Immunol **11**(7): 445-456
- 92) Zigmund, E. and S. Jung (2013). "Intestinal macrophages: well educated exceptions from the rule." Trends Immunol **34**(4): 162-168.
- 93) Henderson, P., J. E. van Limbergen, J. Schwarze and D. C. Wilson (2011). "Function of the intestinal epithelium and its dysregulation in inflammatory bowel disease." Inflamm Bowel Dis **17**(1): 382-395.
- 94) Pavli, P., L. Maxwell, E. Van de Pol and F. Doe (1996). "Distribution of human colonic dendritic cells and macrophages." Clin Exp Immunol **104**(1): 124-132.
- 95) Saleh, M. and G. Trinchieri (2011). "Innate immune mechanisms of colitis and colitis associated colorectal cancer." Nat Rev Immunol **11**(1): 9-20.
- 96) Penney, L., P. J. Kilshaw and T. T. MacDonald (1995). "Regional variation in the proliferative rate and lifespan of alpha beta TCR+ and gamma delta TCR+ intraepithelial lymphocytes in the murine small intestine." Immunology **86**(2): 212-218.

- 97) Poritz, L. S., K. I. Garver, C. Green, L. Fitzpatrick, F. Ruggiero and W. A. Koltun (2007). "Loss of the tight junction protein ZO-1 in dextran sulfate sodium induced colitis." J Surg Res **140**(1): 12-19.
- 98) Cepek, K. L., S. K. Shaw, C. M. Parker, G. J. Russell, J. S. Morrow, D. L. Rimm and M. B. Brenner (1994). "Adhesion between epithelial cells and T lymphocytes mediated by E cadherin and the alpha E beta 7 integrin." Nature **372**(6502): 190-193.
- 99) Ni, J., S. F. Chen and D. Hollander (1996). "Effects of dextran sulphate sodium on intestinal epithelial cells and intestinal lymphocytes." Gut **39**(2): 234-241.
- 100) Renes, I. B., J. A. Boshuizen, D. J. Van Nispen, N. P. Bulsing, H. A. Buller, J. Dekker and A. W. Einerhand (2002). "Alterations in Muc2 biosynthesis and secretion during dextran sulfate sodium-induced colitis." Am J Physiol Gastrointest Liver Physiol **282**(2): G382-389.
- 101) Dharmani, P., P. Leung and K. Chadee (2011). "Tumor necrosis factor-alpha and Muc2 mucin play major roles in disease onset and progression in dextran sodium sulphate induced colitis." PLoS One **6**(9): e25058.
- 102) Johansson, M. E., J. K. Gustafsson, K. E. Sjoberg, J. Petersson, L. Holm, H. Sjovall and G. C. Hansson (2010). "Bacteria penetrate the inner mucus layer before inflammation in the dextran sulfate colitis model." PLoS One **5**(8): e12238.
- 103) Hill, D. A. and D. Artis (2010). "Intestinal bacteria and the regulation of immune cell homeostasis." Annu Rev Immunol **28**: 623-667.
- 104) Takeuchi, O. and S. Akira (2010). "Pattern recognition receptors and inflammation." Cell **140**(6): 805-820.
- 105) Jump, R. L. and A. D. Levine (2004). "Mechanisms of natural tolerance in the intestine: implications for inflammatory bowel disease." Inflamm Bowel Dis **10**(4): 462-478.
- 106) Rakoff-Nahoum, S., J. Paglino, F. Eslami-Varzaneh, S. Edberg and R. Medzhitov (2004). "Recognition of Commensal Microflora by Toll-Like Receptors Is Required for Intestinal Homeostasis." Cell **118**(2): 229-241.
- 107) Janeway CA Jr, Travers P, Walport M, et al. Immunobiology: The Immune System in Health and Disease. 5th edition. New York: Garland Science; 2001. Chapter 9, The Humoral Immune Response. Available from: <http://www.ncbi.nlm.nih.gov/books/NBK10752/>
- 108) Innate Immunity: The First Lines of Defense. (n.d.). Retrieved June 27, 2014, from http://www.garlandscience.com/res/pdf/9780815342434_ch02.pdf

- 109) Oppenheim, J. J., A. Biragyn, L. W. Kwak and D. Yang (2003). "Roles of antimicrobial peptides such as defensins in innate and adaptive immunity." Ann Rheum Dis **62 Suppl 2**: ii17-21.
- 110) Flannagan, R. S., G. Cosio and S. Grinstein (2009). "Antimicrobial mechanisms of phagocytes and bacterial evasion strategies." Nat Rev Microbiol **7**(5): 355-366.
- 111) Dunkelberger, J. R. and W. C. Song (2010). "Complement and its role in innate and adaptive immune responses." Cell Res **20**(1): 34-50.
- 112) Dale, D. C., L. Boxer and W. C. Liles (2008). "The phagocytes: neutrophils and monocytes." Blood **112**(4): 935-945.
- 113) Fang, F. C. (2011). "Antimicrobial actions of reactive oxygen species." MBio **2**(5).
- 114) Iyer, G. Y. and J. H. Questel (1963). "NADPH and NADH oxidation by guinea pig polymorphonuclear leucocytes." Can J Biochem Physiol **41**: 427-434.
- 115) Tainer, J. A., E. D. Getzoff, J. S. Richardson and D. C. Richardson (1983). "Structure and mechanism of copper, zinc superoxide dismutase." Nature **306**(5940): 284-287.
- 116) Winterbourn, C. C., M. C. Vissers and A. J. Kettle (2000). "Myeloperoxidase." Curr Opin Hematol **7**(1): 53-58.
- 117) Nathan, C. F. and R. K. Root (1977). "Hydrogen peroxide release from mouse peritoneal macrophages: dependence on sequential activation and triggering." J Exp Med **146**(6): 1648-1662.
- 118) Imlay, J. A. and S. Linn (1987). "Mutagenesis and stress responses induced in Escherichia coli by hydrogen peroxide." J Bacteriol **169**(7): 2967-2976.
- 119) Keyer, K., A. S. Gort and J. A. Imlay (1995). "Superoxide and the production of oxidative DNA damage." J Bacteriol **177**(23): 6782-6790.
- 120) Keyer, K. and J. A. Imlay (1996). "Superoxide accelerates DNA damage by elevating free iron levels." Proc Natl Acad Sci U S A **93**(24): 13635-13640.
- 121) Harrison, J. E. and J. Schultz (1976). "Studies on the chlorinating activity of myeloperoxidase." J Biol Chem **251**(5): 1371-1374.
- 122) Thomas, E. L. (1979). "Myeloperoxidase, hydrogen peroxide, chloride antimicrobial system: nitrogen-chlorine derivatives of bacterial components in bactericidal action against Escherichia coli." Infect Immun **23**(2): 522-531.

- 123) Albrich, J. M., C. A. McCarthy and J. K. Hurst (1981). "Biological reactivity of hypochlorous acid: implications for microbicidal mechanisms of leukocyte myeloperoxidase." Proc Natl Acad Sci U S A **78**(1): 210-214.
- 124) Fang, F. C. (1997). "Perspectives series: host/pathogen interactions. Mechanisms of nitric oxide-related antimicrobial activity." J Clin Invest **99**(12): 2818-2825.
- 125) Denicola, A., J. M. Souza, R. Radi and E. Lissi (1996). "Nitric oxide diffusion in membranes determined by fluorescence quenching." Arch Biochem Biophys **328**(1): 208-212.
- 126) Szabo, C., H. Ischiropoulos and R. Radi (2007). "Peroxynitrite: biochemistry, pathophysiology and development of therapeutics." Nat Rev Drug Discov **6**(8): 662-680.
- 127) Wink, D. A., K. S. Kasprzak, C. M. Maragos, R. K. Elespuru, M. Misra, T. M. Dunams, T. A. Cebula, W. H. Koch, A. W. Andrews, J. S. Allen and et al. (1991). "DNA deaminating ability and genotoxicity of nitric oxide and its progenitors." Science **254**(5034): 1001-1003.
- 128) Juedes, M. J. and G. N. Wogan (1996). "Peroxynitrite-induced mutation spectra of pSP189 following replication in bacteria and in human cells." Mutat Res **349**(1): 51-61.
- 129) Pacher, P., J. S. Beckman and L. Liaudet (2007). "Nitric oxide and peroxynitrite in health and disease." Physiol Rev **87**(1): 315-424.
- 130) Hausladen, A. and I. Fridovich (1994). "Superoxide and peroxynitrite inactivate aconitases, but nitric oxide does not." J Biol Chem **269**(47): 29405-29408.
- 131) Keyer, K. and J. A. Imlay (1997). "Inactivation of dehydratase [4Fe-4S] clusters and disruption of iron homeostasis upon cell exposure to peroxynitrite." J Biol Chem **272**(44): 27652-27659.
- 132) Wood, Z. A., E. Schroder, J. Robin Harris and L. B. Poole (2003). "Structure, mechanism and regulation of peroxiredoxins." Trends Biochem Sci **28**(1): 32-40.
- 133) Horst, S. A., T. Jaeger, L. A. Denkel, S. F. Rouf, M. Rhen and F. C. Bange (2010). "Thiol peroxidase protects *Salmonella enterica* from hydrogen peroxide stress in vitro and facilitates intracellular growth." J Bacteriol **192**(11): 2929-2932.
- 134) Alfonso-Prieto, M., X. Biarnes, P. Vidossich and C. Rovira (2009). "The molecular mechanism of the catalase reaction." J Am Chem Soc **131**(33): 11751-11761.
- 135) Hebrard, M., J. P. Viala, S. Meresse, F. Barras and L. Aussel (2009). "Redundant hydrogen peroxide scavengers contribute to *Salmonella* virulence and oxidative stress resistance." J Bacteriol **191**(14): 4605-4614.

- 136) De Groote, M. A., U. A. Ochsner, M. U. Shiloh, C. Nathan, J. M. McCord, M. C. Dinauer, S. J. Libby, A. Vazquez-Torres, Y. Xu and F. C. Fang (1997). "Periplasmic superoxide dismutase protects Salmonella from products of phagocyte NADPH-oxidase and nitric oxide synthase." Proc Natl Acad Sci U S A **94**(25): 13997-14001.
- 137) Lindahl, T., B. Demple and P. Robins (1982). "Suicide inactivation of the E. coli O6 methylguanine-DNA methyltransferase." Embo j **1**(11): 1359-1363.
- 138) Richardson, A. R., K. C. Soliven, M. E. Castor, P. D. Barnes, S. J. Libby and F. C. Fang (2009). "The Base Excision Repair system of Salmonella enterica serovar typhimurium counteracts DNA damage by host nitric oxide." PLoS Pathog **5**(5): e1000451.
- 139) Kitajima, S., S. Takuma and M. Morimoto (2000). "Histological analysis of murine colitis induced by dextran sulfate sodium of different molecular weights." Exp Anim **49**(1): 9-15.
- 140) Laroui, H., S. A. Ingersoll, H. C. Liu, M. T. Baker, S. Ayyadurai, M. A. Charania, F. Laroui, Y. Yan, S. V. Sitaraman and D. Merlin (2012). "Dextran sodium sulfate (DSS) induces colitis in mice by forming nano-lipocomplexes with medium-chain-length fatty acids in the colon." PLoS One **7**(3): e32084.
- 141) Kitajima, S., M. Morimoto, E. Sagara, C. Shimizu and Y. Ikeda (2001). "Dextran sodium sulfate-induced colitis in germ-free IQI/Jic mice." Exp Anim **50**(5): 387-395.
- 142) Rose, W. A., 2nd, K. Sakamoto and C. A. Leifer (2012). "Multifunctional role of dextran sulfate sodium for in vivo modeling of intestinal diseases." BMC Immunol **13**: 41.
- 143) Maslowski, K. M., A. T. Vieira, A. Ng, J. Kranich, F. Sierro, D. Yu, H. C. Schilter, M. S. Rolph, F. Mackay, D. Artis, R. J. Xavier, M. M. Teixeira and C. R. Mackay (2009). "Regulation of inflammatory responses by gut microbiota and chemoattractant receptor GPR43." Nature **461**(7268): 1282-1286.
- 144) Sartor, R. B. and S. K. Mazmanian (2012). "Intestinal Microbes in Inflammatory Bowel Diseases." Am J Gastroenterol Suppl **1**(1): 15-21.
- 145) Brown, A. J., S. M. Goldsworthy, A. A. Barnes, M. M. Eilert, L. Tcheang, D. Daniels, A. I. Muir, M. J. Wigglesworth, I. Kinghorn, N. J. Fraser, N. B. Pike, J. C. Strum, K. M. Steplewski, P. R. Murdock, J. C. Holder, F. H. Marshall, P. G. Szekeres, S. Wilson, D. M. Ignar, S. M. Foord, A. Wise and S. J. Dowell (2003). "The Orphan G protein-coupled receptors GPR41 and GPR43 are activated by propionate and other short chain carboxylic acids." J Biol Chem **278**(13): 11312-11319.
- 146) Le Poul, E., C. Loison, S. Struyf, J. Y. Springael, V. Lannoy, M. E. Decobecq, S. Brezillon, V. Dupriez, G. Vassart, J. Van Damme, M. Parmentier and M. Detheux (2003). "Functional characterization of human receptors for short chain fatty acids and their role in polymorphonuclear cell activation." J Biol Chem **278**(28): 25481-25489.

- 147) Maslowski, K. M., A. T. Vieira, A. Ng, J. Kranich, F. Sierro, D. Yu, H. C. Schilter, M. S. Rolph, F. Mackay, D. Artis, R. J. Xavier, M. M. Teixeira and C. R. Mackay (2009). "Regulation of inflammatory responses by gut microbiota and chemoattractant receptor GPR43." Nature **461**(7268): 1282-1286.
- 148) Smith, P. M., M. R. Howitt, N. Panikov, M. Michaud, C. A. Gallini, Y. M. Bohlooly, J. N. Glickman and W. S. Garrett (2013). "The microbial metabolites, short-chain fatty acids, regulate colonic Treg cell homeostasis." Science **341**(6145): 569-573.
- 149) Zackular, J. P., N. T. Baxter, K. D. Iverson, W. D. Sadler, J. F. Petrosino, G. Y. Chen and P. D. Schloss (2013). "The gut microbiome modulates colon tumorigenesis." MBio **4**(6): e00692-00613.
- 150) Zhan, Y., P. J. Chen, W. D. Sadler, F. Wang, S. Poe, G. Nunez, K. A. Eaton and G. Y. Chen (2013). "Gut microbiota protects against gastrointestinal tumorigenesis caused by epithelial injury." Cancer Res **73**(24): 7199-7210.
- 151) Sellon, R. K., S. Tonkonogy, M. Schultz, L. A. Dieleman, W. Grenther, E. Balish, D. M. Rennick and R. B. Sartor (1998). "Resident enteric bacteria are necessary for development of spontaneous colitis and immune system activation in interleukin-10 deficient mice." Infect Immun **66**(11): 5224-5231.
- 152) Arthur, J. C., E. Perez-Chanona, M. Muhlbauer, S. Tomkovich, J. M. Uronis, T. J. Fan, B. J. Campbell, T. Abujamel, B. Dogan, A. B. Rogers, J. M. Rhodes, A. Stintzi, K. W. Simpson, J. J. Hansen, T. O. Keku, A. A. Fodor and C. Jobin (2012). "Intestinal inflammation targets cancer-inducing activity of the microbiota." Science **338**(6103): 120-123.
- 153) Bogdan, C. (2001). "Nitric oxide and the immune response." Nat Immunol **2**(10): 907-916.
- 154) Schwentker, A., Y. Vodovotz, R. Weller and T. R. Billiar (2002). "Nitric oxide and wound repair: role of cytokines?" Nitric Oxide **7**(1): 1-10.
- 155) Witte, M. B. and A. Barbul (2002). "Role of nitric oxide in wound repair." Am J Surg **183**(4): 406-412.
- 156) Guzik, T. J., R. Korbut and T. Adamek-Guzik (2003). "Nitric oxide and superoxide in inflammation and immune regulation." J Physiol Pharmacol **54**(4): 469-487.
- 157) Kobayashi, Y. (2010). "The regulatory role of nitric oxide in proinflammatory cytokine expression during the induction and resolution of inflammation." J Leukoc Biol **88**(6): 1157-1162.
- 158) Wink, D. A., H. B. Hines, R. Y. Cheng, C. H. Switzer, W. Flores-Santana, M. P. Vitek, L. A. Ridnour and C. A. Colton (2011). "Nitric oxide and redox mechanisms in the immune response." J Leukoc Biol **89**(6): 873-891.

- 159) Stallmeyer, B., H. Kampfer, N. Kolb, J. Pfeilschifter and S. Frank (1999). "The function of nitric oxide in wound repair: inhibition of inducible nitric oxide-synthase severely impairs wound reepithelialization." J Invest Dermatol **113**(6): 1090-1098.
- 160) Papanikolaou, A., Q. S. Wang, D. A. Delker and D. W. Rosenberg (1998). "Azoxymethane induced colon tumors and aberrant crypt foci in mice of different genetic susceptibility." Cancer Lett **130**(1-2): 29-34.
- 161) Papanikolaou, A., Q. S. Wang, D. Papanikolaou, H. E. Whiteley and D. W. Rosenberg (2000). "Sequential and morphological analyses of aberrant crypt foci formation in mice of differing susceptibility to azoxymethane-induced colon carcinogenesis." Carcinogenesis **21**(8): 1567-1572.
- 162) Bissahoyo, A., R. S. Pearsall, K. Hanlon, V. Amann, D. Hicks, V. L. Godfrey and D. W. Threadgill (2005). "Azoxymethane is a genetic background-dependent colorectal tumor initiator and promoter in mice: effects of dose, route, and diet." Toxicol Sci **88**(2): 340-345.
- 163) Nambiar, P. R., G. Girnun, N. A. Lillo, K. Guda, H. E. Whiteley and D. W. Rosenberg (2003). "Preliminary analysis of azoxymethane induced colon tumors in inbred mice commonly used as transgenic/knockout progenitors." Int J Oncol **22**(1): 145-150.
- 164) Suzuki, R., H. Kohno, S. Sugie, H. Nakagama and T. Tanaka (2006). "Strain differences in the susceptibility to azoxymethane and dextran sodium sulfate-induced colon carcinogenesis in mice." Carcinogenesis **27**(1): 162-169.
- 165) Liu, P., Y. Lu, H. Liu, W. Wen, D. Jia, Y. Wang and M. You (2012). "Genome-wide association and fine mapping of genetic loci predisposing to colon carcinogenesis in mice." Mol Cancer Res **10**(1): 66-74.
- 166) Inherited Colorectal Cancer. (n.d.). WebMD. Retrieved July 7, 2014, from <http://www.webmd.com/colorectal-cancer/guide/inherited-colorectal-cancer>
- 167) Suzuki, R., H. Kohno, S. Sugie and T. Tanaka (2005). "Dose-dependent promoting effect of dextran sodium sulfate on mouse colon carcinogenesis initiated with azoxymethane." Histol Histopathol **20**(2): 483-492.
- 168) Cooke, M. S., M. D. Evans, M. Dizdaroglu and J. Lunec (2003). "Oxidative DNA damage: mechanisms, mutation, and disease." Faseb j **17**(10): 1195-1214.
- 169) Dizdaroglu, M. and P. Jaruga (2012). "Mechanisms of free radical-induced damage to DNA." Free Radic Res **46**(4): 382-419.
- 170) Boveris, A. and B. Chance (1973). "The mitochondrial generation of hydrogen peroxide. General properties and effect of hyperbaric oxygen." Biochem J **134**(3): 707-716.

- 171) Guidot, D. M., J. M. McCord, R. M. Wright and J. E. Repine (1993). "Absence of electron transport (Rho 0 state) restores growth of a manganese-superoxide dismutase-deficient *Saccharomyces cerevisiae* in hyperoxia. Evidence for electron transport as a major source of superoxide generation in vivo." J Biol Chem **268**(35): 26699-26703.
- 172) Packer, M. A., C. M. Porteous and M. P. Murphy (1996). "Superoxide production by mitochondria in the presence of nitric oxide forms peroxynitrite." Biochem Mol Biol Int **40**(3): 527-534.
- 173) Giulivi, C., J. J. Poderoso and A. Boveris (1998). "Production of nitric oxide by mitochondria." J Biol Chem **273**(18): 11038-11043.
- 174) D'Autreaux, B. and M. B. Toledano (2007). "ROS as signalling molecules: mechanisms that generate specificity in ROS homeostasis." Nat Rev Mol Cell Biol **8**(10): 813-824.
- 175) Ray, P. D., B. W. Huang and Y. Tsuji (2012). "Reactive oxygen species (ROS) homeostasis and redox regulation in cellular signaling." Cell Signal **24**(5): 981-990.
- 176) Kohen, R. and A. Nyska (2002). "Oxidation of biological systems: oxidative stress phenomena, antioxidants, redox reactions, and methods for their quantification." Toxicol Pathol **30**(6): 620-650.
- 177) Karihtala, P. and Y. Soini (2007). "Reactive oxygen species and antioxidant mechanisms in human tissues and their relation to malignancies." APMIS **115**(2): 81-103.
- 178) Wiseman, H. and B. Halliwell (1996). "Damage to DNA by reactive oxygen and nitrogen species: role in inflammatory disease and progression to cancer." Biochem J **313** (Pt 1): 17-29.
- 179) Cheng, K. C., D. S. Cahill, H. Kasai, S. Nishimura and L. A. Loeb (1992). "8-Hydroxyguanine, an abundant form of oxidative DNA damage, causes G----T and A----C substitutions." J Biol Chem **267**(1): 166-172.
- 180) Shibutani, S., M. Takeshita and A. P. Grollman (1991). "Insertion of specific bases during DNA synthesis past the oxidation-damaged base 8-oxodG." Nature **349**(6308): 431-434.
- 181) Nguyen, T., D. Brunson, C. L. Crespi, B. W. Penman, J. S. Wishnok and S. R. Tannenbaum (1992). "DNA damage and mutation in human cells exposed to nitric oxide in vitro." Proc Natl Acad Sci U S A **89**(7): 3030-3034.
- 182) Ohshima, H. and H. Bartsch (1994). "Chronic infections and inflammatory processes as cancer risk factors: possible role of nitric oxide in carcinogenesis." Mutat Res **305**(2): 253-264.

- 183) Stadtman, E. R. (1993). "Oxidation of free amino acids and amino acid residues in proteins by radiolysis and by metal-catalyzed reactions." Annu Rev Biochem **62**: 797-821.
- 184) Marnett, L. J. (2002). "Oxy radicals, lipid peroxidation and DNA damage." Toxicology **181-182**: 219-222.
- 185) Nair, V., G. A. Turner and R. J. Offerman (1984). "Novel adducts from the modification of nucleic acid bases by malondialdehyde." Journal of the American Chemical Society **106**(11): 3370-3371.
- 186) Marnett, L. J., A. K. Basu, S. M. O'Hara, P. E. Weller, A. F. M. M. Rahman and J. P. Oliver (1986). "Reaction of malondialdehyde with guanine nucleosides: formation of adducts containing oxadiazabicyclononene residues in the base-pairing region." Journal of the American Chemical Society **108**(6): 1348-1350.
- 187) Fink, S. P., G. R. Reddy and L. J. Marnett (1997). "Mutagenicity in Escherichia coli of the major DNA adduct derived from the endogenous mutagen malondialdehyde." Proc Natl Acad Sci U S A **94**(16): 8652-8657.
- 188) Meira, L. B., J. M. Bugni, S. L. Green, C. W. Lee, B. Pang, D. Borenshtein, B. H. Rickman, A. B. Rogers, C. A. Moroski-Erkul, J. L. McFaline, D. B. Schauer, P. C. Dedon, J. G. Fox and L. D. Samson (2008). "DNA damage induced by chronic inflammation contributes to colon carcinogenesis in mice." J Clin Invest **118**(7): 2516-2525.
- 189) el Ghissassi, F., A. Barbin, J. Nair and H. Bartsch (1995). "Formation of 1,N6 ethenoadenine and 3,N4-ethenocytosine by lipid peroxidation products and nucleic acid bases." Chem Res Toxicol **8**(2): 278-283.
- 190) Choi, J. Y., H. Zang, K. C. Angel, I. D. Kozekov, A. K. Goodenough, C. J. Rizzo and F. P. Guengerich (2006). "Translesion synthesis across 1,N2-ethenoguanine by human DNA polymerases." Chem Res Toxicol **19**(6): 879-886.
- 191) Delaney, J. C., L. Smeester, C. Wong, L. E. Frick, K. Taghizadeh, J. S. Wishnok, C. L. Drennan, L. D. Samson and J. M. Essigmann (2005). "AlkB reverses etheno DNA lesions caused by lipid oxidation in vitro and in vivo." Nat Struct Mol Biol **12**(10): 855-860.
- 192) Calvo, J. A., L. B. Meira, C. Y. Lee, C. A. Moroski-Erkul, N. Abolhassani, K. Taghizadeh, L. W. Eichinger, S. Muthupalani, L. M. Nordstrand, A. Klungland and L. D. Samson (2012). "DNA repair is indispensable for survival after acute inflammation." J Clin Invest **122**(7): 2680-2689.
- 193) Crohn's & Colitis. (n.d.). *CCFA: Bringing to Light the Risk of Colorectal Cancer among Crohn's & Ulcerative Colitis Patients*. Retrieved July 12, 2014, from <http://www.ccfa.org/resources/risk-of-colorectal-cancer.html>

- 194) Croteau, D. L. and V. A. Bohr (1997). "Repair of oxidative damage to nuclear and mitochondrial DNA in mammalian cells." J Biol Chem **272**(41): 25409-25412.
- 195) Kazak, L., A. Reyes and I. J. Holt (2012). "Minimizing the damage: repair pathways keep mitochondrial DNA intact." Nat Rev Mol Cell Biol **13**(10): 659-671.
- 196) Tchou, J., H. Kasai, S. Shibutani, M. H. Chung, J. Laval, A. P. Grollman and S. Nishimura (1991). "8-Oxoguanine (8-Hydroxyguanine) DNA Glycosylase and Its Substrate Specificity." Proceedings of the National Academy of Sciences of the United States of America **88**(11): 4690-4694.
- 197) Hill, J. W., T. K. Hazra, T. Izumi and S. Mitra (2001). "Stimulation of human 8 oxoguanine-DNA glycosylase by AP-endonuclease: potential coordination of the initial steps in base excision repair." Nucleic Acids Res **29**(2): 430-438.
- 198) Okayasu, I., M. Yamada, T. Mikami, T. Yoshida, J. Kanno and T. Ohkusa (2002). "Dysplasia and carcinoma development in a repeated dextran sulfate sodium-induced colitis model." J Gastroenterol Hepatol **17**(10): 1078-1083.
- 199) Pfohl-Leszkowicz, A., Y. Grosse, V. Carriere, P. H. Cugnenc, A. Berger, F. Carnot, P. Beaune and I. de Waziers (1995). "High levels of DNA adducts in human colon are associated with colorectal cancer." Cancer Res **55**(23): 5611-5616.
- 200) Otteneder, M. and W. K. Lutz (1999). "Correlation of DNA adduct levels with tumor incidence: carcinogenic potency of DNA adducts." Mutat Res **424**(1-2): 237-247.
- 201) Loscalzo, J. (2010). "Antioxidant enzyme deficiencies and vascular disease." Expert Rev Endocrinol Metab **5**(1): 15-18.
- 202) Griffiths, D. F., S. J. Davies, D. Williams, G. T. Williams and E. D. Williams "Demonstration of somatic mutation and colonic crypt clonality by X-linked enzyme histochemistry." Nature **333**(6172): 461-463.
- 203) Kuraguchi, M., H. Cook, E. D. Williams and G. A. Thomas (2001). "Differences in susceptibility to colonic stem cell somatic mutation in three strains of mice." J Pathol **193**(4): 517-521.
- 204) Williams, E. D., A. P. Lowes, D. Williams and G. T. Williams (1992). "A stem cell niche theory of intestinal crypt maintenance based on a study of somatic mutation in colonic mucosa." Am J Pathol **141**(4): 773-776.
- 205) Griffiths, D. F., P. Sacco, D. Williams, G. T. Williams and E. D. Williams (1989). "The clonal origin of experimental large bowel tumours." Br J Cancer **59**(3): 385-387.

- 206) Megaraj, V., X. Ding, C. Fang, N. Kovalchuk, Y. Zhu and Q. Y. Zhang (2014). "Role of hepatic and intestinal p450 enzymes in the metabolic activation of the colon carcinogen azoxymethane in mice." Chem Res Toxicol **27**(4): 656-662.
- 207) Vulliamy, T. J., M. D'Urso, G. Battistuzzi, M. Estrada, N. S. Foulkes, G. Martini, V. Calabro, V. Poggi, R. Giordano, M. Town and et al. (1988). "Diverse point mutations in the human glucose-6-phosphate dehydrogenase gene cause enzyme deficiency and mild or severe hemolytic anemia." Proc Natl Acad Sci U S A **85**(14): 5171-5175.
- 208) Beutler, E. and T. J. Vulliamy (2002). "Hematologically important mutations: glucose-6 phosphate dehydrogenase." Blood Cells Mol Dis **28**(2): 93-103.
- 209) Hagemann, R. F., Sigdestad, C. P. & Lesher S. A quantitative description of the intestinal epithelium of the mouse. *Am. J. Anat.* **129**, 41-51 (1970).
- 210) Loechler, E. L., C. L. Green and J. M. Essigmann (1984). "In vivo mutagenesis by O6 methylguanine built into a unique site in a viral genome." Proc Natl Acad Sci U S A **81**(20): 6271-6275.
- 211) Rossi, S. C. and M. D. Topal (1991). "Mutagenic frequencies of site-specifically located O6-methylguanine in wild-type Escherichia coli and in a strain deficient in ada methyltransferase." J Bacteriol **173**(3): 1201-1207.
- 212) CTNNB1 Gene. (n.d.). Retrieved October 2, 2014, from <http://www.genecards.org/cgi-bin/carddisp.pl?gene=CTNNB1>
- 213) Stamos, J. L. and W. I. Weis (2013). "The beta-catenin destruction complex." Cold Spring Harb Perspect Biol **5**(1): a007898.
- 214) Takahashi, M., S. Nakatsugi, T. Sugimura and K. Wakabayashi (2000). "Frequent mutations of the β -catenin gene in mouse colon tumors induced by azoxymethane." Carcinogenesis **21**(6): 1117-1120.
- 215) Kohno, H., R. Suzuki, S. Sugie and T. Tanaka (2005). "Beta-Catenin mutations in a mouse model of inflammation-related colon carcinogenesis induced by 1,2-dimethylhydrazine and dextran sodium sulfate." Cancer Sci **96**(2): 69-76.
- 216) Chen, J. and X. F. Huang (2009). "The signal pathways in azoxymethane-induced colon cancer and preventive implications." Cancer Biol Ther **8**(14): 1313-1317.
- 217) Fearnhead, N. S., M. P. Britton and W. F. Bodmer (2001). "The ABC of APC." Human Molecular Genetics **10**(7): 721-733.
- 218) Faili, A., S. Aoufouchi, E. Flatter, Q. Gueranger, C.-A. Reynaud and J.-C. Weill (2002). "Induction of somatic hypermutation in immunoglobulin genes is dependent on DNA polymerase iota." Nature **419**(6910): 944-947.

- 219) Balkwill, F. and A. Mantovani (2001). "Inflammation and cancer: back to Virchow?" Lancet **357**(9255): 539-545.
- 220) Tait Wojno, Elia D. and D. Artis "Innate Lymphoid Cells: Balancing Immunity, Inflammation, and Tissue Repair in the Intestine." Cell Host & Microbe **12**(4): 445-457.
- 221) Chen, Y., K. Chou, E. Fuchs, W. L. Havran and R. Boismenu (2002). "Protection of the intestinal mucosa by intraepithelial gamma delta T cells." Proc Natl Acad Sci U S A **99**(22): 14338-14343.
- 222) Martin, P. and S. J. Leibovich (2005). "Inflammatory cells during wound repair: the good, the bad and the ugly." Trends Cell Biol **15**(11): 599-607.
- 223) Eming, S. A., S. Werner, P. Bugnon, C. Wickenhauser, L. Siewe, O. Utermohlen, J. M. Davidson, T. Krieg and A. Roers (2007). "Accelerated wound closure in mice deficient for interleukin-10." Am J Pathol **170**(1): 188-202.
- 224) Sporn, M., A. Roberts, L. Wakefield and R. Assoian (1986). "Transforming growth factor beta: biological function and chemical structure." Science **233**(4763): 532-534.
- 225) Rappolee, D. A., D. Mark, M. J. Banda and Z. Werb (1988). "Wound macrophages express TGF-alpha and other growth factors in vivo: analysis by mRNA phenotyping." Science **241**(4866): 708-712.
- 226) Grotendorst, G. R., G. Smale and D. Pancev (1989). "Production of transforming growth factor beta by human peripheral blood monocytes and neutrophils." J Cell Physiol **140**(2): 396-402.
- 227) Branton, M. H. and J. B. Kopp (1999). "TGF-beta and fibrosis." Microbes Infect **1**(15): 1349-1365.
- 228) Massague, J. (2000). "How cells read TGF-beta signals." Nat Rev Mol Cell Biol **1**(3): 169-178.
- 229) Jeon, S. H., B. C. Chae, H. A. Kim, G. Y. Seo, D. W. Seo, G. T. Chun, N. S. Kim, S. W. Yie, W. H. Byeon, S. H. Eom, K. S. Ha, Y. M. Kim and P. H. Kim (2007). "Mechanisms underlying TGF-beta1-induced expression of VEGF and Flk-1 in mouse macrophages and their implications for angiogenesis." J Leukoc Biol **81**(2): 557-566.
- 230) Nam, E. H., S. R. Park and P. H. Kim (2010). "TGF-beta1 induces mouse dendritic cells to express VEGF and its receptor (Flt-1) under hypoxic conditions." Exp Mol Med **42**(9): 606-613.

- 231) Rappolee, D. A., D. Mark, M. J. Banda and Z. Werb (1988). "Wound macrophages express TGF-alpha and other growth factors in vivo: analysis by mRNA phenotyping." Science **241**(4866): 708-712.
- 232) Schultz, G., D. S. Rotatori and W. Clark (1991). "EGF and TGF-alpha in wound healing and repair." J Cell Biochem **45**(4): 346-352.
- 233) Gartner, M. H., J. D. Benson and M. D. Caldwell (1992). "Insulin-like growth factors I and II expression in the healing wound." J Surg Res **52**(4): 389-394.
- 234) Haase, I., R. Evans, R. Pofahl and F. M. Watt (2003). "Regulation of keratinocyte shape, migration and wound epithelialization by IGF-1- and EGF-dependent signalling pathways." J Cell Sci **116**(Pt 15): 3227-3238.
- 235) Sturm, A. and A. U. Dignass (2008). "Epithelial restitution and wound healing in inflammatory bowel disease." World J Gastroenterol **14**(3): 348-353.
- 236) Werner, S. and R. Grose (2003). "Regulation of wound healing by growth factors and cytokines." Physiol Rev **83**(3): 835-870.
- 237) Jameson, J., K. Ugarte, N. Chen, P. Yachi, E. Fuchs, R. Boismenu and W. L. Havran (2002). "A role for skin gammadelta T cells in wound repair." Science **296**(5568): 747-749.
- 238) Chen, Y., K. Chou, E. Fuchs, W. L. Havran and R. Boismenu (2002). "Protection of the intestinal mucosa by intraepithelial gamma delta T cells." Proc Natl Acad Sci U S A **99**(22): 14338-14343.
- 239) Shahrzad, S., L. Quayle, C. Stone, C. Plumb, S. Shirasawa, J. W. Rak and B. L. Coomber (2005). "Ischemia-induced K-ras mutations in human colorectal cancer cells: role of microenvironmental regulation of MSH2 expression." Cancer Res **65**(18): 8134-8141.
- 240) Onozuka, H., K. Tsuchihara and H. Esumi (2011). "Hypoglycemic/hypoxic condition in vitro mimicking the tumor microenvironment markedly reduced the efficacy of anticancer drugs." Cancer Sci **102**(5): 975-982.
- 241) Hongo, K., N. H. Tsuno, K. Kawai, K. Sasaki, M. Kaneko, M. Hiyoshi, K. Muro, N. Tada, T. Nirei, E. Sunami, K. Takahashi, H. Nagawa, J. Kitayama and T. Watanabe (2013). "Hypoxia enhances colon cancer migration and invasion through promotion of epithelial-mesenchymal transition." J Surg Res **182**(1): 75-84.
- 242) Wike-Hooley, J. L., J. Haveman and H. S. Reinhold (1984). "The relevance of tumour pH to the treatment of malignant disease." Radiother Oncol **2**(4): 343-366.

- 243) Helmlinger, G., A. Sckell, M. Dellian, N. S. Forbes and R. K. Jain (2002). "Acid production in glycolysis-impaired tumors provides new insights into tumor metabolism." Clin Cancer Res **8**(4): 1284-1291.
- 244) Kato, Y., S. Ozawa, C. Miyamoto, Y. Maehata, A. Suzuki, T. Maeda and Y. Baba (2013). "Acidic extracellular microenvironment and cancer." Cancer Cell Int **13**(1): 89.
- 245) Hongo, K., N. H. Tsuno, K. Kawai, K. Sasaki, M. Kaneko, M. Hiyoshi, K. Muro, N. Tada, T. Nirei, E. Sunami, K. Takahashi, H. Nagawa, J. Kitayama and T. Watanabe (2013). "Hypoxia enhances colon cancer migration and invasion through promotion of epithelial-mesenchymal transition." J Surg Res **182**(1): 75-84.
- 246) Zetter, B. R. (1998). "Angiogenesis and tumor metastasis." Annu Rev Med **49**: 407-424.
- 247) Stacker, S. A., M. G. Achen, L. Jussila, M. E. Baldwin and K. Alitalo (2002). "Lymphangiogenesis and cancer metastasis." Nat Rev Cancer **2**(8): 573-583.
- 248) Negus, R. P., G. W. Stamp, M. G. Relf, F. Burke, S. T. Malik, S. Bernasconi, P. Allavena, S. Sozzani, A. Mantovani and F. R. Balkwill (1995). "The detection and localization of monocyte chemoattractant protein-1 (MCP-1) in human ovarian cancer." J Clin Invest **95**(5): 2391-2396.
- 249) Luboshits, G., S. Shina, O. Kaplan, S. Engelberg, D. Nass, B. Lifshitz-Mercer, S. Chaitchik, I. Keydar and A. Ben-Baruch (1999). "Elevated expression of the CC chemokine regulated on activation, normal T cell expressed and secreted (RANTES) in advanced breast carcinoma." Cancer Res **59**(18): 4681-4687.
- 250) Pollard, J. W. (2004). "Tumour-educated macrophages promote tumour progression and metastasis." Nat Rev Cancer **4**(1): 71-78.
- 251) Qian, B. Z. and J. W. Pollard (2010). "Macrophage diversity enhances tumor progression and metastasis." Cell **141**(1): 39-51.
- 252) Gabrilovich, D. I., S. Ostrand-Rosenberg and V. Bronte (2012). "Coordinated regulation of myeloid cells by tumours." Nat Rev Immunol **12**(4): 253-268.
- 253) Quatromoni, J. G. and E. Eruslanov (2012). "Tumor-associated macrophages: function, phenotype, and link to prognosis in human lung cancer." Am J Transl Res **4**(4): 376-389.
- Raulet, D. H. (2003). "Roles of the NKG2D immunoreceptor and its ligands." Nat Rev Immunol **3**(10): 781-790.
- 254) Lamagna, C., M. Aurrand-Lions and B. A. Imhof (2006). "Dual role of macrophages in tumor growth and angiogenesis." J Leukoc Biol **80**(4): 705-713.

- 255) Solinas, G., G. Germano, A. Mantovani and P. Allavena (2009). "Tumor-associated macrophages (TAM) as major players of the cancer-related inflammation." J Leukoc Biol **86**(5): 1065-1073.
- 256) Schoppmann, S. F., P. Birner, J. Stockl, R. Kalt, R. Ullrich, C. Caucig, E. Kriehuber, K. Nagy, K. Alitalo and D. Kerjaschki (2002). "Tumor-associated macrophages express lymphatic endothelial growth factors and are related to peritumoral lymphangiogenesis." Am J Pathol **161**(3): 947-956.
- 257) Murdoch, C., M. Muthana, S. B. Coffelt and C. E. Lewis (2008). "The role of myeloid cells in the promotion of tumour angiogenesis." Nat Rev Cancer **8**(8): 618-631.
- 258) Biswas, S. K. and A. Mantovani (2010). "Macrophage plasticity and interaction with lymphocyte subsets: cancer as a paradigm." Nat Immunol **11**(10): 889-896.
- 259) Boussiotis, V. A., E. Y. Tsai, E. J. Yunis, S. Thim, J. C. Delgado, C. C. Dascher, A. Berezovskaya, D. Rousset, J. M. Reynes and A. E. Goldfeld (2000). "IL-10-producing T cells suppress immune responses in anergic tuberculosis patients." J Clin Invest **105**(9): 1317-1325.
- 260) Taylor, A., J. Verhagen, K. Blaser, M. Akdis and C. A. Akdis (2006). "Mechanisms of immune suppression by interleukin-10 and transforming growth factor-beta: the role of T regulatory cells." Immunology **117**(4): 433-442.
- 261) Gordon, S. and P. R. Taylor (2005). "Monocyte and macrophage heterogeneity." Nat Rev Immunol **5**(12): 953-964.
- 262) Gu, L., S. Tseng, R. M. Horner, C. Tam, M. Loda and B. J. Rollins (2000). "Control of TH2 polarization by the chemokine monocyte chemoattractant protein-1." Nature **404**(6776): 407-411.
- 263) Gordon, S. (2003). "Alternative activation of macrophages." Nat Rev Immunol **3**(1): 23-35.
- 264) Gabrilovich, D., T. Ishida, T. Oyama, S. Ran, V. Kravtsov, S. Nadaf and D. P. Carbone (1998). "Vascular endothelial growth factor inhibits the development of dendritic cells and dramatically affects the differentiation of multiple hematopoietic lineages in vivo." Blood **92**(11): 4150-4166.
- 265) Laxmanan, S., S. W. Robertson, E. Wang, J. S. Lau, D. M. Briscoe and D. Mukhopadhyay (2005). "Vascular endothelial growth factor impairs the functional ability of dendritic cells through Id pathways." Biochem Biophys Res Commun **334**(1): 193-198.
- 266) Fricke, I. and D. I. Gabrilovich (2006). "Dendritic cells and tumor microenvironment: a dangerous liaison." Immunol Invest **35**(3-4): 459-483.

- 267) Moretta, A., C. Bottino, M. Vitale, D. Pende, C. Cantoni, M. C. Mingari, R. Biassoni and L. Moretta (2001). "Activating receptors and coreceptors involved in human natural killer cell-mediated cytotoxicity." Ann Rev Immunol **19**: 197-223.
- 268) Zamai, L., C. Ponti, P. Mirandola, G. Gobbi, S. Papa, L. Galeotti, L. Cocco and M. Vitale (2007). "NK Cells and Cancer." The Journal of Immunology **178**(7): 4011-4016.
- 269) Chan, C. J., M. J. Smyth and L. Martinet (2014). "Molecular mechanisms of natural killer cell activation in response to cellular stress." Cell Death Differ **21**(1): 5-14.
- 270) Rakoff-Nahoum, S. and R. Medzhitov (2009). "Toll-like receptors and cancer." Nat Rev Cancer **9**(1): 57-63.
- 271) Pradere, J. P., D. H. Dapito and R. F. Schwabe (2014). "The Yin and Yang of Toll-like receptors in cancer." Oncogene **33**(27): 3485-3495.
- 272) Lowe, E. L., T. R. Crother, S. Rabizadeh, B. Hu, H. Wang, S. Chen, K. Shimada, M. H. Wong, K. S. Michelsen and M. Arditì (2010). "Toll-like receptor 2 signaling protects mice from tumor development in a mouse model of colitis-induced cancer." PLoS One **5**(9): e13027.
- 273) Fukata, M., A. Chen, A. S. Vamadevan, J. Cohen, K. Breglio, S. Krishnareddy, D. Hsu, R. Xu, N. Harpaz, A. J. Dannenberg, K. Subbaramaiah, H. S. Cooper, S. H. Itzkowitz and M. T. Abreu (2007). "Toll-like receptor-4 promotes the development of colitis-associated colorectal tumors." Gastroenterology **133**(6): 1869-1881.
- 274) Allen, I. C., E. M. TeKippe, R. M. Woodford, J. M. Uronis, E. K. Holl, A. B. Rogers, H. H. Herfarth, C. Jobin and J. P. Ting (2010). "The NLRP3 inflammasome functions as a negative regulator of tumorigenesis during colitis-associated cancer." J Exp Med **207**(5): 1045-1056.
- 275) Matsuda, S., S. Kudoh and S. Katayama (2001). "Enhanced formation of azoxymethane induced colorectal adenocarcinoma in gammadelta T lymphocyte-deficient mice." Jpn J Cancer Res **92**(8): 880-885.
- 276) Germain, R. N. (2002). "T-cell development and the CD4-CD8 lineage decision." Nat Rev Immunol **2**(5): 309-322.
- 277) Palmer, E. (2003). "Negative selection clearing out the bad apples from the T-cell repertoire." Nat Rev Immunol **3**(5): 383-391.
- 278) Mombaerts, P., J. Iacomini, R. S. Johnson, K. Herrup, S. Tonegawa and V. E. Papaioannou (1992). "RAG-1-deficient mice have no mature B and T lymphocytes." Cell **68**(5): 869-877.

- 279) Shinkai, Y., S. Koyasu, K. Nakayama, K. M. Murphy, D. Y. Loh, E. L. Reinherz and F. W. Alt (1993). "Restoration of T cell development in RAG-2-deficient mice by functional TCR transgenes." Science **259**(5096): 822-825.
- 280) Friedl, P., A. T. den Boer and M. Gunzer (2005). "Tuning immune responses: diversity and adaptation of the immunological synapse." Nat Rev Immunol **5**(7): 532-545.
- 281) Coffey, P. J. and B. M. T. Burgering (2004). "Forkhead-box transcription factors and their role in the immune system." Nat Rev Immunol **4**(11): 889-899.
- 282) Harty, J. T., A. R. Tinnereim and D. W. White (2000). "CD8+ T cell effector mechanisms in resistance to infection." Annu Rev Immunol **18**: 275-308.
- 283) Houghton, A. N., P. Guevara, xF, J. o, xE and A (2004). "Immune recognition of self in immunity against cancer." The Journal of Clinical Investigation **114**(4): 468-471.
- 284) Carcinoembryonic Antigen (CEA). (0000, May 3). *WebMD*. Retrieved July 20, 2014, from <http://www.webmd.com/cancer/carcinoembryonic-antigen-cea>
- 285) Pittet, M. J. (2009). "Behavior of immune players in the tumor microenvironment." Curr Opin Oncol **21**(1): 53-59.
- 286) Romagnani, S. (1999). "Th1/Th2 cells." Inflamm Bowel Dis **5**(4): 285-294.
- 287) Zhu, J. and W. E. Paul (2008). "CD4 T cells: fates, functions, and faults." Blood **112**(5): 1557-1569.
- 288) Nathan, C. F., H. W. Murray, M. E. Wiebe and B. Y. Rubin (1983). "Identification of interferon-gamma as the lymphokine that activates human macrophage oxidative metabolism and antimicrobial activity." J Exp Med **158**(3): 670-689.
- 289) Ouyang, W., J. K. Kolls and Y. Zheng (2008). "The biological functions of T helper 17 cell effector cytokines in inflammation." Immunity **28**(4): 454-467.
- 290) Fossiez, F., O. Djossou, P. Chomarat, L. Flores-Romo, S. Ait-Yahia, C. Maat, J. J. Pin, P. Garrone, E. Garcia, S. Saeland, D. Blanchard, C. Gaillard, B. Das Mahapatra, E. Rouvier, P. Golstein, J. Banchereau and S. Lebecque (1996). "T cell interleukin-17 induces stromal cells to produce proinflammatory and hematopoietic cytokines." J Exp Med **183**(6): 2593-2603.
- 291) Cai, X. Y., C. P. Gommoll, Jr., L. Justice, S. K. Narula and J. S. Fine (1998). "Regulation of granulocyte colony-stimulating factor gene expression by interleukin-17." Immunol Lett **62**(1): 51-58.
- 292) Shahrara, S., S. R. Pickens, A. M. Mandelin, 2nd, W. J. Karpus, Q. Huang, J. K. Kolls and R. M. Pope (2010). "IL-17-mediated monocyte migration occurs partially through CC

- chemokine ligand 2/monocyte chemoattractant protein-1 induction." J Immunol **184**(8): 4479-4487.
- 293) Hammond, M. E., G. R. Lapointe, P. H. Feucht, S. Hilt, C. A. Gallegos, C. A. Gordon, M. A. Giedlin, G. Mullenbach and P. Tekamp-Olson (1995). "IL-8 induces neutrophil chemotaxis predominantly via type I IL-8 receptors." J Immunol **155**(3): 1428-1433.
- 294) de Oliveira, S., C. C. Reyes-Aldasoro, S. Candel, S. A. Renshaw, V. Mulero and A. Calado (2013). "Cxcl8 (IL-8) mediates neutrophil recruitment and behavior in the zebrafish inflammatory response." J Immunol **190**(8): 4349-4359.
- 295) Dumoutier, L., E. Van Roost, D. Colau and J. C. Renauld (2000). "Human interleukin-10 related T cell-derived inducible factor: molecular cloning and functional characterization as an hepatocyte-stimulating factor." Proc Natl Acad Sci U S A **97**(18): 10144-10149.
- 296) Xie, M. H., S. Aggarwal, W. H. Ho, J. Foster, Z. Zhang, J. Stinson, W. I. Wood, A. D. Goddard and A. L. Gurney (2000). "Interleukin (IL)-22, a novel human cytokine that signals through the interferon receptor-related proteins CRF2-4 and IL-22R." J Biol Chem **275**(40): 31335-31339.
- 297) Wolk, K., S. Kunz, E. Witte, M. Friedrich, K. Asadullah and R. Sabat (2004). "IL-22 increases the innate immunity of tissues." Immunity **21**(2): 241-254.
- 298) Rutz, S., C. Eidenschenk and W. Ouyang (2013). "IL-22, not simply a Th17 cytokine." Immunol Rev **252**(1): 116-132.
- 299) Andoh, A., Z. Zhang, O. Inatomi, S. Fujino, Y. Deguchi, Y. Araki, T. Tsujikawa, K. Kitoh, S. Kim-Mitsuyama, A. Takayanagi, N. Shimizu and Y. Fujiyama (2005). "Interleukin-22, a member of the IL-10 subfamily, induces inflammatory responses in colonic subepithelial myofibroblasts." Gastroenterology **129**(3): 969-984.
- 300) Ikeuchi, H., T. Kuroiwa, N. Hiramatsu, Y. Kaneko, K. Hiromura, K. Ueki and Y. Nojima (2005). "Expression of interleukin-22 in rheumatoid arthritis: potential role as a proinflammatory cytokine." Arthritis Rheum **52**(4): 1037-1046.
- 301) Wolk, K., E. Witte, E. Wallace, W. D. Docke, S. Kunz, K. Asadullah, H. D. Volk, W. Sterry and R. Sabat (2006). "IL-22 regulates the expression of genes responsible for antimicrobial defense, cellular differentiation, and mobility in keratinocytes: a potential role in psoriasis." Eur J Immunol **36**(5): 1309-1323.
- 302) Zhu, J., H. Yamane, J. Cote-Sierra, L. Guo and W. E. Paul (2006). "GATA-3 promotes Th2 responses through three different mechanisms: induction of Th2 cytokine production, selective growth of Th2 cells and inhibition of Th1 cell-specific factors." Cell Res **16**(1): 3-10.

- 303) Angkasekwinai, P., S. H. Chang, M. Thapa, H. Watarai and C. Dong (2010). "Regulation of IL-9 expression by IL-25 signaling." Nat Immunol **11**(3): 250-256.
- 304) Noelle, R. J. and E. C. Nowak (2010). "Cellular sources and immune functions of interleukin-9." Nat Rev Immunol **10**(10): 683-687.
- 305) Stein, M., S. Keshav, N. Harris and S. Gordon (1992). "Interleukin 4 potently enhances murine macrophage mannose receptor activity: a marker of alternative immunologic macrophage activation." J Exp Med **176**(1): 287-292.
- 306) Doherty, T. M., R. Kastelein, S. Menon, S. Andrade and R. L. Coffman (1993). "Modulation of murine macrophage function by IL-13." J Immunol **151**(12): 7151-7160.
- 307) Van Dyken, S. J. and R. M. Locksley (2013). "Interleukin-4- and interleukin-13-mediated alternatively activated macrophages: roles in homeostasis and disease." Annu Rev Immunol **31**: 317-343.
- 308) de Waal Malefyt, R., C. G. Figdor, R. Huijbens, S. Mohan-Peterson, B. Bennett, J. Culpepper, W. Dang, G. Zurawski and J. E. de Vries (1993). "Effects of IL-13 on phenotype, cytokine production, and cytotoxic function of human monocytes. Comparison with IL-4 and modulation by IFN-gamma or IL-10." J Immunol **151**(11): 6370-6381.
- 309) Shapira, S. K., H. H. Jabara, C. P. Thienes, D. J. Ahern, D. Vercelli, H. J. Gould and R. S. Geha (1991). "Deletional switch recombination occurs in interleukin-4-induced isotype switching to IgE expression by human B cells." Proc Natl Acad Sci U S A **88**(17): 7528-7532.
- 310) Kashiwada, M., D. M. Levy, L. McKeag, K. Murray, A. J. Schroder, S. M. Canfield, G. Traver and P. B. Rothman (2010). "IL-4-induced transcription factor NFIL3/E4BP4 controls IgE class switching." Proc Natl Acad Sci U S A **107**(2): 821-826.
- 311) Van der Pouw Kraan, T. C., J. S. Van der Zee, L. C. Boeije, E. R. De Groot, S. O. Stapel and L. A. Aarden (1998). "The role of IL-13 in IgE synthesis by allergic asthma patients." Clin Exp Immunol **111**(1): 129-135.
- 312) Finkelman, F. D., T. A. Wynn, D. D. Donaldson and J. F. Urban (1999). "The role of IL-13 in helminth-induced inflammation and protective immunity against nematode infections." Curr Opin Immunol **11**(4): 420-426.
- 313) Pope, S. M., E. B. Brandt, A. Mishra, S. P. Hogan, N. Zimmermann, K. I. Matthaei, P. S. Foster and M. E. Rothenberg (2001). "IL-13 induces eosinophil recruitment into the lung by an IL-5- and eotaxin-dependent mechanism." J Allergy Clin Immunol **108**(4): 594-601.

- 314) Coffman, R. L., B. W. Seymour, S. Hudak, J. Jackson and D. Rennick (1989). "Antibody to interleukin-5 inhibits helminth-induced eosinophilia in mice." Science **245**(4915): 308-310.
- 315) Sanderson, C. J. (1992). "Interleukin-5, eosinophils, and disease." Blood **79**(12): 3101-3109.
- 316) Longphre, M., D. Li, M. Gallup, E. Drori, C. L. Ordonez, T. Redman, S. Wenzel, D. E. Bice, J. V. Fahy and C. Basbaum (1999). "Allergen-induced IL-9 directly stimulates mucin transcription in respiratory epithelial cells." J Clin Invest **104**(10): 1375-1382.
- 317) Temann, U. A., P. Ray and R. A. Flavell (2002). "Pulmonary overexpression of IL-9 induces Th2 cytokine expression, leading to immune pathology." J Clin Invest **109**(1): 29-39.
- 318) Fort, M. M., J. Cheung, D. Yen, J. Li, S. M. Zurawski, S. Lo, S. Menon, T. Clifford, B. Hunte, R. Lesley, T. Muchamuel, S. D. Hurst, G. Zurawski, M. W. Leach, D. M. Gorman and D. M. Rennick (2001). "IL-25 induces IL-4, IL-5, and IL-13 and Th2-associated pathologies in vivo." Immunity **15**(6): 985-995.
- 319) Fallon, P. G., S. J. Ballantyne, N. E. Mangan, J. L. Barlow, A. Dasvarma, D. R. Hewett, A. McIlgorm, H. E. Jolin and A. N. McKenzie (2006). "Identification of an interleukin (IL) 25-dependent cell population that provides IL-4, IL-5, and IL-13 at the onset of helminth expulsion." J Exp Med **203**(4): 1105-1116.
- 320) Rubtsov, Y. P., J. P. Rasmussen, E. Y. Chi, J. Fontenot, L. Castelli, X. Ye, P. Treuting, L. Siewe, A. Roers, W. R. Henderson, Jr., W. Muller and A. Y. Rudensky (2008). "Regulatory T cell-derived interleukin-10 limits inflammation at environmental interfaces." Immunity **28**(4): 546-558.
- 321) Taylor, A., J. Verhagen, K. Blaser, M. Akdis and C. A. Akdis (2006). "Mechanisms of immune suppression by interleukin-10 and transforming growth factor-beta: the role of T regulatory cells." Immunology **117**(4): 433-442.
- 322) Maynard, C. L., L. E. Harrington, K. M. Janowski, J. R. Oliver, C. L. Zindl, A. Y. Rudensky and C. T. Weaver (2007). "Regulatory T cells expressing interleukin 10 develop from Foxp3+ and Foxp3- precursor cells in the absence of interleukin 10." Nat Immunol **8**(9): 931-941.
- 323) Sakaguchi, S., K. Wing, Y. Onishi, P. Prieto-Martin and T. Yamaguchi (2009). "Regulatory T cells: how do they suppress immune responses?" Int Immunol **21**(10): 1105-1111.
- 324) de Waal Malefyt, R., J. Abrams, B. Bennett, C. G. Figdor and J. E. de Vries (1991). "Interleukin 10(IL-10) inhibits cytokine synthesis by human monocytes: an autoregulatory role of IL-10 produced by monocytes." J Exp Med **174**(5): 1209-1220.

- 325) Fiorentino, D. F., A. Zlotnik, T. R. Mosmann, M. Howard and A. O'Garra (1991). "IL-10 inhibits cytokine production by activated macrophages." J Immunol **147**(11): 3815-3822.
- 326) Berkman, N., M. John, G. Roesems, P. J. Jose, P. J. Barnes and K. F. Chung (1995). "Inhibition of macrophage inflammatory protein-1 alpha expression by IL-10. Differential sensitivities in human blood monocytes and alveolar macrophages." J Immunol **155**(9): 4412-4418.
- 327) de Waal Malefyt, R., J. Haanen, H. Spits, M. G. Roncarolo, A. te Velde, C. Figdor, K. Johnson, R. Kastelein, H. Yssel and J. E. de Vries (1991). "Interleukin 10 (IL-10) and viral IL-10 strongly reduce antigen-specific human T cell proliferation by diminishing the antigen-presenting capacity of monocytes via downregulation of class II major histocompatibility complex expression." J Exp Med **174**(4): 915-924.
- 328) Fiorentino, D. F., A. Zlotnik, P. Vieira, T. R. Mosmann, M. Howard, K. W. Moore and A. O'Garra (1991). "IL-10 acts on the antigen-presenting cell to inhibit cytokine production by Th1 cells." J Immunol **146**(10): 3444-3451.
- 329) Gazzinelli, R. T., I. P. Oswald, S. L. James and A. Sher (1992). "IL-10 inhibits parasite killing and nitrogen oxide production by IFN-gamma-activated macrophages." J Immunol **148**(6): 1792-1796.
- 330) Buelens, C., V. Verhasselt, D. De Groote, K. Thielemans, M. Goldman and F. Willems (1997). "Interleukin-10 prevents the generation of dendritic cells from human peripheral blood mononuclear cells cultured with interleukin-4 and granulocyte/macrophage colony-stimulating factor." Eur J Immunol **27**(3): 756-762.
- 331) Rissoan, M. C., V. Soumelis, N. Kadowaki, G. Grouard, F. Briere, R. de Waal Malefyt and Y. J. Liu (1999). "Reciprocal control of T helper cell and dendritic cell differentiation." Science **283**(5405): 1183-1186.
- 332) Denis, M. and E. Ghadirian (1993). "IL-10 neutralization augments mouse resistance to systemic Mycobacterium avium infections." J Immunol **151**(10): 5425-5430.
- 333) Greenberger, M. J., R. M. Strieter, S. L. Kunkel, J. M. Danforth, R. E. Goodman and T. J. Standiford (1995). "Neutralization of IL-10 increases survival in a murine model of Klebsiella pneumonia." J Immunol **155**(2): 722-729.
- 334) Laichalk, L. L., J. M. Danforth and T. J. Standiford (1996). "Interleukin-10 inhibits neutrophil phagocytic and bactericidal activity." FEMS Immunol Med Microbiol **15**(4): 181-187.
- 335) van der Poll, T., A. Marchant, C. V. Keogh, M. Goldman and S. F. Lowry (1996). "Interleukin-10 impairs host defense in murine pneumococcal pneumonia." J Infect Dis **174**(5): 994-1000.

- 336) Jinquan, T., C. G. Larsen, B. Gesser, K. Matsushima and K. Thestrup-Pedersen (1993). "Human IL-10 is a chemoattractant for CD8+ T lymphocytes and an inhibitor of IL-8 induced CD4+ T lymphocyte migration." J Immunol **151**(9): 4545-4551.
- 337) Brooks, D. G., K. B. Walsh, H. Elsaesser and M. B. A. Oldstone (2010). "IL-10 directly suppresses CD4 but not CD8 T cell effector and memory responses following acute viral infection." Proceedings of the National Academy of Sciences **107**(7): 3018-3023.
- 338) Cai, G., R. A. Kastelein and C. A. Hunter (1999). "IL-10 enhances NK cell proliferation, cytotoxicity and production of IFN-gamma when combined with IL-18." Eur J Immunol **29**(9): 2658-2665.
- 339) Rook, A. H., J. H. Kehrl, L. M. Wakefield, A. B. Roberts, M. B. Sporn, D. B. Burlington, H. C. Lane and A. S. Fauci (1986). "Effects of transforming growth factor beta on the functions of natural killer cells: depressed cytolytic activity and blunting of interferon responsiveness." J Immunol **136**(10): 3916-3920.
- 340) Castriconi, R., C. Cantoni, M. Della Chiesa, M. Vitale, E. Marcenaro, R. Conte, R. Biassoni, C. Bottino, L. Moretta and A. Moretta (2003). "Transforming growth factor beta 1 inhibits expression of Nkp30 and NKG2D receptors: consequences for the NK mediated killing of dendritic cells." Proc Natl Acad Sci U S A **100**(7): 4120-4125.
- 341) Tada, T., S. Ohzeki, K. Utsumi, H. Takiuchi, M. Muramatsu, X. F. Li, J. Shimizu, H. Fujiwara and T. Hamaoka (1991). "Transforming growth factor-beta-induced inhibition of T cell function. Susceptibility difference in T cells of various phenotypes and functions and its relevance to immunosuppression in the tumor-bearing state." J Immunol **146**(3): 1077-1082.
- 342) Berendt, M. J. and R. J. North (1980). "T-cell-mediated suppression of anti-tumor immunity. An explanation for progressive growth of an immunogenic tumor." J Exp Med **151**(1): 69-80.
- 343) North, R. J. and I. Bursucker (1984). "Generation and decay of the immune response to a progressive fibrosarcoma. I. Ly-1+2- suppressor T cells down-regulate the generation of Ly-1-2+ effector T cells." J Exp Med **159**(5): 1295-1311.
- 344) Shiao, S. L., A. P. Ganesan, H. S. Rugo and L. M. Coussens (2011). "Immune microenvironments in solid tumors: new targets for therapy." Genes Dev **25**(24): 2559-2572.
- 345) Facciabene, A., G. T. Motz and G. Coukos (2012). "T-regulatory cells: key players in tumor immune escape and angiogenesis." Cancer Res **72**(9): 2162-2171.
- 346) Fu, S., A. C. Yopp, X. Mao, D. Chen, N. Zhang, D. Chen, M. Mao, Y. Ding and J. S. Bromberg (2004). "CD4+ CD25+ CD62+ T-regulatory cell subset has optimal suppressive and proliferative potential." Am J Transplant **4**(1): 65-78.

- 347) Yang, S., F. Liu, Q. J. Wang, S. A. Rosenberg and R. A. Morgan (2011). "The shedding of CD62L (L-selectin) regulates the acquisition of lytic activity in human tumor reactive T lymphocytes." PLoS One **6**(7): e22560.
- 348) Girardi, M., D. E. Oppenheim, C. R. Steele, J. M. Lewis, E. Glusac, R. Filler, P. Hobby, B. Sutton, R. E. Tigelaar and A. C. Hayday (2001). "Regulation of cutaneous malignancy by gammadelta T cells." Science **294**(5542): 605-609.
- 349) Moretta, A., C. Bottino, M. Vitale, D. Pende, C. Cantoni, M. C. Mingari, R. Biassoni and L. Moretta (2001). "Activating receptors and coreceptors involved in human natural killer cell-mediated cytotoxicity." Annu Rev Immunol **19**: 197-223.
- 350) Zamai, L., C. Ponti, P. Mirandola, G. Gobbi, S. Papa, L. Galeotti, L. Cocco and M. Vitale (2007). "NK Cells and Cancer." The Journal of Immunology **178**(7): 4011-4016.
- 351) Chan, C. J., M. J. Smyth and L. Martinet (2014). "Molecular mechanisms of natural killer cell activation in response to cellular stress." Cell Death Differ **21**(1): 5-14.
- 352) Raulet, D. H. (2003). "Roles of the NKG2D immunoreceptor and its ligands." Nat Rev Immunol **3**(10): 781-790.
- 353) Desmoplasia. (n.d.). Retrieved September 24, 2014, from <http://medical-dictionary.thefreedictionary.com/desmoplasia>
- 354) Nucleolus. (n.d.). Retrieved September 24, 2014, from <http://www.biology-online.org/dictionary/Nucleolus>
- 355) What is the difference between categorical, ordinal and interval variables? (n.d.). Retrieved September 24, 2014, from http://www.ats.ucla.edu/stat/mult_pkg/whatstat/nominal_ordinal_interval.htm
- 356) What is a contingency table? (n.d.). Retrieved September 24, 2014, from http://www.eumetcal.org/resources/ukmeteocal/verification/www/english/msg/ver_categ_forec/uos1/uos1_ko1.htm
- 357) Handbook of Biological Statistics. (n.d.). Retrieved September 24, 2014, from <http://udel.edu/~mcdonald/statfishers.html>
- 358) Zhang, Y., S. Choksi, K. Chen, Y. Pobeziinskaya, I. Linnoila and Z.-G. Liu (2013). "ROS play a critical role in the differentiation of alternatively activated macrophages and the occurrence of tumor-associated macrophages." Cell Res **23**(7): 898-914.
- 359) Napolitano, L. M., M. M. Buzdon, H. J. Shi and B. L. Bass (1997). "Intestinal epithelial cell regulation of macrophage and lymphocyte interleukin 10 expression." Arch Surg **132**(12): 1271-1276.

- 360) Orsulic, S., O. Huber, H. Aberle, S. Arnold and R. Kemler (1999). "E-cadherin binding prevents beta-catenin nuclear localization and beta-catenin/LEF-1-mediated transactivation." J Cell Sci **112** (Pt 8): 1237-1245.
- 361) Brembeck, F. H., M. Rosario and W. Birchmeier (2006). "Balancing cell adhesion and Wnt signaling, the key role of beta-catenin." Curr Opin Genet Dev **16**(1): 51-59.
- 362) Maher, M. T., A. S. Flozak, A. M. Stocker, A. Chenn and C. J. Gottardi (2009). "Activity of the beta-catenin phosphodestruction complex at cell-cell contacts is enhanced by cadherin-based adhesion." J Cell Biol **186**(2): 219-228.
- 363) Zhang, D. E., C. J. Hetherington, H. M. Chen and D. G. Tenen (1994). "The macrophage transcription factor PU.1 directs tissue-specific expression of the macrophage colony stimulating factor receptor." Mol Cell Biol **14**(1): 373-381.
- 364) Martin, P., D. D'Souza, J. Martin, R. Grose, L. Cooper, R. Maki and S. R. McKercher (2003). "Wound healing in the PU.1 null mouse--tissue repair is not dependent on inflammatory cells." Curr Biol **13**(13): 1122-1128.
- 365) Na, Y. R., Y. N. Yoon, D. I. Son and S. H. Seok (2013). "Cyclooxygenase-2 inhibition blocks M2 macrophage differentiation and suppresses metastasis in murine breast cancer model." PLoS One **8**(5): e63451.
- 366) (1989). Immunodeficient Rodents: A Guide to Their Immunobiology, Husbandry, and Use, The National Academies Press.
- 367) Fischer, A. H., K. A. Jacobson, J. Rose and R. Zeller (2008). "Paraffin embedding tissue samples for sectioning." CSH Protoc **2008**: pdb.prot4989.
- 368) Fischer, A. H., K. A. Jacobson, J. Rose and R. Zeller (2008). "Hematoxylin and eosin staining of tissue and cell sections." CSH Protoc **2008**: pdb.prot4986.
- 369) Frederiks, W. M., H. Vreeling-Sindelarova and C. J. Van Noorden "Loss of peroxisomes causes oxygen insensitivity of the histochemical assay of glucose-6-phosphate dehydrogenase activity to detect cancer cells." Journal of Histochemistry & Cytochemistry **55**(2): 175-181.
- 370) Van Noorden, C. J. and I. M. Vogels (1989). "Polyvinyl alcohol and other tissue protectants in enzyme histochemistry: a consumer's guide." Histochem J **21**(7): 373-379.
- 371) Van Driel, B. E. and C. J. Van Noorden (1999). "Oxygen insensitivity of the histochemical assay of glucose-6-phosphate dehydrogenase activity for the discrimination between nonmalignant and malignant cells." J Histochem Cytochem **47**(5): 575-582.

- 372) Hisada, R. and T. Yagi (1977). "1-Methoxy-5-methylphenazinium methyl sulfate. A photochemically stable electron mediator between NADH and various electron acceptors." J Biochem **82**(5): 1469-1473.
- 373) Saleh, H. A., A. Aburashed, P. Bober and P. Tabaczka (1998). "P53 protein immunohistochemical expression in colonic adenomas with and without associated carcinoma." Am J Gastroenterol **93**(6): 980-984.
- 374) CancerQuest | Tumor Suppressors: P53 Function. (n.d.). Retrieved November 25, 2014, from <http://www.cancerquest.org/p53-function.html>
- 375) Moll, U. M. and O. Petrenko (2003). "The MDM2-p53 interaction." Mol Cancer Res **1**(14):1001-1008.
- 376) Qasim, B. J., H. H. Ali and A. G. Hussein (2012). "Immunohistochemical expression of PCNA and CD34 in colorectal adenomas and carcinomas using specified automated cellular image analysis system: a clinicopathologic study." Saudi J Gastroenterol **18**(4): 268-276.
- 377) Kubben, F. J., A. Peeters-Haesevoets, L. G. Engels, C. G. Baeten, B. Schutte, J. W. Arends, R. W. Stockbrugger and G. H. Blijham (1994). "Proliferating cell nuclear antigen (PCNA): a new marker to study human colonic cell proliferation." Gut **35**(4): 530-535.
- 378) CD34 Gene. (n.d.). Retrieved November 26, 2014, from <http://www.genecards.org/cgi-bin/carddisp.pl?gene=CD34>
- 379) Bornstein, J. C., M. Costa and J. R. Grider (2004). "Enteric motor and interneuronal circuits controlling motility." Neurogastroenterol Motil **16 Suppl 1**: 34-38.
- 380) The Enteric Nervous System. (n.d.). Retrieved December 1, 2014, from http://www.vivo.colostate.edu/hbooks/pathphys/digestion/basics/gi_nervous.htm
- 381) Efferent neuron (n.d.). Retrieved December 1, 2014, from <http://medical-dictionary.thefreedictionary.com/>
- 382) Motoneuron. (n.d.). Retrieved December 1, 2014, from <http://medical-dictionary.thefreedictionary.com/motoneuron>
- 383) Ahmad, R., R. Chaturvedi, D. Olivares-Villagomez, T. Habib, M. Asim, P. Shivesh, D. B. Polk, K. T. Wilson, M. K. Washington, L. Van Kaer, P. Dhawan and A. B. Singh (2014). "Targeted colonic claudin-2 expression renders resistance to epithelial injury, induces immune suppression, and protects from colitis." Mucosal Immunol **7**(6): 1340-1353.
- 384) Kolios, G., V. Valatas and S. G. Ward (2004). "Nitric oxide in inflammatory bowel disease: a universal messenger in an unsolved puzzle." Immunology **113**(4): 427-437.

385) Wink, D. A., H. B. Hines, R. Y. Cheng, C. H. Switzer, W. Flores-Santana, M. P. Vitek, L. A. Ridnour and C. A. Colton (2011). "Nitric oxide and redox mechanisms in the immune response." J Leukoc Biol **89**(6): 873-891.